UNIVERSITY OF SOUTHAMPTON

FACULTY OF NATURAL AND ENVIRONMENTAL SCIENCES

Centre for Biological Sciences

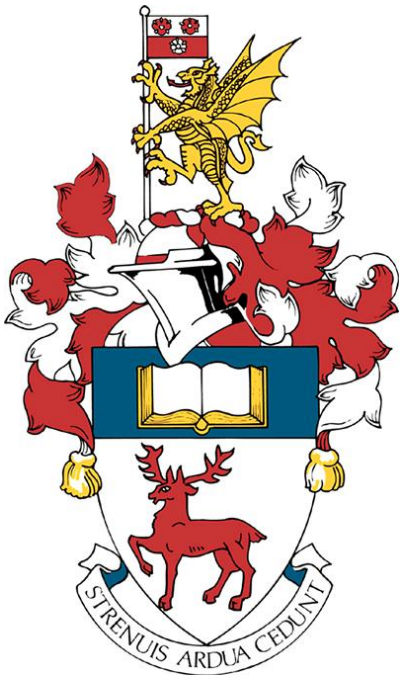

The small GTPase Rho1 couples peptidergic control of circadian behaviour to molecular oscillator function in *Drosophila melanogaster*

by

Miguel Ramírez Moreno

Thesis for the degree of Doctor of Philosophy

September 2017

UNIVERSITY OF SOUTHAMPTON

ABSTRACT

FACULTY OF NATURAL AND ENVIRONMENTAL SCIENCES

Biological Sciences

Thesis for the degree of Doctor of philosophy

THE SMALL GTPASE RHO1 COUPLES PEPTIDERFGIC CONTROL OF CIRCADIAN BEHAVIOUR TO MOLECULAR OSCILLATOR FUNCTION IN *DROSOPHILA MELANOGASTER*

Miguel Ramírez Moreno

The fruit fly *Drosophila melanogaster* constitutes a resourceful and representative model organism for investigation of the circadian clock mechanisms that control daily rhythms. Circadian control of sleep/wake rhythms in both flies and mammals requires not only molecular oscillators inside the clock cells, but also intercellular communication circuits. How these oscillators couple to relevant patterns of signals like neuropeptides or neuronal firing remains, to a large extent, unclear. This project presents evidences that the small GTPase Rho1 (homologue of the mammalian RhoA), a regulator of actin dynamics, controls circadian locomotor behaviour in a dosage-dependent manner. Flies with specific reduction of *Rho1* levels inside their adult *pacemaker* neurons [the ventral lateral neurons (LN_vs) that express the neuropeptide Pigment Dispersing Factor (PDF)] effectively lose their capacity of sustaining rhythms in *free run* devoid of external stimuli. When environmental cues are present, these flies exhibit a heightened sensitivity and their activity rhythms are more dependent of environmental cycles. Remarkable, this happens in the context of normal molecular oscillators across the clock circuitry in the brain. This discoordination between clocks and behaviour points to a disruption at the circuit level that weakens the output response. Diverse experiments have implicated an abnormality in signalling from the small LN_v (s-LN_v) dorsal axons as the cause of this phenotype: 1) the clock-controlled rhythms of remodelling of the s-LN_v dorsal axons are abrogated upon *Rho1* knockdown; 2) The *Rho1* deficit behavioural phenotype is rescued by manipulations that shift pacemaker function from the s-LN_vs to other clock neurons and 3) the *Rho1* knockdown phenotypes in *free run* and under light cycles are hypostatic to the removal of the PDF Receptor (*Pdfr*) gene. These observations suggest that neuronal activity rhythms in PDFR clock neurons and dependent output circuits may also be disrupted. Summarising the results, the Rho1 activity couples the cellular oscillators to the circadian locomotor behaviour by regulating peptidergic s-LN_v signalling. Thus, the characterization of the phenotype caused by the depletion of Rho1 has uncovered a disruption of the clock function at the circuit level without a strong impact on cellular oscillator function.

Table of Contents

List of Tables

List of Figures

List of Supplementary Tables

List of Supplementary Figures

DECLARATION OF AUTHORSHIP

I, Miguel Ramírez Moreno, declare that this thesis and the work presented in it are my own and has been generated by me as the result of my own original research.

The small GTPase Rho1 couples peptidergic control of circadian behaviour to molecular oscillator function in Drosophila melanogaster.....

I confirm that:

1. This work was done wholly or mainly while in candidature for a research degree at this University;
2. Where any part of this thesis has previously been submitted for a degree or any other qualification at this University or any other institution, this has been clearly stated;
3. Where I have consulted the published work of others, this is always clearly attributed;
4. Where I have quoted from the work of others, the source is always given. With the exception of such quotations, this thesis is entirely my own work;
5. I have acknowledged all main sources of help;
6. Where the thesis is based on work done by myself jointly with others, I have made clear exactly what was done by others and what I have contributed myself;
7. None of this work has been published before submission

Acknowledgements (English version)

Thank you, Dr Herman Wijnen, for having chosen me in April 2013 and supervised and taught me for the subsequent four years. Thank you for always having a minute to discuss the last results, and infecting me with excitement when I was taking more pessimistic approaches. Thank you for your patience with ongoing experiments/analysis, Spanglish oddities, and guidance towards the big picture of our circadian story. But also, thank you for helping me accepting the failures, your suggestions, promoting extracurricular activities and contributing to such a good group environment in the lab. Thank you, Dr Amrit Mudher for the support, encouragement and collaborations since the job interview in our joint big fly family.

Thanks to Dr Mark Willet for all the time and experience at the Imaging Centre. Thanks to Tom Broadhead, Maddie Brown, Dave Cook, Rachel Firtzearle and all the technical staff. Thank you to all those that contributed to my project with fly stocks or items, and gave me valuable advice and feedback on the meetings and seminars I have participated at, especially Angélique Lamaze. Thank you to all the former and present members of the Wijnen and Mudher labs, including the undergrads I supervised. I am grateful for the meetings, cross flips, monitor moving, lunches at Mango and solutions for the times of crisis. Thank you to Karolina and Akanksha, and good luck for Alex, Beth and Charlie on your last steps.

Thank you to all the people that have made me enjoy my time in Southampton and my breaks back home, helping me completing my PhD and growing as a person. From the postgrad students from eight cohorts I had the pleasure to meet to the postdocs, Mres and Undergraduates. And above all my board gamers, my BSPS officers, my coffee breakers, my fitness pals, my housemates, my movie and series buddies, my friends from UAM and CBM, my news commentators… Some of you fill several categories, thank you very much for your time and energies. Thank you to the people that has made me enjoy the, sometimes frustrating, detective story research is. I will always be thankful to all my mentors, in every sense of the word, from the UAM, the CBM and UoS. Thanks to the NHS professionals that fixed me when I needed.

I am pleased that my family has always, *always*, been there for me. They supported when I decided it was time to look for jobs abroad. They made me not feeling away these four years with messages, calls, seeing my second cousins grow, holiday meetings, visits, meals, cousin meetings or even weddings. What all of this means is incalculable and cannot be described. The less thing I could do is translating this section for them. And of course, thank you *Drosophila*, because we have been together for six years, and the game is still on. That must mean something.

Agradecimientos (Spanish version)

Gracias al Dr Herman Wijnen por haberme elegido en abril de 2013 y enseñado y dirigido en los siguientes cuatro años. Gracias por tener siempre un minuto para los últimos resultados, y contagiarme con tu entusiasmo cuando yo los veía con malos ojos. Gracias por tu paciencia con experimentos y análisis de estos, mis rarezas en spanglish y tu guía para completar nuestra historia circadiana. Pero también gracias por ayudarme a aceptar los fallos, tus ideas, tus sugerencias para actividades extracurriculares y tus contribuciones al buen ambiente del grupo fuera del laboratorio. Gracias también a la Dr Amrit Mudher por el apoyo, el estímulo y las colaboraciones desde la entrevista de trabajo in nuestra gran familia de moscas.

Gracias al Dr Mark Willet por todo su tiempo y experiencia en el centro de microscopía. Gracias a Tom Broadhead, Maddie Brown, Rachel Firtzearle y todo el personal técnico. Gracias a todos los que contribuyeron a mi proyecto con moscas o reactivos, y que me proporcionaron ayuda y consejo en las diferentes reuniones y seminarios en los que he participado, especialmente Angélique Lamaze. También a todos los antiguos y actuales miembros de los grupos Wijnen y Mudher, incluyendo a mis estudiantes. Gracias por las reuniones, el cuidado de mis cruces y experimentos, y las soluciones en los momentos de crisis. Gracias sobre todo a Karolina y Akanksha, y buena suerte para Alex, Beth y Charlie en lo que os queda de tesis.

Gracias a toda la gente que me ha permitido disfrutar Southampton y descansos vacacionales, porque me han ayudado a completar la tesis y crecer como persona. Desde los doctorandos de ocho promociones que he tenido el placer de conocer a los postdocs y estudiantes de grado y de máster. Y por encima de todo a mis colegas para juegos de mesa, pausas para el café, vida saludable, series o películas; a mis compañeros de piso, mis amigos de la UAM y el CBM y mis comentaristas de cómo va el mundo. Muchas gracias por vuestro tiempo y energías. Gracias a toda la gente que me ha permitido disfrutar de esta historia de detectives, a veces frustrante, que es la investigación. Siempre estaré agradecido a todos mis maestros, en todos los sentidos, de la UAM, el CBM y la UoS. Y a los profesionales del NHS que me arreglaron cuando lo necesité.

Estoy encantado de que mi familia siempre, siempre, ha estado allí por mí. Me apoyaron cuando decidí que tocaba buscar trabajo afuera. Me hicieron no sentirme lejos durante estos cuatro años con sus mensajes y llamadas, ver crecer a mis primos pequeños, reuniones en vacaciones, quedadas de primos, comidas e incluso bodas. Lo que todo esto ha significado para mi es incalculable e imposible de describir, y por eso al menos he traducido esta parte para vosotros. Y por supuesto, gracias a ti, *Drosophila*, por estos seis años juntos y lo que nos queda. Será por algo.

Definitions and Abbreviations

Notes about *Drosophila melanogaster* nomenclature on this thesis

• Gene names: italic font and lower-case letter except the first one for genes discovered with dominant mutations. Acronym names with first upper case letter only (*per*, *Pdf*, *Rho1*).

• Protein names: regular font. The first letter is upper case, except with acronyms, with all the letters on upper case which the first one on capital letters or all of them in case of acronym (Per, PDF, Rho1).

In both cases, the curated nomenclature found on Flybase is employed (like in WASp), except for DBT (whose official name is Dco).

List of terms

aMe: accesory Medulla

Antp: *Antennapedia*

AOT: anterior optic tract

AR: Arrhythmic

AVP: Arginine Vasopressin

BMAL1: Brain and Muscle ARNT-Like 1

bHLH: basic Helix-Loop-Helix

bHLH-O: basic Helix-Loop-Helix-Orange

bp: base pairs

cAMP: cyclic adenosine monophosphate

CGRP: Calcitonin Gene-Related Protein

Chic: Chickadee

Clk: Clock

CLOCK: Clock Locomotor Output Kaput

CNS: Central Nervous System

CRF: Corticotropin-Releasing Factor

Cry: Cryptochrome

CtBP: C-terminal Binding Protein

CT: Circadian Time

Cy^1: *$Curly^1$* (*$Duox^{Cy}$*)

Cwo: Clockwork Orange

Cyc: Cycle

Cul3: Cullin-3

Dia: Diaphanous

Dbt: Doubletime

DD: Dark-Dark/*free run*

DH31: Diuretic Hormone 31

DH44: Diuretic Hormone 44

DN(s): Dorsal Neuron(s)

DN1(s): Dorsal Neuron(s) type 1 (anterior and posterior subtypes included)

DN1a(s): Dorsal Neuron(s) type 1 anterior

DN_1p(s): Dorsal Neuron(s) type 1 posterior

DN_2(s): Dorsal Neuron(s) type 2

DN_3(s): Dorsal Neuron(s) type 3

Duox: Dual oxidase

EMi: Evening-Morning index

EMS: ethylmethanesulfonate

FAD: Flavin Adenin Dinucleotide

FASPS: Familial Advanced Phase Syndrome

FFI: Fatal Familial Insomnia

Flw/*flw*: Flapwing

GABA: γ-Aminobutyric acid

GAP: GTPase Activating Protein

GDP: Guanosine Diphosphate

GRASP: GPF Reconstitution Across Synaptic Partners

GS: GeneSwitch

GSK3β: Glycogen Synthase Kinase-3β

GTP: Guanosine Triphosphate

H-B e: Hofbauer-Buchner eyelets

Hid: Head involution defective

Hu: *Humeral* ($Antp^{Hu}$)

If^{1}: *Irregular facets* (Kr^{If})

ITP: Ion Transport Peptide

Jet: Jetlag (E3 ligase)

Kay-α: Kayak-α

Kr/*Kr*: Kruppel/*gene*

LD: Light-Dark conditions

LL: constant Light conditions

l-LN_v(s): large ventrolateral neuron(s)

LN_d(s): dorsolateral neuron(s)

lNPF: long Neuropeptide F

Lar: Leukocyte antigen-related

LPN(s): lateral posterior neuron(s)

Me: Medulla

MHC: Myosin Heavy Chain

MLC: Myosin Light Chain

MLCK: MLC Kinase

MLCP: MLC Phosphatase

Mmp: matrix metalloproteinase

MRLC: Myosin Regulatory Light Chain (alternate name for MLC)

NLS: Nuclear Localization Signal

Nocte: No circadian temperature entrainment

$N^{f\text{-}g}$: *facet-glossy Notch (*allele of the *Notch* gene*)*

NPF: Neuropeptide F

PAS: Per-Arnt-Sim

Pbl: Pebble

PDF/*Pdf*: Pigment Dispersing Factor/*gene*

PDFR/*Pdfr*: Pigment Dispersing Factor receptor/*gene*

PDF-Tri: PDF^{+} tritocerebral cell population

PDH(s): Pigment Dispersing Hormone(s)

PDP1: Par-domain protein1

PDZ: Postsynaptic density protein (PSD95), *Drosophila* disc large tumor suppressor (Dlg1), and Zonula occludens-1 protein (zo-1)

Per/*per*: Period/*gene*

PFD: Photon Flux Density ($\mu mol\ m^{-2}\ s^{-1}$)

PH: Pleckstrin homology

PHR: Photolyase-related (Cry protein region)

PI: Pars Intercerebralis

PI3K: Phosphoinositide 3-kinase

PKA: Protein Kinase A

POT: Posterior Optic Tract

Pyx: Pyrexia

R: Rhythmicity

RD: Red Light-Dark entrainment conditions

repo: *reversed polarity*

RR: Constant Red Light conditions

Rho1: Ras homolog 1

RhoGEF: Rho Guanine Exchange Factor

RNAi: (1) Ribonucleic Acid-mediating interference (process). (2) Interfering RNA (agent).

ROCK: Rho-associated Coiled-coil Kinase

Rok: Rho-associated, coiled-coil-containing protein kinase (adapted from the mammalian homologue ROCK)

Ser^{1}: *Serrate*

SCN: Suprachiasmatic Nuclei

Sco: *Scutoid* (*sna^{Sco}*)

s-LN_v(s): small ventrolateral neuron(s)

Slmb: Supernumerary limbs or Slimb

sna: *snail*

Sqh: Spaguetti-squash

SR: Strongly Rhythmic/Strong Rhythmicity

τ: tau, endogenous period lenght

TARGET: Temporal And Regional Gene Expression Targeting

Tb^{1}: T*ubby*^{1}

Tim/*tim*: Timeless/*gene*

TRPC: Transient Receptor Potential cation Channel

TRPA1/*TrpA1*: Transient Receptor Potential A1

Tsr: Twinstar

Tub/*Tub*: Tubulin/*gene*

UAS: Upstream Activation Sequence

Vri: Vrille

VS: Vibration-Silence environmental cycle

w: *white*

WR: Weakly Rhythmic/Weak Rhythmicity

WASP: Wiscott-Aldrich Syndrome Protein

Wnt: Wingless-related integration site

Wg: Wingless

Zip: Zipper

ZT: Zeitgeber Time

Chapter 1: Introduction

1.1 Introduction to this chapter

The purpose of this project has been to understand how the circadian adult locomotor behaviour of *Drosophila melanogaster* is affected by the disruption of the proper expression and signalling of a critical actin regulator. As a consequence, two major fields of study, circadian rhythms, and Rho1-signalling pathway, are explained in this chapter. Chapter 1.2 introduces circadian rhythms in nature, from their basic characteristics to its evolutionary importance and implications in human welfare and physiology. Chapter 1.3 further develops and reviews the current knowledge of circadian rhythms in *Drosophila melanogaster*, with comparisons with the mammalian mechanisms when homologies or differences are present. Chapter 1.4 introduces Rho1-signalling pathway, again mostly but not only focused on the fruit fly, including previous and concurrent interactions upon circadian rhythms. Finally, Chapter 1.5 described the broad aims of the PhD project.

1.2 Circadian rhythms in nature

1.2.1 Concept

The Earth has a current rotational period of approximately 24 hours with respect to the Sun. Although unappreciable by us as discreet observers, moon tidal forces are slowing down this rotation, and a day on Earth was actually almost two milliseconds longer one century ago (McCarthy and Seidelmann, 2009). Despite this gradual trend, exposure to constant and predictable environmental cycles for millions of years have caused deep effects upon the living beings, manifested as circadian rhythms. The term “circadian” was coined by Franz Halberg during the 1950s, as an effort into unifying the terminology among specialists (Halberg *et al.*, 2003). Circadian research is part of the broader field of chronobiology, which also studies ultradian rhythms (shorter than 24 hours), infradian rhythms (longer than 24 hours), or seasonal/ circannual rhythms, all of them with multiple occurrences even within the same organism (Wollnik, 1989; Lloyd and Stupfel, 1991; Sensi, Pace Palitti and Guagnano, 1993). A circadian rhythm (as defined in the next section) is the observable output of a causative mechanism, the circadian clock. For example, the circadian rhythm of the adult fly locomotor activity is controlled by the circadian clock inside the fly brain (see chapter 1.3).

1.2.2 Characteristic of circadian rhythms

The diversity of circadian rhythms in nature is astonishing, but any given one accomplishes three defining features, described since the earliest classic studies (Pittendrigh, 1954; Dunlap, 2004). These characteristics also introduce a series of concepts widely employed by circadian researchers:

- A circadian clock displays a self-sustained cycle of approximately 24 hours in the absence of external stimuli. The temporal study employs the so-called Circadian Time (CT), denoting constant conditions, or *free run*, where the clock works on its own. Usually, these are DD conditions (Dark-Dark) albeit it always refers to previous conditions (see next characteristic). On the most basic level, a circadian rhythm is generated by an oscillatory mechanism, usually a negative feedback transcription-translation loop. As will be discussed in further chapters, with a focus in the fruit fly, different clocks have arisen on different lifeforms, constituting analogous mechanisms with a similar functional significance.
- A circadian clock can be adjusted or modulated by external cues. Despite the clock's ability to run autonomously, its phase can be modified by external input. External cues capable of working on its own, its phase can me modified with external input. External cues able of controlling circadian clocks are called synchronizers or *zeitgebers*, a term coined by Aschoff (Aschoff, 1960). The process of a zeitgeber modifying a clock phase is usually named entrainment, with a clock being entrained once it is synchronous with the external stimuli. The presence of an external stimuli is indicated by the use of Zeitgeber Time or ZT. For example, for a 24-hour cycle in 12:12 Light-Dark (LD) conditions, ZT00 denotes the beginning of the day (dawn or "*lights-on*" event), and ZT12 represents the end of the light phase (or "*lights-off*" event). The extinction of the external cues changes the time to ZT to CT, so CT12 represents the *subjective* or *virtual* end of the light phase, if a 24-hour rhythm is present. A number of external factors can entrain the clock (and thus, representing ZT time), and are further explained for the case of the fruit fly in the chapter 1.3.4.
- Finally, a circadian clock has a mechanism of temperature compensation. This effect is particularly counterintuitive, with temperature acting as a zeitgeber (see Chapter 1.3.4.2). It is important to distinguish the ability of an organism to feel temperature environmental cycles (and couple its rhythms to it, by phase change) from the change in reaction speeds caused by temperature (slowing or speeding the clock). Circadian homeostasis is necessary because an increase in temperature speeds up the chemical reactions; thus, this could lead to period disturbances as a result of changes in temperature. Different types of clocks exhibit different ways of compensation, many not yet characterized (Majercak *et al.*, 1999; Gould *et al.*, 2006; Kidd, Young and Siggia, 2015; Shinohara *et al.*, 2017). Temperature compensation is found in

both poikilothermic and homeothermic organisms, albeit with reported limitations (Pittendrigh, 1954; Sweeney and Hastings, 1960; Gibbs, 1981; Barrett and Takahashi, 1995; Shinohara *et al.*, 2017).

1.2.3 Historical background of circadian research

Long before the term "circadian" appeared, many observations of behavioural differences in living beings between day and night had been found in historical records. In 400 BC, the geographer Androsthenes of Thasos, admiral of Alexander the Great, reported changes in the leaf position in different tree species (Devlin, 2002). In 1729 Jacques d'Ortous de Mairan went further by demonstrating a light-independent rhythm in the opening and folding of *Mimosa pudica* leaves. De Mairan observed that this behaviour, although in synch with the day-night cycle, was actually an endogenous process (de Mairan, 1729). This casual observation gave birth to chronobiology.

Investigation of human endogenous rhythms in the absence of external time cues is difficult to realize. With an undeniable curiosity, Dr Nathaniel Kleitman and his assistant Bruce Richardson locked themselves in 1938 at Mammoth Cave (Kentucky, USA). Their aim was showing that in absence of external cues, they would be capable to switch to a 28-hour period. After 32 days, they desisted, as their endogenous clocks persisted in a 24-hour long rhythm. Similar results had already been discovered 20 years before in goldfish by J.S. Szymanski (Singh, Sharma and Malviya, 2012). Experiments conducted by Jürgen Aschoff determined that in humans the endogenous period is slightly longer than 24 hours in absence of external stimuli. This is the reason of the "circa" component in the circadian term (Pittendrigh, 1958; Aschoff, 1960).

Also, during the 1960s, circadian rhythms were found in microscopic life with studies in *Paramecium*, *Euglena* or *Gonyaulax* (Sweeney and Hastings, 1960; Sweeney, 1963; Johnson, 2007). Several of these experiments were highly significant, showing for the first time that circadian rhythms were a cell-autonomous phenomenon and not an emergent property of complex organisms (Sweeney, 1963). Many classical studies of microscopic circadian behaviour used the fungus *Neurospora* and the green alga *Chlamydomonas* as model organisms (Matsuo and Ishiura, 2010; Baker, Loros and Dunlap, 2012). These experiments discarded the early assumption that circadian rhythms were exclusive to higher eukaryotes (Dunlap, 1999). In theory, a 24-hour cycle would not be useful for a being that divides and complete its life cycle in less time. Also, scientists considered that circadian rhythms were too evolutionally "complex" for prokaryotes. Despite these assumptions, several groups during the 1960s found daily oscillation in cyanobacteria nitrogen fixation (Golden *et al.*, 1997). Further experiments found circadian clocks in other prokaryotes and archaebacteria (Dvornyk, Vinogradova and Nevo, 2003; Whitehead *et al.*, 2009).

Once circadian rhythms were found to be a rather common phenomenon in nature, researchers focused on the quest for the responsible mechanisms. While performing brain lesions on rats, Stephan and Zucker determined that the Suprachiasmatic Nuclei (SCN, previously known to be involved in visual function) were the core of the mammalian circadian clock (Stephan and Zucker, 1972). Following the pioneering steps by Colin Pittendrigh, Seymour Benzer and Ron Konopka started a series of mutant studies with the fruit fly (*Drosophila melanogaster*), based on genetic defects in circadian behaviour (Konopka and Benzer, 1971). These experiments gave origin to the circadian research in the fruit fly, further detailed in Chapter 1.3.

1.2.4 Evolutionary implications of circadian rhythms

Our current understanding of chronobiology evidences that, although some species and phyla apparently lack them, circadian rhythms are very common throughout the diversity of living beings (Barrett and Takahashi, 1995; Moran, Softley and Warrant, 2014). This suggests a high degree of conservation and importance, along the mechanistic diversity and found advantages of clock-bearing organisms (Highkin and Hanson, 1954; Costa *et al.*, 1992; Beaver *et al.*, 2002; Dvornyk, Vinogradova and Nevo, 2003; Dodd *et al.*, 2005; Johnson, 2005). Several theories have tried to explain how circadian rhythms produce adaptive advantages in living beings (Pittendrigh, 1993). Energy conservation and protection of DNA as benefits of internal daily time keeping are usually suggested, as well as perception of seasonality (Pittendrigh, 1993; Johnson, 2005; Bradshaw and Holzapfel, 2010; Hut and Beersma, 2011; Meuti and Denlinger, 2013). Many studies both in laboratory and field have found advantaged responses for individuals carrying functional clocks in bacteria (Ouyang *et al.*, 1998), *Arabidopsis* (Green *et al.*, 2002), the fruit fly (Katewa *et al.*, 2016) or mammals (DeCoursey and Krulas, 1998; DeCoursey, Walker and Smith, 2000). On the other hand, while persistence of endogenous rhythms in controlled constant conditions may still confer advantages (Sheeba *et al.*, 1999) some species may lose them when evolving in environments devoid of external cues (Moran, Softley and Warrant, 2014).

As researchers discovered with experiments in microorganisms, any cell carrying the components of a given molecular clock can act as an autonomous oscillator (Michel *et al.*, 1993; Nagoshi *et al.*, 2004). This has allowed *Drosophila* researchers for example employ modified S2 cells (a clockless cell line) as a workbench to study the working of the oscillator (Tataroglu and Emery, 2014). For multicellular organisms, clock-bearing cells are usually restricted to discreet clusters which are coordinated to establish a common response. Traditionally, researchers have distinguished between a *main* core clock (usually found in the brain), and a series of slave or peripheral clocks which control secondary or local roles. Although the main clock works as an independent element and is subjected to most of circadian studies (including this thesis), the question whether the so-

called *peripheral* clocks are slaved to the former is at least vague and context-dependent (Mohawk, Green and Takahashi, 2012; Ito and Tomioka, 2016).

1.2.5 Circadian rhythms in mammals

In the case of mammals, the main clock is constituted by a selected population of approximately 20.000 neurons located in the SCN. (Honma *et al.*, 2012; Evans, 2016). This discrete brain region, located above the optic chiasm, was known for long before the discovery of its role in daily timekeeping (Gray, 1918). Despite their connections, SCN neurons remain capable of functioning as independent oscillators, as shown when the SCN is dissociated and cultured *ex vivo* (Welsh *et al.*, 1995). In a living mammal, SCN neurons need to keep their clocks coupled to sustain strong output rhythms, and this is made by connexins at the gap junctions (Aton and Herzog, 2005; Long *et al.*, 2005; Scemes, Spray and Meda, 2009). The SCN communicates with the rest of the brain, and clocks throughout the body via many signalling pathways (An *et al.*, 2013; Belle *et al.*, 2014). Tissue and organ peripheral clocks (See Chapter 1.3.8 for information about them in *Drosophila*) account for some degree of circadian oscillation in ~10% of their total mRNA (Mohawk, Green and Takahashi, 2012).

Mammalian clock neurons have a molecular oscillator that exhibits remarkable homology to those found in insects. Relevant similarities, as well as differences, will be detailed across chapter 1.3.

1.2.6 Circadian rhythms, human physiology and wellbeing

Circadian rhythms affect many processes of human life, both in health and disease. A series of factors from genetics to age determine the strength of a person's clock. Humans are mostly diurnal animals, but the population range varies from "morning people" or larks to "Evening people" or owls (Alward, 1988; Preckel *et al.*, 2013). As with every other physiological process, circadian rhythms may be disturbed by a number of intrinsic or extrinsic factors, many of them related to developed societies (Wittmann *et al.*, 2006; Dominoni *et al.*, 2013). Short wavelength light exposure during night affects human circadian rhythms (Zaidi *et al.*, 2007; Tosini, Ferguson and Tsubota, 2016). A simple way of assessing this effect is with melatonin levels, a hormone which normally exhibits rhythms in accumulation in the bloodstream and saliva (Brainard *et al.*, 2001).

Arguably, the most well-known circadian disturbance is the phenomenon of circadian desynchronisation or *Jet lag*. Effects greatly vary among individuals but are due to conflict between environmental cues and our body clocks. However, many other apparently less severe circadian disruptors can be present on a daily basis. They include shift work, social jet lag,

abnormal exposure to artificial light cycles, or even daylight-saving times (Costa, 2003; Kantermann *et al.*, 2007; Chang *et al.*, 2015). Shift workers and others suffering circadian desynchronisation constitute a risk group for a number of maladies, including metabolic and heart diseases (especially diabetes), psychiatric disorders and even cancer (Maury, Ramsey and Bass, 2010; Zimberg *et al.*, 2012; Kelleher, Rao and Maguire, 2014; Bechtel, 2015; West and Bechtold, 2015; Sridhar and Sanjana, 2016). Conversely, clinical researchers are increasingly leveraging circadian rhythms as a therapeutic tool, e.g., in drug delivery (Levi and Schibler, 2007; Levi *et al.*, 2010; Ortiz-Tudela *et al.*, 2014).

Sleep is a homeostatic multifactorial process modulated by the circadian clock (Campbell and Tobler, 1984; Fuller, Gooley and Saper, 2006). Despite the importance of sleep and the noticeable symptomatic effects, not all sleep disturbances are related to circadian rhythms. For example, the Fatal Familiar Insomnia (FFI) is a rare disease not caused by circadian defects, although the rhythms of the patients are affected by the disease (Portaluppi *et al.*, 1994). Circadian and sleep disorders therefore usually present co-morbidity, although the cause/effect relationship can greatly vary. This is the case for circadian symptoms such as *sundowning* or evening confusion, which is common among Alzheimer's Disease patients and others forms of dementia (Bedrosian and Nelson, 2013). On the other hand, sleep homeostasis, as a circadian-regulated process, could be involved in the progression of these diseases (Xie *et al.*, 2013; Lim, Gerstner and Holtzman, 2014; Musiek, Xiong and Holtzman, 2015; Musiek and Holtzman, 2016).

There exist some human diseases directly caused by mutations in clock genes (Iwase *et al.*, 2002; Jones *et al.*, 2013). Familial Advanced Phase Syndrome (FASPS) shortens the endogenous period length by different causes that lead to a fastened molecular oscillator (Toh *et al.*, 2001). The accelerated clock affects activity/sleep rhythms but also body temperature and melanotin rhythms (Jones *et al.*, 1999; Xu *et al.*, 2005).

1.3 Circadian rhythms in *Drosophila melanogaster*

1.3.1 *Drosophila melanogaster* as a model organism

Drosophila melanogaster (domain *Eukarya*, kingdom *Animalia*, phylum *Arthropoda*, class *Insecta*, order *Diptera*, family *Drosophilidae*)(Meigen, 1830; ITIS, 1996), colloquially known as the fruit fly, is a widely used model organism that has provided researchers in experimental biology with many tools an data. Its usage as model organism was firstly suggested by Charles W. Woodworth (University of Harvard) and received a huge impulse with the works of Thomas Hunt Morgan

(1933 Nobel Prize in Physiology or Medicine)(Markow, 2015). Its success is due to several key advantages such as its short life cycle (which takes around ten days at 25° C), small size, easy manipulation and a well-known genome (Ashburner, Golic and Hawley, 2005). Classical studies have employed the isolation of artificially generated mutations for elucidating their genetic role via phenotypic characterization. Because of this, many *Drosophila* genes are named because of the mutant phenotype (like the gene *timeless*). After decades of use, researchers now can easily control spatial and temporal expression of genes and other elements of interest with new or refined techniques and tools (see Chapter 2).

Flies are holometabolous insects (they undergo complete metamorphosis) with several life stages (Ashburner, Golic and Hawley, 2005). Embryo-containing eggs are layed by females after being fertilized by male sperm. After approximately 24 hours the embryo hatches and reaches the larva stage, composed of three different instars and devoted to feeding (Lawrence, 1992). L1, L2 and L3 instars are separated by cuticle moulting and characterized by a progressive size increase. Late L3 instar larvae (approximately 7 days old) start a wandering phase to look for a suitable place to attach themselves to start the pupariation stage. Metamorphosis then occurs, where the imaginal discs developed during the larval stages assemble around the guts and nervous system to form the pharate (Bainbridge and Bownes, 1981). The pharate is the contained imago or adult organism, which emerges approximately ten days since the cycle started at room temperature (Ashburner, Golic and Hawley, 2005).

The majority of this chapter, as well as the results of this project, involve the main clock circuits located in the fly brain, whose most studied output is the adult locomotor behaviour. There are, however, several secondary oscillators, the peripheral clocks, that control local physiological aspects. They are briefly introduced in Chapter 1.3.8.

1.3.2 Molecular oscillator of *Drosophila melanogaster*

The molecular clock of *Drosophila melanogaster* shares many homologies with its mammalian counterpart. Some of the participant genes have solely circadian roles, while certain essential cellular genes have also a role in regulating the molecular oscillator. Except when specified, this chapter employs the nomenclatures guidelines of the FlyBase community (Attrill *et al.*, 2016). The *Drosophila* molecular clock circuit is represented in Figure 1.1.

1.3.2.1 Primary negative feedback loop of the *Drosophila* circadian clock

1.3.2.1.1 Period and Timeless

The unravelling of the genes and proteins involved in circadian rhythms began in the 1970s with the work of Ron Konopka, then a graduate student at the laboratory of Seymour Benzer. He generated hundreds of X-chromosome mutant lines using ethyl methanesulfonate (EMS, an alkylating agent). Konopka then subjected these lines to a genetic screen consisting of the characterization of eclosion rhythms. Wild-type flies tend to hatch within the first (humid) hours after dawn (hence the genus name *Drosophila*, *lover of the dew*), so disruption of these rhythms in *free run* would point to an affected circadian gene. Among the screened lines, they found three mutants with abnormalities in circadian eclosion rhythms. One showed a longer period (~29 hours), another a shorter period (~19 hours), and the last one showed no rhythm at all. Further analysis determined that the three different phenotypes were caused by different mutations affecting the same gene, that was then named *period* (*per*) (Konopka and Benzer, 1971). Subsequently, these mutant alleles were named per^{L} (*long*), per^{S} (*short*) and per^{01} (null) respectively.

Period protein has 1224 aminoacids and its sequence contains two Per-Arnt-Sim (PAS) repetition domains (PAS A and PAS B) and two helixes (αE and αF) (King *et al.*, 2011). PAS domains are common in basic Helix-Loop-Helix (bHLH)-like transcription factors and have a role in dimerization. The protein has additional domains that allow its interaction with other components of the clock (as indicated in the following sections) (Kim *et al.*, 2007). Per does not contain, however, DNA binding domains, making a direct interaction with DNA not possible (Huang, Edery and Rosbash, 1993). Therefore, although Per is able to form homodimers, it requires to establish heterodimers with other proteins in order to affect the daily time keeping (Zeng *et al.*, 1996; Allada *et al.*, 1998; Landskron *et al.*, 2009; King *et al.*, 2011). Notably, the Per^{L} mutant protein has a defect in the PAS A domain because of a point mutation (King *et al.*, 2011).

Analysis of *per* expression showed that its mRNA levels cycles through the day, increasing during light hours, peaking in the evening and then decreasing during night time (Hardin, Hall and Rosbash, 1990). A similar but delayed cycle was observed for Per protein levels, which reach their highest level before dawn (ZT00) and the minimum before dusk (ZT12) (Zerr *et al.*, 1990; Curtin, Huang and Rosbash, 1995; Shafer, Rosbash and Truman, 2002). This time cue is maintained in DD conditions, where Per maintains expression rhythms (Zerr *et al.*, 1990; Shafer, Rosbash and Truman, 2002). Taken together, these data seemed to suggest Per was involved in a feedback loop for sensing time, and that it would cooperate with more proteins, probably forming heterodimers. There are three Per proteins in mammals, Per1, 2 and 3, which share several

functional similarities (Shearman *et al.*, 1997; Sun *et al.*, 1997; Archer *et al.*, 2003). It has been proposed than Per1 and 2 are the closest equivalents to *Drosophila* Per, with Per3 acting as a supporting element (Bae *et al.*, 2001; Archer *et al.*, 2003). The effects of mutations in Per2 related to FASPS (See Chapter 1.2.6) share similarities with the *Drosophila per*^{s} mutant (Toh *et al.*, 2001; Kivimäe, Saez and Young, 2008).

More than twenty years after Per's discovery, Michael Young and colleagues characterized *timeless* (*tim*), the gene that codifies its partner (Sehgal *et al.*, 1994; Myers *et al.*, 1995). Timeless protein has 1389 aminoacids and contains a Nuclear Localisation Signal (NLS), but again not a DNA binding domain (Myers *et al.*, 1995). *per* and *tim* transcript and protein levels oscillated synchronously, suggesting that they may share a joint mechanism of expression control (Sehgal *et al.*, 1994). The rhythms in subcellular localization for both proteins also show many similarities (Shafer, Rosbash and Truman, 2002). However, after dawn, while Per levels slowly decrease, Tim levels abruptly fall, suggesting a different and faster method of degradation (Hunter-Ensor, Ousley and Sehgal, 1996). This led scientists to believe that light could induce Tim protein degradation and that this degradation could function in light-mediated synchronization (See Chapter 1.3.4.1)(Zeng *et al.*, 1996). It was also discovered that Per and Tim indeed associate as heterodimers, and this happens when Tim binds to the PAS and α-helix repeats of Per (Saez and Young, 1996; King *et al.*, 2011). In fact, the formation of the heterodimeric complex is required for a critical process of the molecular oscillator to take place, the nuclear translocation of Per which is at its maximum when the protein levels are the highest (Saez and Young, 1996; Shafer, Rosbash and Truman, 2002). Although Per sequence contains information for nuclear translocation, the absence of the 14-aminoacid-long NLS of Tim increases the period length by delaying Tim nuclear entry (Nawathean, Stoleru and Rosbash, 2007; Saez *et al.*, 2011). Without a DNA-binding region of their own, it was clear that Per and Tim required other interactors to establishing a transcriptional feedback loop.

1.3.2.1.2 Clk and Cyc

The promoter region of *per* gene contains a 69 bp sequence that is sufficient for daily cycling of a reporter gene, as long as Per-Tim complex is present. Inside this sequence there is a smaller element known as an E-Box, CACGTG. This sequence is also found in the *tim* promoter region, and it is required for high-level transcription, but not for the daily cycle (Hao, Allen and Hardin, 1997; Darlington *et al.*, 1998; Hao *et al.*, 1999). The consensus E-Box sequence is a binding site for basic Helix-Loop-Helix (bHLH) transcription factors, many of whom bind to DNA as heterodimers (Murre *et al.*, 1989).

One of these transcription factors is encoded by *Clock* (*Clk*), which was discovered in 1998 by Michael Rosbash group, and originally named *Jerk* (*Jrk*)(Allada *et al.*, 1998). The gene was renamed once it was identified as homologue of the murine CLOCK (Clock Locomotor Output Kaput)(Vitaterna *et al.*, 1994; King *et al.*, 1997). Clk is a bHLH-PAS transcription factor (Gekakis *et al.*, 1998). *Clk* mRNA has complex regulation, both pre- and post-transcriptional, that results in a protein expression profile slightly in antiphase to Per (Glossop, Lyons and Hardin, 1999; Kim *et al.*, 2002a). Non-functional mutants of Clk show a reduced expression of *per* and *tim*, but also an increase in *Clk* mRNA levels (Allada *et al.*, 1998; Glossop, Lyons and Hardin, 1999). Microarrays showed that virtually all the genes with circadian oscillation were directly or indirectly dependent on Clk levels (McDonald and Rosbash, 2001). To become a functional transcription factor, Clk forms a heterodimer with the protein Cycle (Cyc). Cyc is a homologue of the mammalian BMAL1 (Brain and Muscle ARNT-Like 1), and also a bHLH-PAS transcription factor (Darlington *et al.*, 1998; Rutila *et al.*, 1998). Experiments in mice showed that mutations affecting CLOCK-BMAL1 function exhibit the same behavioural phenotype as their fly counterparts (Vitaterna *et al.*, 1994; Gekakis *et al.*, 1998; Chiou *et al.*, 2016).

The interaction between Per-Tim and Clk-Cyc heterodimers leads to a reduction of the DNA-binding activity of the latter (Lee, Bae and Edery, 1999). This interaction is found only during the dark phase of the cycle when Tim is present and thus heterodimerizes with Per(Lee, Bae and Edery, 1998). The event causes a reduction in *per* and *tim* expression during night. Therefore, the repressor activity of Tim- Per leads to the repression of *per* and *tim* transcripts, establishing the hypothesised negative feedback loop (Darlington *et al.*, 1998). Based on experimental conditions, Per is considered to be the actual repressor component of the heterodimer (Rothenfluh, Young and Saez, 2000). Per also intervenes in the control of Clk phosphorylation and destabilization via recruitment of the kinase Doubletime (Dbt, see Chapter 1.3.2.3) (Yu *et al.*, 2006). Recently, it has been proposed that C-terminal Binding Protein (CtBP) can act as a co-factor for Clk-Cyc activity. Its overexpression leads to period lengthening or arrhythmic behaviour (Itoh, Matsumoto and Tanimura, 2013).

1.3.2.2 Regulation of *Clk* expression and Secondary feedback loop

Besides *per* and *tim*, more genes contain E-Boxes in their regulatory regions, making them potential targets for the Clk-Cyc heterodimer. *Clk* expression is *anti-phase* to *per*/*tim* and exhibits a complex regulation with many intervening factors. The Per-Tim complex itself exerts some indirect influence over *Clk* expression, among others(Bae *et al.*, 1998; Darlington *et al.*, 1998).

Two Clk-controlled genes are *vrille* (*vri*) and *Par-domain protein1* (*Pdp1*, specifically the isoform PDP1 epsilon, or PDP1ϵ). Both are expressed cyclically and are required for circadian locomotor

activity (Blau and Young, 1999; McDonald and Rosbash, 2001; Cyran *et al.*, 2003). Moreover, the two proteins can bind to the V/P box of *Clk* promoter as members of the Leucine Zipper DNA binding subfamily. They have however antagonistic roles when binding to the sequence, with PDP1 activating *Clk* transcription and Vri acting as a repressor (Reddy *et al.*, 2000; Cyran *et al.*, 2003; Zheng *et al.*, 2009b). This is usually referred to as a secondary feedback loop in the oscillator. Additionally, both PDP1ϵ and Vri exert roles in the *Drosophila* circadian rhythms without directly affecting the molecular clock (See chapters 1.3.5.1 and 1.3.6)(Benito, Zheng and Hardin, 2007; Gunawardhana and Hardin, 2017). Another gene controlled by Clk activity is *clockwork orange* (*cwo*). Cwo belongs to the family of transcriptional repressors bHLH-O, named because of the conserved Orange domain (Davis and Turner, 2001; Kadener *et al.*, 2007). The protein regulates its own transcription by binding to the E-boxes, competitively reducing Clk-Cyc activity (Kadener *et al.*, 2007; Matsumoto *et al.*, 2007). Although not directly clock-controlled, Kayak-α (Kay-α) carries a dual function in the oscillator by repressing Clk function but also protecting it from the activity of Vri (Ling, Dubruille and Emery, 2012).

Apart from these known mechanisms, clock genes are equally subjected to several regulatory ways affecting their expression, including microRNAs (Kadener *et al.*, 2009; Staiger and Koster, 2011; Mehta and Cheng, 2013; Chen and Rosbash, 2016).

1.3.2.3 Posttranslational control of the clock components

The main feedback loop involving Per-tim and Clk-Cyc complexes has numerous regulatory mechanisms that lead to the endogenous 24-h period. Many of the characterised ones are posttranslational modifications, frequently phosphorylation events, mostly but not exclusively for Per protein. As in many other cell processes, these are usually carried by kinases. Some of these phosphorylation events can affect Per stability or the nuclear import, having a subsequent effect on the period length and rhythmicity. Many phosphorylation events allow or inhibit later ones, establishing a complex chain of sequential steps based on the covering/uncovering of phosphorylation site or changing the affinity of kinases for the subtract (Garbe *et al.*, 2013). Several of these kinases were previously known because of their additional critical roles in cellular life (Jursnich *et al.*, 1990; Pinna and Meggio, 1997; Kalderon, 2002).

The kinase Doubletime (Dbt, also known as Dco) is arguably the most important and best characterized kinase acting upon Period (Kloss *et al.*, 1998; Price *et al.*, 1998). Dbt is the fly homologue of the mammalian Casein kinase 1ε (CK1ε), which also impacts circadian clock function (Kloss *et al.*, 1998; Lowrey *et al.*, 2000; Toh *et al.*, 2001). Dbt binds to Per via the Period

Doubletime Binding domain (PDBD) (Kim *et al.*, 2007). The Dbt-Per-Tim complex allows Dbt to enter the nucleus and phosphorylate Per on several sites, preventing its activity and tagging it for degradation (Kloss *et al.*, 2001; Chiu *et al.*, 2008; Kivimae, Saez and Young, 2008). The latter process is mediated by Supernumerary limbs or Slimb (Slmb), an E3 Ubiquitin ligase (Grima *et al.*, 2002). Slmb specifically requires Dbt-mediated phosphorylation to recognise Per (Grima *et al.*, 2002; Ko, Jiang and Edery, 2002; Chiu *et al.*, 2008). Dbt activity is promoted by early phosphorylation events on Per by the CMGC kinase Nemo (Chiu, Ko and Edery, 2011). Despite its role as repressor of Per activity, Dbt exerts a more complex regulation of the protein. In the cytoplasm, Dbt inhibits the nuclear translocation of monomeric Per when Tim is not present (Cyran *et al.*, 2005). The removal of 27 specific amino acids of Per is sufficient to dramatically reduce Dbt-mediated phosphorylation. This sequence, also conserved in the mammalian Per proteins, promotes nuclear import and subsequent repressor activity (Nawathean, Stoleru and Rosbash, 2007). The removal of the PDBD domain also increases Per stability by reducing phosphorylation events, but the molecular clock is disrupted and leads to behavioural arrhythmia (Kim *et al.*, 2007).

Tim acts a protector of Per against phosphorylation events that compromise Per stability leading to Slmb activity. The slmb mutant background shows aberrant Tim rhythms, maybe as a consequence of altered Per cycles (Grima *et al.*, 2002). Tim is, however, targeted by a different Ubiquitination complex including Cullin-3 (Cul3) in a light-independent manner (Grima *et al.*, 2012). When Tim is removed by this mechanism or by exposure to blue light (see Chapter 1.3.4.1), Per starts to be slowly degraded (Hunter-Ensor, Ousley and Sehgal, 1996; Kloss *et al.*, 2001).

Many phosphorylation events in the Per-Tim heterodimer are related to its nuclear import. Shaggy (Sgg) is the fly orthologue of Glycogen Synthase Kinase-3β (GSK3β) and its overexpression was found to correlate with a shorter period (Martinek *et al.*, 2001). The kinase phosphorylates Tim and promotes the faster nuclear entry of Per-Tim heterodimer (Martinek *et al.*, 2001; Fang, Sathyanarayanan and Sehgal, 2007). Sgg also phosphorylates Per, at least on the S657 residue. This phosphorylation follows a similar event of the S661 residue, by a yet-unidentified Proline-directed kinase. Together, they promote further phosphorylation events leading to Per nuclear translocation (Ko *et al.*, 2010). Casein Kinase 2 (CK2) is a Serine/Threonine kinase with a tetrameric structure (two α catalytic and 2 β regulatory subunits) (Dahmus *et al.*, 1984; Allende and Allende, 1995). CK2 phosphorylates Per and promotes nuclear entry (Lin *et al.*, 2002; Lin, Schroeder and Allada, 2005). The kinase also phosphorylates Tim, again promoting nuclear translocation (Meissner *et al.*, 2008). Another kinase, p90 Ribosomal Kinase (S6KII) interacts with CK2 (via β regulatory subunit) and phenotypic comparisons suggests it acts as inhibitor (Akten *et al.*, 2009).

Although not as extensively studied, Clk phosphorylation also plays a role in the molecular oscillator (Mahesh *et al.*, 2014). Low phosphorylation levels precede nuclear translocation, whereas hyperphosphorylated Clk is set to degradation (Hung *et al.*, 2009). Dbt is also involved in Clk regulation and destabilises the transcription factor (Kim and Edery, 2006; Yu *et al.*, 2006).

Phosphorylation events are usually balanced by dephosphorylating reactions. Phosphatases constitute a counter-mechanism to kinase activity, and also act on the molecular clock by dephosphorylating Per or Tim. Protein Phosphatase 2A (PP2A) stabilizes Per, shortening the period length and strengthening the rhythm opposing to Dbt activity (Sathyanarayanan *et al.*, 2004; Fang, Sathyanarayanan and Sehgal, 2007). This kinase/phosphatase equilibrium is also seen for Clk phosphorylation levels (Kim and Edery, 2006). Protein Phosphatase 1 (PP1) also promotes nuclear translocation, but by dephosphorylating Tim, with a non-antagonistic interaction with Sgg, as an example of the complexity of the phosphorylation code of these proteins (Fang, Sathyanarayanan and Sehgal, 2007).

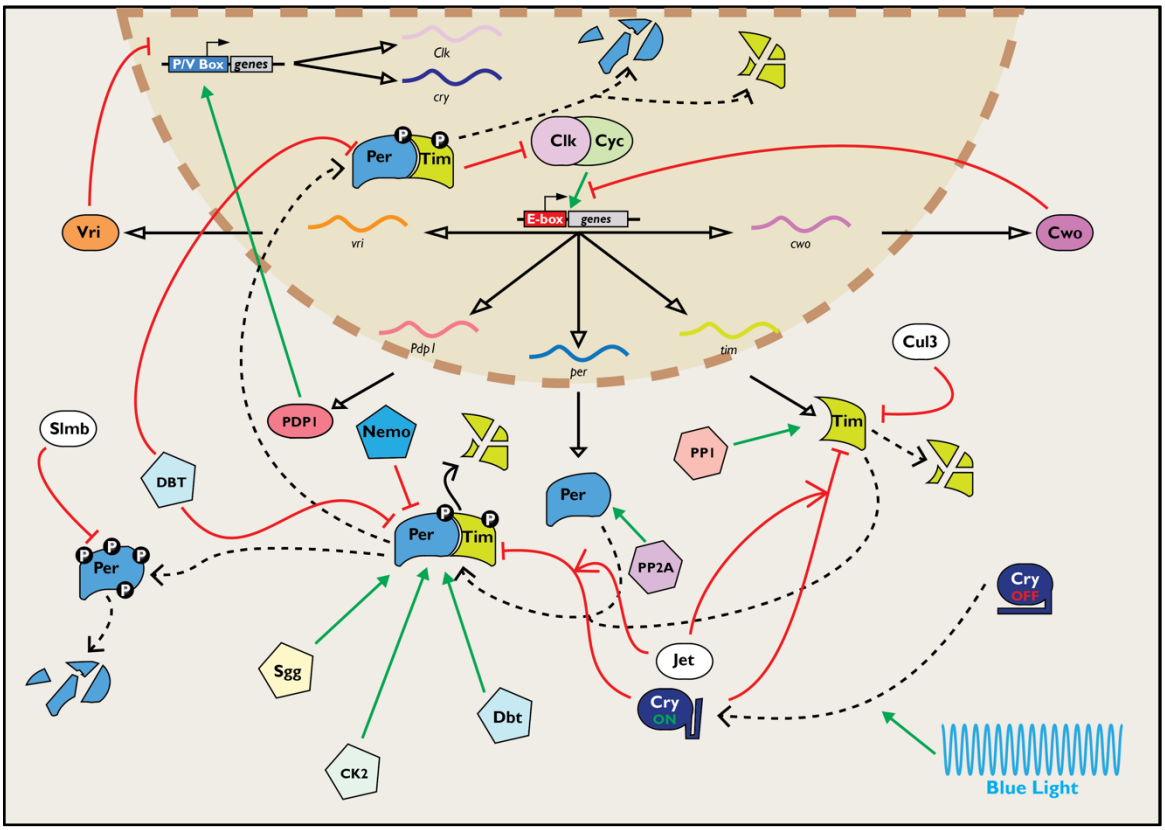

Figure 1.1. ***Drosophila melanogaster*** **molecular clock**. Indicated elements are, in alphabetical order: Casein Kinase 2 (Ck2); Clock (Clk); Cryptochrome (Cry); Cullin-3 (Cul3); Cycle (Cyc); Clockwork orange (Cwo); Doubletime (Dbt); Jetlag (Jet); Nemo Kinase (Nemo); PAR Domain Protein 1 (PDP1); Period (Per); Protein Phosphatase 1 (PP1); Protein Phosphatase 2A

(PP2A); Shaggy (Sgg); Supernumerary limb or Slimb (Slmb); Timeless (Tim) and Vrille (Vri). Black lines indicate transcription/translation. Green lines indicate promotion of expression or further steps of the molecular clock. Red lines indicate inhibition/repression. Dashed lines indicate transport or conformational change.

1.3.3 Anatomical characteristics of the neuronal circuitry

Compared to the ~50.000 cells of the SCN, only approximately 150 neurons (75 cells per cerebral hemisphere) comprise the *Drosophila melanogaster* core clock circuitry (Helfrich-Forster, 2004; Förster, 2010).

All these clock cells display rhythmic cycles of Per, as their subsequent characterizations are intrinsically linked to studying the expression of this protein (Ewer *et al.*, 1992; Helfrich-Forster, 1995; Kaneko and Hall, 2000). Because of their anatomical layout, these clusters were initially identified and named by their location inside the brain (Helfrich-Förster, 1996). However, a more sophisticated organization is suggested by molecular and functional profiles as explained in this chapter. A functional clock inside the circuitry is sufficient for driving the circadian locomotor behaviour in a *free run* state throughout the output pathways (see Chapters 1.3.6 and 1.3.7) (Ewer *et al.*, 1992; Frisch *et al.*, 1994; Grima *et al.*, 2004). The contribution by the different subsets is, however, unequal and dependent of the environmental conditions, as detailed in Chapters 1.3.4-1.3.7. Besides the clock neurons, cycling Per and Tim proteins are present at some brain glial populations (Zerr *et al.*, 1990; Jackson, 2011).

A basic anatomical classification is based on the coronal (anterior-posterior) and horizontal (ventral-dorsal) planes, with hemispheres separated by the sagittal plane. Clock cell clusters are divided into Lateral and Dorsal neurons (LNs and DNs, respectively). LNs can be divided into ventrolateral neurons (LN_vs, including two subclasses, small and large), dorsolateral neurons (LN_ds) and Lateral Posterior Neurons (LPNs). DNs are divided in three main classes: DN_1s (two subclasses), DN_2s and DN_3s (Figure 1.2).

1.3.3.1 Ventrolateral Neurons (LN_vs)

There are approximately 10 ventrolateral neurons per brain hemisphere. Defined by their smaller soma size, five are named small ventrolateral neurons (s-LN_vs), in contrast to the 4-6 large ventrolateral neurons (l-LN_vs) (Helfrich-Forster, 1995; Kaneko, 1998; Kaneko and Hall, 2000). Both subclasses have their cell bodies on the edge of the optic lobes and central brain (Figure 1.2), but

their dendritic and axonal ramifications are easily distinguished (Helfrich-Forster and Homberg, 1993; Park and Griffith, 2006).

Four of the s-LN_vs have ipsilateral projections. Short neurites are sent into the nearby accessory medulla (aMe), a neuropil known to function in circadian peacemaker in arthropods (Helfrich-Forster, Stengl and Homberg, 1998; Loesel and Homberg, 2001; Reischig and Stengl, 2003; Helfrich-Forster *et al.*, 2007a). They also display longer axonal projections that form a bundle and reach the dorsal part of the brain. There, the axons display a characteristic dorsal horn or turn, and arborize constituting the s-LN_v dorsal projections, dorsal termini and others (Helfrich-Forster *et al.*, 2007a). The arborisation pattern of these axons is subjected to circadian regulation, as the branching is more expansive during the first hours of the day than early the evening. This daily remodeling is normally clock-controlled as requires both *per* and *tim* expression (Fernandez, Berni and Ceriani, 2008). GRASP data suggest the s-LN_v dorsal projections contact with the DN_{1p} neurons (See chapter 1.3.3.4) and the LN_ds (See chapter 1.3.3.2) (Gorostiza *et al.*, 2014). The s-LN_vs are also connected to brain areas such as the Pars Intercerebralis (PI) and the mushroom bodies (Helfrich-Forster, 1997; Helfrich-Forster, Wulf and de Belle, 2002; Allada and Chung, 2010).

The l-LN_vs display both ipsi- and contralateral projections reaching the accessory medulla (aMe), as well as an expanded complex structure in the optic medulla. The contralateral arborisation consists of three to five nerve fibers that reach the other side of the brain through the Posterior Optic Tract (POT)(Park and Griffith, 2006; Helfrich-Forster *et al.*, 2007a). Researchers discovered the contralateral ramifications of l-LN_vs by using *disconnected* (*disco*) mosaic mutants, which can eliminate the lateral neurons of a single hemisphere (Helfrich-Forster *et al.*, 2007a).

Finally, the remaining fifth s-LN_v is separated by both genetic profile and function from the other ventrolateral neurons (See chapter 1.3.5 and 1.3.7). The cell body of this neuron is often found near those of the the l-LN_vs, and its dorsal termini reach the opposite hemisphere (Schubert, Helfrich-Forster and Rieger, 2016).

1.3.3.2 Lateral neurons (LN_ds)

The dorsolateral neurons (LN_ds) constitute a population of 6 neurons per hemisphere, with their cell bodies arranged in a characteristic balloon-like array near the s-LN_v dorsal axons (but not in the same anteroposterior plane)(Helfrich-Forster, 2005a; Helfrich-Forster *et al.*, 2007a). They project into the dorsal part of the brain, where their neurites contribute to an intricate bundle, making their clear distinction difficult (Kaneko and Hall, 2000). Some projections loop around the anterior optic tract (AOT) and reach the other side of the brain through the Dorsal-Fusion-Commissure (DFC). The aMe receives projections from the LN_ds in a contralateral and ipsilateral

way, depending on the specific single studied LN_d neuron(Helfrich-Forster *et al.*, 2007a; Schubert, Helfrich-Forster and Rieger, 2016). The LN_ds exemplify the limits of the anatomical classification because of their diversity regarding expression profiles of different clock-related signals and molecules (See chapter 1.3.5.2)(Johard *et al.*, 2009).

1.3.3.3 Lateral Posterior Neurons (LPNs)

The Lateral Posterior Neurons (LPNs) are currently the least characterised of the clock neurons. They number 3-4 per hemisphere and, previously, were considered Tim-expressing non-clock neurons (Kaneko and Hall, 2000; Shafer *et al.*, 2006). As their name suggests, LPNs are found in the posterior part of the brain, consistently near the midway of the s-LN_v dorsal projections (Shafer *et al.*, 2006). Little is known about these cells, apart from being neurons displaying rhythmic diurnal Per and Tim expression and their receptiveness to temperature cues (see Chapter 1.3.4.2) (Yoshii *et al.*, 2005; Shafer *et al.*, 2006; Busza, Murad and Emery, 2007).

1.3.3.4 Dorsal neurons (DNs)

Anatomical and genetic differences divide DNs into different classes:

- Class 1 (DN_1s, 14- 16 per hemisphere). This group is further divided into *anterior* and *posterior* subclasses (DN_{1a} and DN_{1p} respectively) based on their distribution in the coronal plane (Shafer *et al.*, 2006). Most of them are DN_{1p} cells, which express the transcription factor Glass and contact with the s-LN_v dorsal termini (Shafer *et al.*, 2006; Seluzicki *et al.*, 2014). The two DN_{1a}s are usually found in a more dorsal position, projecting to the aMe and expressing the neuropeptide IPNamide (IPNa)(see Chapter 1.3.5.2)(Shafer *et al.*, 2006). Most of the DN_1 projections cross the midline of the brain throughout the DFC without reaching the aMe (Helfrich-Forster *et al.*, 2007a).
- Class 2 (DN_2s, two neurons per hemisphere). The DN_2s are found within the proximity of the s-LN_v dorsal projections without apparent afferences (Shafer *et al.*, 2006). Besides expressing Per and Tim, there is little known information about their genetic profiles albeit their role is more characterized than for the LPNs (see Chapter 1.3.6). Projections of these neurons are also detected at the DFC (Helfrich-Forster *et al.*, 2007a).
- Class 3 (DN_3s, approximately 40 per hemisphere). The most numerous group shows a wide range of cell body sizes, with 3-5 of them having bigger somas than the others. As with the DN_2s, they have been poorly studied (Shafer *et al.*, 2006). DN_3s projections are directed to the midline of the brain but do not reach the other hemisphere. Two of these neurons project towards the aMe along the LN_d processes (Helfrich-Forster *et al.*, 2007a).

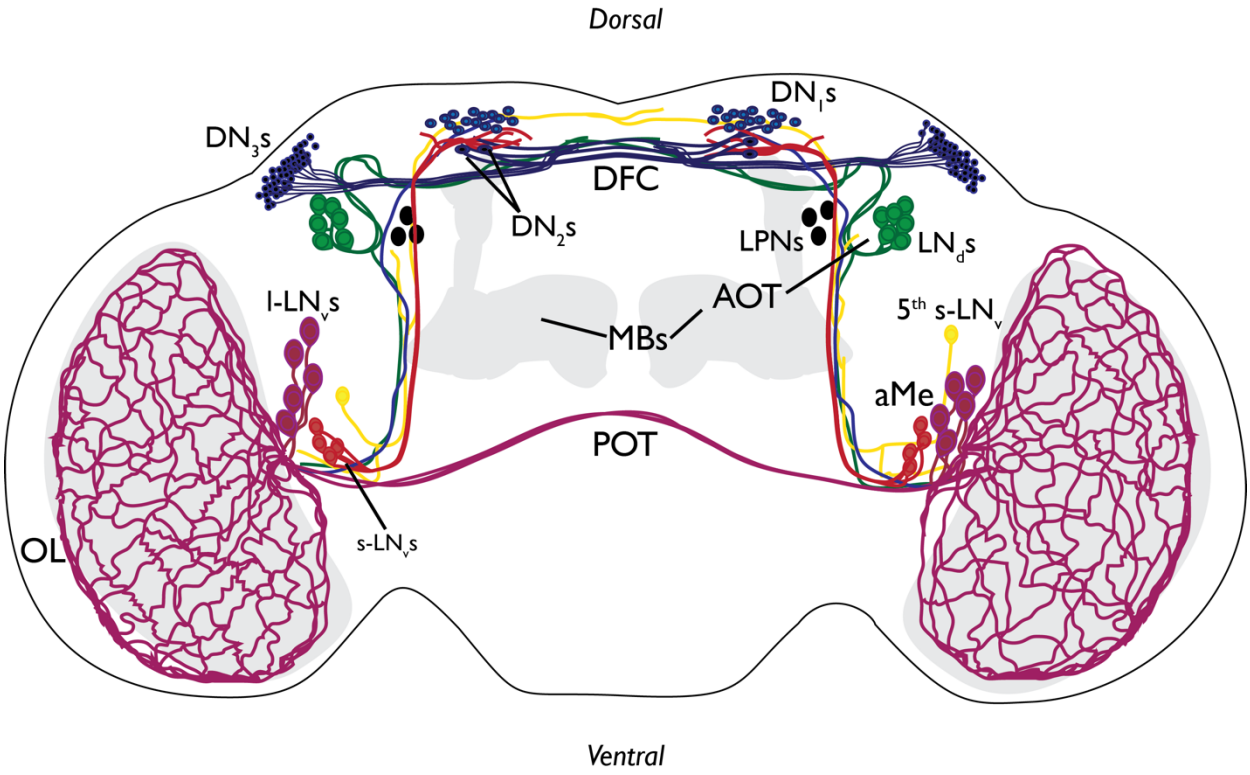

Figure 1.2 The circuitry of the core *Drosophila melanogaster* clock. Horizontal (dorsoventral) plane of the adult brain. Clock neurons are divided by clusters and colour code: dorsal neurons class 1 (DN_1s); dorsal neurons class 2 (DN_2s), dorsal neurons class 3 (DN_3s), dorsolateral neurons (LN_ds), large ventrolateral neuros (l-LN_vs), lateral posterior neurons (LPNs, in black without projections) and small ventrolateral neurons (s-LN_vs). The following anatomical regions of the brain are also shown: accessory Medulla (aMe), Anterior Optic Tract (AOT), Dorsal-Fusion-Commissure (DFC), Mushroom Bodies (MBs), Optic Lobes (OL) and Posterior Optic Tract (POT). Anatomical information is gathered from different sources (Helfrich-Forster, 2005a; Helfrich-Forster *et al.*, 2007a; Sheeba, 2008; Schubert, Helfrich-Forster and Rieger, 2016).

1.3.4 Zeitgeber input and synchronization

As stated in Chapter 1.2.2, a circadian clock needs to be both self-sustained and entrainable by zeitgebers. "Resetting the clock" implies the removal of the Per-Tim heterodimer, and therefore the free activity of Clk-Cyc as transcriptional factors (Sidote *et al.*, 1998; Peschel and Helfrich-Forster, 2011). This subchapter details some of the better known zeitgeber, as well as the involved clock components.

1.3.4.1 Cryptochrome and Blue light

Light is the zeitgeber inducing the strongest response in flies, with the organism being extremely sensitive to it (Hirsh *et al.*, 2010). Brief pulses of light can advance (if happening during late night) or delay (if happening during early night) the current rhythm (Myers *et al.*, 1996). One major question arisen from early research on the core molecular clock was the light-dependent Tim-degradation. This process is in part caused by the active role of Cryptochrome (Cry) (Emery *et al.*, 1998; Ceriani *et al.*, 1999; Lamba *et al.*, 2014). Cryptochromes are flavonoid proteins with structural similarities to the DNA-repairing enzyme photolyase, accomplishing different roles across organisms upon blue light stimulation (Lin and Todo, 2005; Yu *et al.*, 2010). While the *Drosophila* Cry retains its photosensitivity, it is absent in other insect groups and in the mammalian cryptochromes (Lin and Todo, 2005). The "mammalian Cryptochrome" type actually assumes the role of the *Drosophila* Tim in the oscillator loop, heterodimerizing with the Per proteins (Dodson, Hore and Wallace, 2013; Engelen *et al.*, 2013). The mammalian TIM has its equivalent in the Drosophila Tim2 or Timeout (with *tim* being actually a duplication of *timeout*), which is involved in light entrainment from the visual systems and other non-circadian roles (Benna *et al.*, 2010).

In *Drosophila*, *cry* expression is repressed by Vri activity (Glossop *et al.*, 2003), while promoted by PDP1 (Zheng *et al.*, 2009b). The protein is sensitive to low wavelengths, with two peaks in the ultraviolet spectrum (<400 nm) and visible blue light (450 nm)(Stanewsky *et al.*, 1998; Berndt *et al.*, 2007; VanVickle-Chavez and Van Gelder, 2007). It displays many structures common in cryptochromes like the Photolyase-related (PHR) Region and the carboxiterminal tail. In *Drosophila*, PHR represents the active domain of the protein and the tail acts as a regulator (Busza *et al.*, 2004; Lin and Todo, 2005). Cry activation causes a conformational change in the tail which promotes binding to Tim (Ceriani *et al.*, 1999; Busza *et al.*, 2004; Czarna *et al.*, 2013; Vaidya *et al.*, 2013). The mechanism involves redox reactions with the Flavin Adenin Dinucleotide (FAD) cofactor and changes in the interaction between PHR and the C-tail (Busza *et al.*, 2004; Ozturk *et al.*, 2014). Conflicting models exist regarding the ground state of the FAD cofactor (oxidized or reduced) and the actual causative agent of the conformational change (the cofactor excitation or Cry reacting with the reduced state) (Ozturk *et al.*, 2007; Ozturk *et al.*, 2011). Besides Tim, activated Cry also displays affinity for Jetlag (Jet), a component of the E3 ubiquitin ligase complex (Ozturk *et al.*, 2011). The association allows Jet to interact with Tim and ubiquitinate both proteins, thus tagging them for proteasomal degradation (Koh, Zheng and Sehgal, 2006; Peschel *et al.*, 2009). Several proteins interact with Jet and modulate its function (Knowles *et al.*, 2009). There are therefore two known separated mechanisms for Tim degradation: a light-dependent processes relaying on Jet and an interaction with ubiquitination complexes that keeps acting

under *free run* conditions or input from other clock cells (see chapter 1.3.7)(Grima *et al.*, 2002; Knowles *et al.*, 2009; Grima *et al.*, 2012).

Clock cells expressing Cry act as deep brain photoreceptors and are able of gather light information by themselves, resulting in entrained behaviour (Emery *et al.*, 2000b). Antibodies for Cry locate the protein in the ventrolateral neurons (small and large), three of the LN_ds, the two DN_{1a}s and some DN_{1p}s (Stoleru *et al.*, 2004; Yoshii *et al.*, 2009b; Yoshii, Hermann and Helfrich-Forster, 2010; Yoshii, Rieger and Helfrich-Forster, 2012). As it will be seen in the Chapter 1.3.7, this classifies the clock neurons based on their function. The constant exposure to LL without any other stimuli (LL conditions) causes behavioural arrhythmia because of Cry activity. Null mutants like cry^{01} or cry^{b} are easily detected because they retain rhythmicity under these conditions (Stanewsky *et al.*, 1998; Emery *et al.*, 2000a; Emery *et al.*, 2000b; Dolezelova, Dolezel and Hall, 2007). The amount of Cry protein or posttranslational modifications of it or its substrate Tim can modulate the light sensitivity (Emery *et al.*, 1998; Martinek *et al.*, 2001; Dubruille *et al.*, 2009).

Visual systems are obviously also able of receiving light input. They include the compound eyes, the ocelli, and a minor contribution from the Hofbauer–Buchner (H–B) eyelets (Stanewsky *et al.*, 1998; Helfrich-Forster *et al.*, 2001; Veleri *et al.*, 2007; Umezaki and Tomioka, 2008). The gathered light cues from visual systems allow the fly to remain rhythmic in LL unlike Cry activity (Emery *et al.*, 2000a). This means there is some degree of redundancy for blue light reception, as a fly must lack Cry and the external photoreceptors (cells or associated pathways) to becoming insensitive to external light input, or residual entrainment will still be present (Stanewsky *et al.*, 1998; Helfrich-Forster *et al.*, 2001; Rieger, Stanewsky and Helfrich-Forster, 2003; Veleri *et al.*, 2003). Deep brain photoreceptors are present in many animals, but are not still totally characterised in mammals (Vigh *et al.*, 2002; Nakane *et al.*, 2010; Hang, Kitahashi and Parhar, 2016).

Cry has additional roles besides light resetting of the clock, including magnetosensation and morning arousal (Kumar, Chen and Sehgal, 2012; Dodson, Hore and Wallace, 2013; Fedele *et al.*, 2014; Guerra, Gegear and Reppert, 2014).

1.3.4.2 Temperature

Independently of the temperature compensation mechanisms, the presence of a temperature cycle (with a peak or thermophase and a trough or cryophase) can drive rhythms in *Drosophila* in DD conditions, and to some degree LL conditions (Pittendrigh, 1954; Yoshii *et al.*, 2005; Glaser and Stanewsky, 2007; Currie, Goda and Wijnen, 2009).

The fly sensitivity to a temperature cycle is remarkable, synchronizing behavioural rhythms with a 2-3°C amplitude cycle (Wheeler *et al.*, 1993; Glaser and Stanewsky, 2007; Chen *et al.*, 2015).

Temperature is however a weak cue compared to blue light, requiring more time when facing a phase shift, up to three days if the cycles are in *anti-phase* (Currie, Goda and Wijnen, 2009; Sehadova *et al.*, 2009). Both zeitgebers provide synchronised stimuli in nature (daylight usually bring warmer temperatures than night), and light is usually mentioned to be a stronger cue than temperature cycle. Temperature cycles can rescue, however, the arrhythmia induced under LL conditions (see Chapter 1.3.7)(Yoshii *et al.*, 2005). The presence conflicting environmental cues in the laboratory can modify the response of flies, providing information about the working of the clock circuitry (See Chapter 1.3.7)(Currie, Goda and Wijnen, 2009; Gentile *et al.*, 2013). While light stands over temperature when the two zeitgebers are in *anti-phase*, intermediate situations can severely alter the locomotor behaviour and even the molecular clocks (Currie, Goda and Wijnen, 2009; Harper *et al.*, 2016).

Similar to light, there are several ways of temperature sensing for flies. The zeitgeber can entrain the molecular clock inside some clock cells, including the LN_vs, LPNs and members of the three dorsal clusters (Yoshii *et al.*, 2005; Busza, Murad and Emery, 2007; Miyasako, Umezaki and Tomioka, 2007; Zhang *et al.*, 2010b). Cold temperature can promote *per* expression inside the whole head, in synch of the expected response during the dark phase (Goda, Sharp and Wijnen, 2014). The Transient Receptor Potential Cation Channel (TRPC) A1 (TRPA1) is not required for temperature entrainment but can affect the locomotor behaviour in the presence of high temperatures (Lee and Montell, 2013; Roessingh, Wolfgang and Stanewsky, 2015). *TrpA1* mutants show affected but resilient temperature-driven rhythms, that are almost eliminated with combined genetic ablation of the *cry*-expressing cells (Lee and Montell, 2013; Roessingh, Wolfgang and Stanewsky, 2015). Besides its role in temperature, TRPA1 can influence the fly behaviour under LD cycles (see Chapter 1.3.7)(Das, Holmes and Sheeba, 2015;2016). Pyrexia (Pyx) is another TRPC involved in responses when flies face low temperature cycles (Wolfgang *et al.*, 2013).

Diverse genes and organs are involved in temperature transduction pathways to the clock neurons. The chordotonal organs, proprioceptive organs found in the joints, express No circadian temperature entrainment (Nocte) which allows them to act as sensory organs for temperature entrainment (Glaser and Stanewsky, 2005; Sehadova *et al.*, 2009). While Nocte is required for the entrainment, the aforementioned precise temperature sensitivity is achieved with Ionoctropic Receptor 25a (IR25a), pointing to a complex and adaptive mechanism (Chen *et al.*, 2015). Intriguingly, *no receptor potential A* (*norpA*) mutants, a phospoliphase C involved in visual phototransduction, also lose their capacity of temperature entrainment (Glaser and Stanewsky, 2005; Szular *et al.*, 2012).

Many body parts and tissues can entrain molecular rhythms in their peripheral clocks with temperature cues in LL (see Chapter 1.3.8) (Glaser and Stanewsky, 2005;2007; Sehadova *et al.*, 2009). On its own, temperature can drive clock-independent rhythms in the activity of flies. Those activity patterns follow the external temperature cycle, but are easily deemed as non-circadian because of the lack of anticipation of the cycle peak. Depending of the environment, a working clock counteract these activity bouts (Currie, Goda and Wijnen, 2009).

1.3.4.3 Red Light

Blue light can act both through Cry and the visual systems (see Chapter 1.3.4.1), but red light is restricted to the latter. Mutant interactions have shown that both Rhodopsin 1 and 6 (Rh1, Rh6) can receive red light information at the compound eyes activity, and *Rh1*/*Rh6* double mutants or eyeless flies are blind to red light cycles (Hanai, Hamasaka and Ishida, 2008). Information is then thought to be relayed to the clock neurons via the l-LN_v projections at the medulla or optic lobes (Helfrich-Forster *et al.*, 2007a). Visual systems react to red light probably in the same way that to blue, but without the associated response by Cry. Indeed, other wavelengths can be sensed by visual systems in a similar fashion involving other Rhodopsins, and maybe Cry (Hanai and Ishida, 2009).

Opposite to their arrhythmic state caused by LL conditions, flies under constant red light exposure (RR conditions) maintain a circadian behaviour as Cry remains unresponsive (Helfrich and Engelmann, 1983; VanVickle-Chavez and Van Gelder, 2007). As a consequence, RR conditions act as a *de facto free run* state, similar to *cry* mutants in LL (Emery *et al.*, 2000a; Dolezelova, Dolezel and Hall, 2007). Published works, as well as unpublished results from our lab, indicate that RR conditions change the hierarchical disposition of the clock neurons, marginalising the contribution of PDF-signalling to rhythmicity (Cusumano *et al.*, 2009). Red-Dark (RD) entrainment conditions may alter the normal behavioural response of flies (see more details in Chapter 1.3.7)(Cusumano *et al.*, 2009). Red light is a weaker cue than blue light, requiring more time to entraining and being outcompeted by the latter if environmentally conflicted (Hanai, Hamasaka and Ishida, 2008).

1.3.4.4 Other zeitgebers

Although lights and temperature are the best widely studied zeitgebers, other external cues can at least promote entrainment of the clocks inside *Drosophila*. Chordotonal organs can drive behavioural rhythms under Vibration-Silence (VS) cycles in absence of other stimuli (Simoni *et al.*, 2014). Populations can provide time cues to incoming individuals via olfactory cues (pheromones) which can respectively be subjected to entrained rhythms (Krupp *et al.*, 2013). In males, DN_1

neurons can be entrained by sexual activity, but this time cue (or the DN_1s on their own) cannot modify the adult locomotor behaviour (Levine *et al.*, 2002; Hanafusa *et al.*, 2013).

1.3.5 Communication across the clock circuit

As neurons, clock cells rely on different ways of communicating information among them. The establishment of a precise and unique rhythm requires the collaboration of the different cell clusters, which employ different ways of communication across the circuit (Beckwith and Ceriani, 2015). In normal conditions, a clock cell carries a working oscillator within (temporal cue) which can influence ways of communication like the firing rate, which is an output of its clock but can act as a temporal cue for others. Therefore, albeit the molecular clocks are cell-autonomous mechanisms, at any given time or environmental conditions some clock cells are receiving external input, and "blind" ones are receiving temporal cues from the former. Each of the following described elements take a role into the (not fully understood) grand mechanism that determines the unifying and rhythmic response of the core brain clock.

1.3.5.1 Pigment Dispersing Factor (PDF)

Among neuronal signals there are several neuropeptides, small protein-like sequences involved in many diverse roles in fly physiology (Nassel and Winther, 2010). Previous studies had characterized the Pigment Dispersing Hormones (PDHs) in crustacean and other arthropods (Rao and Riehm, 1988;1993). Interestingly, it was then found that some of the previously discovered clock neurons were inmunoreactive to PDH antibody (Helfrich-Forster and Homberg, 1993; Nassel *et al.*, 1993). The responsible neuropeptide (NSELINSLLSLPKNMNDA-NH_2), whose gene was characterized in 1998, received the name of Pigment Dispersing Factor(PDF)(Park and Hall, 1998; Nassel and Winther, 2010).

PDF seems to have a sole circadian role based on being exclusively found at the l-LN_vs, four of the s-LN_vs (hence identifying the 5^{th} s-LN_v by its absence), two short-lived tritocerebral (PDF-tri) neurons and abdominal cells in the adult (Renn *et al.*, 1999; Im and Taghert, 2010) More importantly, the null mutant (Pdf^{01}) is viable and normal excepting its aberrant circadian behaviour (see Chapter 1.3.7 for more information)(Nassel *et al.*, 1993; Renn *et al.*, 1999). Moreover, they start losing their rhythmicity in *free run*, although some of the flies retain weak but shorter than 24-h rhythms (Renn *et al.*, 1999; Klarsfeld, Leloup and Rouyer, 2003; Lin, Stormo and Taghert, 2004; Wulbeck, Grieshaber and Helfrich-Forster, 2008). The same phenotype appears when the PDF-expressing neurons are genetically ablated or silenced. These phenotypic similarities are the ones that have classified these neurons as pacemaker cells in *free run* (see Chapter 1.3.7)(Renn *et al.*, 1999; Wu, Cao and Nitabach, 2008).

PDF receptor (PDFR, alternatively named Han or Gop), a class II G-protein coupled receptor, was firstly described in 2005 (Helfrich-Forster, 2005b; Hyun *et al.*, 2005; Lear *et al.*, 2005; Mertens *et al.*, 2005). There is a remarkable phenotypical resemblance between Pdf^{01} and the loss of *Pdfr* function, like with the $Pdfr^{5304}$ mutant (Hyun *et al.*, 2005; Lear *et al.*, 2005). There exist conflicting reports about which clock cells express the receptor, although s-LN_vs, three of the LN_ds, and some DN_1s and DN_3s are commonly cited (Helfrich-Forster, 2005b; Hyun *et al.*, 2005; Lear *et al.*, 2005; Mertens *et al.*, 2005; Im and Taghert, 2010; Im, Li and Taghert, 2011). The presence of PDFR at the l-LN_vs has been contradictory across literature, as albeit they express the correspondent Gal4 driver they are normally insensitive to PDF (Helfrich-Forster, 2005b; Shafer *et al.*, 2008; Im and Taghert, 2010; Im, Li and Taghert, 2011). PDFR interacts to a lesser extent with several other ligands *in vitro* and *in vivo* like Diuretic Hormone 31 (DH31), the homologue of Calcitonin Gene-Related Peptide (CGRP) (see Chapter 1.3.6)(Mertens *et al.*, 2005; Goda *et al.*, 2016).

PDF is firstly involved into synchronizing the different cell clusters across the clock circuitry, by having different effects upon each population. The s-LN_vs for example can maintain Per expression rhythms in DD without PDF, although their phase as a group is gradually lost (Lin, Stormo and Taghert, 2004). Comparatively, the LN_ds experience a phase advance as a group but they cannot maintain the Per molecular rhythms further in DD (Lin, Stormo and Taghert, 2004). Therefore, clock neurons react differently in a Pdf^{01} background, from rhythm weakening to unresponsiveness (Peng *et al.*, 2003; Lin, Stormo and Taghert, 2004; Yoshii *et al.*, 2009b). At least in the PDF-expressing neurons, the neuropeptide increases Per stability, and these neurons can modify the molecular clock of the PDF- neurons by direct effects on Tim by PDF-controlled PKA (Li *et al.*, 2014b; Seluzicki *et al.*, 2014). Curiously, $PDFR^{-}$ l-LN_vs are often reported as unable of maintaining molecular rhythms in DD(Yang and Sehgal, 2001; Veleri *et al.*, 2003; Grima *et al.*, 2004).

This effect of PDF is one of the very few known evidences of cell communication across the circuit having an effect upon the molecular oscillators, but the neuropeptide can cause further responses in clock neurons (see Chapter 1.3.5.3). PDF administration increases cyclic adenosine monophosphate (cAMP) and calcium levels in many clock neurons (Shafer *et al.*, 2008; Yao *et al.*, 2012; Zhang and Emery, 2013; Cavey *et al.*, 2016). This increases the firing rate in neurons like the s-LN_vs or the DN_{1p}s, which have been traditionally challenging for electrophysiological studies (Sheeba *et al.*, 2008b; Kunst *et al.*, 2014; Seluzicki *et al.*, 2014; Cavey *et al.*, 2016). Innovative recent studies have shed more light to the way PDF affects the different oscillators, showing for example that PDF-signalling keeps a forced desynchrony of Ca^{2+} currents among the different clock clusters (Liang, Holy and Taghert, 2016; Sabado *et al.*, 2017).

Despite the importance of PDF as circadian mediator, little is known about how the clock itself regulates its expression. Although *Pdf* mRNA does not display clear rhythms, gene and neuropeptide are affected by Clk and Vri (Park and Hall, 1998; Blau and Young, 1999; Mezan *et al.*, 2016; Gunawardhana and Hardin, 2017). The neuropeptide can negatively affect Clk activity, establishing a feedback mechanism which currently is not fully characterised (Mezan *et al.*, 2016). The complicated post-translational regulation of PDF results in a daily rhythm of accumulation at the s-LN_v dorsal termini, peaking shortly after the (real or subjective) dawn and exhibiting a trough after the beginning of the night. Vri is specifically required inside the s-LN_vs for the persistence of this rhythm, which is on the other hand impervious to PDF overexpression (Helfrich-Forster *et al.*, 2000; Park *et al.*, 2000; Gunawardhana and Hardin, 2017). PDF in the s-LN_v soma display milder oscillations, and there are no reported PDF rhythms in the l-LN_vs (Park *et al.*, 2000).

PDF and related peptides are exclusively found in arthropods. In the mammalian SCN, Vasoactive Intestinal Peptide (VIP) and Arginine Vasopressin (AVP) perform similar roles in communication among neurons (Piggins and Cutler, 2003; Aton *et al.*, 2005; Ono, Honma and Honma, 2016).

1.3.5.2 Other neuropeptides and neurotransmitters

Although PDF is the best characterized neuropeptide related to circadian rhythms in *Drosophila*, others have been under study in recent years. These neuropeptides, along other signals detailed in this subchapter, are probably the reason some Pdf^{01} flies (or individuals with genetic ablation of PDF^+ cells) retain some rhythmicity in DD (Renn *et al.*, 1999). Ion Transport Peptide (ITP) is naturally found in just a few neurons inside the brain, including the 5^{th} small s-LN_v and one of the Cry^+ LN_ds (Dircksen *et al.*, 2008; Johard *et al.*, 2009). Similar to PDF, ITP levels oscillate at the dorsal projections of these cells, while the soma levels remain constant. This rhythm is, however, bimodal with peaks around noon and midnight, and troughs around the *lights-on* and *lights-off* events (Hermann-Luibl *et al.*, 2014). These neuropeptide expression peaks tend to merge in DD conditions, mirroring a similar pattern found in the adult locomotor activity (see chapter 1.3.7)(Hermann-Luibl *et al.*, 2014).

Three LN_ds (only one of them Cry^+), the 5^{th} s-LN_v and half of the l-LN_vs express Neuropeptide F (NPF), invertebrate homologue of the mammalian YPF, inside the clock circuitry (Yannielli and Harrington, 2001; Hermann *et al.*, 2012). Interestingly, the expression at the three LN_ds has been reported to be more common in males, which would make this neuropeptide a component of the sexual dimorphism in the clock (see chapter 1.3.9)(Lee, Bahn and Park, 2006; Hermann *et al.*,

2012). Its receptor is found at some LN_ds and DN_1s (He *et al.*, 2013). The neuropeptide is therefore found in cells with known roles in the circadian behaviour (see chapter 1.3.7) albeit its precise function is not known. Related to NPF, short neuropeptide F (sNPF) is expressed in the PDF-expressing s-LN_vs and two LN_ds (all of them expressing Cry)(Johard *et al.*, 2009). sNPF inside the s-LN_vs promote sleep and it is thought to repress the same cAMP synthesis that PDF promotes (Shang *et al.*, 2013; Vecsey, Pirez and Griffith, 2014). As previously stated, the neuropeptide IPNamide is found with daily oscillations in the $DN1_a$s, albeit little is known besides linking them to lateral neurons (Verleyen *et al.*, 2004; Shafer *et al.*, 2006).

Besides these more specific transmitters, *Drosophila* clock cells are capable of responding to classic well-known neuronal mediators. PDF^+ neurons express γ-aminobutyric acid A ($GABA_A$, ionotropic) receptors, and seems to be partially inhibited by GABAergic sleep-promoting neurons. This communication seems to reduce light sensitivity and wakefulness response during night (Parisky *et al.*, 2008; Chung *et al.*, 2009). The s-LN_vs requrie $GABA_B$-mediated (G-coupled) signalling for their role as pacemaker cells (see chapter 1.3.7)(Dahdal *et al.*, 2010). Lateral neurons receive glumatate-signalling (maybe inhibitory) from the dorsal clusters as a way of reinforcing the circuit synchrony (Hamasaka *et al.*, 2007; Collins *et al.*, 2014; Guo *et al.*, 2016). Presence of receptors and transporters of other neurotransmitters, along associated roles are found across the circuit (Hamasaka and Nassel, 2006; Johard *et al.*, 2009; Frenkel *et al.*, 2017).

1.3.5.3 Firing rate and neuronal state

Transmission of currents constitutes one of the important functions of clock neurons. The most immediate association between the clock and neuronal qualities like firing rate or membrane potential can be uncovered by studying these throughout the day. Because of the discrete nature of the clock clusters, several techniques have been developed to study them, ranging from classical electrophysiological techniques to Ca^{2+} current sensors, fluorescence-based techniques and known locomotor output of the adult organisms. For example, patch-clamp recordings of the l-LN_vs and fluorescence-based assays of the s-LN_vs show these neurons decrease their excitability during the day and increase it throughout the night in the presence of a working clock (Cao and Nitabach, 2008; Cao *et al.*, 2013). Light-induced clock reset is associated with acute increase of the firing rate in the l-LN_vs, which can be kept further on DD (Sheeba *et al.*, 2008b). The DN_{1p}s display elevated excitability in the first hours of the day compared to the last ones (Flourakis *et al.*, 2015). How the molecular oscillator can regulate the neuronal state is not fully understood. Pre- and post-transcriptional control of ionic channels constitutes a versatile tool for this (Flourakis *et al.*, 2015).

As introduced in Chapter 1.3.5.1, PDF-signalling promotes neuronal excitability, while sNPF reduces it (Vecsey, Pirez and Griffith, 2014). For example, the neuropeptide binding to PDFR increases the firing rate of the DN_1s during late evening/early morning. The intricate association between PDF-signalling, the neuronal state and the communication across the circuit (see also Chapter 1.3.6 and 1.3.7) may explain why the phenotype of electrical silencing of the PDF-expressing neurons matches the lack of the neuropeptide (Wu, Cao and Nitabach, 2008), or why the l-LN_v neuronal state is sensitive to the lack of PDFR in other clock neurons (Yao *et al.*, 2012).

While neuronal output can be affected by the clock, the neuronal state can also influence the molecular oscillator. Input from morning cells causes Tim Cul3-dependent degradation inside the E-cells (Guo *et al.*, 2014). This effectively allows elements like the firing rate to act as external cues for other clock neurons.

1.3.6 Output centres of the circadian clock

Despite the persistent interrogation of the mechanisms inside the clock circuitry, and the characterized behavioural phenotypes, how the circadian clocks links with the adult locomotor behaviour remains a poorly answered question. Many of the known or partially discovered circuits are related to the locomotor behaviour, already defined as the most well-known output of the *Drosophila* circadian clock.

One of the best characterised locomotor output circuits involves the Pars Intercerebralis (PI) part of the neuroendocrine insect system and equivalent to the mammalian hypothalamus (Hartenstein, 2006; de Velasco *et al.*, 2007). The PI at the dorsal protocerebrum exhibits some circadian gene expression and contains many neurosecretory neurons like those expressing Diuretic Hormone 44 (DH44), homologue of the Corticotropin-Releasing Factor from mammals (CRF) (Jaramillo *et al.*, 2004; Park *et al.*, 2008; Cavanaugh *et al.*, 2014). Six of these neurons are required for the behavioural output, by regulating their activity with input from the s-LN_vs and relayed through the DN_{1p}s (Cavanaugh *et al.*, 2014; Cavey *et al.*, 2016). Although PDF-expressing neurons are involved, this circuit relies on transmission of neuronal activity (Cavanaugh *et al.*, 2014; Cavey *et al.*, 2016).

Albeit the aforementioned PDF-tri cells may contact the PI, they die or at least lose the neuropeptide expression shortly after hatching, suggesting relationship with eclosion rhythms but not adult locomotor behaviour (Myers, Yu and Sehgal, 2003; Im and Taghert, 2010). PDF-signalling contributes before dawn to sleep inhibition (constituting an example of circadian regulation of the later) by causing the DN_1s to release DH31 (Kunst *et al.*, 2014). Other studies have found links between the PI and sleep, with no known circadian regulation (Crocker *et al.*, 2010; Park *et al.*,

2014). The s-LN_vs can, maybe indirectly, inhibit dorsal non-clock neurons involved in leucokinin-signalling, required for circadian behaviour (Cavey *et al.*, 2016).

DN_2s constitute the output efference to establish the daily temperature preference rhythm (TFR), which urges flies to seek for low temperature in the morning and higher in the evening, with parallelisms to internal temperature rhythms of endothermic organisms (Kaneko *et al.*, 2012). *Trpa1*-expressing anterior cells (which also gather input from *Pyx*-expressing antennal cells) send temperature information to the DN_2s via the s-LN_vs and serotonin signalling, independent from the temperature entraining circuits (Tang *et al.*, 2013; Tang *et al.*, 2017). This circuit is highly dependent of PDFR activation of the DN_2s by DH31 of unknown origin (Goda *et al.*, 2016).

Other possible locomotor output mechanisms remain obscure at the current time. It has been proposed than PDP1ϵ is involved in the output of the clock and not in its regulation (Benito, Zheng and Hardin, 2007; Lim *et al.*, 2007). The cause of the reported discrepancies is the diverse effects gene targeting of *Pdp1* causes in the clock genes, and the associated locomotor defects that cannot be rescued by actions on the secondary oscillatory loop (Zheng *et al.*, 2009b). Further studies have linked this transcription factor to metabolic pesticide response (Beaver *et al.*, 2010).

1.3.7 Establishment of adult Drosophila *locomotor* behaviour

The interaction of the clock components inside the diverse clock neuronal clusters, along external zeitgebers and other internal factors like sleep, result in the widely studied adult locomotor behaviour (Allada and Chung, 2010). Temporal information of the clock neurons needs to be integrated and transmitted to generate detectable adult locomotor behaviour. Behavioural study allows to interrogate the clock circuitry because of the differential contribution of the clock clusters and the diverse intercellular communications. Circadian experiments often refer to single flies being tested at a time, as interactions between individuals alter the behavioural response in a clock-independent way, especially when mixing males and females (Hanafusa *et al.*, 2013).

The first behavioural data suggested to researchers that *Drosophila* activity, like many other examples in animals, had a bi-modal component (Pittendrigh and Daan, 1976; Helfrich-Forster, 2000;2009). Pittendrigh and Daan experiments were the firsts that proposed the so-called dual oscillator model, based on the responses to light cycles. One of the two components would be responsible for the morning (M) activity, while the other would cause the evening (E) activity. A wild-type record of the average activity of a fly (or group of flies) in a 12:12 LD cycle at constant temperature conditions exhibits a stereotyped shape with peaks occurring around the artificial dawn and dusk (*lights-on* and *lights-off* events, respectively) (Figure 1.3, A). They are named anticipatory activity peaks or bouts, and their dependence on a working clock is proven by their

absence in *per*^{01} mutants (Grima *et al.*, 2004; Rieger *et al.*, 2009). The peaks are separated by a period of inactivity frequently called *siesta* (Spanish for nap), which is affected by both light and temperature and is more pronounced in males (see chapter 1.3.9)(Ho and Sehgal, 2005; Khericha, Kolenchery and Tauber, 2016).

With the available tools, genetic targeting of specific cell clusters allowed to identify the responsible neurons by phenotypic detection (Figure 1.3, B). With this approach, PDF-expressing neurons were confirmed to be responsible for morning activity as predicted by the model (Stoleru *et al.*, 2004). As a consequence, they are also named Morning- or M-cells (considering this name indicates their function, but not their genetic lineage). An opposite approach, consisting of selectively rescuing *per* gene in a *per*^{01} mutant, as well as the behaviour of the *Pdf*^{01} mutant provided the same response (Renn *et al.*, 1999; Grima *et al.*, 2004). Similar experiments identified the Evening- or E-cells: the 5th s-LN$_v$, the LN$_d$s and some DN$_1$s (Grima *et al.*, 2004; Stoleru *et al.*, 2004; Rieger *et al.*, 2006). This means that with the possible exception of the heterogeneous DN$_1$s, all the clock cells known to be involved in the LD behaviour are Cry$^+$ (see chapter 1.3.4.1). It marks another distinction between the classic oscillators, as while PDF is associated to M-Cells, ITP is only found at some E-cells (Johard *et al.*, 2009).

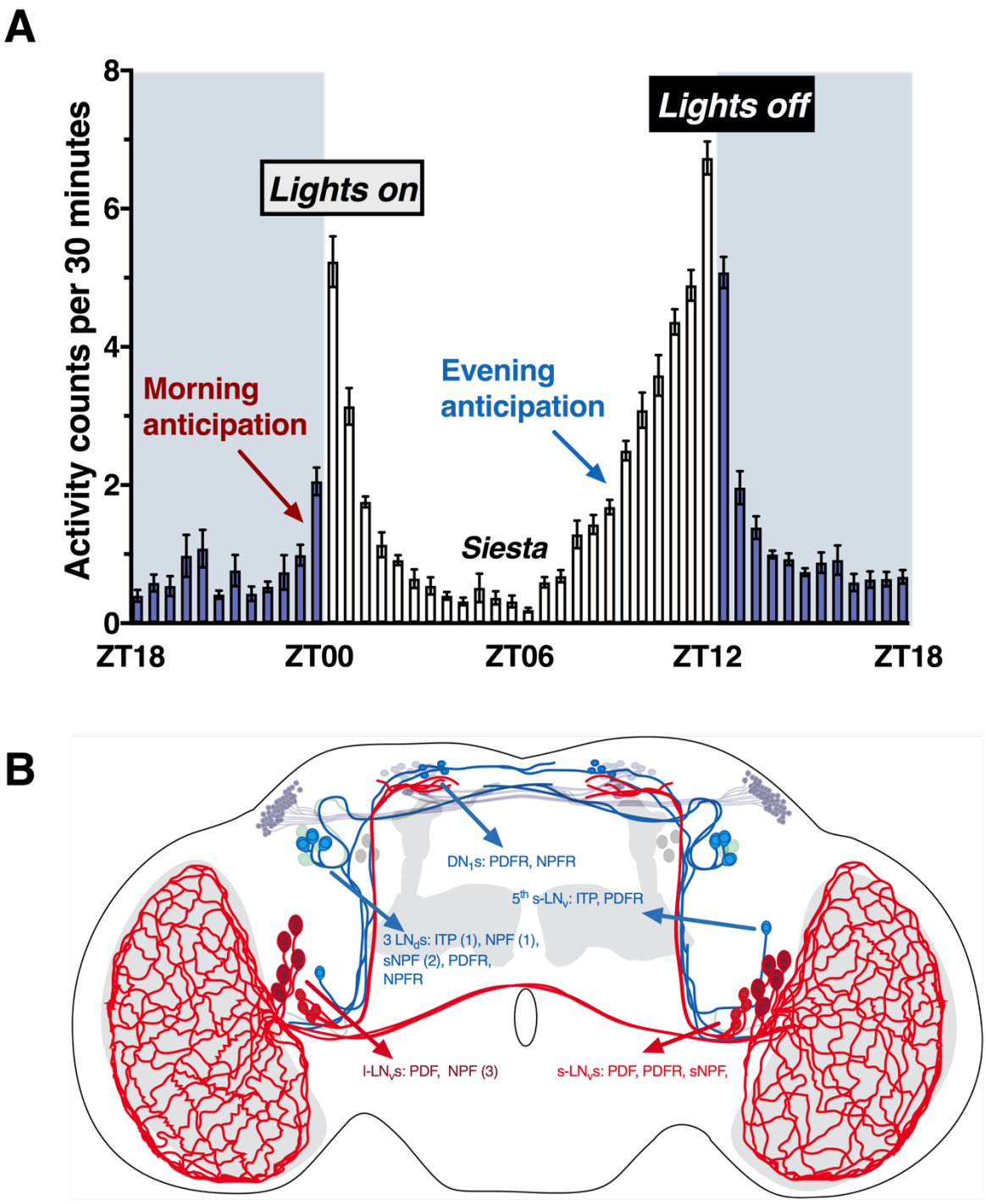

Figure 1.3 Dual oscillator model for the LD behaviour of *Drosophila melanogaster*. A) Activity profile of an averaged male population. The 12:12 Light-Dark (LD) cycle at constant room temperature represents an average of six days starting at midnight (ZT18). *Lights-on* event marks the beginning of the day (ZT00) and *lights-off* event the beginning of the night (ZT12). The profile shows the morning anticipatory activity (in red, promoted by M-cells based on the dual oscillator model), the evening anticipatory activity (in blue, promoted respectively by the E-cells) and the siesta throughout middle hours of the day. **B)** Horizontal plane of the adult brain displaying the clock-bearing cells involved in the dual oscillator model. The Morning (M-) cells, in red, are the PDF^+ s-LN_vs and l-LN_vs. The Evening (E-) cells

are the PDF- 5th s-LN$_v$, 3 of the LN$_d$s and some DN$_1$s. All the identified cells are also Cry$^+$. The picture indicates the neuropeptides (and corresponding receptors) as presented in Chapter 1.3.5). Further details about the different cell clusters are detailed in Chapter 1.3.3, and about the relationship between M-/E- cells and the resulting behaviour in this chapter. ITP: Ion Transport Peptide; NPF: Neuropeptide F; NPFR: NPF Receptor; PDF: Pigment Dispersing Factor; PDFR: PDF Receptor; sNPF: short Neuropeptide F.

Current data suggest PDF-signalling is a critical component of the interaction between the M- (PDF-expressing) and E- cells. The neuropeptide is considered to be mostly a late night/dawn signal, coinciding with its strongest accumulation at the s-LN$_v$ dorsal termini, and with the expansion of these (Park *et al.*, 2000; Taghert and Shafer, 2006; Fernandez, Berni and Ceriani, 2008). Targeting of PDF-signalling indicates that the neuropeptide causes the morning anticipatory activity, while it delays the evening anticipatory activity promoted by the E-cells (Renn *et al.*, 1999; Zhang *et al.*, 2010a; Schlichting *et al.*, 2016). The traditional conception of the dual oscillator cannot resolve the complete clock circuitry organisation (Yoshii, Rieger and Helfrich-Forster, 2012), but is nevertheless supported by cellular data, like the Per phase delay found at the LN$_d$s upon PDF-signalling (Lin, Stormo and Taghert, 2004). The l-LN$_v$s, lacking PDFR, contribute to the morning anticipatory activity, but also to the evening one (Sheeba *et al.*, 2008a). At the same time, restoring the clock only inside the l-LN$_v$s (*per* rescue with the *c929-Gal4* driver) does not rescue any locomotor rhythms at all, showing that these neurons require a working oscillator inside the s-LN$_v$s for promoting activity (Grima *et al.*, 2004). Both oscillators cooperate during light-dependent resets (Lamba *et al.*, 2014). Moreover, PDF-signalling to the DN1$_p$s is sufficient for rescuing both the morning anticipatory activity and the short period in DD, although evening anticipatory activity and overall poor rhythmicity are not (Zhang *et al.*, 2010a). DN$_1$s exert an inhibitory role over M- and E- cells via glutamate-signalling, limiting the maximum evening activity and promoting sleep during mid-day (Guo *et al.*, 2016).

All these results were gathered during LD cycles with other environmental variables remaining unchanged. The activity profile of the fly changes with different conditions, and this is a reflex of the hierarchical change inside the clock circuitry. When LD cycles are removed, the *free run* behaviour of the fly mostly resembles a unimodal peak with the disappearance of the *siesta*. While M- and E-cells are required for the stereotypical LD profile, the PDF-expressing neurons are sufficient to drive rhythms in DD. This is the reason why these clock cells, particularly the s-LN$_v$s, are traditionally named *pacemaker* neurons (not to be confused with the use of the term pacemaker for the 150 clock neurons) (Dubruille *et al.*, 2009).

There exists some controversy regarding the true nature of the standardized 12:12 LD behavioural profile, as it is greatly changed when flies face more natural conditions. Particularly, certain environmental conditions with gradual changes causes the appearance of the so-called Afternoon (A-) peak instead of the expected *siesta* (Green *et al.*, 2015a). The A-peak is especially dependent on gradual temperature cycles sensed by TRPA1 (see Chapter 1.3.4.2), which also causes the apparition of a *siesta* if the temperature transitions are abrupt (Das, Holmes and Sheeba, 2015; Green *et al.*, 2015a; Das, Holmes and Sheeba, 2016). As a consequence, the *siesta* itself has been proposed to be an experimental artefact and a response to gated cycles, as it tends to disappear with more natural-like conditions (Vanin *et al.*, 2012; Green *et al.*, 2015b). This response is regardless regulated by the clock circuitry and can be modulated by environmental cues, providing ecological adaptability (like resistant to desiccation during the hottest hours of the day) (Majercak *et al.*, 1999; Collins, Rosato and Kyriacou, 2004; Wijnen and Young, 2008). The DN_1s increase their excitability when facing warm temperatures, linking this mechanism to their sleep promoting role and to the apparition of *siestas* under both light and temperature gated cycles (Rieger *et al.*, 2007; Guo *et al.*, 2016). Therefore, as previously mentioned in Chapter 1.3.6, DN_1s seem to promote both activity and sleep, and have been therefore a clock cluster of interest in recent years (Cavanaugh *et al.*, 2014; Kunst *et al.*, 2014).

What is unanimously defined as an artefact currently is the *masking*, the promotion of activity following the *lights-on* and its decrease after *lights-off,* obscuring clock-driven behaviours (Rieger, Stanewsky and Helfrich-Forster, 2003). These behavioural changes are present even in clockless mutants, as they do not rely on any type of anticipation at all (Wheeler *et al.*, 1993). This means that mutant flies can "follow" external cycles, but they cannot be entrained by them. While its apparition is dependent on the photoreception systems linked to circadian rhythms, it is possible that masking-derived activity could influence the clock in normal individuals (Rieger, Stanewsky and Helfrich-Forster, 2003).

As mentioned in chapter 1.3.4.3, flies can also be entrained by red light in a similar fashion to blue light. The process takes more consecutive days, probably because indirect entrainment of the clock cells like in the cry^{01}/cry^{b} mutants (Hanai, Hamasaka and Ishida, 2008). RD conditions make the flies display activity profiles very similar to animals in LD (Cusumano *et al.*, 2009). Flies maintain a robust rhythmicity in RR conditions as long as some yet uncharacterised clock cells have working clocks within. These rhythms usually display longer period lengths than those in DD (Helfrich and Engelmann, 1983; Cusumano *et al.*, 2009). Intriguingly, red light affects flies lacking PDF-signalling differentially. While an advance evening anticipatory activity is a highlight of these flies in LD, this evening anticipation is absent in RD conditions, unless PDF-signalling is specifically restored towards clock-bearing E-cells (Cusumano *et al.*, 2009). How exactly red light promote

evening activity in wild-type flies but decreases it in *Pdf*^{01} mutants is not known, but evidences the versatility of the clock circuit when facing different environmental conditions. In RR conditions, these flies keep displaying shorter rhythms, but their rhythmicity is considerably improved, at least in males (Cusumano *et al.*, 2009).

When flies face a gradient temperature cycle in DD, the activity peak phase synchronises with the temperature one, and the effect is similar with abrupt cold:warm transitions (Currie, Goda and Wijnen, 2009; Tang *et al.*, 2017) . Despite temperature is a weaker cue than light, temperature cycles can rescue wild-type flies from the LL-induced arrhythmia (Glaser and Stanewsky, 2007; Sehadova *et al.*, 2009; Chen *et al.*, 2015).

As already discussed, flies with compromised clocks are still able of responding to external cues (Wheeler *et al.*, 1993), and they also react differently when exposed to combined environmental cycles. An entrained clock to a given LD cycle can inhibit the activity-promoting effects of a temperature increase. These effects are particularly evident when a temperature cycle is in *anti-phase* to the LD cycle, where flies lacking clocks "follow" the temperature increase up until *lights-on* (Currie, Goda and Wijnen, 2009; Menegazzi, Yoshii and Helfrich-Forster, 2012).

1.3.8 Peripheral clocks in *Drosophila melanogaster*

Like in many animals including mammals, several rhythmic outputs in *Drosophila* involve peripheral clocks. Peripheral rhythms are sometimes named slave oscillators because of their presumptive submissive or secondary nature towards the main clock in the brain, but that notion has been challenged in *Drosophila* (Ito and Tomioka, 2016). Peripheral clocks are cell-autonomous oscillators with a varied interaction with the core clock and sensory neurons that entrain them (Plautz *et al.*, 1997). *Drosophila* peripheral rhythms were firstly identified with studies of luciferase expression under circadian gene drivers. Fly bodies exhibited then an expected daily rhythm of the enzyme expression, but explanted parts of the animal maintained the rhythms despite the lack of a brain and, more importantly, could be reset by light or temperature (Plautz *et al.*, 1997; Glaser and Stanewsky, 2005; Sehadova *et al.*, 2009).

As mentioned in Chapter 1.3.2.1.1, the characteristic that gave origin both to circadian research in *Drosophila* and to the genus name is curiously the most slaved peripheral rhythm. Eclosion rhythms, as Benzer studied, requires PDF-signalling from the lateral neurons, but is ultimately controlled by a clock in the Prothoracic Gland, the endocrine gland that secretes ecdysone (Myers, Yu and Sehgal, 2003). On the other hand, the circadian clock of the sensorial olfaction system in the antenna is completely independent of the core clock (Tanoue *et al.*, 2004). The

Drosophila oenocytes also display an independent peripheral clock that can be modulated by PDF, and this has an effect in sexual behaviour (Krupp *et al.*, 2013).

1.3.9 Sexual dimorphism and circadian rhythms

Gender-specific differences in circadian rhythms and associated processes are found across many species, with *Drosophila melanogaster* not being an exception (Wever, 1984; Helfrich-Forster, 2000; Hendricks *et al.*, 2003; Paul *et al.*, 2006; Zimmerman *et al.*, 2012; Krizo and Mintz, 2014). In many species, males are the most studied gender for circadian rhythms, in part because of controversial gender bias related to the severely disputed intrinsic female sensitivity to hormonal cycles (Krizo and Mintz, 2014; Prendergast, Onishi and Zucker, 2014). Male flies are also the most studied individuals, mostly because of practical reasons like the disruptive effect of fertilized eggs and larval propagation.

Although this can be bypassed by different means, the current stereotyped behaviour of a fly facing a LD cycle has a strong gender component (Khericha, Kolenchery and Tauber, 2016). The *siesta* is more pronounced in males, effectively sleeping twice as much as females in the day total (Helfrich-Forster, 2000; Isaac *et al.*, 2010; Zimmerman *et al.*, 2012). Different assays have shown of sleep pattern of males and females differ in the response (Catterson *et al.*, 2010). Feminization or masculinization of the opposed neuronal circuits have failed to fully reverse the behavioural differences (Khericha, Kolenchery and Tauber, 2016). This difference is not entirely genetic, as virgin females exhibit a similar profile which is irreversibly changed after sexual activity (Helfrich-Forster, 2000; Ho and Sehgal, 2005; Isaac *et al.*, 2010). This is dependent of the male sex peptide, produced by the accessory gland and transmitted to females during mating with long lasting effects in the receptor animal (Kubli, 1992). It is thought this behavioural change has consequences in resource acquisition for egg-laying individuals (Isaac *et al.*, 2010).

Some gender features regarding genetic profile and function of the clock cells are known, albeit with little currently known effects. The male DN_1s exhibit a higher excitability than the female ones, correlating with the quantifiable differences between the *siestas* (Guo *et al.*, 2016) and with the male cells responding to sexual cues (Hanafusa *et al.*, 2013). Other circuit-specific gender differences are the reported differential expression of NPF (see Chapter 1.3.5.2)(Lee, Bahn and Park, 2006) and *Pdf* (Park and Hall, 1998). The gender component of PDF-signalling has not been documented in scientific literature beyond possible differences in *Pdf* expression (Park and Hall, 1998), but some differences emerge with studies in Red Light (See Appendix B). Finally, clock components have been found to influence male sex-related behaviours like sex drive (DN_1s) or pheromone production (PDF, via a peripheral rhythm) (Fujii and Amrein, 2010; Krupp *et al.*, 2013).

Therefore, the specific differences on a circuit level for the behavioural difference for males and females are not understood yet. Just like the neurons driving male courtship can be ectopically activated in females, similar experiments could provide information regarding circadian behaviour in the future (Rezaval *et al.*, 2016).

1.3.10 Circadian rhythms and clocks during *Drosophila* development

Origins of the clock neuronal circuitry during fly development are not currently fully understood. One of the reasons being the numerous differences in the nervous system across different life cycle stages (Truman, 1990). Embryogenic neurogenesis originates in the neuroblast populations of the neuroectodermic layer (Truman, 1990; Landgraf, 2016). These neuroblast clusters exhibit a stem cell-like quiescent behaviour, with some of them dividing and differentiating into larval CNS neurons during these stages. Most of them however, are reactivated during metamorphosis, where they mature into the adult CNS neurons (Truman and Bate, 1988; Spindler and Hartenstein, 2010). The larval-to-adult transition is further complicated because along larval tissue programmed death, fly neurons exhibit synaptic remodelling and pruning (Rusconi, Hays and Cagan, 2000; Tissot and Stocker, 2000; Watts, Hoopfer and Luo, 2003).

As early as the embryonic stages, the presence of proteins such as Per and Clk distinguishes precursors of many of the neuronal clock subsets, with Tim showing a different pattern more associated with glia precursors (Houl *et al.*, 2008; Ruiz *et al.*, 2010). During the larva stages, clock clusters can be found, and the s-LN_vs express PDF since first instar larval stage (Helfrich-Forster, 1997; Kaneko, Helfrich-Forster and Hall, 1997). The l-LN_vs and their arborisation pattern appear halfway during the pupa stage (Helfrich-Forster, 1997). The two 5^{th} s-LN_v precursors are found in early larva in close proximity to the PDF-positive s-LN_vs, suggesting a common origin before the neuropeptide is expressed (Kaneko, Helfrich-Forster and Hall, 1997; Rieger *et al.*, 2006; Helfrich-Forster *et al.*, 2007b). Three dorsal neuron clock clusters are also found during larva stage (Kaneko, Helfrich-Forster and Hall, 1997). As important as the time of formation is the moment where the clock clusters display a working clock. The larval clock neurons rhythmically express Per if exposed to light cycles (with the exception of the DN_3s), but only s-LNv s maintain strong rhythms further in DD (Kaneko, Helfrich-Forster and Hall, 1997). Interestingly, the rhythms in the DN_2 precursors are in *anti-phase* to the rest of clusters, while in synch with them in the adult fly under constant temperature at DD (Kaneko, Helfrich-Forster and Hall, 1997; Yoshii *et al.*, 2009a). These data suggest the existence of a working morning oscillator (PDF^+ neurons), and possibly an evening one (the 5^{th} s-LN_v, at least).

Circadian rhythms are found in larvae, for example modulating their characteristic response to light (Konopka and Benzer, 1971; Mazzoni, Desplan and Blau, 2005). This behavioural rhythm requires the larval Bowlig Organ (photoreception) and a working clock, establishing an input circuit not present in the adult organism. The requirement of the photoreception pathway contrast with the lack of necessity for both Cry and PDF. The precise requirement of Cry for entraining the molecular clock is not fully understood, although it can overcome the lack of visual phototransduction (and vice versa)(Kaneko, Hamblen and Hall, 2000; Mazzoni, Desplan and Blau, 2005). Temporal information can persist inside the fly since the end of the embryonic stage, with adults Per rhythms in synch with environmental cycles from early larva if no other cues are received (Sehgal, Price and Young, 1992; Kaneko, Hamblen and Hall, 2000). Some cells express clock components during development, only to lose them or simply disappear (Ruiz *et al.*, 2010).

The question whether circadian clocks have a role in development is not intuitive at first glance. This is because of the constant presence of Light-Dark cycles in nature and the normal development of *per* and *tim* mutants (Konopka and Benzer, 1971; Sehgal *et al.*, 1994). Besides the independent cellular function of some clock components, the regulation of at least Clk-Cyc function by the molecular oscillator has developmental consequences (Goda *et al.*, 2011). Intriguingly, selective targeting of the clock inside the steroid hormone-producing prothoracic gland results in developmental lethality because of larvae failing to reach pupa stage (see Chapter 2.1.1.1) (Di Cara and King-Jones, 2016). While this points to a required synchrony between hormone signalling and external cycles, it is not known how this is not achieved in this experimental setup like in the viable null mutants (Konopka and Benzer, 1971; Sehgal *et al.*, 1994; Di Cara and King-Jones, 2016).

1.4 The small GTPase Rho1 and the Rho1-signalling pathway

1.4.1 Rho1 GTPases and Rho1

Our current understanding of living beings considers the ability to respond to the environment one of their core characteristics (Koshland, 2002). Cells require elements that interact with the outer medium and that transform the received signals in intracellular changes, contributing to the complex cell signalling pathways. A common feature is the employment of the so-called molecular switches. These are proteins with alternate on/off states that trigger downstream biochemical cascades and modify cell processes (Alberts *et al.*, 2002). The outcomes of cell signalling include proliferation, differentiation, apoptosis or survival, adhesion, and particularly for the case of this

thesis, a dynamic cytoskeleton. Cells have three types of cytoskeleton components: microtubules, intermediate filaments and actin filaments. The Rho GTPases constitute a family of molecular switches with the role, among others, of regulating the last two (Boureux *et al.*, 2007).

The Rho GTPases are one of the nine protein families that comprise the Ras superfamily, composed of small guanosine triphosphatases (GTPases) (Wennerberg, Rossman and Der, 2005). The small GTPases are monomeric G Proteins with a shared structure related to the α subunit of the heterotrimeric G proteins (Wennerberg, Rossman and Der, 2005). In their resting ("off") state, they contain Guanosine Diphosphate (GDP), which is substituted by Guanosine Triphosphate (GTP) when activated ("on" state). An activated GTPase hydrolyses GTP into GDP (dephosphorilation), releasing a free phosphate (Pi, the third or γ-phosphate) and energy. This reaction can lead to a phosphorylation cascade and further events in cell signalling (Denhardt, 1996).

The mammalian RhoA gave its name to the family being the first discovered. RhoA stands for "Ras homolog gene family, member A" and its structure was originally predicted from the genetic sequence ((Madaule and Axel, 1985). As GTPases, Rho proteins have conserved domains: a N-terminal region with a phosphate-binding loop, as well as the Switch I, Switch II and C-terminal regions. The two critical Switch regions, bound to the γ-phosphate via NH groups, undergo conformational change between the two states (Vetter and Wittinghofer, 2001; Lartey and Lopez Bernal, 2009). Switch regions are also binding sites for positive and negative regulators (Li and Zheng, 1997; Dvorsky and Ahmadian, 2004). The C-terminal region contains a hypervariable region and the CAAX motif (Cys, two aliphatic residues and any other residue), which is involved in posttranslational regulations required for the protein to be anchored to the cell membrane (Gao, Liao and Yang, 2009; Lartey and Lopez Bernal, 2009).

Rho GTPases are exclusive to eukaryotic cells, where they show remarkable sequence conservation. Three subfamilies are known, named Rho, Cdc42 and Rac because of their founding members (Boureux *et al.*, 2007). Each of the three proteins sits at the core of a signalling pathway, and the cooperative role between the three regulates actin cytoskeleton, but also signal transduction (Etienne-Manneville and Hall, 2002). The Rho1-signalling has mostly been studied for its role in the formation of the actin stress fibers (Ridley and Hall, 1992).

Drosophila melanogaster expresses Rho1, homologue of RhoA, which constitutes the core of the Rho1-signalling pathway. The protein contains 193 aminoacids and weights 22 kDa, with a high sequence homology with other invertebrate Rho1s and the human RhoA proteins (Pham *et al.*, 2009). A similar degree of conservation is found in many components of the fly Rho1-signalling pathway (Bernards, 2003; Verdier, Guang Chao and Settleman, 2006). Rho1 is an essential

component of cellular life and loss-of-function mutants die during embryonic stage, although heterozygous individuals are perfectly viable(Magie *et al.*, 1999). The Rho1-signalling pathway, with related elements, is represented in Figure 1.4.

1.4.2 Upstream regulators of Rho1

The "on"/ "off" switch of Rho1 depends on its interaction with several positive and negative regulators. Many of them are firstly activated by extracellular signals, often mediated by integrin-cadherin signalling (Wei *et al.*, 2000; Huveneers and Danen, 2009; Watanabe, Sato and Kaibuchi, 2009; Ojelade, Acevedo and Rothenfluh, 2013). The Guanine nucleotide Exchange Factors (GEFs) act as the positive regulators or activators of GTPases. They stimulate the release of GDP allowing the binding of GTP, setting the "switch on" state for Rho1(Cherfils and Zeghouf, 2013). RhoGEFs usually have a Dbl homology (DH) domain, which takes on several roles, including that of nucleotide exchange and it is considered to be necessary to their activity (Brugnera *et al.*, 2002). The Pleckstrin homology (PH) domains allow the GEFs to retain a near-to-membrane location, and both activate and inhibit the DH domain (Bishop and Hall, 2000; Brugnera *et al.*, 2002; Cherfils and Zeghouf, 2013).

Several RhoGEFs have been discovered in *Drosophila*. Pebble (Pbl) was firstly studied via its role in cytokinesis (Prokopenko *et al.*, 1999; Gregory, Lorensuhewa and Saint, 2010). Concurrently, RhoGEF2 has attracted attention of developmental biology because of its role during embryonic stages (Barrett, Leptin and Settleman, 1997; Wenzl *et al.*, 2010). Trio is a non-specific GEF whose activity has been found in different contexts within *Drosophila*, especially development of nervous system (Bateman, Shu and Van Vactor, 2000; Iyer *et al.*, 2012; Shivalkar and Giniger, 2012).

In contrast, the GTPase Activating Proteins (GAPs) increase GTP hydrolysis activity and thus work as negative regulators by causing GTP hydrolysis without the expected substrates (Moon and Zheng, 2003; Boureux *et al.*, 2007). They have not been as studied as GEFs, although they are equally necessary to establishing the RhoGTPase cycle (Jacobs T. and Hall, 2005). Therefore, their disruption lead to consequences in similar models (Billuart *et al.*, 2001; Greenberg and Hatini, 2011; Nahm and Lee, 2011; Pilgram *et al.*, 2011). RhoGAPs contain the homonymous 140 aa RhoGAP domain, involved in the binding to RhoGTPases (Lamarche and Hall, 1994; Moon and Zheng, 2003). Genome and sequencing analysis indicate that the RhoGAP group interestingly outnumbers the RhoGTPases (Moon and Zheng, 2003; Jacobs T. and Hall, 2005). A third group of proteins, Guanine Nucleotide Dissociation Inhibitors or GDIs, forms complexes with GDP-bound GTPases and sequester them in the inactivated state (Wennerberg, Rossman and Der, 2005; Cherfils and Zeghouf, 2013).

Extracellular signals that activate the pathway are usually mediated via the cell surface integrin and cadherin signalling (Wei *et al.*, 2000; Huveneers and Danen, 2009; Watanabe, Sato and Kaibuchi, 2009; Ojelade, Acevedo and Rothenfluh, 2013). Phosphoinositide 3- kinases (PI3Ks) often activate GEF activity (Innocenti *et al.*, 2003). The GEF Trio interacts with the receptor protein tyrosine phosphatase Lar (Bateman *et al.*, 2000).

1.4.3 Downstream effectors and targets of Rho1

The Rho1-signalling pathway contains many proteins that interact among themselves while also exhibiting crosstalk with other pathways, including the Cdc42 and Rac pathways. One of the main immediate downstream targets of Rho1 activity is Rok, (Drosophila Rho-Kinase). Rok shares homology with the mammalian Rho-associated Coiled-coil Kinase (ROCK) and directly interacts with Rho1 (Mizuno *et al.*, 1999; Amano, Nakayama and Kaibuchi, 2010). Another Rho1 effector is Diaphanous (Dia). Unlike Rho1 and Rok, Dia was discovered firstly in *Drosophila*, and afterwards in mammals because of their homology (Castrillon and Wasserman, 1994; Watanabe *et al.*, 1997). Both effectors act on different downstream products, contributing to the complexity of the network. Dia phosphorylates Chickadee (Chic, the *Drosophila* homologue of mammalian Profilin), which promotes actin nucleation (Pantaloni and Carlier, 1993). Respectively, Rok activates several signalling cascades, like the one starting with Lim-kinase1(Limk1)(Ohashi *et al.*, 2000b). This protein phosphorylates and activates the *Drosophila* homologue of Adf/Cofilin, Twinstar (Tsr) (Gunsalus *et al.*, 1995; Ohashi *et al.*, 2000a). Tsr protein promotes re-structuration of actin by severing fibres and actin turnover (Carlier *et al.*, 1997; Chen *et al.*, 2001). Rok also exerts its function with nonmuscle Myosin II. The hexameric protein is closely related to the one found in mammalian smooth muscle, hence its name. Nonmuscle Myosin II is composed of three pairs of subunits: the heavy chain (MHC), encoded by *zipper* (*zip*), the regulatory light chain (MLC or sometimes MRLC), codified by the gene *spaguetti-squash* (*sqh*) and the essential light chain (Mlc-c) (Edwards and Kiehart, 1996; Aldaz, Escudero and Freeman, 2013). Rok phosphorylates Sqh, leading to contraction of the actin fibres (Karess *et al.*, 1991; Ito *et al.*, 2004; Vicente-Manzanares *et al.*, 2009). Rok also inhibits MLC Phosphatase (MLCP, also known as Flapwing or Flw), one of the several dephosphorylating agents which inhibiting Sqh (Ito *et al.*, 2004; Vereshchagina *et al.*, 2004; Wang *et al.*, 2009). Activity of Sqh can also be promoted with the MLC Kinases (MLCK)(Kojima *et al.*, 1996; Totsukawa *et al.*, 2000).

1.4.4 Interactions with other actin regulator modules

According to the interactome of the Rho1-signalling pathway frequently interacts with Rac, Cdc42 and downstream components to constitute the dynamics of the actin cytoskeleton (Boureux *et*

al., 2007; Mack and Georgiou, 2014). Collaboration between different actin regulators are often seen with interactions with cellular routes like Wnt (Wingless-related integration site, derived from the *Drosophila* Wingless or Wg) -signalling (Winter *et al.*, 2001; Habas, Dawid and He, 2003; Schlessinger, Hall and Tolwinski, 2009). Many of these interactions are promoted by RhoGEFs, whose differential specificity towards Rho1/RhoA, Rac or Cdc42 lead to a diversity of response cascades (Shivalkar and Giniger, 2012; Kher *et al.*, 2014; Li *et al.*, 2014a), but can also occur downstream. For example, Chic activity in actin elongation is promoted by Dia, but also by Arp2/3, activated by Wiskott-Aldrich Syndrome Protein (WASP), downstream effector of Cdc42 and collaborator of Rho1-signalling (Wear, Schafer and Cooper, 2000; Liu *et al.*, 2009). The serine-threonine kinase Pak is activated by both Rac and Cdc42 and also promotes Lim kinases activity (Harden *et al.*, 1996; Ridley, 2001) . As an example of antagonistic interactions, at least in some cellular context, Cdc42-signalling pathway negatively regulates Sqh activity by targeting the MLCKs (Vlachos and Harden, 2011).

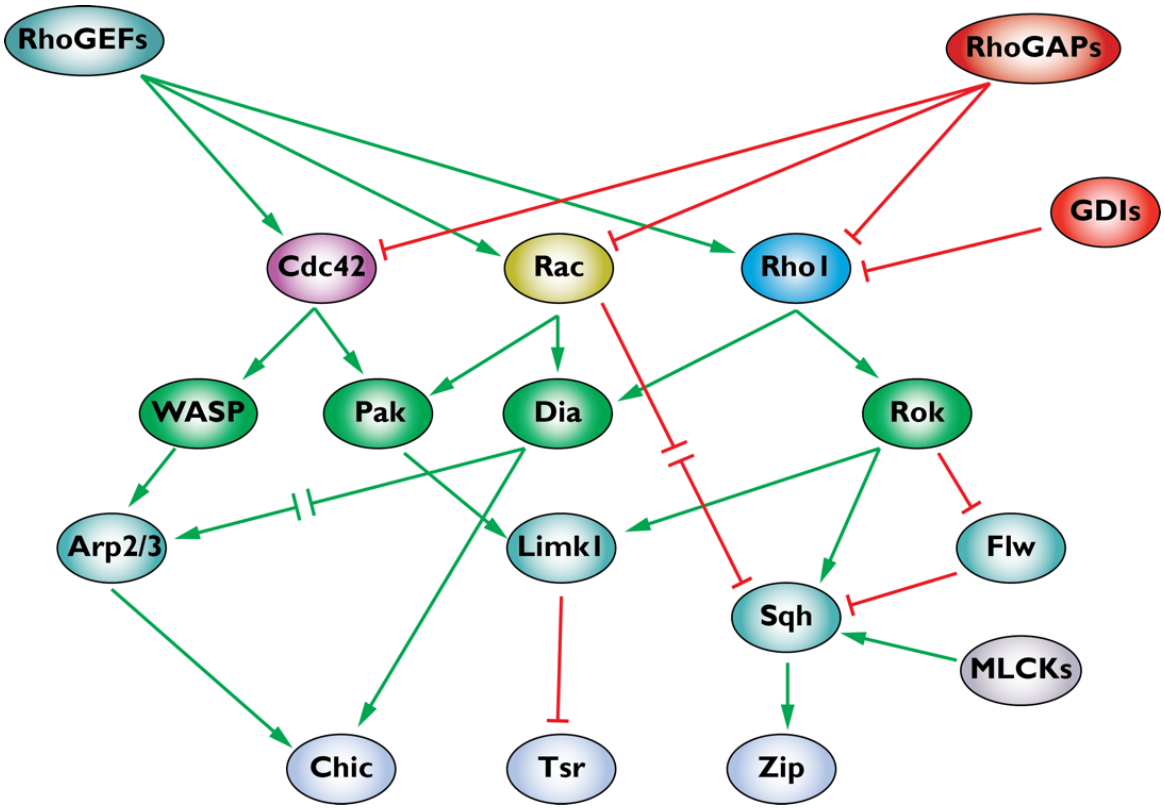

Figure 1.4. The Rho1-signalling pathway in *Drosophila melanogaster*. Main interactors of Rho1-signalling are shown, as well as related actin regulators. Rho1 is activated from the inactive GDP-bound form by Guanine nucleotide Exchange Factors (GEFs) such as Pbl, RhoGEF2 and Trio, while GTPase Activating Proteins (GAPs) promote the inverse reaction. Guanine Nucleotide Dissociation Inhibitors (GDIs) sequester RhoGTPases in an inactivated state. Downstream effectors of Rho1 include Diaphanous (Dia), which together with Chickadee (Chic) promotes the nucleation and elongation of actin filaments; and Rok, which promotes

stabilization of actin via LIM kinase (Limk1) by inhibiting Twinstar (Tsr) and actomyosin assembly contraction via non-muscle Myosin II (Spaguetti Squash, Sqh, and Zipper, Zip), both directly and indirectly (Flapwing, Flw) along other proteins (MLC kinases, MLCKs). The pathway interacts with Rac and Cdc42 signalling pathway, mostly through WASP and Arp2/3 (actin branching). Proteins like Pak further link the different actin dynamics regulators. Interrupted lines indicate indirect interaction throughout other components of the pathway.

1.4.5 Functions of Rho1 and the Rho1-signalling pathway

The multiple functions of the Rho1-signalling pathway make it one of the critical modules of cellular life. They include cell contraction, cell division, cell motility, morphology, neurogenesis, and cell polarity. These functions are often shared with other cellular pathways (Castrillon and Wasserman, 1994; Magie *et al.*, 1999; Ridley, 2001; Schlessinger, Hall and Tolwinski, 2009; Hall and Lalli, 2010; Tolias, Duman and Um, 2011). It is considered that Rok is a critical component, both for its mediator role between Rho1 and effectors and for its relay role for connecting the pathway with others like Wnt-signalling and related processes like planar epithelial polarity (Winter *et al.*, 2001; Riento and Ridley, 2003; Amano, Nakayama and Kaibuchi, 2010). Consequently, Rho1-signalling can also be involved in disease, particularly cancer (Li and Lim, 2003; Guan *et al.*, 2013; Khoo *et al.*, 2013; Ba *et al.*, 2016).

In neuronal development, The Rho1-signalling pathway, as well as Rac and Cdc42, intervene in different functions, including microtubule growth and stabilization. Some components of these pathways have been well studied in neuronal context, like a specific WASP found in neurons (NWASP)(Rohatgi, Ho and Kirschner, 2000). RhoGTPases have critical roles in the development of the nervous system, where Trio has been extensively studied (Bateman, Shu and Van Vactor, 2000; Iyer *et al.*, 2012) and Rho1 specifically promotes neurite retraction (Lee *et al.*, 2000). Axon development also requires the function of these pathways in formation, guidance and stabilization stages (Ruchhoeft *et al.*, 1999; Luo, 2000; Kim *et al.*, 2002b). Actin dynamics also intervene in established synapsis, where they mediate in the effects and responses of both pre- and post-synaptic neuron contributing to neuronal plasticity (Matus, 1999; Dillon and Goda, 2005; Cingolani and Goda, 2008; Ojelade, Acevedo and Rothenfluh, 2013). The role of actin inside the cell nucleus remains not fully understood, but several data point to a role of this cytoskeleton and its regulators in interactions with cytoplasm, nuclear transport and genic expression (Zheng *et al.*, 2009a; Pawlowski *et al.*, 2010; Weston, Coutts and La Thangue, 2012; Falahzadeh, Banaei-Esfahani and Shahhoseini, 2015).

1.4.6 Interactions of Rho1-signalling and the circadian behaviour

As a core component of neurons and any other associated cell types in their environment, researchers have proposed links between actin cytoskeleton and animal behaviour (Ojelade, Acevedo and Rothenfluh, 2013). Many of the proposed interactions rely in the way synaptic plasticity can modulate external and behavioural responses and the known role of actin dynamics on different neuronal contexts (Matus, 1999; Dillon and Goda, 2005; Hlushchenko, Koskinen and Hotulainen, 2016; Sweatt, 2016). Actin cytoskeleton, its regulators and binding proteins can exert different effects over communicating neurons (Cingolani and Goda, 2008; Ojelade, Acevedo and Rothenfluh, 2013)

However, a more specific connection between Rho1-signalling and the circadian behaviour was found by Dr Neethi Varadaraja Rao, who obtained her PhD under the supervision of Dr Herman Wijnen at the University of Virginia (USA), in the year 2013. Some of the results of that project constitute the basis of the current proposed project. Through a genetic screen, it was discovered that Rho1 was involved in the re- entrainment of circadian rhythms by temperature. Deficiencies of *Rho1* genetic dosage led to an early temperature re-entrainment. As temperature input remained unaffected, it was determined that the reason was a weakened clock. This was further confirmed by the reduced rhythmicity of the given flies in *free run*. It was also found that gene targeting of *Rok* inside the PDF-expressing neurons extended the endogenous period length of the flies. The *Rok* knockdown phenotype was related to alterations in the neuronal state or PDF-signalling, but with a delay in the molecular clock.

During the realisation of this project, we kept in contact with Justin Blau group, which uncovered a circadian regulation of Rho1 inside the s-LN_vs as a way of controlling the dorsal termini remodelling of these neurons (Petsakou, Sapsis and Blau, 2015). Because of the phenotypical similarities (and differences) with the presented research project, the experimental results presented in this thesis will be further compared to this work. It constitutes an example of how a critical component of cellular life can specifically interact inside discrete neurons to regulate the behaviour of an organism (Petsakou, Sapsis and Blau, 2015). The complete behavioural consequences of this interaction, and the underlying mechanisms, remain elusive.

1.5 Project aims

The precise mechanisms that organise the *Drosophila melanogaster* clock cells into a neuronal circuit that relays time information from an established molecular clock to an effective output in the activity of the animal is still a puzzling question. This is partially because of the unknown circuitry pathways and also because of the uncharacterized interlinking components. Previous

experiments from our group showed that chromosome deficiencies associated with the small GTPase *Rho1* gene correlate with a circadian phenotype. Therefore, based on the information gathered from literature and early experimental results, this project proposed to address the mechanisms by which the small GTPase Rho1 interacts with molecular time keeping in clock neurons to control locomotor activity rhythms.

This can be further detailed into four main aims, outlined here and presented throughout Chapter 3:

- **Is the small GTPase Rho1 required for the normal establishment of the adult *Drosophila melanogaster* circadian behaviour? (Chapter 3.2 and subsequent).** To answer this question, it is precise to specifically link the *Rho1* gene product to found circadian phenotypes. This means different ways of targeting the small GTPase must reproduce the same behavioural output. The employment of classic mutants and more advance and precise techniques will allow to provide with an answer.
- **What are the spatial and temporal requirements for Rho1 function for the adult behavioural rhythms? (Chapter 3.3)** As the circadian behaviour is controlled by discreet populations of neurons inside the fly brain, any given circadian phenotype could uncover a specific requirement of the protein under study inside the clock circuitry. Rho1 could be specifically required inside some clock cell clusters for acting upon circadian behaviour. With the clock neurons interacting with each other in an established hierarchy, the place of Rho1 function itself can give cues to answer the third question.
- **How does Rho1 interact with the circadian clock? (Chapter 3.4 and 3.5)** This question represents the ultimate aim of the project. The circadian behaviour of the adult fly is the final quantifiable output of a series of information transmissions from the acquisition of external cues to the resulting activity:rest rhythm. The characterization of Rho1-associated phenotypes, and the spatial/temporal requirements for them will allow to develop hypothesis that will be further tested by interrogating the clock circuitry and subjecting the flies to different experimental conditions.
- **What are the effects on environmental sensitivity related to the role of Rho1 in the circadian behaviour of *Drosophila*? (Chapter 3.6).** The last question deviates from the previous three. Instead of studying the circadian behaviour (in *free run*), the last subchapter characterises the behavioural response of the fly while facing environmental cues. As the animal output under these conditions resembles natural conditions more than laboratory ones and it is still clock-controlled, it constitutes a major and necessary point to be addressed for the characterisation of the role of Rho1.

Therefore, the project has the main goal of providing insight into the possible relationship between a well characterised cellular process and a highly tissue-specific mechanism. The resolution of the detailed aims will expand the current knowledge of the *Drosophila melanogaster* circadian clock. The different experiments will characterise behavioural phenotypes affecting the whole organisms but emerging from specific targeting of a restricted number of cells. The shared homologies between flies and humans (where discreet clock neurons can also profoundly alter the behaviour) as well as the evolutionary conservation of many of the involved genes and proteins, confers this project the possibility of granting useful information about the mammalian circadian rhythms. Increasing the knowledge of animal systems will have positive effects over our understanding our own physiology, and will improve human health and welfare.

Chapter 2: Methodology

2.1 *Drosophila melanogaster* as model organism

2.1.1 *Drosophila melanogaster* culture

2.1.1.1 Life cycle and culture

Drosophila melanogaster individuals develop in approximately ten days at room temperature (RT, 23° C) after egg laying. The embryonic stage (24 hours) is followed by three larva stages or instars (approximately five days) and the pupa stage (three days). Flies were kept in glass or plastic vials containing approximately 10 ml of solidified fly food media. Unless specified otherwise, flies were raised and kept at 23 °C inside Environmentally Controlled Rooms (ECRs) with a constant humidity of 70%. Flies were sometimes raised at 17 °C or 29 °C for experimental purposes, always specified in the results presentation in Chapter 3.

The food composition is based on the recommendations of the Bloomington Drosophila Stock Centre (BDSC) at Indiana University (Indiana, USA) and contains, per each litre of distilled water:

- 9 g *Drosophila* agar
- 17.5 g yeast
- 10 g soya flour
- 73.1 g yellow maize meal
- 46.2 g light malt extract
- 48 g dry weight sucrose
- Anti-fungal agents: 5 ml Propionic acid (final concentration of 0.005%) and 7 ml methyl paraben (Tegosept, Genesee Scientific) (10% m/v in EtOH 95%, final concentration of 0.07%).

Unused, uninteresting or old flies were discarded inside a morgue (EtOH 70%) or frozen inside the vials as part of the Health and Safety protocols of the University of Southampton. All the flies and fly-containing items were incinerated or autoclaved as part of the DEPHRA guidelines of GMO handling.

2.1.1.2 Cross scheme

Many of the employed experimental protocols required crossing two different fly strains to achieve experimental individuals. Flies carry four pairs of chromosome, with the first pair determining the gender based on the X/autosomes ratio (usually XX for females, and XY for males.

Many of the transgenic constructs are available for the X and the second and third pair of chromosomes because of the small size of the Y and fourth pair. Stable lines usually carry the chromosomes of interest as homozygotic or with a balancer chromosome. These are artificially altered chromosomes with a functional set of genes, yet unable of lining up and recombining with their homologues, resulting in a lack of genetic recombination with the chromosome of interest. As balancer chromosomes are lethal in homozygosis, this is an ideal method for conserving unaltered genetic constructs, especially those with lethal effects if homozygotic. Balancer chromosomes usually carry visual markers that allow researchers to identify them (and therefore, identifying the construct because of the lack of this cues). Usually, fly lines are made in a *white* (w^{1118}) mutant background, so the flies would normally have white-coloured eyes as opposed to the wild-type red. Many transgenic constructs include a working copy of the gene (named w^{+} or *miniwhite*), so the eye colour indicates the presence of the construct. As *w* gene is located at the X-chromosome, male eyes are usually more sensitive to the presence of *miniwhite* constructs, as they normally carry a single copy of the gene.

Crosses consist of the combination of virgin females and males (whose virginity is not required). Virgins were collected based on the physical characteristics displayed by newly hatched flies and in the fact that flies do not engage in mating behaviour during at least the first eight hours after eclosion. Maternal stocks were chosen based on the requirement of constructs inside the X chromosome, as the single copy in males is always inherited from the mother. Adults were kept inside the vials for approximately four days, and always moved to a new vial before offspring hatch. Individuals from the F1 were collected during the successive days, always before the F2 larva reached the pupa stage.

Cross schemes were designed to achieve when possible isogenic controls, that is, siblings of the experimental flies and therefore a similar genomic composition excluding genetic variables of interest. When not possible, one of the paternal stocks was employed, and always with flies that hatched at the same time than the experimental individuals. Flies were divided, unless specified, by gender during the experiments. This is because of both dosage-dependent effects, like the expression of transgenes in the X chromosome (like *UASDcr2w*), and possible gender differences (see Chapter 1.3.9). Minimizing genetic background differences is a way of controlling the experimental conditions, as they in some cases can affects circadian behaviour (Zimmerman *et al.*, 2012). The balancer chromosomes CyO^{1} (II, containing an allele of dual oxidase (*Duox*), $Duox^{Cy}$, curly wings) and $TM6B,Tb^{1}$ [III, identified by $Tubby^{1}$ (Tb^{1}) larvae and *Humeral* (Hu, neomorphic allele of *Antennapedia*, *Antp*) bristles] balancer chromosomes proved not to affect fly rhythmicity and were consistently used as isogenic controls (Lindsley and Zimm, 1992). The second chromosome markers *Scutoid* (*Sco*, missing scutellar bristles; allele of *snail*, sna^{Sco}) and *Irregular*

facets (*If*^{1}, aberrant eye formation; allele of *kruppel*, *kr*^{If}) were used sometimes in conjunction with *CyO*^{1} for established stocks (McGill *et al.*, 1988; Carrera *et al.*, 1998). Both markers were discarded to be used in experiments as they seemed to reduce rhythmicity in the carriers. The balancer *TM3Ser'* (III) also showed to cause locomotor defects. As a way of action, *TM3Ser*^{1} was only used as balancer chromosome during cross schemes and for experiments where rhythmicity was not tested (like expression analysis). *If*^{1} and *Sco* were never used without the balancer chromosome *CyO*^{1}.

2.1.1.3 The Gal4/UAS system: spatial control

The development of the Gal4/UAS system by Andrea Brand and Norbert Perrimon is considered a milestone in the recent *Drosophila* research (Figure 2.1 A)(Brand and Perrimon, 1993). Gal4/UAS is a refined binary expression system that allows express any genetic construct inside selective cells or tissues. It is based on the yeast transcription activators, key finding in the studies of genetic expression (Johnston and Hopper, 1982; Ptashne, 1988). The presence of the exogenous transcription factor Gal4 does not normally cause detrimental effects of the fly. The protein is introduced via the insertion of the codifying sequence inside the fly genome, either randomly next to a promoter/enhancer sequence (*enhancer trap* technique) or with a preceding promoting sequence of interest. That way, the expression of Gal4 is controlled by a cis-element (usually denominated *driver*) that will restrict it to specific cells or lineages. Because of this many available Gal4 lines carry the name of the gene whose driver is used (total or partially), like *elav-Gal4* (neuron lineages), or *Pdf-Gal4* (neurons expressing this neuropeptide). Additionally, the genome of the fly also contains the Upstream Activating Sequence (UAS), a yeast enhancer that allows Gal4 to drive expression. UAS will then drive the expression of any element of interest, from reporter genes (foreign elements like Green Fluorescent Protein or GFP, β-galactosidase, or Calcium sensors, among many others) to exogenous genes (like apoptotic genes like *reaper* for genetic ablation; ionic channels for silencing or exciting neurons; and many other possibilities). Keeping Gal4 and UAS lines independently guarantees the great versatility of the system, with many experiments requiring only one single cross. The Gal4/UAS system can be combined with others for more combinatorial and mosaic possibilities (Pfeiffer *et al.*, 2010). Despite the system being an extremely powerful tool, it is not perfect. Some works have reported side effects and off-target of the Gal4 protein (Fischer *et al.*, 1988; Liu and Lehmann, 2008). One of the system limitations is also the temporal control of the genetic expression, which is restricted to the temporal window of the driver sequence.

2.1.1.4 The TARGET system: temporal control

There exist several ways of achieving temporal control of genetic expression in *Drosophila*. Usually, these techniques relay in a change of an environmental variable to act as an on/off switch of the Gal4/UAS system. For example, the modified GeneSwitch (GS) Gal4 system expresses a modified Gal4 protein only active when RU-486 (mifepristone) is added to the diet (Nicholson et al., genetics 2008). The repressor Gal80 is another component of the galactose regulon in yeast and blocks the activity of Gal4 proteins (Johnston and Hopper, 1982). A modified, temperature-sensitive Gal80 protein ($Gal80^{TS}$) is the basis of the Temporal And Regional Gene Expression Targeting (TARGET) system (Figure 2.1 B). This repressor is inactivated at 29 °C (*restrictive* conditions for Gal80), and is fully efficient at 17 °C (*permissive* conditions for Gal80), both temperatures inside the range tolerated by flies (McGuire *et al.*, 2003). This way, Gal4/UAS system will only be active when flies are at the high temperature, thus reaching temporal control of gene targeting, albeit once conditions are permissive again, the already expressed construct will cause its effect until degraded by cell machinery. $Gal80^{TS}$ was expressed inside all the fly cells with the ubiquitous *tubulin* driver (*tub-*$Gal80^{TS}$). Gal80 can also be expressed with a driver just like Gal4 and permanently restrict the spatial domain of the Gal4 expression (Suster *et al.*, 2004).

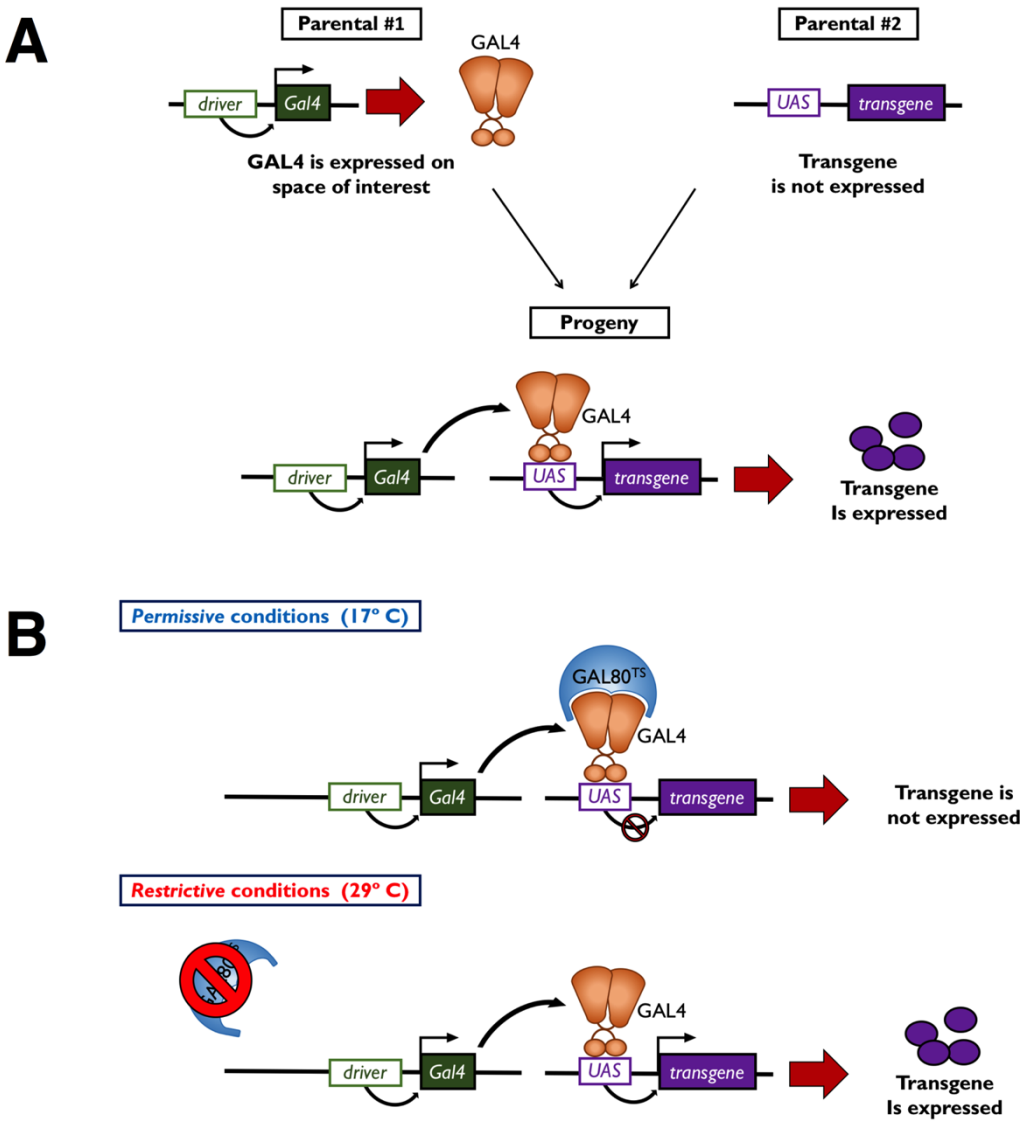

Figure 2.1. Spatial and temporal control of genetic expression with Gal4/UAS and TARGET systems. **A)** Gal4/UAS system as developed by Brand and Perrimon (Brand and Perrimon, 1993). Experimental progeny receives the *Gal4* driver with the promoter sequence of a gene of interest from one parental, and the *UAS* construct with the transgene of interest from the other. Both elements are therefore found in the same genome inside the progeny, and Gal4 protein is only expressed inside the tissues or cells ruled by the driver sequence. **B)** TARGET system enhances the Gal4/UAS system by adding an on/off switch to refine temporal control (McGuire *et al.*, 2003). *Permissive* conditions (approx. 17° C) allow the Gal80 repressor to block Gal4 activity, while *restrictive* conditions (29° C) inactivate the repressor, allowing the Gal4/UAS to be functional. $Gal80^{TS}$ is usually expressed across all the fly cells with a ubiquitous driver (for example, *tubulin*).

2.1.1.5 RNA interference: genetic knockdown

RNA interference (RNAi) consists of the reduction of expression levels of a determined gene by using double-stranded interfering RNAs (dsRNAs, also named RNAis). The sequence is complimentary to the gene to be targeted, and employs an existing cell mechanism (RNA-Induced Silencing Complex or RISC) involved in protection against foreign RNA (Fire *et al.*, 1998; Jana *et al.*, 2004). As a way of increasing the cellular mechanism efficiency, the endoribonuclease Dicer-2, involved in the long hairpin dsRNA processing, is overexpressed with the *UASDcr2w* construct (the w indicates it carries a w^+ rescue for visual detection)(Dietzl *et al.*, 2007; Okamura *et al.*, 2008). The RNAi stocks are available usually from large transgenic fly stock collections. This work employed lines acquired at BDSC (NIH P40OD018537) (Indiana, USA), National Institute of Genetics (NIG-fly stock centers, Kyoto, Japan) and Transgenic RNAi Project (TRiP, Harvard Medical School, USA). Specific details about each RNAi lines can be found in the next subchapter.

2.1.2 List of fly stocks

Genotype sections specified information regarding the spatial location in the *Drosophila* genome of the gene/construct. Complete genotypes are named as follows: "X chromosome/X chromosome" ; "second chromosome/second chromosome" ; "third chromosome/third chromosome". The lack of dashes indicates homozygosity, and an empty space indicates wild-type/unaffected chromosome. For constructs, information about the location is provided for X (I), second (II), or third (III) chromosomes. Constructs were kept with balancer chromosomes (*CyO* for the second and *TM6B* or *TM3Ser'* for the third) or in homozygosity.

2.1.2.1 Mutants and strains

Genotype	Description	Source and Reference
w^{1118};;	Wild-type control (w mutant background).	Bloomington stock (Hazelrigg, Levis and Rubin, 1984)
w^{1118}; Df(2R)ED2457/SM6a;	Chromosome deletion of XX genes (2R:16000309; 2R:16130157).	Bloomington #8915 (DrosDel Project) (Ryder *et al.*, 2007)
w^{1118}; $Rho1^{1B}$/CyO;	Loss-of-function Rho1 allele with deletion of 52 C-terminal aminoacids.	Bloomington #9477 (Magie and Parkhurst, 2005)
w^{1118}; $Rho1^{E3.10}$;	Missense mutation (C189Y) at the Rho1 CAAX box reduces	Bloomington #3176

	the membrane-bound amount.	(Halsell, Chu and Kiehart, 2000)
Pdfr^{5304}; ;	Loss-of-function allele with deletion of transmembrane domain	Bloomington #33068 (Hyun *et al.*, 2005)
; ; Pdf^{01}	Loss-of-function allele with nonsense point mutation (Y21)	Bloomington #26654 (Renn *et al.*, 1999)
ywper^{01}; ;	Null mutant with nonsense point mutation (Q464)(Yu *et al.*, 1987)	Donated by M Young. (Konopka and Benzer, 1971)

Table 2.1. Mutant stocks.

2.1.2.2 Gal4 and Gal80 lines

This list details the precise names of the employed drivers and associated constructs. In the results chapter, they are often abbreviated (*tim(UAS)-Gal4* being *tim$_p$* for example).

Construct (Chromosome)	Description (adult brain)	Source and Reference
***tim(UAS)-Gal4* (II)**	Expresses Gal4 in all the clock-bearing cells.	Gift from M Young. Developed by S. Martinek in unpublished work. (Blau and Young, 1999)
***Pdf-Gal4* (II)**	Expresses Gal4 in PDF-expressing neurons.	Bloomington #6900 (Renn *et al.*, 1999)
***cry-Gal4-13* (III)**	Expresses Gal4 in morning and evening cells.	Gift from P Emery (Emery *et al.*, 2000b; Zhao *et al.*, 2003)
***R6-Gal4* (II)**	Expresses Gal4 in the s-LN$_v$s, with a very dim and rare expression in the l-LN$_v$s	Gift from P Taghert. (Helfrich-Forster *et al.*, 2007a)
***c929-Gal4* (II)**	Expresses Gal4 in DIMM-expressing cells, including many neuropeptidergic neurons and the l-LN$_v$s.	Bloomington #25373 (Taghert *et al.*, 2001; Park *et al.*, 2008)
***tubulin$_p$-Gal4* (III)**	Expresses Gal4 ubiquitously.	Bloomington #32184 (Lee and Luo, 1999)
***Mai179-Gal4* (II)**	Expresses Gal4 in the five 5 s-LN$_v$ pairs, 3 of the LN$_d$s, and	Gift from F Rouyer

	some of the l-LN_vs.	(Grima *et al.*, 2004)
***GMR78G02-Gal4* (III)**	Expresses Gal4 with part of the promoter sequence of *Spr*, in the 5th s-LN_v and the three cry$^+$ LN_ds	G Rubin (HHMI, USA) Bloomington #40010 (Schlichting *et al.*, 2016)
***GMR54D11-Gal4* (III)**	Expresses Gal4 with the promoter of *CG11448* in the ITP-expressing cells.	G Rubin (HHMI, USA) Bloomington #41279 (Yoshii *et al.*, 2015)
***Clk4.1M-Gal4* (III)**	Expresses Gal4 in 8-10 DN_1p neurons.	Bloomington #36316 (Zhang *et al.*, 2010a)
***Clk4.5F-Gal4* (III)**	Expresses Gal4 in 4 DN_1ps.	Bloomington #37526 (Zhang *et al.*, 2010a)
***Clk.1-3M9-Gal4* (II)**	Expresses Gal4 in the PDF$^+$ s-LN_vs and DN_2s.	Bloomington #41810 (Kaneko *et al.*, 2012)
***DvPdf-Gal4* (II)**	Expresses Gal4 in the *Pdf* domain of *D virilis*.	Gift from J Park (Bahn, Lee and Park, 2009)
***Pdf-Gal80* (II)**	Expresses the Gal80 repressor in the PDF-expressing clock neurons.	Gift from M Rosbash (Stoleru *et al.*, 2004)
***Cry-Gal80* (III)**	Expresses the Gal80 repressor in the Cry-expressing neurons.	Gift from M Rosbash (Stoleru *et al.*, 2004)
***Repo-Gal80* (II)**	Expresses Gal80 repressor in glial cells.	Gift from T. Lee (Awasaki *et al.*, 2008)
***tub_pGal80^{TS}* (II)**	Expresses Gal80^{TS} ubiquitously.	Bloomington #7108 (McGuire *et al.*, 2003)

Table 2.2. Gal4 drivers and complements.

2.1.2.3 UAS transgenic constructs

Construct (Chromosome)	Description	Source and Reference
***UAS-Dcr2w* (I and III)**	Expresses Dicer-2, component of the RNAi cellular machinery.	Bloomington stocks 24648 (X) and 24651 (III) (Dietzl *et al.*, 2007)

***UAS-mCD8::GFP* (III)**	Expresses GFP protein fused with the transmembrane murine CD8.	Gift from J Blau (Lee and Luo, 1999)
***UAS-Rho1.Sph* (III)**	Expresses wild-type copy of Rho1.	Bloomington #7334 (Weber and Mlodzik, 2003)
***UAS-Rho1^{V14}* (III)**	Expresses constitutively-active Rho1.	Bloomington #8144 (Fanto *et al.*, 2000; Weber and Mlodzik, 2003)
***UAS-Rho1^{N19}* (III)**	Expresses dominant negative Rho1.	Bloomington #7238 (Strutt, Weber and Mlodzik, 1997; Weber and Mlodzik, 2003)
***UAS-Rok.CAT* (III)**	Expresses a constitutively activated Rok kinase.	Bloomington #6669 (Luo, 2002; Neisch *et al.*, 2010)
***UAS-RhoGEF2$^{\Delta PDZ}$* (III)**	Expresses a mutant isoform of RhoGEF2 lacking the PDZ domain	Bloomington #6669 (Barrett, 2005)
***UAS-hid* (II)**	Expresses the pro-apoptotic protein Head involution defective (Hid)	Bloomington #65403 (Goyal *et al.*, 2000)
***UAS-luc* (III)**	Expresses firefly luciferase, employed as control for TRiP RNAi lines	Bloomington #35788 (Johnson, 2005)
***UAS-per16* (III)**	Expresses Period protein	F Rouyer (Blanchardon *et al.*, 2001)
***UAS-Wasp* (III)**	Expresses the WASP protein	Bloomington #39724 (Bellen, 2012)

Table 2.3. UAS constructs (excluding RNAi lines)

2.1.2.4 UAS RNAi stocks

For the *Rho1* RNAis, the numbers 1-4 indicate their designation in the Chapter 3. Unless specified, the construct 1 (*JF02809*) should be considered the default employed RNAi in the experimental setups.

Gene	Construct (Chromosome) (Stock)	Origin and references
Rho1	*1: JF02809* (III) (B27727)	Transgenic RNAi Project (TRiP, HMS, USA)
	2: HMS00375 (III) (B32383)	(Ni *et al.*, 2009; Ni *et al.*, 2011b)
	3: Rho1.325-786.dsRNA (III) (B29002)	(Warner and Cook, 2009; Warner and

	4: Rho1.770-1310.dsRNA (II) (B29003)	Longmore, 2009)
Rok	*NM_080535.2* (II) (9774R-3)	National Institute of Genetics Fly Stock
	NM_080535.2 (III) (9774R-2)	Cente (NIG, Japan)
Pbl	*GL01092* (III)(B36841)	TRiP (Ni *et al.*, 2011a)
RhoGEF2	*JF01747* (III) (B31239)	TRiP (Ni *et al.*, 2008)
	NM_057969.3 (II) (9635-R)	NIG, Japan
WASp	*JF01975* (III) (B25955)	TRiP (Ni *et al.*, 2008)
	HMS01534 (II) (B36119)	TRiP (Ni *et al.*, 2011a)
chic	*HMS00550 (III) (B34523)*	TRiP (Ni *et al.*, 2010)
Pdf	*JF01820* (III) (B25802)	TRiP (Ni *et al.*, 2009)

Table 2.4. UAS RNAi lines

2.2 Characterization of RNAi effectivity on genetic expression

2.2.1 Longevity/Survival assay

In order to measure the average lifespan of a fly population, males and females were collected within four days after eclosion. Flies were kept in small groups (up to five individuals) inside vials, and their identities were randomized and coded to avoid bias. Every two or three days, vials were inspected at morning, the dead flies were counted, and finally the surviving individuals were moved to a fresh vial. This way, escaped or accidentally stuck flies were excluded (censored) from the analysis. Daily observations were collected, analysed and plotted with GraphPad Prism 6 (GraphPad software, Inc.). In order to determine if there were survival differences among populations, Log-Rank (Mantel-Cox) test was performed (Mantel, 1966).

For the assayed flies in this project, the already described TARGET system was used to quantify the effect of post-developmental *Rho1* RNAi expression in the fly organism (*tubulinGal4* driver, targeting all the cells) (McGuire *et al.*, 2003). Flies were raised at 17 °C and moved to 29 °C when the experiment started. 3 different crosses were used with flies added in batches every two or three days.

2.2.2 Quantitative PCR assay

Quantitative PCR (qPCR) was utilised to measure the expression levels of the *Rho1* gene, a crucial requirement when employing RNAi techniques.

For flies carrying the $Rho1^{1B}$ mutant allele, as well as respective controls, adults were raised at 23 °C and then collected and kept at 17 °C for some days until the cross batch was completed.

Then the flies were frozen and the heads collected and stored at -80 °C. For flies expressing RNAis, *tubGal4* driver was again employed because of the limited spatial resolution of clock-related genes inside the whole head. The process was similar to mutant individuals but raising the flies at 17 °C to keep the RNAi expression off. Then, adult individuals were moved to 29 °C just like in the survival assay, with the heads being collected and frozen after a fixed amount of time (48 hours). All the qPCR experiments involved at least three biological replicates per genotype, with a different cross acting as each replicate.

Total RNAi was extracted from frozen heads with the the RNAqueous®-4pcr Kit (ThermoFisher Scientific). The RNA amounts were then measured with a Nanodrop® ND-100 spectophotometer (with the employed Elution buffer as blank). The qPCR reaction itself was performed with the Precision OneStep™ qRT-PCR Mastermix (Primerdesign) and run with a MJ Research PTC-200 (Bio-Rad). For the fixed volume of 20 µl, equal solutions were prepared to provide 25 ng of RNA per reaction (working concentration of 5 ng/µl).

Standard curves were run for *Rho1* and the selected housekeeping gene, *rpl32* (also known as *Ribosomal Protein 49*, or r*p49*) with a primer final concentration of 0.4 µM (Figure 2.2). *rp49* has a long usage as housekeeping gene in *Drosophila*, including circadian studies (Gabler *et al.*, 2005; Goda *et al.*, 2011; Pan *et al.*, 2015; Nikhil, Abhilash and Sharma, 2016). The employed primers were: *dmdydasrpl32F* (CAC TTC ATC CGC CAC CAGT), *dmrpl32R* (CGC TTG TTC GAT CCG TAA CC) (both Invitrogen), *Rho1qF1* (GGT GCC TGC GGT AAA ACT TG) and *Rho1qR1* (AGC TCC ACC TGT TTG CCA TC) (both Eurofins Genomics). New primers were designed with the NCBI online tool (Ye *et al.*, 2012), with additional validation for off targets with the DRSC/TRiP online tool (Perrimon, 2003).

Three technical replicates were run per each biological replicate. Reactions were run based on the detection of SYBR Green with the following program:

- 55 °C for 10 minutes.
- 95 °C for 8 minutes.
- Reaction cycle, repeated 40 times:
    - 95 °C for 10 seconds
    - 60 °C for 1 minute
    - Plate reading
- Measurement of melting curves between 60 and 95 °C each 0.2 °C (1 second holding) as *in silico* validation of results. Selected technical replicates were run in a 3% agarose gel (product lengths: 140 bp for *rp49* and 125 bp for *Rho1*).

Reactions were measured with Opticon Monitor Software (Bio-Rad), and the Rho1 levels (Relative to rp49) were determined by using the comparative Cycle threshold (Ct) method (Δct) (Schmittgen and Livak, 2008). Each biological replicated received a number consisting of the average of the validated technical replicates. Data were further processed and analysed in Microsoft Excel ® and SPSS® (IBM) with the t-test, o when assumptions were not accomplished with the Mann-Whitney *U* test (α= 0.05).

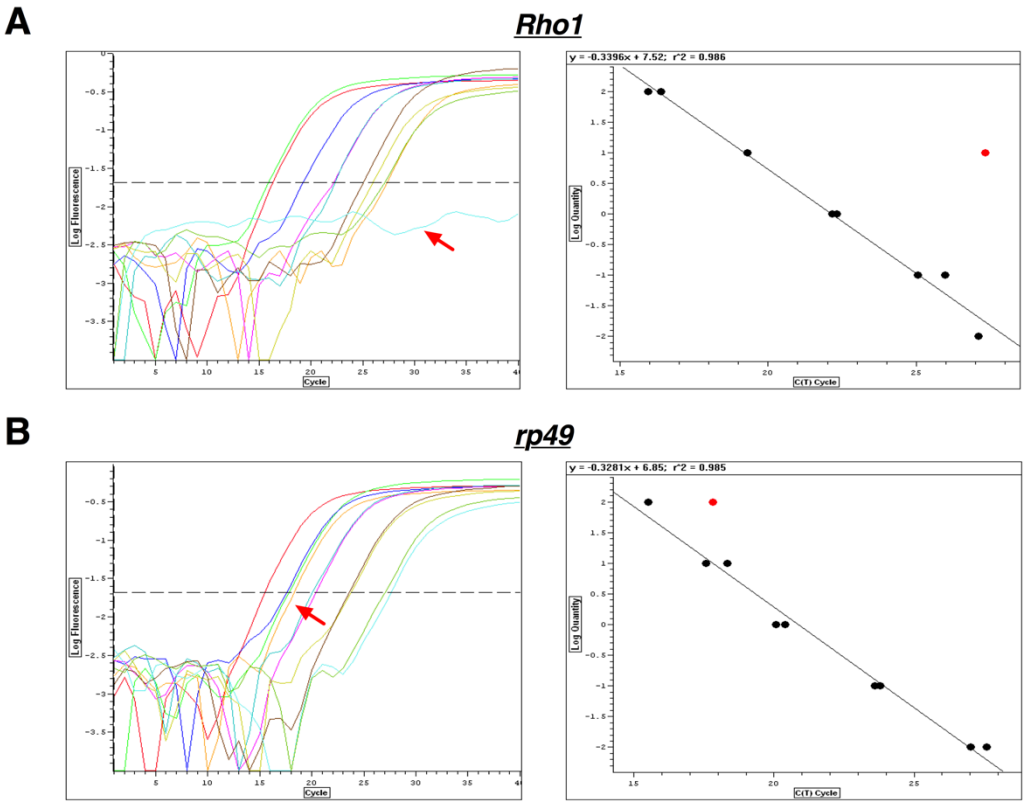

Figure 2.2. Standard curves for *Rho1* and *rp49* qPCR expression analysis. Left panels depict the fluorescence of the SYBR Green signal (log scale) in subsequent amplification cycles for *Rho1* (**A**) and *rp49* (**B**). Right panels show the Ct value (X axis) against the known RNA quantity (in 1/10 serial dilutions: 100, 10, 1, 0.1 and 0.01 ng/µl, Y axis) in order to establish the quantity formulas (Log quantity = -0.3396*C(t) + 7.52 for *Rho1*, and -0.3281*C(t) + 6.85 for *rp49*). By applying the formulas to subsequent C(t) readings of both genes, log quantity was achieved, and the quantity values were used to calculate the *Rho1*/*rp49* ratio per each biological replicate. Standard curves were calculated for the given primer concentration: 0.8 µl of a working solution 10 µM, resulting in a final concentration per reaction (total volume of 20 µl) of 0.4 µM. The graphs include, highlighted in red, a faulty technical replicate not used for the calculations.

2.3 Locomotor behaviour study

The most extensively utilised protocol in the experiments presented here is the study of the daily locomotor activity of adult flies. Typically, the assay involves the study of the circadian behaviour in *free run* following an entrainment phase under a given environmental cycle (usually, 12 hours of light followed by 12 hours of dark, or 12:12 LD). There exist experimental differences based on the different conditions and the specific period of analysis.

2.3.1 Fly maintenance and data acquisition

For these experiments, flies were held in 5 mm diameter glass tubes containing standard restricted diet food. The purpose of this type of diet is to provide adults with sufficient energy to live (sucrose) but to also avoid the development of offspring in the female-containing vials, as this would disrupt the experiment.

The restricted diet food has the following composition, for each 10 ml (1 set of 32 tubes) of medium:

- 0.5 g sucrose (final concentration of 5%)
- 0.1 g agar (final concentration of 1%)
- 70 µl methyl paraben (Tegosept) as anti-fungal preservative agent (Genesee Scientific, San Diego, CA, USA) (final concentration of 0.07%)

Activity for individual flies inside the tubes was recorded using Drosophila Activity Monitor (DAM) System (TriKinetics, Waltham, MA), with 32 tubes per monitor. For most of the assays, data were recorded for 14 days: 6 days of entrainment (i.e., LD cycles) and 8 days in *free run* (i.e., DD). The day of transition was not considered for analysis, and therefore *free run* behaviour was analysed on days 8-14 (7 in total). During the total length of the experiment, activity of individual flies was recorded within 5-minute long intervals (bin size: five minutes). Occasionally, counts were accidentally skipped because of monitor moving or hardware/software crashes. In the case of a system crash longer than twelve hours, the correspondent data were discarded. Activity logs were recorded in .txt files to be analysed with the specific software later detailed.

DAM system monitors were stored inside incubators, consisting of containers inside environmentally controlled rooms. Trays storing the monitors inside these incubators contained the sets of lights and were covered to guarantee light isolation. Room temperature (RT) conditions will always refer to experiments taking place at 23 °C with a relative humidity of 70%. Additional ECRs were employed when temperatures of 17 °C (*permissive* conditions for TARGET

assay) or 29 °C (*restrictive* conditions for TARGET assay) were used, always with a relative humidity of 70%. Temperature cycles inside the ECRs were also employed when indicated.

Environmental light testing by Karolina Mirowska provided the following intensities, measured at Photon Flux Density or PPF (µmol m^{-2} s^{-1}):

- Light for LD cycles: 0.97 PPF, with peaks at 441 and 541 nm. This is equivalent to approximately 50 Lux (as there is no direct conversion system).
- Red light inside the incubators: 0.57 PPF with a single peak at 630 nm
- Lights at Environmental Controlled Rooms: 1.53 PPF with several peaks.
- Red torch for *free run* handling (close contact): 1.75 PPF with single peak at 631 nm. However as supported by experimental data and literature, short exposition to red light is not sufficient to affect the fly clock (Hanai, Hamasaka and Ishida, 2008).

Multi-environmental locomotor assays were run in Percivall incubators, in order to precisely couple LD and temperature cycles of interest (see Chapter 2.3.3).

2.3.2 Analysis of adult circadian behaviour

Most of the data processing and early analysis of the DAM system output was performed with ClockLab, a Matlab-based program (Actimetrics)(Figure 2.3)(Pfeiffenberger *et al.*, 2010). First, visual observation of individual actograms (see next section) allowed to discard dead flies during the assay. Typically, for any given genotype, the following data were generated:

- **Actograms** of a given population (Figure 2.3, B). These figures visually depict the activity of a fly (or an averaged population) throughout the course of the experiment length. They typically two days per row, with the second day being repeated on the first day of the next row (day 1, day 2; day 2, day 3 and so on). This allow an easier interpretation and depiction of occurrences like a shorter or longer period, which cause displacement of the daily patterns towards left (shorter than 24-h period) or right (longer than 24-h period). Actograms were made by selecting "normalised" mode, averaging populations, with a bin size of 30 minutes (that is, gathering the 5 minute bins in groups of six) and start time at ZT12/CT12 (lights-off). Actograms were prepared for presentation in Microsoft Powerpoint® and Adobe Photoshop® (Adobe) in order to include environmental conditions, with no further modifications.
- **Activity profiles** of a given population (Figure 2.3, C). Activity profiles were made for average populations, with a bin size of 5 minutes (maximum possible resolution) and with a start date at ZT18 (six hours before *lights-on* event). Activity profiles are only presented for LD phase although during the course of the project were also generated sometimes for *free run*

days, adjusting the day length based on the endogenous rhythm of the fly (see next part). A series of days can be represented also with a **time series**, for a better observation of progressive changes. Activity profiles were also prepared for presentation in Microsoft Powerpoint® and Adobe Photoshop® (Adobe) in order to include environmental conditions and differentiate genotypes or conditions by colour, with no further modifications. Further analysis of the flies during the entraining period is described in Chapter 2.3.3.

- **Chi-squared (χ^2) Periodogram** analysis for individual flies (Figure 2.3, D). This analysis provided quantifiable data to be used for comparison among populations. χ^2 is one of the most widely used methods for assessing the rhythmicity of animals (Hamblen *et al.*, 1986; Blanchardon *et al.*, 2001). The test allows the program to identify not only the endogenous Period length (represented as Tau) of the circadian rhythm of the fly, but also its strength, measured with the Relative Rhythmic Power (RRP). This mathematical test runs individual fly files looking for a detectable rhythm from within a given period length range. This was set between 15 and 35 hours, with a bin size of 30 minutes, in order to avoid false positives with the harmonics at 12, 36 and 48 hours but also detect possible period length disruptions. The χ^2 test were always performed with a confidence level of 99%, so each test must reach a significance of less than 0.01 in order to discard the null hypothesis (no detectable period). The resulting period length is the one with the highest amplitude compared to the significant threshold (that is, the one with the strongest statistic evidence). Flies failing the test provide an error value and are therefore deemed as arrhythmic (AR) with no period length at all. RRP was calculated by dividing the test score by the significance threshold at that period length. This provides a value always higher than 1, with arrhythmic flies having a RRP between 0 and 1 that the program is unable to compute. Flies were scored as strongly rhythmic (SR, when 1.5<RRP), or weakly rhythmic (WR, when 1<RRP<1.5). Further data processing was performed in Microsoft Excel®. Analysis of period length (Tau) and RRP was conducted in SPSS® (IBM) with Mann-Whitney *U* non-parametric tests (α= 0.05) because of the inconsistent variance and normality. Analysis of the distribution of the different rhythmicity categories frequencies (SR, WR or AR flies) was performed with the Fisher's Exact Test, and this allowed to assess the arrhythmic flies of a given population, as otherwise RRP comparison would always underestimate possible differences.

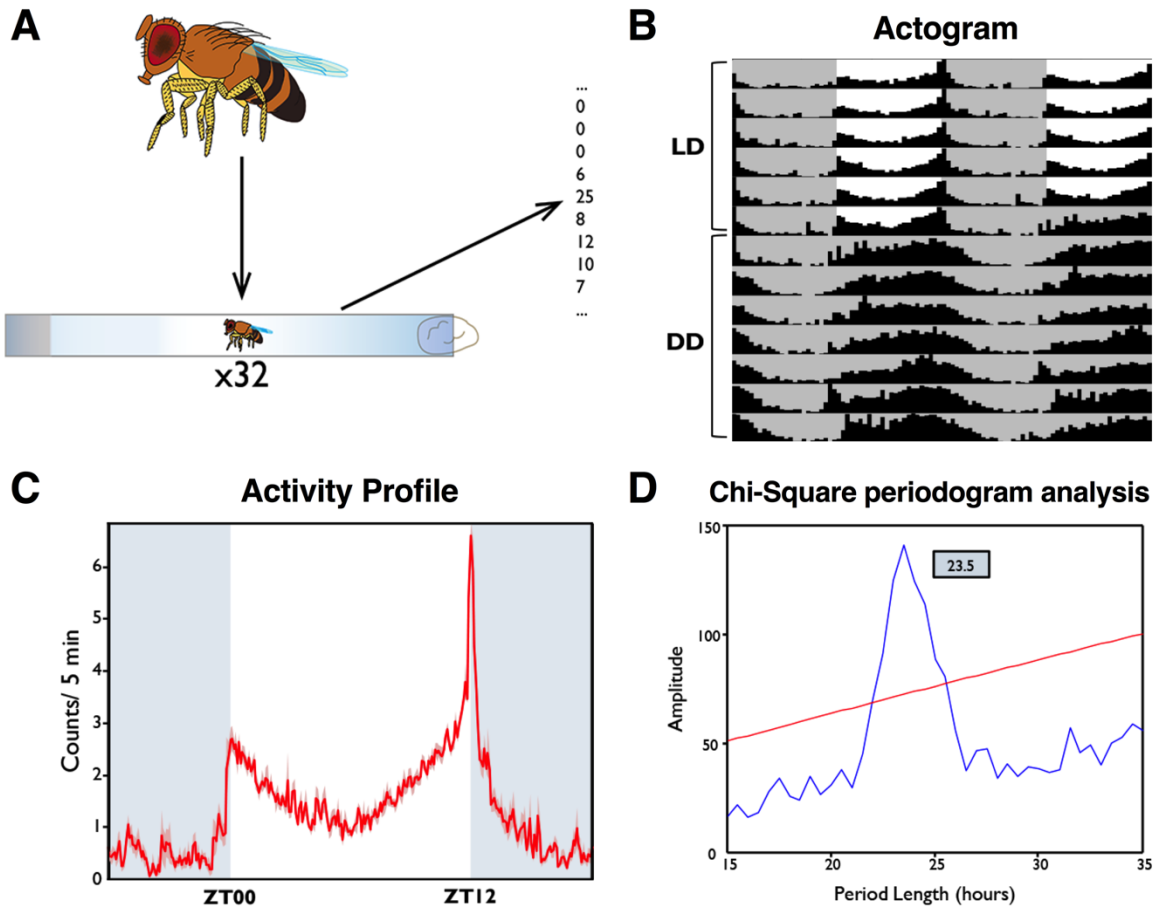

Figure 2.3 Study of the circadian behaviour of *Drosophila melanogaster*. The figure represents examples of the aforementioned output data from Drosophila Activity Monitor (DAM) System (trikinetics) and further processing in Clocklab (Actimetrics). **A)** Individual flies are loaded inside glass tubes, with up to 32 individuals per monitor. The daily activity is read and downloaded in bins, generating an output text file, which can be used in Matlab for processing and representation. **B)** Actogram representing the activity of a population during 14 days, with 6 days of Light-Dark (LD) entrainment and 8 days in *free run* or Dark-Dark (DD) conditions. As explained in the main text, actograms typically double plot the days (second day of a given row, and first day of the next row). Grey background indicates the dark phase. **C)** Activity Profile corresponding to the average (Mean ±SEM). The profile displays the maximum possible resolution with a bin size of 5 minutes. **D)** Visual depiction of the Chi-squared (χ2) Periodogram analysis of a single fly during 7 days in *free run*. The test shows a unique rhythm with a period length of 23.5 hours (amplitude of the test score, blue line, is higher than significance threshold, red line). The test has analysis all the rhythms between 15 and 35 hours as instructed, with a bin size of 30 minutes or 0.5 hours.

2.3.3 Analysis of locomotor activity under environmental cycles.

As activity profiles (see Chapter 2.3.2) provide only with visual observation when comparing two different animals/populations, a method to obtain quantifiable data was developed by using Clocklab. Within the entraining period (i.e. the previously described six days in LD cycles for most of the experiments), data regarding the total activity for the complete (averaged) day and time ranges of interest was gathered. As many data files employed at *free run* analysis were proven to be useful for this approach also, later experiments were also carried by keeping the flies at six complete days under the conditions of interest.

Along 12:12 LD cycles at constant 23° C, genotypes of interest were subjected to additional environmental cycles (Figure 2.4, A):

- 12:12 LD cycles coupled with *in-phase* temperature cycle. For this cycle, temperature starts in a cryophase (18 °C) at *lights-on*, progressively ramping up to the thermophase (25 °C) at *lights-off*, and decreasing throughout the dark phase until reaching the cryophase.
- 12:12 LD cycles coupled with *anti-phase* temperature cycle. Under these conditions, the cryophase (18 °C) is reached at *lights-off*, with the temperature descending throughout the light phase. Thermophase (25 °C) is reached at *lights-off* after increasing during the dark phase.

Additional cycles were used for specific assays at constant 23 °C but with differences in the LD conditions. Long and short photoperiod were used as a way of emulating more semi-natural conditions in different seasons, with 14:10 LD representing “summer days”, and 10:14 LD representing “winter days” (although the temperature remained unchanged). 12:12 Red Light-Dark (RD) conditions were also tested as a method of entrainment.

Firstly, with the interest of gathering as many data as possible, four time ranges of interest within the average day were chosen. With a given bin size of ten minutes and the employed computer times, these were:

- Activity four hours after *lights-off* event (ZT12-ZT16): 12:10 am to 4 am computer time
- Activity four hours before *lights-on* event (ZT20-ZT24): 8 am to 11:50 am computer time
- Activity four hours after *lights-on* event (ZT00-ZT04): 12:10 pm to 4 pm computer time
- Activity four hours before *lights-off* event (ZT08-ZT12): 8 pm to 11:50 pm computer time

While the time ranges include exactly 4 hours or 24 readings (including first and last reading at the given times) they do not include the actual expected *lights-on* and *off* events (12 pm and 12 am computer time). The data gathering was designed this way because of the inconsistent synchrony between the DAM computer clock and the different timers throughout the years this project took

place. As a consequence, actual events could happen some minutes before or after the scheduled computer time. While this was not necessarily significant for the post-event peaks because of the masking effect, this guaranteed that activity preceding *lights-on* and *off* was not affected by post-event activity bouts. Clocklab automatically provided the activity within the given time range (number of counts in 4 hours), the percentage that number represented for the total activity and the associated remaining activity counts and percentage from the total daily. Percentages were taken as variables because they remained more consistent and unaffected by individual variability, length of the vial, etc.

For experiments involving long photoperiod, the time ranges were modified:

- Activity four hours after *lights-off* event (ZT14-ZT18): 2:10 am to 6 am computer time
- Activity four hours before *lights-on* event (ZT20-ZT24): 8 am to 11:50 am computer time
- Activity four hours after *lights-on* event (ZT00-ZT04): 12:10 pm to 4 pm computer time
- Activity four hours before *lights-off* event (ZT10-ZT14): 10 pm to 1:50 am computer time

And respectively, for short photoperiod days:

- Activity four hours after *lights-off* event (ZT10-ZT14): 10:10 pm to 2 am computer time
- Activity four hours before *lights-on* event (ZT20-ZT24): 8 am to 11:50 am computer time
- Activity four hours after *lights-on* event (ZT00-ZT04): 12:10 pm to 4 pm computer time
- Activity four hours before *lights-off* event (ZT06-ZT10): 6 pm to 9:50 pm computer time.

As will be shown in Chapter 3.6, these data, particularly the ones corresponding to anticipatory activity, were used to develop a tool to asset the response of a fly under a given environmental cycle. The final resulting output was named *Evening-Morning Index* (E-M Index) (Figure 2.4, B). The E-M Index was developed with the next formula (in Microsoft Excel ®):

$$\frac{(\%Activity\ four\ hours\ before\ lights\ off) - (\%\ Activity\ four\ hours\ before\ lights\ on)}{(\%Activity\ four\ hours\ before\ lights\ off)}$$

With the index displaying a value between 0 and 1, depending of the anticipatory/preceding activity of the animal (See chapter 3.6). in the rare cases where the activity preceding lights-on were quantitatively bigger than the one preceding lights-off, the Index was automatically converted to 0 in order not to affect the rest of the population. When comparing two populations, Mann-Whitney *U* test was employed in SPSS (α= 0.05). When more than two groups were compared (i.e., a same genotype under different environmental cycles), analyses were performed with Kruskal-Wallis test instead (non-parametric equivalent to ANOVA test) (α= 0.05).

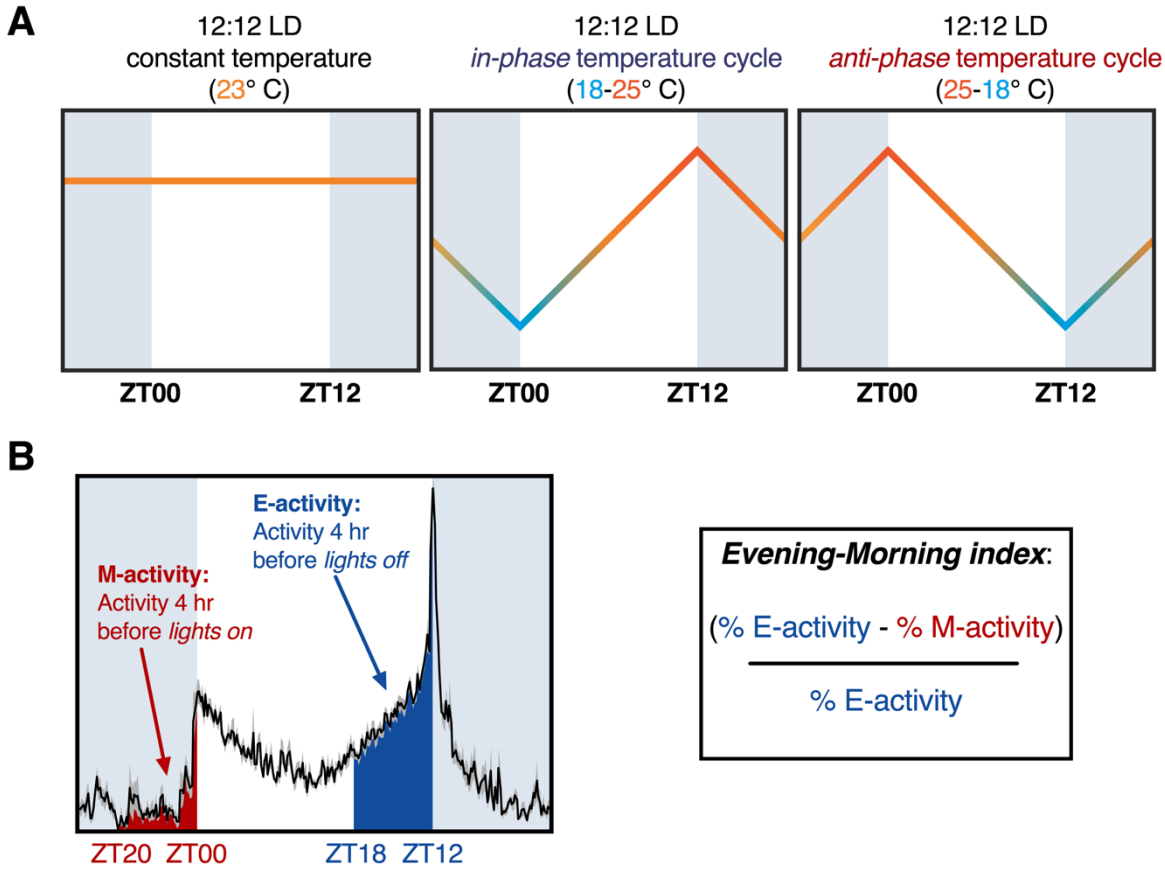

Figure 2.4 Characterisation of the *Drosophila melanogaster* behavioural response facing different environments. Scheme of the three different environmental cycles genotypes of interest were subjected two. The three conditions are 12:12 LD with constant temperature (23° C, RT), an in-phase temperature cycle (cryophase,18 °C at *lights-on*, thermophase, 25 °C at *lights-off*) and an anti-phase temperature cycle (thermophase, 25 °C at *lights-on*, cryophase,18 °C at *lights-off*). **B)** Calculation of the *Evening-Morning* index (E-M Index) showing the time ranges where activity was collected: 4 hours before *lights-on* (M-activity) and 4 hours before *lights-off* (E-activity). Both variables, as a percentage of the total absolute activity, were related with the E-M Index.

2.4 Inmunocytochemistry of the central nervous system

Inmunoytochemistry protocol closely followed a published work centred about the dissection of the fly CNS (Wu and Luo, 2006).

2.4.1 Preparation of flies

Adult flies of the same age (between one and four days after hatching, kept at 17° C) were moved to vials separated by genotype or gender, and kept in incubators under the desired conditions of entrainment and/or *free run*. In order to cause the minimal disruption to the molecular clock, vials with flies dissected during any dark phase were collected in darkness and immediately put on ice, keeping them protected of light until the moment of dissection. The ice also anaesthetised the flies, facilitating their manipulation.

2.4.2 *Drosophila* central nervous system extraction

Flies on ice at 4 °C were dissected in batches (genotype/gender/time point). The anesthetized animals were placed on a pre-cooled metal thermoblock, with micro-scalpel and sharp forceps used as tools. Heads were firstly detached from the bodies, followed by the removal of the proboscises. The resulting hole was used to gently push the brain out of the rest of the head cuticle. Brains were cleaned of trachea, eyes and other tissues that would affect its floatability in further protocol steps, but always without compromising its physical integrity. The resulting moisture from the cold block and brain extractions was used to avoid tissue desiccation. Brains were then transferred to 0.2 ml PCR tubes with freshly thawed 4% paraformaldehyde (PFA). Tubes containing flies were kept in ice until all the batches of flies were dissected.

The 4% paraformaldehyde solution formula, from CSH Protocol (2006), per 100 ml of solution:

- 4 g of EM grade Paraformaldehyde powder, to be gently dissolved by stirring on a heating block at 60° C
- 10 mL of 10X PBS, made of:
  - 800 mL distilled H_2O
  - 80 g NaCl
  - 2 g KCl
  - 14.4 g Na_2HPO_4
  - 2.4 g KH_2PO_4
  - HCl 1M to adjust the pH to 7.4
- Variable amount of HCl 1M (approximately 1 ml) to adjust the pH to 7.4. 1M NaOH was employ to counter the possible acidity excess.
- distilled H_2O to adjust the final volume to 100 ml.

PFA solution was stored in aliquots at -20 °C until day of dissections.

2.4.3 Immunocytochemistry assay

Once all the different fly sets were dissected (all the genotypes corresponding to the same time point usually), brains in PFA 4% were place in a nutator for fixation at room temperature for 20 minutes. This was followed by the removal and discard of most of the PFA volume and two quick (pouring, tube flicking and discarding) 0.1 M Phosphate Buffer with 0.3% Triton X-100 or PBT. This was followed by three consecutive 20 min PBT washes at the RT nutator, always trying not to disrupt the delicate brains inside the solution. Non-specific antigen blocking was performed with a blocking solution consisting of 5% Normal Goat Serum (NGS) in PBT. Brain were then subjected to primary antibody incubation, again in a block solution and for the course of two consecutive nights at 4 °C (primary antibodies are summarized in Table 2.5. The same washing procedure (2 quick washes followed by 3x20 min with PBT) was performed to remove the primary antibody, before starting the secondary antibody incubation. Secondary antibodies were again dissolved in blocking solution but protecting the fluorophores from light during 2 consecutive nights at 4° C.

The last day, brains were subjected to the same washing protocol one last time before removing all the exceeding PBT volume and embedding the brains inside the mounting medium hard-set Vectashield® (Vector Labs). Brains were then gently aspired with a cut pipette tip and placed on a glass slide. Medium leaks and brain squishing was avoided by locking them with polish nail, which was also used to seal the coverslip on the slide. Slides were stored protected from light at -20 °C until imaging experiments.

The PB solution includes at the same concentration (0.1 M) both sodium hydrogen phosphate (Na_2HPO_4) and sodium dihydrogen phosphate (NaH_2PO_4) (CSHP, 2010) and was stored at room temperature both at 1 and 10X dilutions. Triton X-100 (Sigma-Aldrich) was freshly added to PB (0.3% vol/vol) for each experiment. The block solution was also made fresh the same day of usage, by adding a 5% of NGS (Sigma-Aldrich).

The following antibodies where used

Class	Description	Concentration	Origin and reference
Primary	Rabbit Anti-Period (pc)	1:10000	Gift from JC Hall (Liu *et al.*, 1992; Stanewsky *et al.*, 1997)
	Mouse C7 anti-PDF (mc)	1:300	Deposited by J Blau at Developmental Studies Hybridoma Bank (Cyran *et al.*, 2005)
	Chicken ab13970 anti-GFP (pc)	1:2000	Abcam (Chen and Condron, 2008)
Secondary	Goat A11077 Anti-Rabbit 568	6.5 µg/ml	Life Technologies (ThermoFisher Scientific)
	Goat A11029 Anti-Mouse 488	6.5 µg/ml	

Goat Anti-Chicken 488	1:250	Molecular Probes (ThermoFisher Scientific)

Table 2.5. List of antibodies. Class: Description of the primary antibodies include its origin as polyclonal (pc) or monoclonal (mc).

2.4.4 Antibody pre-absorption

The use of antibodies for immunocytochemistry requires selective antigen specificity in order to guarantee the specific imaging of the element of interest. This is guaranteed by monoclonal antibodies, produced from a source that has been in contact with one single antigen. However, the anti-Per antibody, kindly provided by Jeffrey C Hall (Liu *et al.*, 1992), was polyclonal; that is, extracted from a serum with multiple antigens. In order to make the solution selective to Per protein only, the antibody was pre-cleared by incubating with per^{01} embryos. Embryos were dechorionated with 50% bleach, washed with 0.7% NaCl, 0.05% Triton X-100 and fixed with methanol (stored at 4°C) following existing protocols (Rothwell and Sullivan, 2007). Pre-absorption was performed with the antibody diluted 1:100 in PBT, 5% Normal Goat Serum (NGS, Sigma-Aldrich) for two days at 4°C. Pre-absorbed solution was stored at -20°C with 0.1% Sodium Azide.

The 10X Embryo wash solution formula is:

- 1 litre of distilled H_2O
- 70 g NaCl (final concentration of 7%)
- 5 mL of Triton X-100 (final concentration of 0.5%)

2.5 Imaging and analysis

2.5.1 Data acquisition and presentation

Pictures were taken with either an SP2 (Per signal quantification) or SP8 (s-LN_v dorsal projections) Leica® confocal microscopy, based on the available hardware at the Imaging and Microscopy Centre (IMC). No microscope changes were done within any given experiment.

The microscope was controlled with the Leica Imaging Suite®. Pictures were taken by using the same acquisition profile (resolution, pinhole, laser intensity, range acquisition and offset) per channel for all the samples involved in an experiment. The exception was the GFP signal, employed only for anatomical information. The type of objective and optical zoom was equally constant for all the samples of an experiment. For the acquisition of xyz stacks, the distance

between slides was 1 µm. The resulting data were contained within .tiff or .lei files to be used on further analysis Double-blinding was applied before any quantification in order to avoid biases.

Representative figures of microscopy results were assembled in FigureJ (ImageJ plugin)(Mutterer and Zinck, 2013). Adobe Photoshop® was employed for framing the representative figures at some instances, with no further modifications.

2.5.2 Antibody signal quantification

Composite z-projections were generated from the original stacks files for each individual item (cells or s-LN$_v$ dorsal projections) (Figure 2.5 A). For the levels of Per protein, a selection mask was drawn with the mGFP channel, and the signal intensity was measured in the Per channel. Background signal was randomly measured in three z-projections in the same z-width than the analysed object, by using the same selection mask (Figure 2.5 B). The normalised signal was obtained with the formula $S = (I-B)/B$; where I stands for *Integrated Density* (total sum of pixel intensities, or Average (0-255) pixel intensity x Area) and B stands for average background Integrated Density ($n = 3$). Comparison among genotypes/timepoints was done in SPSS (IBM), with the signal levels analysed with the Mann-Whitney U test ($\alpha = 0.05$). The rare instances of a signal below 0 (when S and B are virtually identical) were transformed into 0 as they were considered to be protocol artefacts.

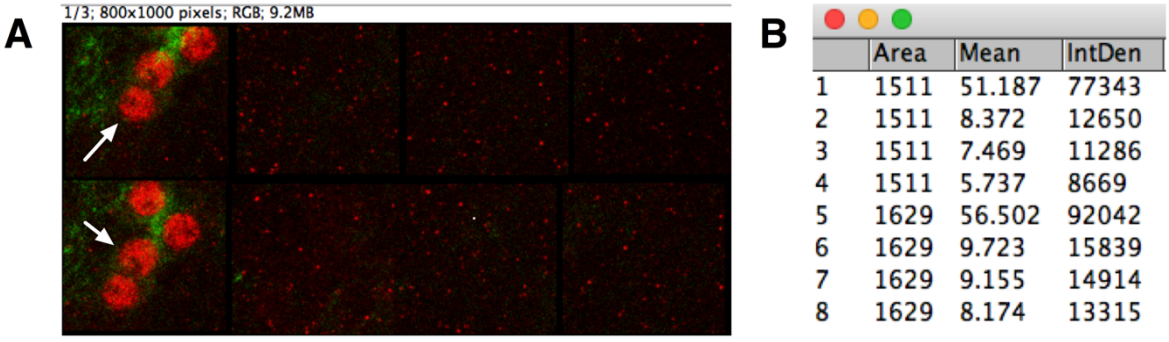

	Area	Mean	IntDen
1	1511	51.187	77343
2	1511	8.372	12650
3	1511	7.469	11286
4	1511	5.737	8669
5	1629	56.502	92042
6	1629	9.723	15839
7	1629	9.155	14914
8	1629	8.174	13315

Figure 2.5. Quantification of antibody signal by ImageJ. **A)** Example screenshot of Maximum z-projection files used for anti-Per signal quantification. Each row depicts the maximum z-projection of a single cell inside the same s-LN$_v$ cell cluster (arrows, with different z-planes for each cell) and three correspondent background screenshots taken at the same z-projection than the cells. mGFP channel (green) was used to draw a selection mask around the cell body, and to then quantify the signal from the Per channel (red). **B)** Example of output at ImageJ of the two s-LN$_v$s. Measures 1-4 correspond to first cell (top row in A) and measures 5-8 to second one (bottom row in A). The first measure is the intensity of Per antibody inside the cell (*IntDen* column, from *Integrated density*), and the three subsequent correspond to the background measurements in the respective screenshots. As a

consequence of using the same selection mask, the *Area* remains unchanged per each cell + backgrounds set. Mean column represents IntDen/Area.

2.5.3 Per protein subcellular localisation analysis

By comparing the anti-Per signal with the cytoplasmic GFP, cells were scored Nuclear, Cytoplasmic/Nuclear-Cytoplasmic or Absent. The distribution of frequencies was analysed with the Fischer's Exact Test (Soper, 2014). Cytoplasmic and Nuclear-Cytoplasmic categories were combined into one in order to make the data eligible for 2x3 contingence table analysis and because the number Nuclear-Cytoplasmic cells were negligible or absent in all the conditions.

2.5.4 Quantification of axonal arborisation

The complexity of the axonal arborisation of the s-LN_v dorsal termini was quantified with information gathered from the anti-PDF antibody (Figure 2.6 A). xyz stacks were transformed into single xy files by the method of maximum projection as previously stated. These files were quantified by the Sholl Analysis method, originally developed for measuring the complexity of dendritic arborisations (Sholl, 1953). The method was successfully adapted previously to detect the daily remodelling of the s-LN_v dorsal termini (Fernandez, Berni and Ceriani, 2008). 7 concentric circles were made with the Concentric Circles plug in, with the radius constantly increasing by 10 µm up until 70 µm (Figure 2.6 B)(Rasband, 2007). The centre point was marked at the point of the first branching of the axonal termini. The number of crosses per circle was annotated, and the resulting sum was deemed as the "Sholl score" of the given hemisphere. Sholl score was proved not to accomplish all the requirements for t-test in all the conditions, so Mann-Whitney *U* test ($\alpha = 0.05$) was used instead.

The same maximum projection stacks were also used for measuring the anti-PDF antibody signal as previously described (Chapter 2.5.2), except in the cases where the signal was too bright or low to obtain reliable structural information. In these instances, a second stack was taken with modified parameters to analyse the axonal complexity, but only the former ones were used for antibody quantification in order to avoid photobleaching. Antibody signal was used to draw the selection mask in the dorsal termini as it has been proved to finely represent the axonal morphology (Fernandez, Berni and Ceriani, 2008; Gatto and Broadie, 2009).

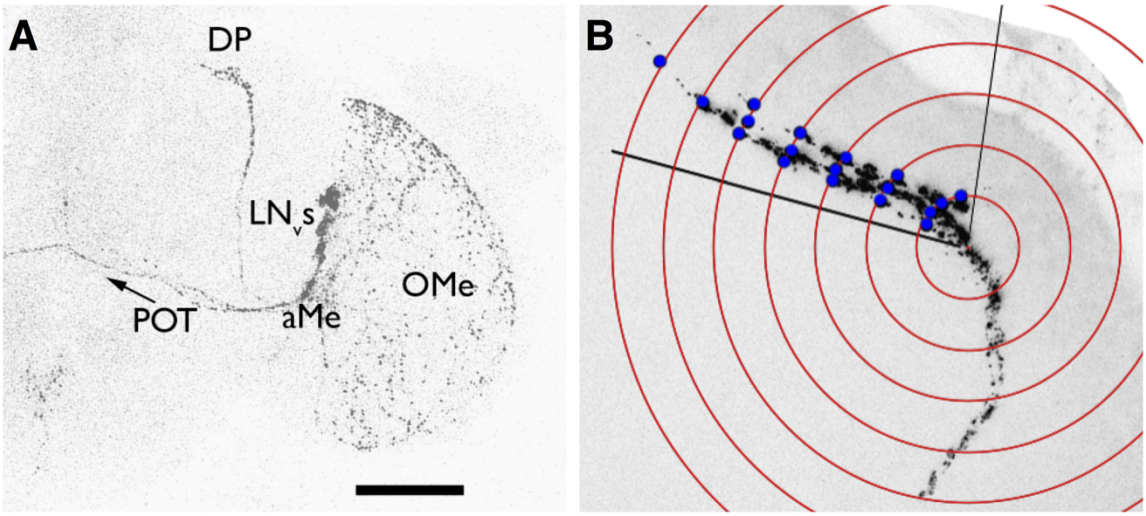

Figure 2.6. Quantification of the arborisation complexity of s-LN_v dorsal projections with Sholl analysis. A) anti-PDF staining (grayscale-inverted) displaying significant anatomical features of the fly brain: cell bodies of the ventrolateral neurons (LN_vs); Dorsal Projections of the s-LN_vs (DP); l-LN_v projections across the Posterior Optic Tract (POT); and accessory Medulla (aMe). Scale bar represents 100 µm. **B)** Example of Sholl analysis of the s-LN_v dorsal projections, with seven concentric circles (r1= 10 µm, r7= 70 µm) and the intersections points in blue. The Sholl score for this given axonal bundle would be 18. This protocol reproduced the original approach (Fernandez, Berni and Ceriani, 2008).

Chapter 3: Experimental results

3.1 Introduction to this chapter

Chapter five, divided in five subchapters, addresses the questions that were raised in the project aims (See Chapter 1.5). Each subchapter includes experimental results that try to accomplish the different aims, but all of them take a part in the characterisation of the Rho1-related locomotor phenotype.

The effects of reduced *Rho1* genic product on the adult locomotor activity are firstly described and characterised in Chapter 3.2. Chapter 3.3 extensively details results that specify the causative relationship between Rho1 and the found phenotype, and the place where the small GTPase is having a role as well within the clock circuit. Chapter 3.4 presents the interrogation of the core clock cells of *Drosophila* upon depletion of *Rho1* levels. The found cellular effects lead to the establishment of a hypothesis for the role of Rho1 in the circadian behaviour. This one is subjected to test in Chapter 3.5, with additional experiments targeting the way the clock cells communicate with each other. On the other hand, Chapter 3.6 investigates the behaviour of the flies under different entrainment conditions, required for all the previous experiments but not further described upon this point. Although the main conclusions of each subchapter are briefed at the end as being necessary for interpreting subsequent results, the majority of the overall discussion of the project is found in the Chapter 4.

Some results can be found in the Appendix A, which includes supplementary information for this chapter, along summary tables. Appendix B, on the other hand, introduces, explains and discusses an independent group of results gathered from experiments with red light (See Chapter 1.3.4.2 and 1.3.7). Despite their independent nature regarding the study of Rho1 and its interaction with the circadian behaviour, they provide additional (and unpublished) context to some experiments described in Chapter 3.5.2).

3.2 Heterozygous loss of function of *Rho1* impacts circadian behaviour.

The *Rho1* gene is located on the R arm of the second chromosome (chromosome coordinates 2R:16,102,687-16,107,229)(Attrill *et al.*, 2016). Because of the numerous studies focused on this gene there are many available tools to target its expression. One of the classic techniques is the employment of chromosome deficiencies, particularly useful for mappings studies based on quantitative trait loci (Mackay, 2001). The chromosome deficiency *(2R)ED2457* deletes 130.000

base pairs and entails the loss of 26 recognized loci, including *Rho1* (Shao *et al.*, 2010; Attrill *et al.*, 2016). It was made with FRT-dependent recombination as part of a library comprising up to 60% of the fly euchromatin (DrosDel Project, 2007; Ryder *et al.*, 2007). This aberrant chromosome is identified by the presence of a w^{+} marker and balanced with *SM6A* (*Cy/Duox*^{Cy} as external marker). The balancer chromosome is necessary because of the risk of recombination and the developmental lethality of the homozygous individuals for the deficiency. The background similarity allowed to employ w^{1118};; as the parental line. Virgin females from this stock were crossed with males carrying the respective deficiencies and mutants.

Population actograms for control and experimental isogenic groups can be found at Figure 3.1 A, and the corresponding analysis of the DD period in Figure 3.2 A, B, C. Flies developed normally with no noticeable differences from parental stocks, but the presence of the chromosome deficiency increased the number of flies displaying arrhythmia in both genders, especially in females (Figure 3.2 A). Importantly, this arrhythmia was caused by erratic activity rather than lack of it, discarding possible locomotive defects of these flies. Relative Rhythmic Power (RRP, see Chapter 2.3.2) analysis of strongly and weakly rhythmic flies (Mann-Whitney *U* test) equally showed reduced rhythms for the deficiency-carrying females. (Figure 3.2 B). Differences were not found for males, probably because of the weak rhythmicity of the controls (Figure 3.2 B). Period Length was not seemingly affected by the presence of the deficiency besides an increased variability associated to a weaker rhythm (Figure 3.2 C). This experiment proved that the chromosome deficiency *(2R)ED2457* affects rhythmicity in *Drosophila*, but it was impossible to determine if any of the other 25 identified deleted genes could be contributing to the phenotype.

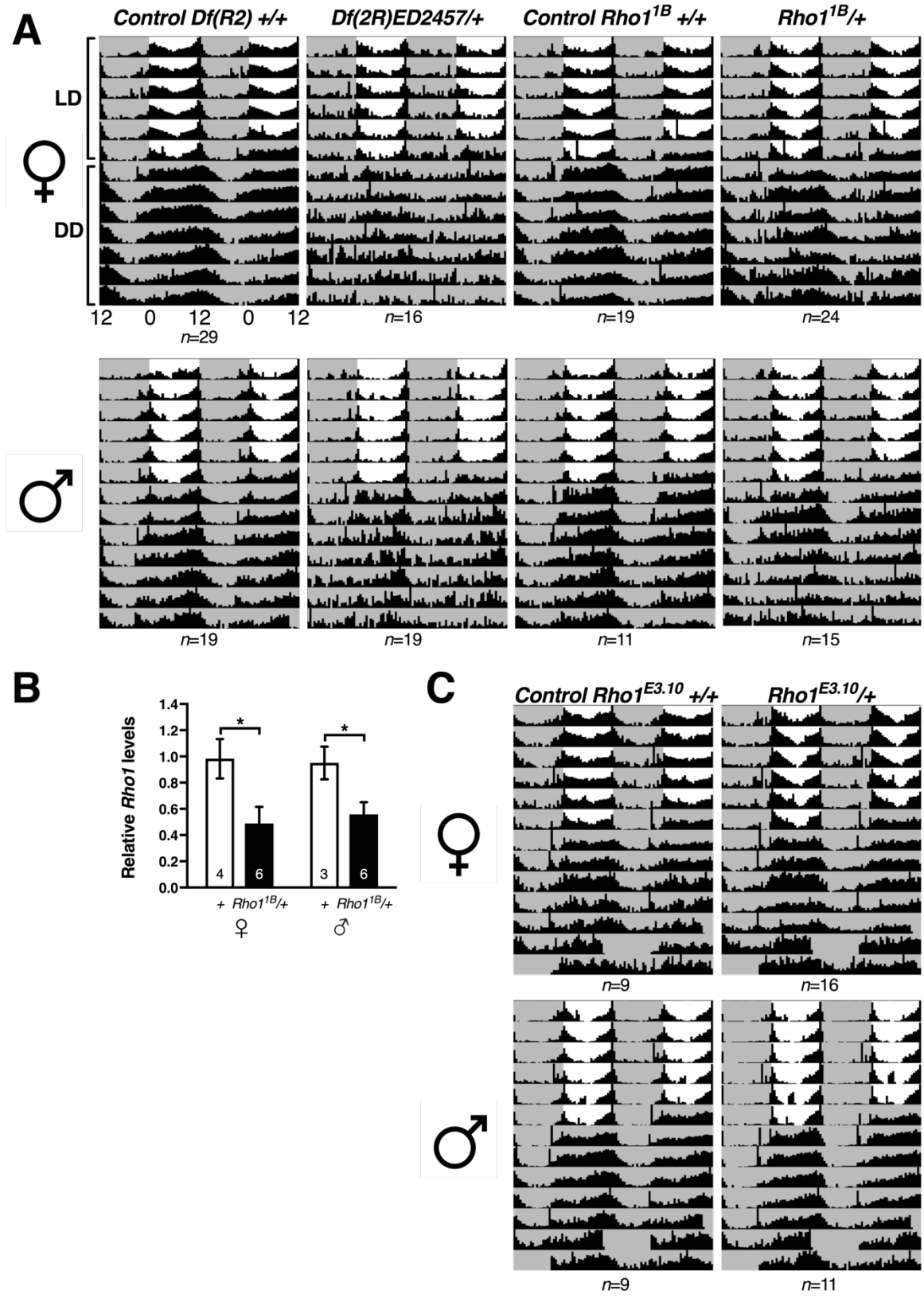

Figure 3.1. Circadian locomotor activity of *Drosophila melanogaster* with compromised *Rho1* genetic dosage. **A)** Adults of both genders with two wild-type copies of the *Rho1* gene or heterozygotic for the chromosomic deficiency encompassing *Rho1* or the *Rho1^{1B}* null allele

are entrained for 6 days in LD and transferred to DD conditions on day 7, at a constant temperature of 23 °C. The quantified data from the next 7 days in DD are found in Figure 3.2. Column titles indicate given genotype, and rows represent females (top) and males (bottom). White background, light period; grey background, dark period. Actograms represent the normalised population average. *n* numbers are indicated below the actograms. Control genotypes consist of isogenic siblings carrying a balancer chromosome (*SM6A* for the deficiency, and CyO^{1} for the $Rho1^{1B}$ mutant allele). **B)** *Rho1* gene levels (relative to *RpL32*) inside fly heads for the given genotypes in both genders. $Rho1^{1B}$ heterozygous mutants and isogenic controls were harvested after hatching at 23 °C. Bars represent Mean ±SEM and numbers indicate number of biological replicates. **C)** Adults of both genders carrying two wild-type copies of the *Rho1* gene or heterozygotic for the $Rho1^{E3.10}$ allele are entrained for 6 days in LD and transferred to DD conditions on day 7, at a constant temperature of 23 °C. The quantified data from the next 7 days in DD are found in Figure 3.2. Column titles indicate given genotype, and rows represent females (top) and males (bottom). White background, light period; grey background, dark period. Actograms represent the normalised population average. *n* numbers are indicated below the actograms. Control genotypes consist of isogenic siblings carrying a balancer chromosome (CyO^{1}). Activity gaps in the actograms are due to an overnight system crash.*p<0.05 and by t-test [$Rho1^{1B}$ females: t(8)=-2.489, p=0.038; $Rho1^{1B}$ males: t(7)=-2.494, p=0.041]. As $Rho1^{1B}$ male ratio failed the Shapiro-Wilk test for Normality (but passed the Kolmogorov-Smirnov with Lilliefors correction), Mann-Whitney *U* test was also performed with a similar result (p=0.024).

Due to the disruptive nature of a severe chromosome deficiency for genomic and homeostatic fitness, it was aimed to demonstrate that the deletion of *Rho1* was the reason of the locomotor phenotype associated to the *(2R)ED2457* deficiencty. $Rho1^{1B}$ is a loss of function allele created by an imprecise P-element excision that removes the last 52 aminoacids (exons 3 and 4) and leaves no protein to be detected by immunofluorescence in embryos (Magie and Parkhurst, 2005). The homozygous $Rho1^{1B}$ allele is lethal like the *(2R)ED2457* deficiency, with individuals displaying major defects in the embryonic stage (Magie and Parkhurst, 2005; Xu, Keung and Myat, 2008). w^{1118}; $Rho1^{1B}/CyO^{1}$ males were again crossed with w^{1118};; virgin females, maintaining the same cross scheme as the deficiency. qPCR analysis confirmed that flies carrying the $Rho1^{1B}$ allele have their mRNA levels halved, consistent with previous immunostaining-based reports (Magie and Parkhurst, 2005)(Figure 3.1 B). The population of females carrying the $Rho1^{1B}$ allele exhibited a

greater degree of arrhythmia than the isogenic controls (Actograms in Figure 3.1 A, Figure 3.2 D), as well as a reduced RRP of flies displaying rhythmic behaviour (Figure 3.2 E). Both tests found no differences when comparing the two male populations (Figure 3.1 A, Figure 3.2 D, E). Consistent with data from *(2R)ED2457* deficiency, females with reduced *Rho1* levels were again more affected than males regarding their circadian behaviour. No differences were found again for the endogenous period lengths in any of the genders (Figure 3.2 F).

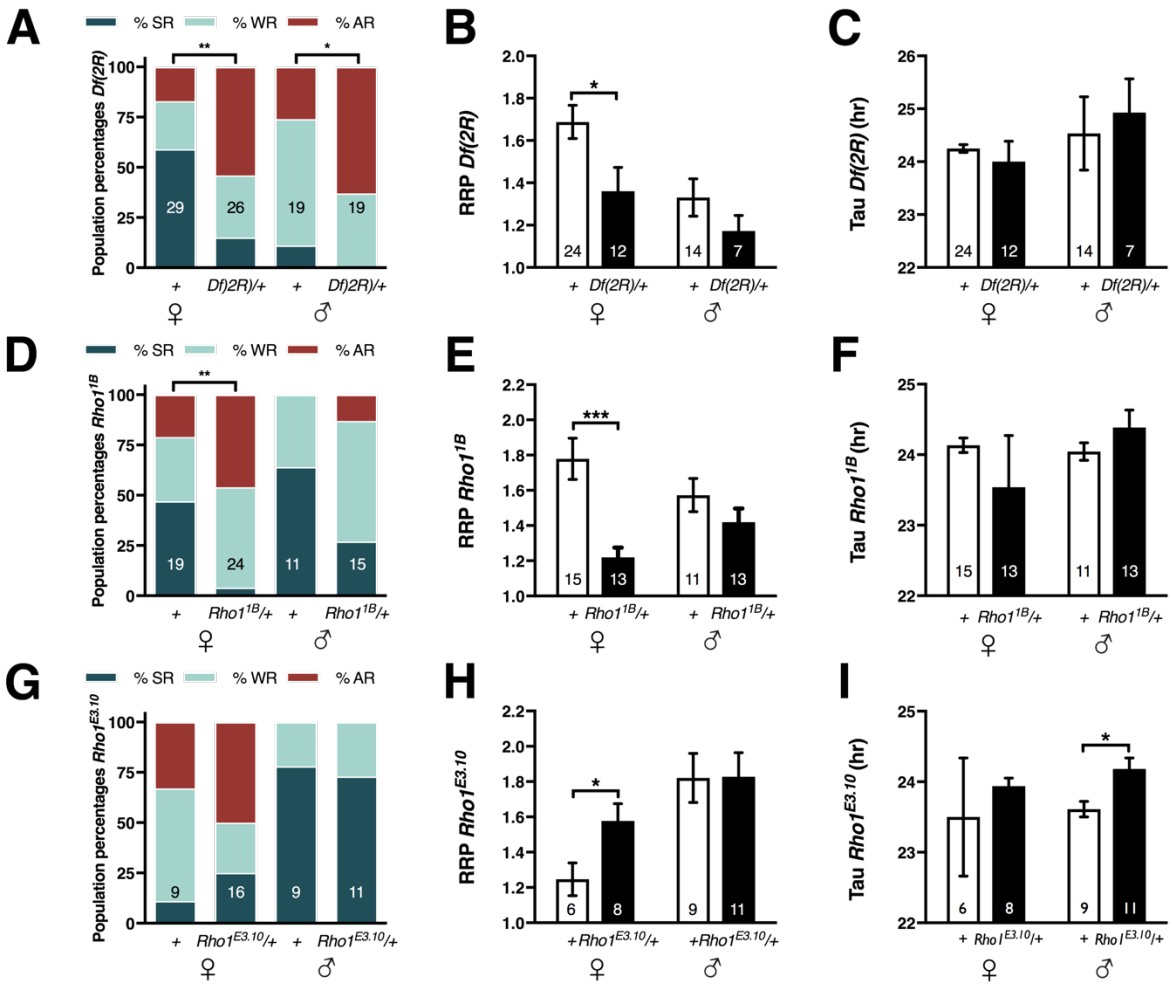

Figure 3.2. Effects of reduced *Rho1* levels in *Drosophila melanogaster* circadian behaviour. A, B, C) Distribution of frequencies (Strongly Rhythmic, SR; Weakly Rhythmic, WR or Arrhythmic, AR) (A), Relative Rhythmic Power (RRP) of SR and WR flies (B) and Period Length (Tau) of SR and WR flies (C) for flies carrying the chromosome deficiency *(2R)ED2457*, as well as isogenic controls. **D, E, F)** Distribution of frequencies (D), RRP of SR and WR flies (E) and Tau of SR and WR flies (F) for flies carrying the $Rho1^{1B}$ mutant allele, as well as isogenic controls. **G, H, I)** Distribution of frequencies (G), RRP of SR and WR flies (H) and Tau of SR and WR flies (I) for flies carrying the $Rho1^{E3.10}$ mutant allele, as well as isogenic controls. Bars represent Mean ±SEM and numbers in bars indicate *n*, with the total number of flies

originated from 5 (*Df(2R)*, 5 (*Rho1*^{1B} allele) and 1 (*Rho1*$^{E3.10}$ allele) crosses. For population percentages column (A, D, G), *p<0.05 and **p<0.01 by Fisher's Exact test. For RRP (B, E, H) and Tau (C, F, I) columns, *p<0.05 and ***p<0.001 by Mann-Whitney *U* test (α= 0.05).

A third chromosome defective for *Rho1* was utilised, carrying the *Rho1*$^{E3.10}$ allele. This allele is not null as the protein is expressed, but a missense point mutation in the cysteine of the CAAX motif (C189Y) reduces its membrane attachment in epithelial tissue and renders the allele recessive lethal (Halsell and Kiehart, 1998; Halsell, Chu and Kiehart, 2000; Neisch *et al.*, 2010). For this allele, the results were negative, and in the case of females even suspicious (Figure 3.1 C and Figure 3.2 G, H, I). Fisher's Exact test failed to find differences between carriers and controls for both genders (Figure 3.2 G). RRP comparisons showed an apparent improved rhythmicity in females carrying the allele (Figure 3.2 H). RRP of the males was not affected by *Rho1*$^{E3.10}$ allele (Figure 3.2 H) but the endogenous period was lengthened, something not found in females (Figure 3.2 I). The genetic background of this cross could explain the abnormal result found only in females. The X chromosome of the parental stock for this allele carrying a dominant *facet-glossy Notch (N*$^{f-g}$*)* marker could be affecting neuronal development of the females, maybe explaining the found effect (Larson, Liberman and Cagan, 2008). As the phenotypic effects of the *Rho1*$^{E3.10}$ allele were apparently negligible, and the effects by this allele are characterised in different contexts other than neurons, no further experiments were performed with it.

These experiments with chromosome deficiencies and mutants evidence that genetic dosage of *Rho1* can impact the circadian behaviour of the adult flies. Specifically, they point to *Rho1* displaying haploinsufficiency in establishing the circadian behaviour. These results are striking because *Rho1* is considered to be haplosufficient for the development of the fly (Magie *et al.*, 1999). With the obtained results employing somatic mutants, diverse techniques available in *Drosophila* research allow to refine the experiments and confirm the involvement of Rho1, as well as specific places of action for the small GTPase.

3.3 Spatial and temporal mapping of the *Rho1* knockdown phenotype

3.3.1 Selective knockdown of *Rho1* inside the clock cells is sufficient to cause behavioural arrhythmia

Due to the intrusive nature of aberrant alleles inside all the somatic cells, classic experiments with mutants represent limitations regarding the obtainable information. The found circadian phenotype could be due to diverse non-clock-related factors (like locomotor defects or overall unhealthy phenotype). The high specificity of RNA interference process, combined with the Gal4/UAS system, constituted a valuable tool in order to study the function of Rho1 specifically inside tissues related to the circadian behaviour (Van Roessel *et al.*, 2002; Pili-Floury *et al.*, 2004). As stated in Chapter 2, the *UASdcr2* construct was included in all the experiments involving RNAis in order to enhance the efficiency of the process (Dietzl *et al.*, 2007). The construct was included even when the RNAis were not long hairpin and thus not processed by Dicer-2 (like *TRiP.HMS00375*)(Okamura *et al.*, 2008) , in order to both facilitate the cross schemes and maintain a similar genetic background.

A series of available RNAi lines for *Rho1* were tested first employing the *tim(UAS)-Gal4* driver, in order to target the complete clock circuitry. The construct includes 5 UAS sequences upstream the driver in order to enhance its effectivity (Blau and Young, 1999). This driver has been previously used for RNAi-mediated gene targeting inside the clock cells with behavioural consequences (Matsumoto *et al.*, 2007; Hermann-Luibl *et al.*, 2014). Except for one of the RNAis (*Rho1.770-1310*), all the flies expressing the RNAi were compared with isogenic siblings lacking the driver (CyO balancer instead) but carrying the UAS construct. For the former construct, isogenic driver-only flies were used as controls instead. The virgin line *UASDcr2w; tim(UAS)-Gal4/CyO*, was tested in later experiments as an additional control (See Chapter 3.3).

The first RNAi, *JF02809* (Bloomington stock 27727), expresses a double strand RNAi targeting the first three exons of *Rho1* along part of the 5'UTR region. Similar to previous experiments with mutants and deficiencies, RNAi-expressing flies with the *tim* driver developed normally without any detectable difference from undriven controls. Locomotor assays showed that populations with targeted *Rho1* knockdown inside the clock cells failed to maintain strong rhythms in *free run* (Figure 3.3). Quantitative analysis indicated that these populations displayed an elevated percentage of flies with behavioural arrhythmia, up to 75% in the case of females (Figure 3.4 A). A similar effect was found when comparing the rhythmic power of flies displaying a rhythm, with greater effects than in the former experiments with mutants (Figure 3.4 B). The gender

component was still present however, as the differences among the two female groups were quantitatively higher than in the male ones (Figure 3.4 B, C). While females had an internal period length equal to the isogenic controls, experimental males showed an increase by ≈1 hour (Figure 3.4 C). However, the presence of the *tim(UAS)-Gal4* extended the period in driver-only flies, clearly indicating an insertion site effect rather than a phenotype caused by *Rho1* knockdown (See Chapter 3.3.3). Further observation of later experiments makes us to assume that *Rho1*-deficit has no effect in the endogenous period length, and that this one is increased by extrinsic factors related to the Gal4/UAS system. The reason of the lack of a detectable period extension in the RNAi-expressing females is probably the very poor rhythmicity, which makes easier for the ClockLab software to find aberrant periods, and therefore increasing the population variance.

Strikingly, as was already apparent in experiments with the chromosome deficiency *(2R)ED2457* or the $Rho1^{1B}$ mutant (Figure 3.1 A), experimental flies displayed an apparent wild-type behaviour during their entrainment (Figure 3.3). This is not found in many clock or clock output mutants, whose phenotypes already manifest during LD cycles, usually because of failing to entrain. Contrary to this, visual observation indicated that *Rho1* knockdown flies anticipate the lights-off event normally, which prompted further experiments in the entrainment phase (see Chapter 3.6). Importantly, this behaviour provides information about the state of the circadian behaviour of the flies. Firstly, it implies flies are able of following LD cycles, but they rely on them in order to establish locomotor rhythms, so it could be assumed these flies have lost their circadian behaviour as it cannot be maintained in *free run*. Secondly, it is unlikely that *Rho1* knockdown had caused cell death inside the clock circuitry, as the presence of stereotyped LD activity suggest the persistence of some kind of clock inside the brain. This is an assumption based on behavioural assays that needs to be further corroborated by inspecting the *Rho1*-deficient clock cells (see Chapter 3.4).

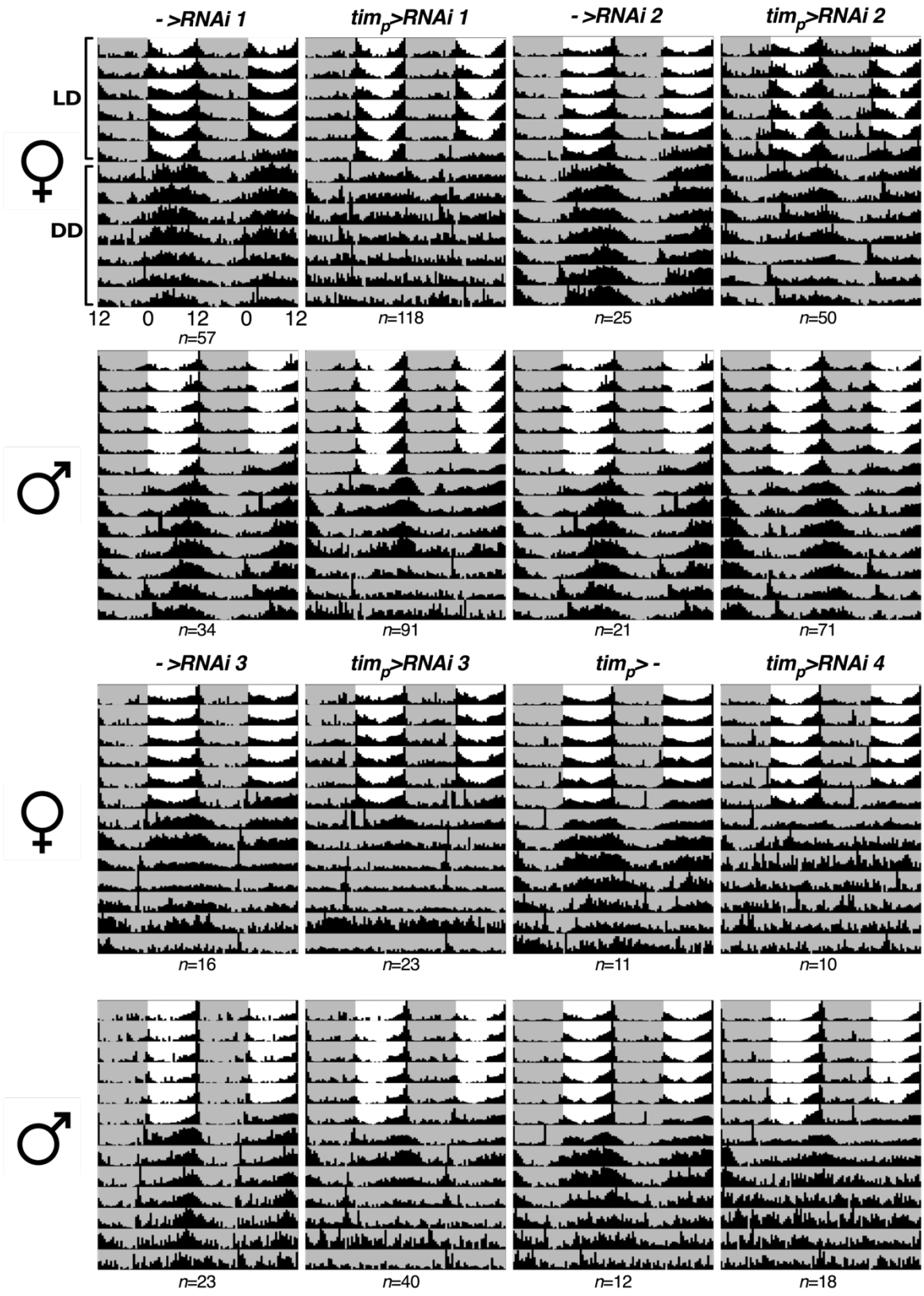

Figure 3.3. Circadian locomotor activity of *Drosophila melanogaster* with *Rho1* knockdown inside the clock cells. Adults of both genders are entrained for 6 days in LD and transferred to DD conditions on day 7, at a constant temperature of 23 °C. The quantified data from the

next 7 days in DD are found in Figure 3.4. Column titles indicate given genotype, and rows represent females (top) and males (bottom). White background, light period; grey background, dark period Actograms represent the normalised population average. *n* numbers are indicated below the actograms. All the flies in this assay have the *UASDcr2w* construct in the X chromosome (heterozygously in the case of females). Isogenic controls represent flies lacking the *tim(UAS)-Gal4* driver (represented as tim_p in the figure) but carrying the correspondent *UASdsRNAi* construct; the exception being the RNAI 4 (*Rho1.770-1310)* line, where the controls are isogenic flies carrying the driver and not the RNAi construct (see main text in this subchapter).

A second construct, *TRiP.HMS00375*, (Bloomington stock 32383), expresses a short hairpin RNAi targeting a sequence in the third exon. Expression of this RNAi ("Rho1 RNAi 2") reduced again the rhythmicity of the female population, albeit in a milder way (Figure 3.4 D). This effect was even milder for the male population, whose rhythmic individuals displayed quite strong rhythms (Figure 3.4 D, E). If the efficiency of this RNAi is more limited than *JF02809*, these results keep supporting the notion that female flies exhibit a higher degree of sensitivity to *Rho1* levels inside their clock cells. Analysis of period length indicated the experimental set up with this RNAi caused the same effects than with the *JF02809* construct, lengthening the period length on males. As this effect was found even when the effects on male rhythmicity were very mild, it seemed again caused by the presence of the *tim(UAS)-Gal4* construct rather than (Figure 3.4 E).

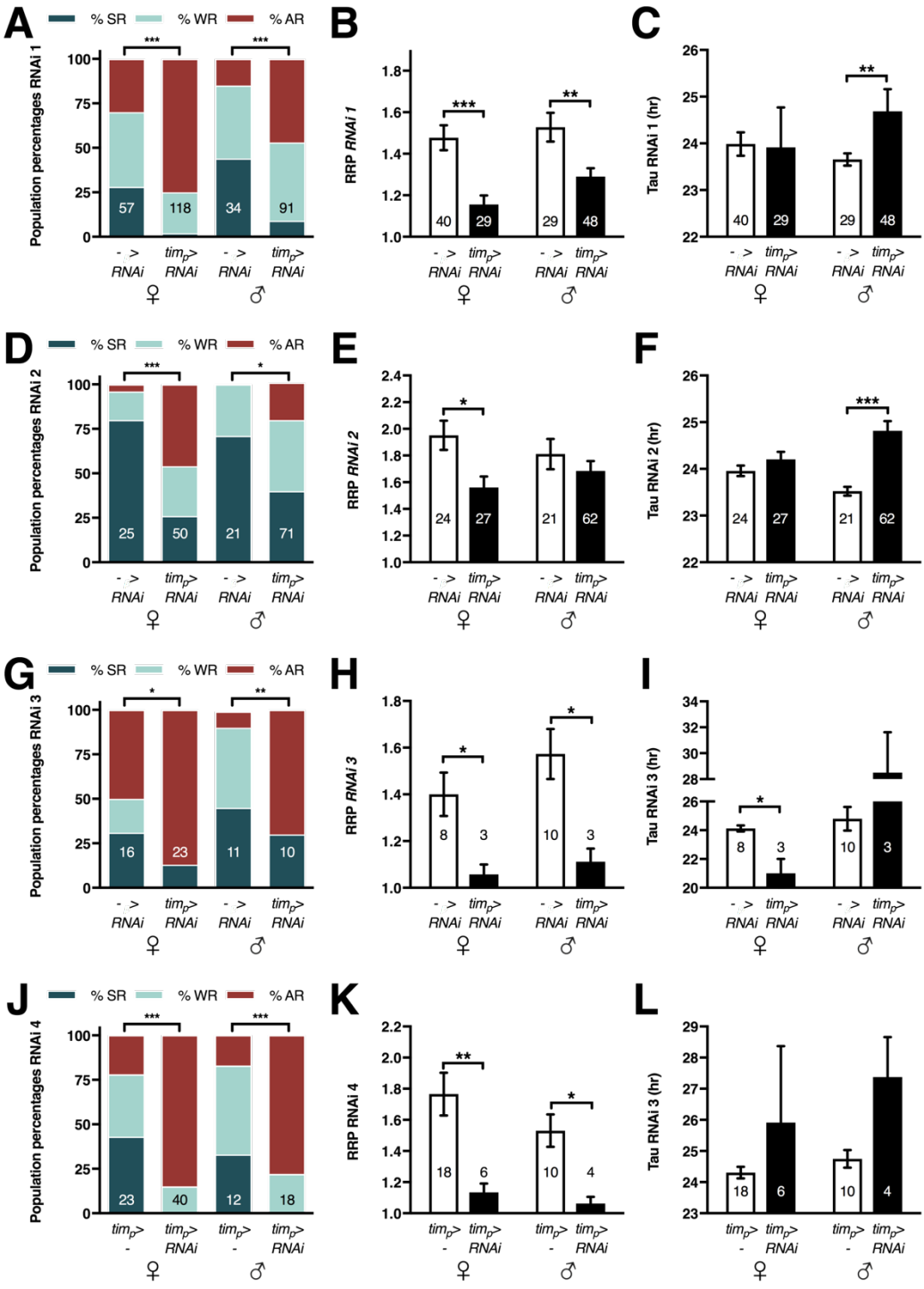

Figure 3.4. Effects of reduced *Rho1* levels inside the clock cells in *Drosophila melanogaster* circadian behaviour. A, B, C) Distribution of frequencies (Strongly Rhythmic, SR; Weakly Rhythmic, WR or Arrhythmic, AR) (A), Relative Rhythmic Power (RRP) of SR and WR flies (B) and Period Length (Tau) of SR and WR flies (C) for flies expressing the *JF02809 Rho1* RNAi construct inside the clock cells, as well as isogenic controls. **D, E, F)** Distribution of frequencies (D), RRP of SR and WR flies (E) and Tau of SR and WR flies (F) for flies expressing

the *TRiP.HMS00375 Rho1* RNAi construct inside the clock cells, as well as isogenic controls. **G, H, I)** Distribution of frequencies (G), RRP of SR and WR flies (H) and Tau of SR and WR flies (I) for flies expressing the *325-786 Rho1* RNAi construct inside the clock cells, as well as isogenic controls. **J, K, L)** Distribution of frequencies (J), RRP of SR and WR flies (K) and Tau of SR and WR flies (L) for flies expressing the *770-1310 Rho1* RNAi construct inside the clock cells, as well as isogenic (driver only) controls. Bars represent Mean ±SEM and numbers in bars indicate *n*, with the total number of flies originated from 10 (*JF02809*), 3 (*TRiP.HMS00375*), 2 (*325-786*) and 3 (*770-1310*) crosses. For population percentages column (panels A, D, G, J) *p<0.05; **p<0.01 and ***p<0.01 by Fisher's Exact test. For RRP (panels B, E, H, K) and Tau (panels C, F, I, L) columns, *p<0.05; **p<0.01 and ***p<0.001 by Mann-Whitney *U* test (α= 0.05).

Two more RNAis were tested (Figure 3.3), corresponding to constructs designed by Stephen Warner and with published results for *Rho1* phenotypes (Warner and Cook, 2009; Warner and Longmore, 2009). The lines target the 5'UTR and part of the first exon (*Rho1.770-1310*, Bloomington Stock 29003 and Rho1 RNAi 4 in this chapter) and sequences from the third and fourth exons (*Rho1.325-786*, Bloomington Stock 29002 and Rho1 RNAi 3 in this chapter). Notice that these RNAi lines are named RNAi 4 and 3 respectively not because of their order in the sequence but because their stock number. The second chromosome carrying the *Rho1.770-1310* (RNAi 4) construct, balanced with CyO^1, was proven to be lethal in homozygosis, probably due to insertion effects and unrelated to Gal4/UAS system. Therefore, the crossing scheme was modified by employing homozygous driver females and heterozygous males, yielding *tim(UAS)-Gal4/UASRNAi* progeny as experimental group, and *tim(UAS)-Gal4*/CyO^1 as isogenic control group.

Rho1.325-786 (RNAi 3) was tested in the same way that *JF02809* and *TRiP.HMS00375* against isogenic undriven controls. The expression of the construct rendered again many of the experimental flies arrhythmic, even compared with undriven females whose circadian behaviour showed some degree of disruption (Figure 3.4 G). Both genders showed reduced RRP (Figure 3.4H). The very few females displaying any rhythm at all showed a period length reduction, probably due their very poor rhythmicity (Figure 3.4 H). For *Rho1.770-1310* (RNAi 4) the driver-only controls represented another proof that the expression of Gal4 with the *tim(UAS)-Gal4* driver per se is not detrimental to rhythmicity (See Chapter 3.3.4). The knockdown dramatically increased the arrhythmic phenotype of the experimental populations (Figure 3.4 J), and equally reduced the RRP of rhythmic flies (Figure 3.4 K). There was no apparent effect on the period

length, although all the genotypes displayed longer than 24 h rhythms as expected because of the presence of the *tim(UAS)-Gal4* construct (Figure 3.4 L). Like with *JF02809*, flies expressing the other three RNAis displayed relatively normal activity during LD cycles (Figure 3.3).

In summation, expression of different RNAi lines targeting *Rho1* inside the clock cells successfully replicated the behavioural phenotype of whole-organism *Rho1* deficiencies. The arrhythmic phenotype was found in all the instances for the females, while males exhibited a higher resilience, or barely no effect for the case of the *TRiP.HMS00375* construct. While the RNAi expressing system could be affected by the differential dosage of Dicer-2 protein (with *UASDcr2* construct in the X chromosome), the same effect was found for the case of the $Rho1^{1B}$ mutation. With the different RNAi lines targeting different regions of the *Rho1* gene (with some overlapping between pairs), gathered data confirm that controlled levels of the small GTPase are required, inside specific cells, for the proper establishment of a circadian behaviour in *Drosophila melanogaster*. This fulfils the first of the aims of this project but leads to several open questions. Given the nature of the employed driver, we aimed to determine where inside the clock circuitry Rho1 is required for its function. This constitutes the Chapter 3.3.3, but at the same time further experiments were required to address possible problems of the RNAi system. These are described in the next subchapter, and were done to confirm and refine the first conclusion of this project.

3.3.2 The *Rho1*-deficit behavioural arrhythmia is caused by a specific role carried by Rho1, with at least post-developmental contribution

As presented in the introduction, circadian rhythms are present during the larval stages preceding the adult imago fly (Sehgal, Price and Young, 1992; Mazzoni, Desplan and Blau, 2005; Ruiz *et al.*, 2010). As a consequence, clock bearing cells have to cope with reduced *Rho1* levels in mutant organisms, which may cause permanent effects. Despite heterozygote individuals consistently reported as "wild-type"-like and without detrimental effects (Xu, Keung and Myat, 2008), a precise mechanism like the circadian clock could be more sensitive to these conditions if Rho1 was involved with it. The use of Gal4 lines and RNAi constructs carries similar problem because of: 1) the need of establishing a correlation between arrhythmia and *Rho1* reduced levels; 2) active drivers during developmental stages as clock components are found during larval phases; and 3) possible off-clock targets of these drivers.

With *JF02809* construct becoming the most widely used in further experiments, its specificity to target *Rho1* was tested. Because *tim* driver specifically targets to a minimum part of the cells constituting the adult fly brain (plus cells in the visual systems), the *tubulin* (*tub*) driver was

employed, being expressed in all the cells of the organism (Lee and Luo, 1999). This systemic driver was co-expressed along the Gal80^{TS} construct from the TARGET system, constituting a useful on/off switch (McGuire *et al.*, 2003). Because these experiments did not involve locomotor assays, isogenic undriven controls carrying the *TM3Ser*^{1} balancer chromosome were employed. Therefore, unlike with the timeless driver shown in previous assays targeting the clock neurons; these flies, if uncontrolled, expressed the RNAi in all their cells.

Unsurprisingly, expression of the RNAi inside all the cells during development by switching off Gal80^{TS} at 29 °C impeded the emergence of experimental flies (non-*Ser*^{1} individuals) while assessing the progeny (data not shown). The lack of dead pupas suggested that experimental individuals died before reaching this stage, consistent with reported data from *Rho1* mutants dying of massive defects in the embryo-to-larva morphological changes (Magie *et al.*, 1999). In juxtaposition, these animals survived until adulthood when the RNAi expression was inhibited at 17 °C, with no apparent deviations from the expected proportions due to 50-50 chances of F1 animals receiving either the driver or the balancer chromosome. No specific developmental delays were either found for any of the genotypes in both genders.

Next, emerged adults were transferred to 29 °C, activating RNAi expression in experimental organisms, and subjected to a longevity assay. Flies with acute expression of the RNAi inside their cells died faster than the control counterparts under these conditions (Figure 3.5). The median survival for experimental females was only 4 days (undefined for controls because of low mortality in the time range) and 12 days for male individuals (30 for controls). These data are consistent with the notion that the expression of the *JF02809* construct is removing a critical element of cell life, and thus its post developmental expression is sufficient for compromising survival.

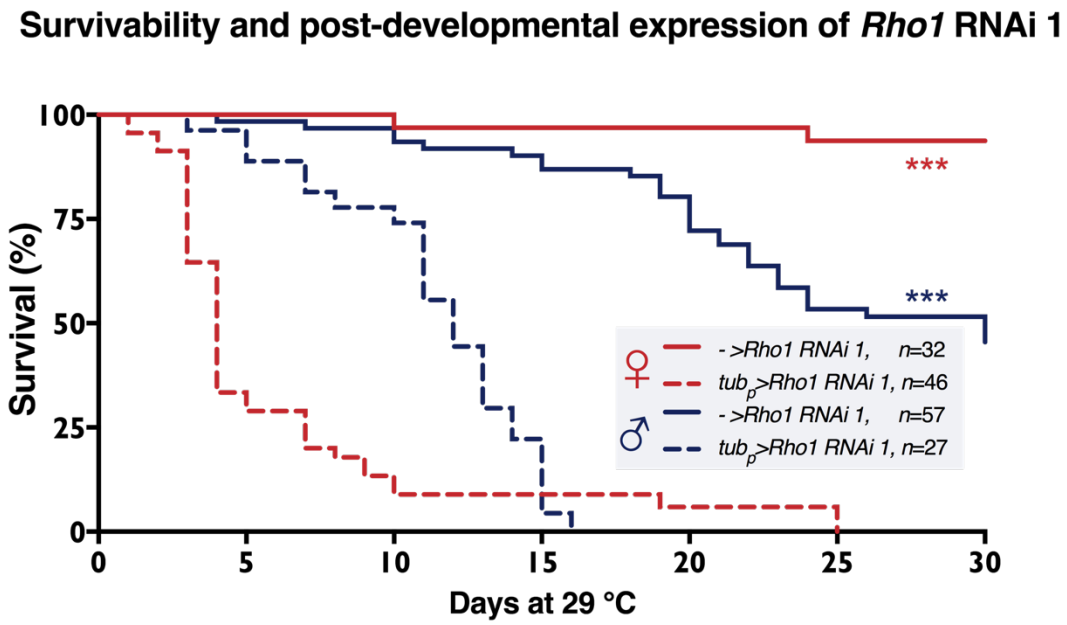

Figure 3.5. Effects of *JF02809 Rho1* RNAi overexpression upon survivability. Survival curves of flies raised at 17°C (*permissive* conditions for the TARGET system) and transferred to 29 °C (*restrictive* conditions) with *Rho1* RNAi 1 (*JF02809*) expression driven by tub_p> (absent in undriven isogenic controls). *n* is indicated per genotype/gender in the legend and flies are originated from 4 different crosses. For both genders, ***p<0.0001 by Log-rank/Matel-Cox test while comparing experimental and control populations. Flies come from four different crosses.

Once the reduced survival of RNAi-expressing flies was confirmed, individuals from the different genotypes were collected at defined time points following RNAi expression, in order to quantify the *Rho1* levels. qPCR analysis revealed that only 48 hours of the construct expression was sufficient to dramatically reduce *Rho1* mRNA levels in both genders (Figure 3.6 A). While the heterozygous mutant flies maintained, as expected, half of the normal *Rho1* levels, 48 hours of RNAi expression were sufficient for reach a similar expression level. Although *tub* and *tim* cannot be completely compared (it is not possible to assay tub_p>*RNAi* flies in a locomotor assay because of the decreased survival), these data support that RNA interference is a more powerful tool than the heterozygous mutant. This resembles the results with locomotor assays, where three of the four RNAi lines showed greater effects on fly rhythmicity than the $Rho1^{1B}$ heterozygous mutant (See Chapter 3.3.1).

Expression analysis of the *Rho1.770-1310* (RNAi 4) construct, albeit showing a similar trend, did not provide conclusive results (Figure 3.6 B). This may be related to the detrimental effects of the chromosome carrying this construct, which forced the employment of driver-only controls (See Chapter 3.3.1). While *JF02809* showed no off targets (size 18 bp or more) for a search at NIN and TRiP databases (Perrimon, 2003; Ye *et al.*, 2012), the sequence of the *Rho1.770-1310* RNAi was found to target also the yet-uncharacterised gene CG8909 at the X chromosome (Warner and Longmore, 2009; Attrill *et al.*, 2016). Experiments carried out by Joshua Mahler also showed no detectable differences when the RNAi 2 line (*TRiP.HMS00375* construct) was expressed (Figure 3.6 C), although these results correlate with the mild (almost null in the case of males) effect of this RNAi in rhythmicity (Figure 3.4 D, E).

Nevertheless, the three RNAis show the same correlation between effects in *Rho1* gene levels and rhythmicity of adult flies, even by comparing the effects of two different drivers and not including in the analysis the arrhythmic percentage of the population (Figure 3.6 D).

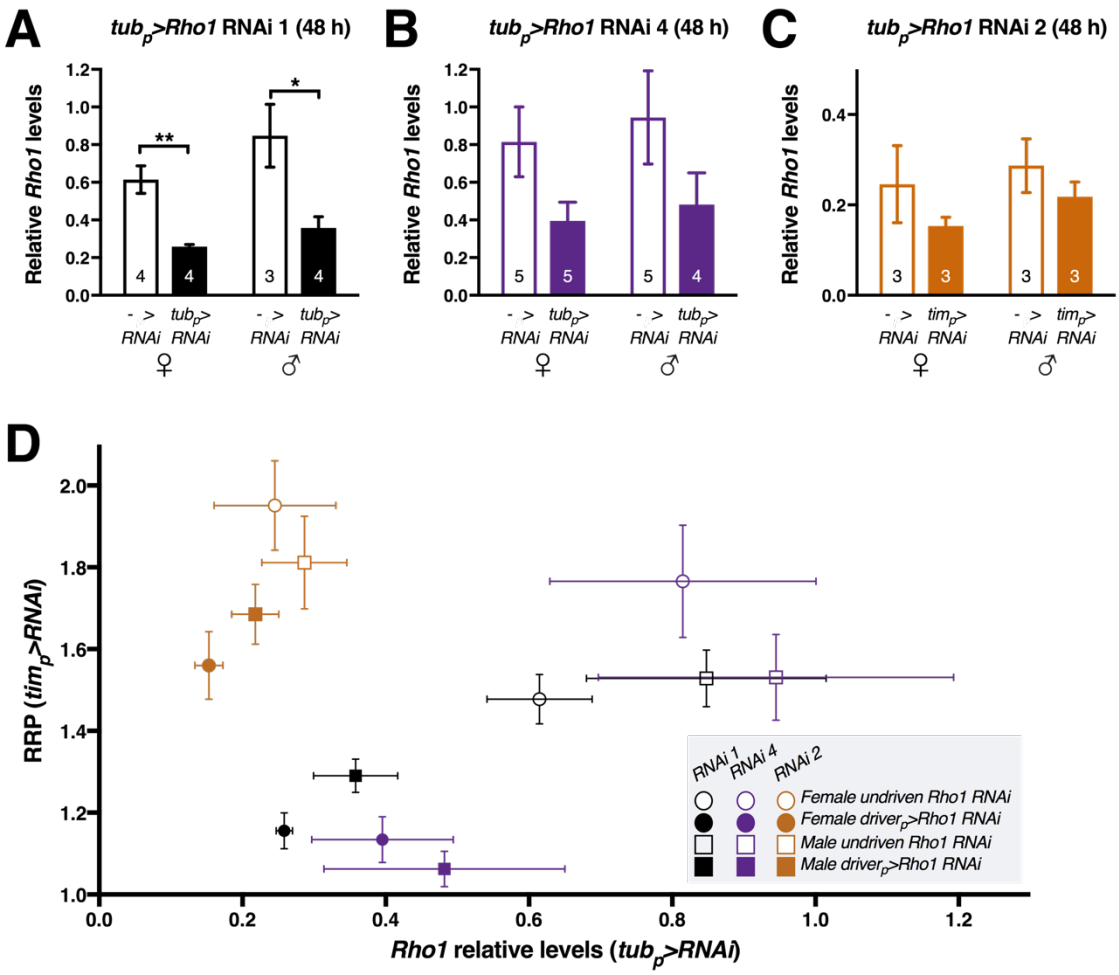

Figure 3.6 Expression levels of *Rho1* under RNAi knockdown inside the *tim* cells. A, B, C) *Rho1* gene levels (relative to *RpL32*) inside fly heads under post-developmental expression of the *JF02809* (RNAi 1, A, *Rho1.770-1310* (RNAi 4, B) or *TRiP.*HMS00375 (RNAi 2, C) constructs. Flies were raised at 17°C (*permissive* conditions for the TARGET system) and transferred to 29 °C (*restrictive* conditions) for 48 h before head harvesting. Undriven isogenic controls lack the tub_p> driver for both RNAis. Bars represent Mean ±SEM and numbers indicate number of different biological extractions. *p<0.05 and **p<0.01 by t-test [tub_p>$dsRho1^{JF20809}$ females: t(6)=-4.798, p=0.003; and tub_p>$dsRho1^{JF20809}$ males: t(5)=-3.133, p=0.026]. No significance was found for the RNAi 4 [tub_p>$dsRho1^{Rho1.770-1310}$ females: t(8)=-1.994, p=0.081; and tub_p>$dsRho1^{Rho1.770-1310}$ males: t(7)=-1.457, p=0.188] and RNAi 2 [tub_p>$dsRho1^{TRiP.HMS00375}$ females: t(4)=-1.055, p=0.351; and tub_p>$dsRho1^{TRiP.HMS00375}$ males: t(4)=-1.01, p=0.37]. Experiments including RNAi 2 were carried out by Joshua Mahler. **D)** Comparison of the *Rho1* levels presented at panels A and B against the Relative Rhythmic Power (RRP) when the RNAi lines are expressed with *tim(UAS)-Gal4* driver as presented in

Figure Figure 3.4 C, L (weakly or strongly rhythmic flies only). Notice that controls for RNAi 1 and RNAi 2 are undriven individuals, while they are driver-only flies for RNAi 4.

In an alternate approach to changing *Rho1* levels inside the clock cells overexpression of the wild-type *Rho1* gene (Weber and Mlodzik, 2003) inside the *tim* cells led to similar effects as knockdown in female rhythmicity, with no effect on males (Figure 3.7 A, B). This experiment was then repeated in a $Rho1^{1B}$ mutant heterozygous background to test for rescue. Indeed, overexpression of *Rho1* inside the female $Rho1^{1B}$/+ clock cells improved their rhythmicity, while no rescue was found in the case of the males (Figure 3.7 A, B). These results represent a contradiction with the recently published studies regarding the locomotor arrhythmia induced by Rho1 overexpression inside the PDF neurons (part of the *tim* cells)(Fanto *et al.*, 2000; Petsakou, Sapsis and Blau, 2015) that cannot be explained with the results and conditions of this group of experiments.

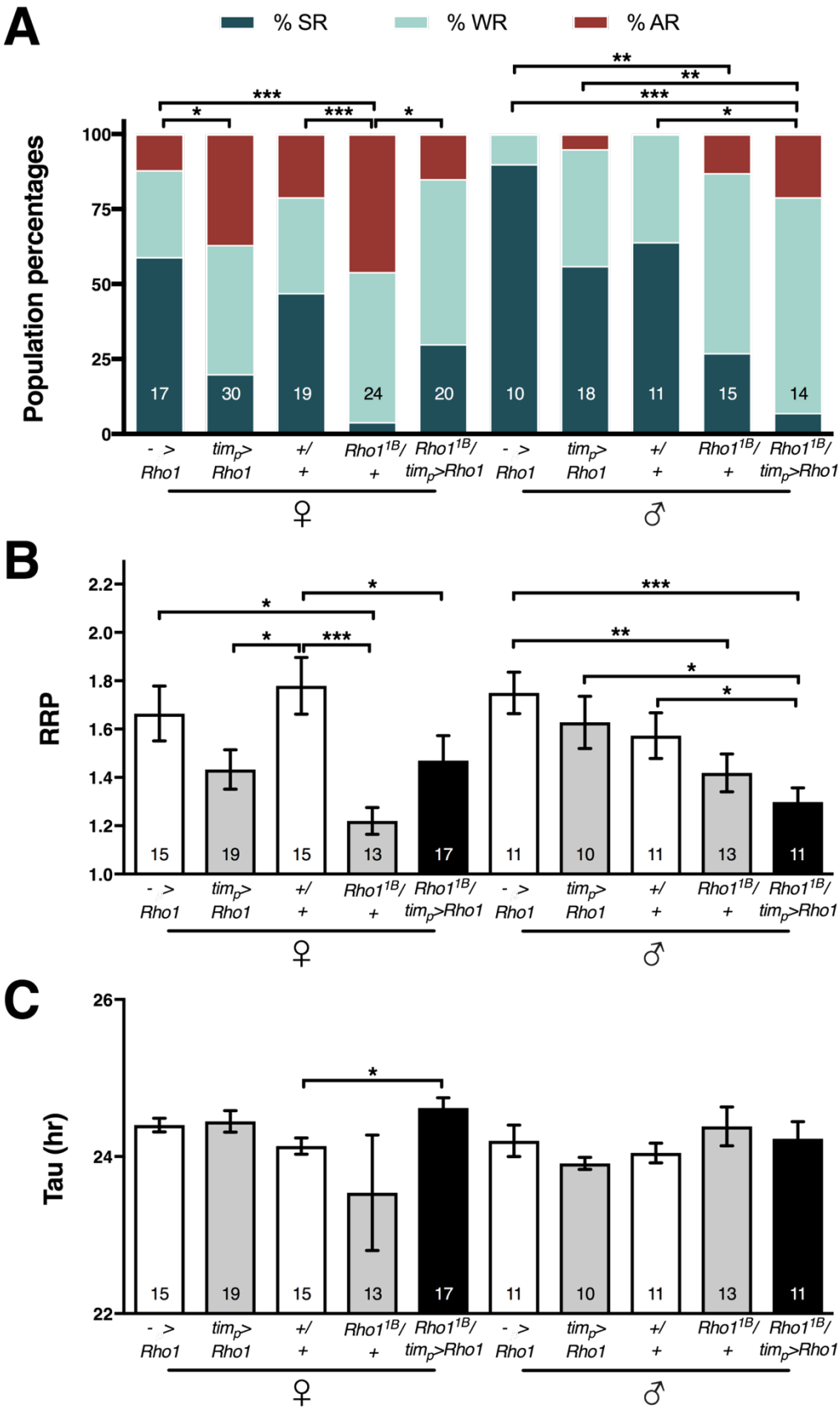
A
% SR
% WR
% AR
Population percentages
100
75
50
25
0
17
30
19
24
20
10
18
11
15
14
- > Rho1
timp> Rho1
+/ +
Rho1^1B/ +
Rho1^1B/ timp>Rho1
♀
♂
B
RRP
2.2
2.0
1.8
1.6
1.4
1.2
1.0
15
19
15
13
17
11
10
11
13
11
C
Tau (hr)
26
24
22

Figure 3.7. Effects of *Rho1* overexpression and interactions with the *Rho1^{1B}* mutant allele in *Drosophila melanogaster* circadian behaviour. Distribution of frequencies (Strongly Rhythmic, SR; Weakly Rhythmic, WR or Arrhythmic, AR) for the given genotypes. **B)** Relative Rhythmic Power (RRP) of SR and WR flies for the given genotypes. **C)** Period Length (Tau) of SR and WR flies for the given genotypes. Bars represent Mean ±SEM and numbers in bars indicate *n*, with the total number of flies originated from 4 (*Rho1* overexpression), 6 (*Rho1^{1B}* allele, as firstly presented in Figure 3.2), and 4 (*Rho1* overexpression in the *Rho1^{1B}/+* background) crosses. White bars represent isogenic controls for *tim$_p$>Rho1* (first bar) or the *Rho1^{1B}* allele (third bar, as previously shown in Figure 3.2). For population percentages panel (A), *p<0.05, **p<0.01 and ***p<0.001 by Fisher's Exact test. For RRP (B) and Tau (C) panels, *p<0.05, **p<0.01 and ***p<0.001 by Mann-Whitney *U* test (α= 0.05).

A final approach involving manipulations of Rho1 employed two different functional mutant lines. Rho1^{V14} is a constitutively activated isoform that can be selectively expressed thanks to the Gal4/UAS system (Lee *et al.*, 2000; Weber and Mlodzik, 2003). This expression replicated the phenotype of wild-type Rho1 overexpression in females, with barely any effect in the male population (Figure 3.8 A, B, C). Despite both experiments being set in different backgrounds, Overexpression of the mutant seemed to be more detrimental to the rhythmicity of the animals, which is consistent with its activated state. The second mutant isoform, Rho1N^{19}, is a dominant negative protein which causes a loss-of-function state when interacting with the intrinsic Rho1 pool (Strutt, Weber and Mlodzik, 1997; Weber and Mlodzik, 2003). Expression of this isoform inside the clocks cells reduced the female RRP (Figure 3.8 D, E). Despite the low number of control counterparts, experimental males remained fundamentally unaffected by this isoform, similar to previous assays (Figure 3.8 D, E). The mild and female-only phenotypes with both isoforms again contrasts with the presented results of the dominant negative isoform inside the PDF neurons and its detrimental effect upon rhythmicity (Petsakou, Sapsis and Blau, 2015). Genetic background could account for the discrepancy between RNAi and dominant negative expression in this project.

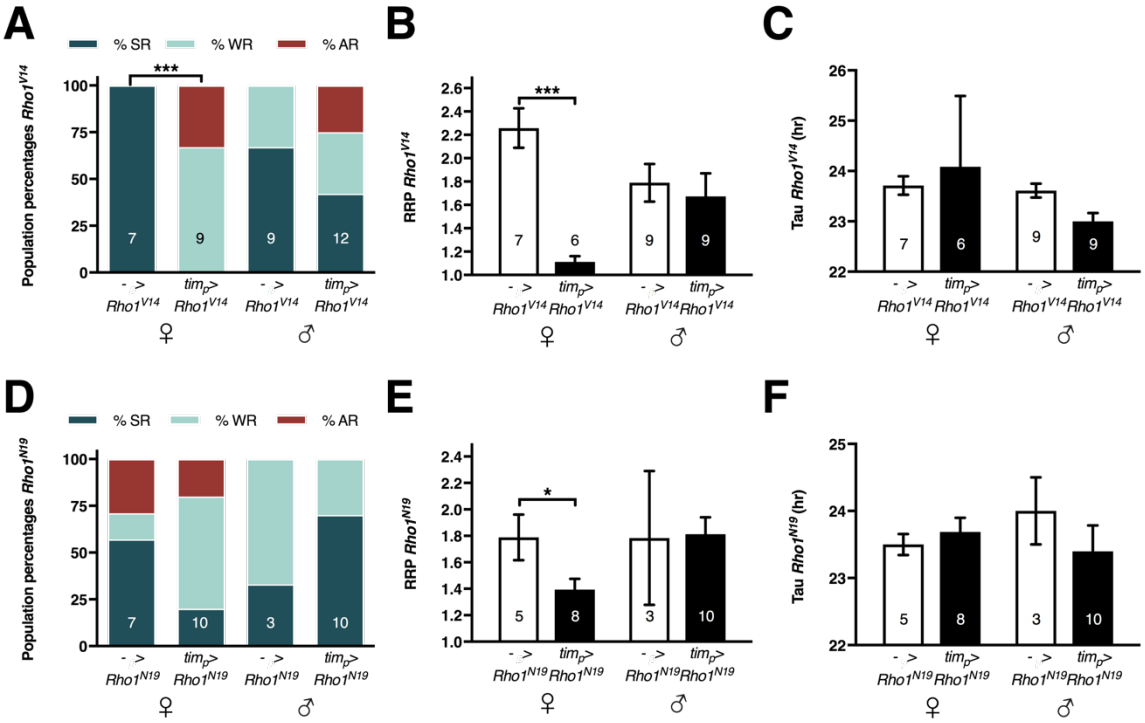

Figure 3.8 Effects of overexpression of *Rho1* isoforms inside the clock cells in *Drosophila melanogaster* circadian behaviour. A, B, C) Distribution of frequencies (Strongly Rhythmic, SR; Weakly Rhythmic, WR or Arrhythmic, AR) (A), Relative Rhythmic Power (RRP) of SR and WR flies (B) and Period Length (Tau) of SR and WR flies (C) for flies expressing the constitutively activated $Rho1^{V14}$ construct inside the clock cells, as well as isogenic (undriven) controls. **D, E, F)** Distribution of frequencies (D), RRP of SR and WR flies (E) and Tau of SR and WR flies (F) for flies expressing the dominant negative ^{Rho1N19} construct inside the clock cells, as well as isogenic (undriven) controls. Bars represent Mean ±SEM and numbers in bars indicate *n*, with the total number of flies originated from a single cross for each of the two isoforms. For population percentages panels (A, D) ***p<0.01 by Fisher's Exact test. For RRP (B, E) and Tau (C, F) panels, ***p<0.001 by Mann-Whitney *U* test (α= 0.05).

The results included so far in this subchapter are related specifically to Rho1 function, as it will be in the rest of this chapter. During the first year of the project, however, a genetic screen was performed with the goal of targeting other components of the Rho1-signalling pathway (See Chapter 1.4). The locomotor phenotypes are detailed in Appendix A1, but interpretation of the screen data provided further support to keeping the study around Rho1. The selective knockdown of the Rho1 activator RhoGEF2 (Barrett, Leptin and Settleman, 1997) reproduced the phenotype of *Rho1* knockdown with two different RNAi (Supplementary Table 1). The targeting of the

downstream effector Rok (Mizuno *et al.*, 1999) only reduced the female rhythmicity (Supplementary Table 1). Furthermore, overexpression of a constitutively activated isoform of Rok (and thus, bypassing the need of Rho1 if Rok were the one acting upon the circadian behaviour) failed to totally rescue the *Rho1* knockdown phenotype (Supplementary Table 1). These inconclusive results, along the previously mentioned recent publication (Petsakou, Sapsis and Blau, 2015) indicate that the Rho1-signalling pathway inside the clock cells could intervene in the establishment of the adult circadian behaviour of the fly. These results are further discussed in Chapter 4.

Once the correlation between locomotor arrhythmia and reduced *Rho1* levels (both for the $Rho1^{1B}$ mutant and the RNAi system) was confirmed, the next question to ask was whether a long term *Rho1* deficit could have led to defects in the clock cells. In other words, could *Rho1* knockdown be causing developmental effects that would irreversibly impact upon the adult locomotor circadian behaviour? The TARGET system allowed to address this possible issue by blocking the RNAi (*JF02809* construct) expression inside the *tim* cells until flies reached adulthood.

The first experimental setups were met with a series of problems, ranging from low overall rhythmicity of the flies at 17 °C and the compromised survivability of animals at 29 °C (data not shown). Hence, we failed to subject the flies to long term RNAi expression only during adulthood. The last employed protocol kept experimental and control flies at 17 °C during the developmental stages while being subjected to a 12:12 LD cycle as programmed for the environmentally controlled room. Flies were then loaded into monitors and moved, at the end of the light phase, to either 17 °C or 29 °C in DD. This means that flies at 29 °C started to express the RNAi at the same time they were released in constant conditions.

While experimental and control populations exhibited no differences at 17 °C (Figure 3.9 B, C, D), acute adult-only expression of the RNAi at 29 °C impacted on the behaviour of the experimental flies (Figure 3.9 E, F, G). Many female flies lost their rhythmicity when exposed to restrictive conditions after a week of RNAi knockdown expression, while males did not exhibit this phenomenon (Figure 3.9 E). Quantitative analysis of the RRP of weakly or strongly rhythmic flies indicated than *Rho1* RNAi expression reduced rhythmicity of the carrier flies in both genders (Figure 3.9 F). The lesser effect compared to previous assays (Figure 3.4) can be explained by the shorter expression window in this assay, which may also account for the “wild-type”-like actograms (Figure 3.9 A). Therefore, these assays proved that acute reduction of *Rho1* levels inside adult clock cells is sufficient to reduce the rhythmicity of the flies in *free run*. Developmental effects cannot be totally discarded though, as they could still contribute to the

phenotype with our current data. This possibility would fit with the mild phenotype uncovered with this assay. The reason for the reduced arrhythmia outcome could also simply rely on the short expression time of the RNAi which, as already stated, started at the same time than the analysis in DD. This experiment revealed, regardless, a post-developmental contribution of the small GTPase levels to the adult rhythmicity in DD.

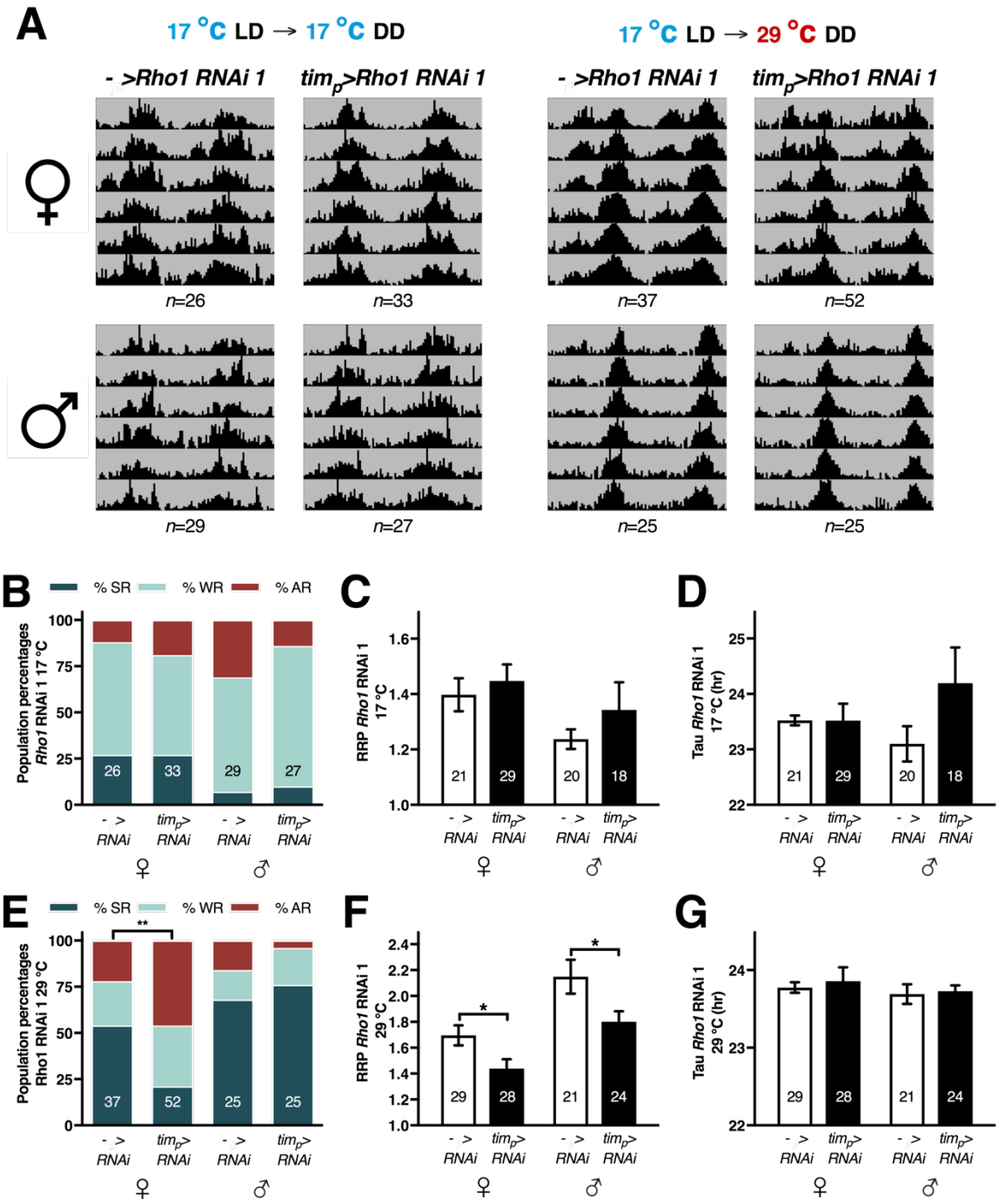

Figure 3.9. Post-developmental impact of *Rho1* knockdown inside the clock cells. Developing flies are raised at 17 °C with a 12:12 LD cycle to be entrained with (data not gathered)

with the Gal80^{TS} repressor switching Gal4/UAS system off. Adults are then maintained at 17 °C (RNAi expression *off*, left actograms) or transferred to 29 °C (RNAi expression *on*, right actograms), both in DD conditions. The quantified data from the next 7 days in DD are found in the next panels. Column titles indicate given temperature and genotype, and rows represent females (top) and males (bottom). Grey background represents dark period. *n* numbers are indicated below the actograms. Actograms represent the normalised population average. Isogenic control genotypes lack the *tim(UAS)-Gal4 driver*. **B, C, D)** Distribution of frequencies (Strongly Rhythmic, SR; Weakly Rhythmic, WR or Arrhythmic, AR) (B), Relative Rhythmic Power (RRP) of SR and WR flies (C) and Period Length (Tau) of SR and WR flies (D) for flies not expressing the *JF02809 Rho1* RNAi construct at 17 °C, as well as isogenic (lacking the driver) controls. **E, F, G)** Distribution of frequencies (E), RRP of SR and WR flies (F) and Tau of SR and WR flies (G) for flies expressing the *JF02809 Rho1* RNAi construct at 29 °C, as well as isogenic (lacking the driver) controls. Bars represent Mean ±SEM and numbers in bars indicate *n*, with the total number of flies originated from 4 (flies tested 17 °C) and 7 (flies tested 29 °C) crosses. For population percentages column (B, E), **p<0.01 by Fisher's Exact test. For RRP (C, F) and Tau (D, G) columns, *p<0.05 by Mann-Whitney *U* test (α= 0.05).

The results from this chapter suggest that Rho1 has a function in the adult clock neurons, and that changes in its expression levels are detrimental to the rhythmicity of the flies. *Rho1* knockdown could still cause detrimental effects for the clock neurons fitness, although the presence of anticipatory rhythms in LD conditions, in contrast to the phenotypes of *per*^{01} and *Pdf*^{01} mutants, points to the presence of relatively functional clock neurons, able at least of transmitting temporal information where subjected to environmental cycles. The cited mutants, although exhibiting responses to *lights-on* and *lights-off* event, display a prominent change in their anticipatory activity (*Pdf*^{01} flies) or no anticipation at all (*per*^{01} mutants and every other selective disruption of clock-specific components) (Renn *et al.*, 1999; Grima *et al.*, 2004; Lee *et al.*, 2016). Further studies will be presented regarding the state of the clock neurons (Chapter 3.4) and the precise nature of the behavioural responses under environmental cycles (Chapter 3.6). But the next question was, once a relationship between *Rho1* gene product and the behavioural rhythms was confirmed, to determine which of the clock neuron subsets was responsible for the characterised phenotype.

3.3.3 Spatial mapping reveals specific requirement of Rho1 inside the PDF-expressing neurons

The fact that flies expressing Rho1 RNAis with the *tim(UAS)-Gal4* driver reached adulthood was interesting, because of the developmental consequences of tampering with the targeted cells (Stoleru *et al.*, 2004; Keene *et al.*, 2011). Indeed, expression of the pro-apoptotic gene *Head involution defective* (Hid) with this driver caused the animals to die during pupa stage (data not shown). This is most likely due to wide-spread activity of this driver in not only clock neurons, but also peripheral clock cells and some other cell types, including glia (identified by the *repo* lineage) (Kaneko and Hall, 2000; Nagoshi *et al.*, 2010; Chen *et al.*, 2014). It has been reported that glial cells, besides expressing clock components, can indeed affect the circadian behaviour (Ewer *et al.*, 1992; Ng, Tangredi and Jackson, 2011; Ng and Jackson, 2015).

The results with *Rho1* knockdown inside the *tim* domain allowed the possibility that reduced *Rho1* levels inside some of the members of the glial subpopulation contributed to the emergence of the arrhythmic behaviour (Chen *et al.*, 2014). This could represent an issue for the found phenotype with selective *Rho1* knockdown, because some glial cells inside the brain exhibit Per protein circadian rhythms (Zerr *et al.*, 1990; Jackson, 2011). While this rhythm is not necessary for the locomotor behaviour in *free run*, disruption of glia leads to detrimental effects upon rhythmicity, maybe caused by an actual contribution of glia to the circadian clock (Suh and Jackson, 2007; Ng, Tangredi and Jackson, 2011; Ng and Jackson, 2015). Reduced *Rho1* levels could compromise glial activity and in turn disrup brain fitness as a consequence of reduced homeosthasis, with manifested effects in the circadian behaviour among other uncovered features. This hypothesis was tested by the addition of a *repo-Gal80* construct, kindly provided by Tzumin Lee (Awasaki *et al.*, 2008). The construct drives the repressor with the glial-specific *reversed polarity* (*repo*) gene promoter (Awasaki *et al.*, 2008), restricting the Gal4/UAS system to the actual clock-bearing cells. The presence of the construct failed to increase the percentage of flies exhibiting rhythmicity with *Rho1* knockdown (Figure 3.10 A, B), or to improve the RRP of the rhythmic ones (Figure 3.10 C). Concurrently *Repo-Gal80* did not affect the rhythmicity of the flies when the RNAi was not expressed (Figure Figure 3.10 A, B, C). System crashes during the entrainment phase did not allow further analysis during LD days, albeit LD response was apparently normal for these genotypes (Figure 3.10 A). These data showed that the contribution of *Rho1*-defective tim^{+} glial cells to the locomotor phenotype is negligible, if existent at all.

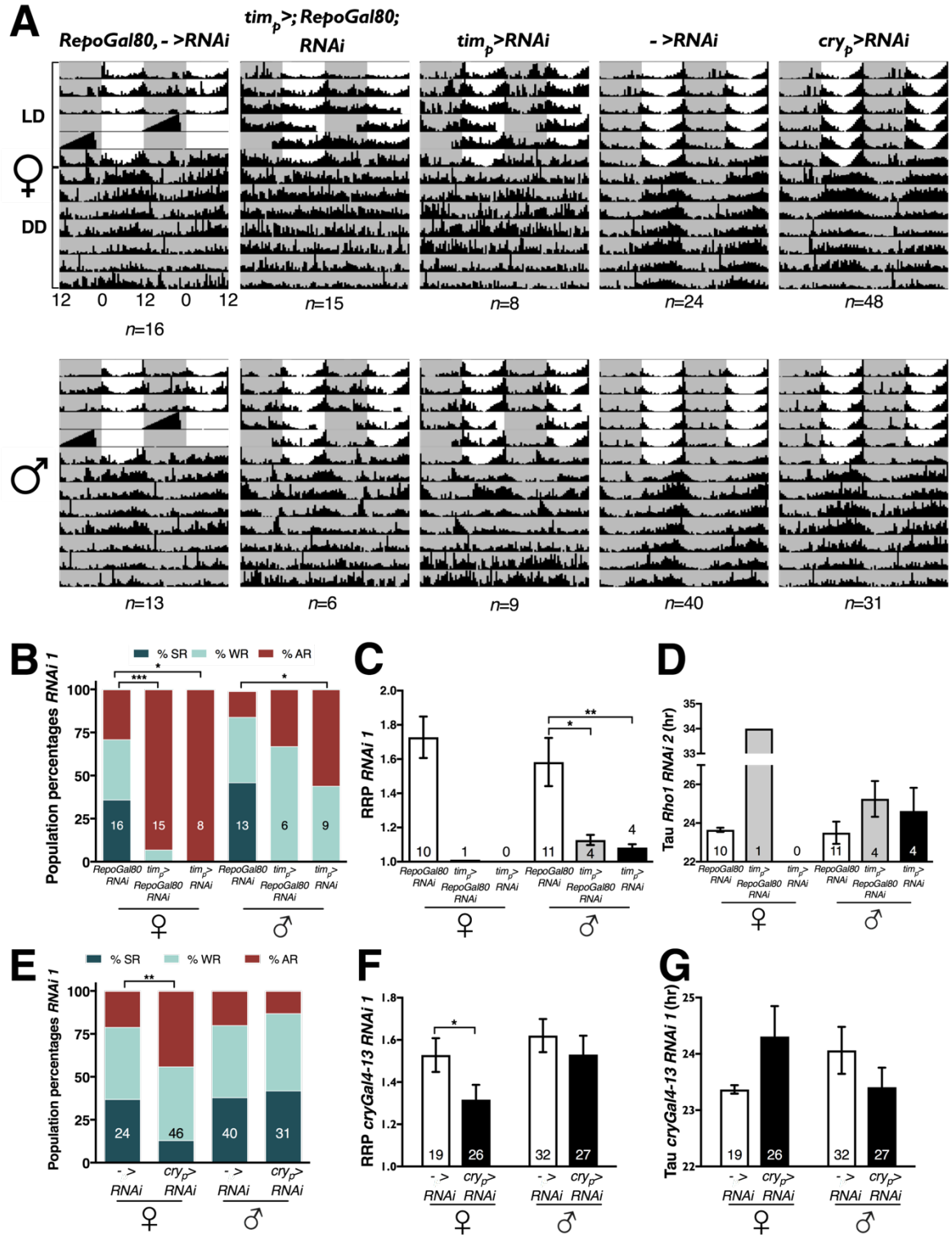

Figure 3.10. Lack of contribution of glial cells to *Rho1* deficit behavioural arrhythmia and selective knockdown inside *cry*-expressing neurons. A) Adults of both genders are entrained for 6 days in LD and transferred to DD conditions on day 7, at a constant temperature of 23 °C. The quantified data from the next 7 days in DD and *n* numbers are found in the next panels. Column titles indicate given genotype, and rows represent

females (top) and males (bottom). White background, light period; grey background, dark period. Actograms represent the normalised population average. The first three actograms for both genders contain data gaps during the LD phases because of DAM system crashes. As environmental conditions remained unchanged and DD phase was not affected, *free run* analysis of these populations remained unaffected. The first genotype constitutes the parental line and carries the *Repo-Gal80* (II) construct **B, C, D)** Distribution of frequencies (Strongly Rhythmic, SR; Weakly Rhythmic, WR or Arrhythmic, AR) (B), Relative Rhythmic Power (RRP) of SR and WR flies (C) and Period Length (Tau) of SR and WR flies (F) for flies expressing the *JF02809 Rho1* RNAi construct inside the *tim* cells with contribution or not of the *repo* glial population, as well as one of the parental lines carrying the *repo-Gal80* and RNAi constructs but not the *tim(UAS)-Gal4* driver (first actogram, the other parental line carrying the driver is shown in Figure 3.8). **E, F, G)** Distribution of frequencies (E), RRP of SR and WR flies (F) and Tau of SR and WR flies (G) for flies expressing the *JF02809 Rho1* RNAi construct inside the Cry-expressing clock neurons, as well as isogenic controls. Bars represent Mean ±SEM and numbers in bars indicate *n*, with the total number of flies originated from 1 (*Repo-Gal80* assay) and 6 (*cry-Gal4-13* assay) crosses. For population percentages column (B, E) *p<0.05; **P<0.001 and ***p<0.01 by Fisher's Exact test. For RRP (C, F) and Tau (D, G) columns, *p<0.05 and **p<0.01 by Mann-Whitney *U* test (α= 0.05).

Once the lack of contribution of glial cells to the phenotype was proven, more selective Gal4 drivers were tested in order to narrow down the targeted cells inside the *tim* domain. The *cry-Gal4-13* construct drives expression inside the classical M- (PDF-expressing) and E-cells (Emery *et al.*, 2000b; Zhao *et al.*, 2003)(See Chapter 1.3.7), constituting a more restrictive set of clock neurons inside the circuitry. Reduction of *Rho1* levels inside the dual oscillator cells was sufficient to reduce the female rhythmicity, but males remained mostly unaffected (Figure 3.10 A, E, F, G). These results again showed therefore a gender dimorphism in the *Rho1* knockdown phenotype, which consistently denotes males as more resilient to alterations in the small GTPase levels.

Diverse characterised drivers were screened for the expression of the *JF02809* construct. Many of these drivers finely restrict expression inside specific neuron clusters across the clock circuitry, but have broader domains during developmental stages or outside brain. As a consequence, many of these drivers caused developmental lethality during the metamorphosis stage. This was the case of different Gal4 lines derived from the *Clk* gene promoter *Clk gene* like *Clk4.5F* and *Clk4.1M*, that target 10 or 4 neurons of the DN_1p subclass (Zhang *et al.*, 2010a), or *Clk1.9*, expressing inside the

s-LN_v and the DN_2s (Kaneko *et al.*, 2012). The same effect was found for the *Mai179-Gal4* driver, which specifically targets E- and M- cells inside the adult brain (Grima *et al.*, 2004). Because of the attention focus on the DN_1p clock neurons in recent years (See Chapter 1.3.7), the *Clk4.1M* driver was combined with the TARGET assay in order to achieve post-developmental RNAi expression. Like with the others experimental setups with the $Gal80^{TS}$ construct (See Chapter 3.3.2), the flies were arrhythmic regardless of the presence of the Gal4 driver (data not shown).

In parallel, a complementary approach was followed by restricting the expression pattern of the *tim(UAS)-Gal4* driver. This was achieved with Pdf-Gal80, that blocks the system inside the PDF-expressing cells (Stoleru *et al.*, 2004). For the experimental setup presented in Figure 3.11, both parental lines (*tim* driver individuals and Pdf-Gal80 + RNAi individuals) were tested along F1 individuals which always carried both the driver and the RNAi construct. Some of these flies also carried the Pdf-Gal80 construct (RNAi expression allowed in all the clock cells but the PDF-expressing ones) and others the *CyO* balancer chromosome (RNAi expression in all the clock circuitry). These genotypes revealed that expression of the RNAi inside all the clock cells except the PDF-expressing neurons was not sufficient to induce the behavioural arrhythmia (Figure 3.11 A, B, C). The phenotypical rescue was total in males, with female individuals still showed a slightly compromised rhythmicity compared to paternal lines. This would indicate that Rho1 was specifically carrying a role in the sixteen clock neurons expressing the neuropeptide, with no phenotypical contribution of other members of the clock circuitry. Period length data was consistent with previous assays (Figure 3.11 D), although experimental males carrying the *Pdf-Gal80* construct did not exhibited a lengthening of their endogenous period length.

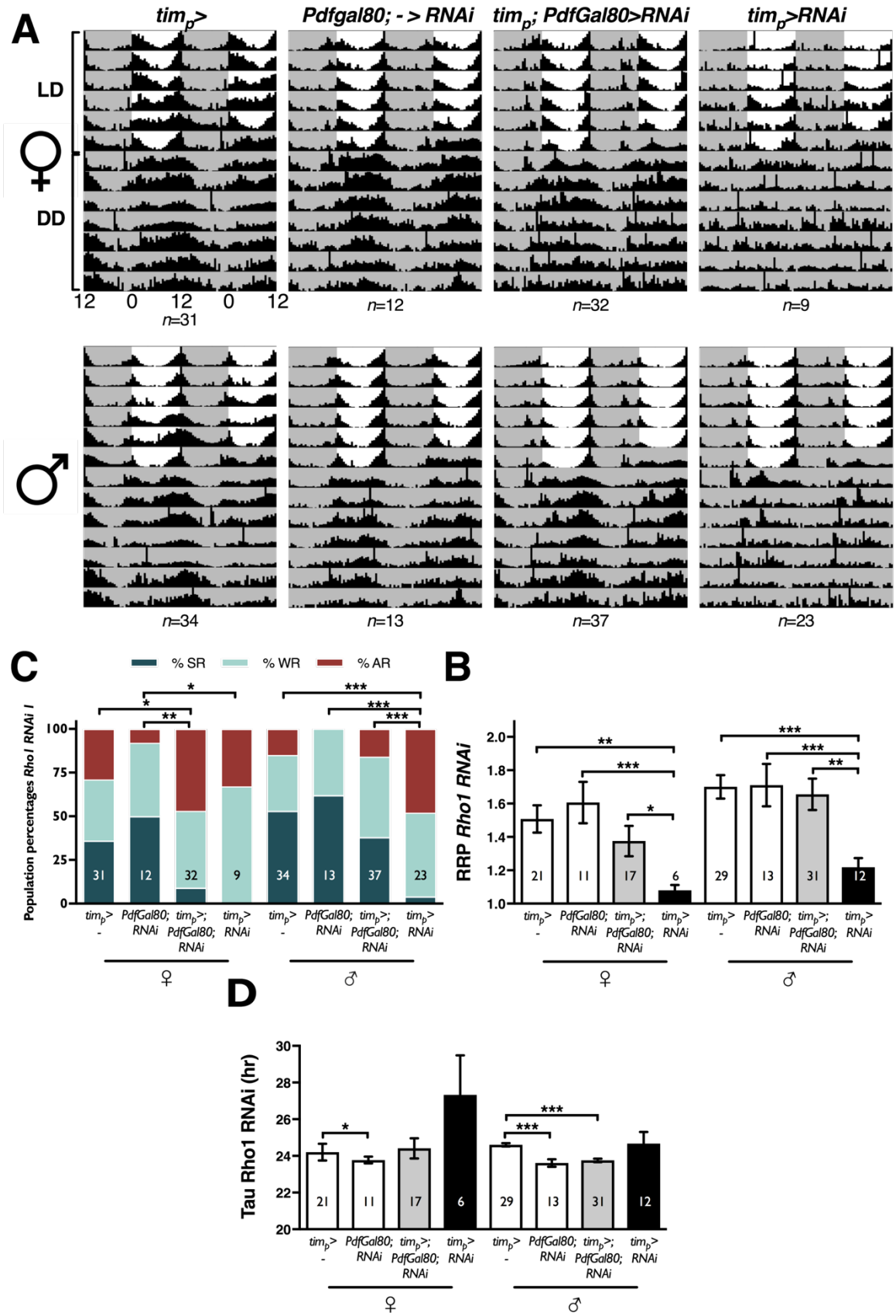
A
timp>
Pdfgal80; - > RNAi
timp; PdfGal80>RNAi
timp>RNAi
LD
DD
12 0 12 0 12
n=31
n=12
n=32
n=9
n=34
n=13
n=37
n=23
C
% SR
% WR
% AR
Population percentages Rho1 RNAi
B
RRP Rho1 RNAi
D
Tau Rho1 RNAi (hr)
timp> -
PdfGal80; RNAi
timp>; PdfGal80; RNAi
timp> RNAi
♀
♂

Figure 3.11. *Rho1* knockdown inside the clock cells requires the PDF-expressing neurons to lead to behavioural arrhythmia. Adults of both genders are entrained for 6 days in LD and transferred to DD conditions on day 7, at a constant temperature of 23 °C. The quantified data from the next 7 days in DD and *n* numbers are found in the next panels. Column titles indicate given genotype, and rows represent females (top) and males (bottom). White background, light period; grey background, dark period. Actograms represent the normalised population average. The first two genotypes are the parental lines (the RNAi line carries the *Pdf-Gal80* construct), with the last two isogenic populations from the progeny (with or without *Pdf-Gal80)* in the subsequent panels. **B)** Distribution of frequencies (Strongly Rhythmic, SR; Weakly Rhythmic, WR or Arrhythmic, AR) for flies corresponding to the displayed genotypes. **C)** Relative Rhythmic Power (RRP) of SR and WR flies corresponding to the displayed genotypes. **D)** Period Length (Tau) of SR and WR flies corresponding to the displayed genotypes. Bars represent Mean ±SEM and numbers in bars indicate *n*, with the total number of flies originated from 5 (*tim-Gal4* driver line) and 3 (*Pdf-Gal80* assay) assays/crosses. For population percentages column (B) *p<0.05; **p<0.01 and ***p<0.01 by Fisher's Exact test. For RRP (C) and Tau (D) columns, *p<0.05; **p<0.01 and ***p<0.001 by Mann-Whitney *U* test (α= 0.05).

It was then reasoned that the specific knockdown of *Rho1* in the PDF-expressing neurons would phenocopy the results with the *tim* driver, if these neurons were indeed the responsible of the phenotype. The *Pdf-gal4* construct allows to precisely express Gal4 inside these clock cells with no known off-targets, which has allowed its usage for behavioural studies with genetic ablation (Renn *et al.*, 1999). The presence of the construct, like with *tim(UAS)-Gal4*, extended the period length with no further effects upon rhythmicity (Figure 3.12 A-D). Corroborating the hypothesis, expression of the *JF02809* construct within these clock neurons reproduced the behavioural phenotype found with the *tim(UAS)-Gal4* driver (Figure 3.12 A-D). The gender component was present again, as experimental males were mostly rhythmic, yet statistically different from isogenic controls (Figure 3.12 B, C). Consistent with assays involving the *tim* driver, the extended period length seemed mostly attributed to the presence of Gal4, with driver-only flies displaying the longest Tau probably because of the increased variance in experimental genotypes (Figure 3.12 D). The *Rho1.770-1310* (RNAi 4) construct (See Chapter 3.3.2) was also tested with this driver, causing the same behavioural arrhythmia, even enhanced in the case of the experimental males (Figure 3.12 A, E, F, G). Like

with *tim(UAS)-Gal4* assays, these experimental flies were again tested along isogenic driver-only controls because of the construct being homozygous lethal (See Chapter 3.3.2).

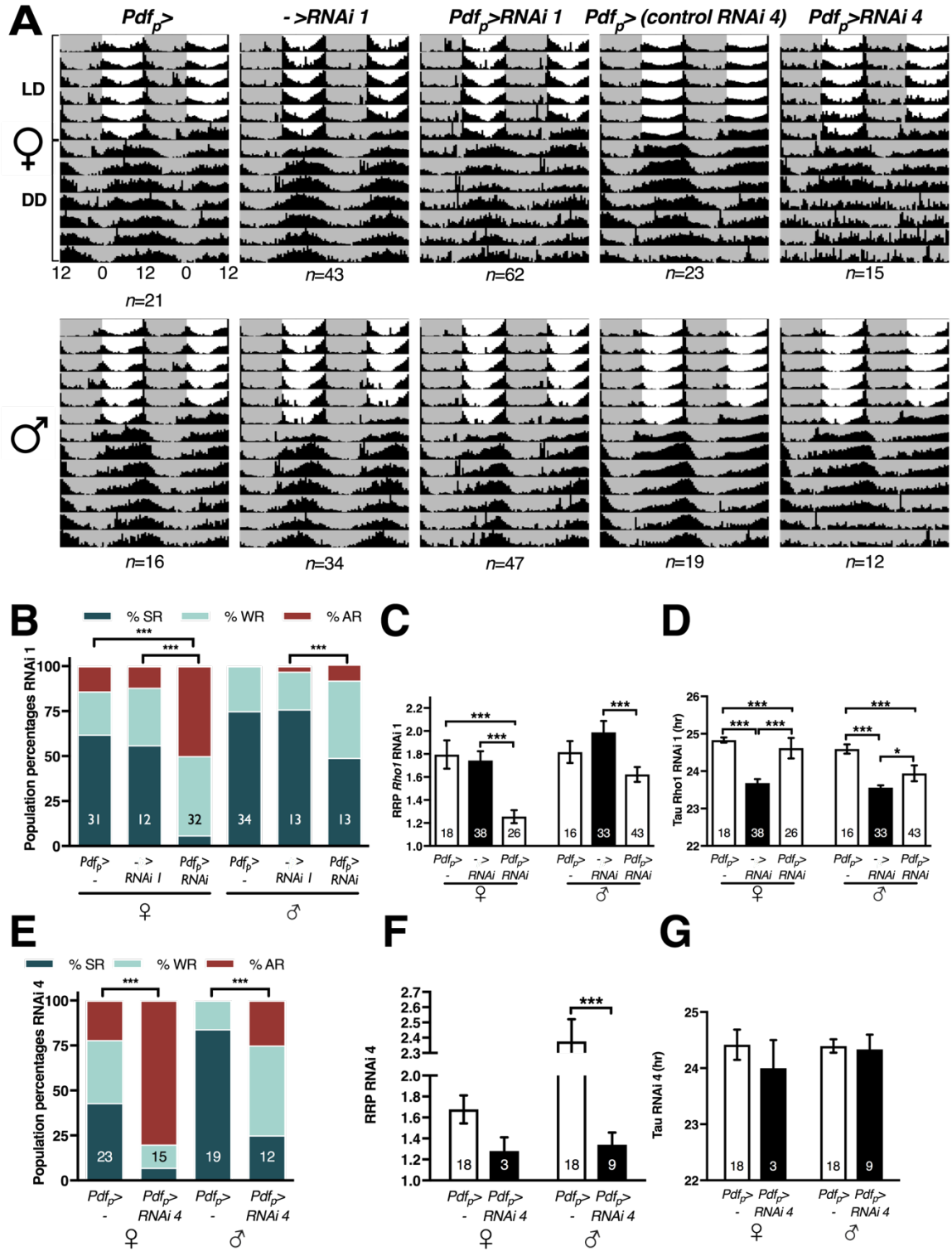

Figure 3.12. *Rho1* knockdown inside the PDF-expressing neurons is sufficient to lead to behavioural arrhythmia. Adults of both genders are entrained for 6 days in LD and

transferred to DD conditions on day 7, at a constant temperature of 23 °C. The quantified data from the next 7 days in DD and *n* numbers are found in the next panels. Column titles indicate given genotype, and rows represent females (top) and males (bottom). White background, light period; grey background, dark period. Actograms represent the normalised population average. Notice than the first *Pdf-Gal4* (Pdf_p) actograms correspond to the original driver line, while the second to last actograms correspond to the isogenic controls of the *770-1310 Rho1* RNAi construct. **B, C, D)** Distribution of frequencies (Strongly Rhythmic, SR; Weakly Rhythmic, WR or Arrhythmic, AR) (B), Relative Rhythmic Power (RRP) of SR and WR flies (C) and Period Length (Tau) of SR and WR flies (F) for flies expressing the *JF02809 Rho1* RNAi construct inside the *Pdf* neurons, as well as isogenic controls. **E, F, G)** Distribution of frequencies (E), RRP of SR and WR flies (F) and Tau of SR and WR flies (G) for flies expressing the *770-1310 Rho1* RNAi construct inside the *Pdf* neurons, as well as isogenic (driver only) controls. Bars represent Mean ±SEM and numbers in bars indicate *n*, with the total number of flies originated from 3 (*Pdf-Gal4* driver line) and 3 (*Pdf-Gal4* assay) assays/crosses. For population percentages column (B, E) *p<0.05 and ***p<0.01 by Fisher's Exact test. For RRP (C, F) and Tau (D, G) columns, *p<0.05; **p<0.01 and ***p<0.001 by Mann-Whitney *U* test (α= 0.05).

The drivers *c929* and *R6*, that can subdivide the PDF^+ subpopulations (the l-LN_vs and the 4 pairs of s-LN_vs, respectively) were aimed to be tested. This resulted however again in developmental lethality, much more like previous drivers during the pupa stage. We therefore believed that RNAi expression outside the clock circuitry led to death, consistent with the lethality of the tub_p*-Gal4* driver (See Chapter 3.3.2). For example, *c929* is reportedly expressed in over a hundred neurons inside the adult brain (Taghert *et al.*, 2001). The *R6-Gal4* driver is expressed in parts of the tracheal system (observations by P Taghert) and has produced instances of developmental lethality before (Helfrich-Forster *et al.*, 2007a; Head *et al.*, 2015). Because of the detrimental locomotor effects caused by $Gal80^{TS}$ in previous assays, none of these drivers was tested in an adult-only context.

Altogether, results from this subchapter indicate that the small GTPase Rho1 intervenes in the establishment of the adult Drosophila circadian behaviour by having a role inside the clock neurons expressing PDF. This satisfactorily fulfils the spatial and temporal characterization of the original phenotype found in mutant individuals, but still brings into question the precise role Rho1 has inside the clock cells.

3.4 Effects of *Rho1* knockdown in anatomy and function of *Drosophila* clock cells

3.4.1 Purpose of the CNS examination

The previous subchapters have highlighted a role of the small GTPase Rho1 in the establishment of the adult circadian locomotor behaviour of the fruit fly. The locomotor activity of the flies is the resulting output of a series of steps that start with a molecular oscillator inside the clock neurons (Yoshii, Rieger and Helfrich-Forster, 2012). Therefore, interrogating the clock cells inside the arrhythmic flies can clarify in which stage Rho1 is acting upon the resulting locomotor behaviour.

A previously detailed (Chapter 1.3.2), the molecular oscillator of *Drosophila melanogaster* consists of a negative feedback transcriptional loop. The heterodimer Clk-Cyc upregulates the expression of different proteins like Per and Tim. These proteins accumulate in the cytoplasm during early hours of the night, when they form a stable heterodimer and translocate to the nucleus (Shafer, Rosbash and Truman, 2002). Per-Tim then represses Clk-Cyc activity, which downregulates the expression of its components (Curtin, Huang and Rosbash, 1995; Darlington *et al.*, 1998).

The purpose of the imaging of the clock cells was to test if the function of the molecular oscillator is affected by reduced *Rho1* levels. To this aim, Per protein immunostaining was used as a proxy of the state of the molecular clock with its characteristic nuclear accumulation during the late night and early hours of the day, leading to degradation and absence during the rest of the day (Shafer, Rosbash and Truman, 2002). There exist different ways the small GTPase Rho1 or its signalling pathway could interact with the oscillatory feedback loop. Nuclear actin could act in the clock, probably as a consequence of a systemic cellular mechanism rather than specific interactions (Hofmann, 2009). The actin cytoskeleton is a highly dynamic structure involved in many processes including nuclear transport, hence its disruption could indirectly disrupt the clock (Pawlowski *et al.*, 2010). The alternate hypothesis stated that the clock circuitry remains at least in part intact was tested, as this would fit with the locomotor rhythms found in LD cycles for these adult flies. It is worth remembering that flies with genetic ablation of the PDF-expressing neurons can follow LD cycles, but fail to maintain the rhythms in DD (Renn *et al.*, 1999).

CT02 and CT14 time points (two hours after subjective dawn and two hours after subjective dusk, respectively) were chosen in order to maximize the expected differences in terms of Per protein

expression, PDF subcellular location and complexity of the s-LN_v axonal projections (Zerr *et al.*, 1990; Park *et al.*, 2000; Shafer, Rosbash and Truman, 2002; Fernandez, Berni and Ceriani, 2008). It is therefore important to consider the temporal resolution limits of the experiments. Fly brains were dissected on the second day of exposure to DD conditions. This is, after 26 (CT02) or 38 (CT14) hours in DD, when the animals are already exhibiting arrhythmic behaviour.

3.4.2 *Rho1* knockdown inside the clock cells does not disrupt the molecular oscillator

Expression of the *UASmCD8::GFP* construct with the *tim(UAS)-Gal4* driver was employed to mark and locate the clock circuitry inside the brain (Lee and Luo, 1999). The experimental cross consisted of female flies with these constructs being crossed with males carrying the *JF02809 Rho1* RNAi transgene (RNAi 1 in previous subchapters). The need of a driver in order to tag the cells with mGFP discarded the employment of isogenic (undriven) controls, so the flies from the mother stock (driver only) were used as controls instead. These flies were carefully collected at the same time that the experimental progeny, thus guarantying to be the same age. Unlike in some research works, all the flies from a given genotype were dissected without previously dividing the individuals into categories based on their response in a locomotor assay. When the rhythmicity of flies from the same genotype (sometimes even from the same batches) was tested, it was curiously found that the GFP construct caused detrimental effects on female rhythmicity, while male rhythmicity was exclusively dependent on the expression of the RNAi construct as previously shown (See Chapter 3.3.1 and Supplementary Table 4).

The experiment presented a series of limitations regarding the identification of the different cell clusters. The dorsal region proved to be especially challenging because of the high density of cells and tangled neuronal processes. Only clearly identified DN_2s were classified that way, and therefore some of them may have contributed to the DN_1 group. Because of their poor visualization and challenging imaging, DN_3s were ruled out from the assay, as well as the barely characterised LPNs.

The first immediate result of the imaging of the clock circuitry was the confirmation that these neurons remained alive despite *Rho1* knockdown (Figure 3.13 and Figure 3.14). Although no further analysis was done, the morphology of the affected neurons remained wild-type, without displaying any striking gross morphological defect. The tangling of the different projections made however impossible to find specific abnormalities (if any) for specific cell clusters. Quantification of the Per protein signal and comparison between CT02 and CT14 time points drew a surprising result: while *Rho1* knockdown flies exhibited immediate arrhythmia once deprived of external

cues (see Chapter 3.3), their cell clocks kept strong molecular rhythms during the first hours in DD (Figure 3.13 and Figure 3.14).

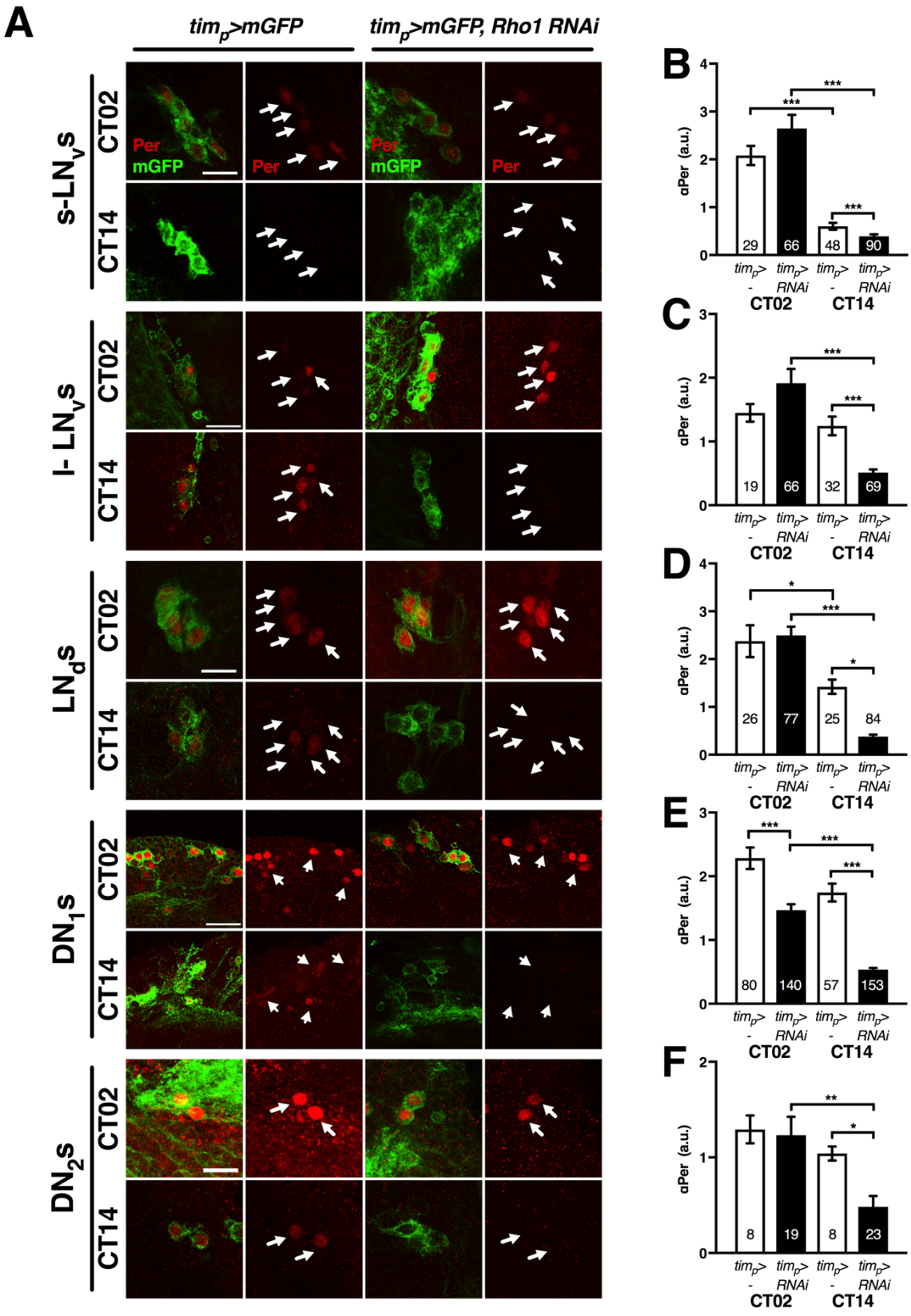

Figure 3.13. Persistence of Per molecular rhythms upon *Rho1* RNAi (*JF02809*) knockdown in the female clock cells. A) Representative pictures of the analysed clock cell clusters at CT02 (top rows) and CT14 (bottom rows) on the second day of exposure to DD (26 and 38 hours

after last lights-off, respectively). Per each given genotype (columns), left panels display mGFP and Per channel, with Per channel alone in right panels. White arrows indicate nuclei or nuclei cluster for DN_1s. Scale bar represents 10 µm (s-LN_vs, LN_ds and DN_2s) or 20 µm (l-LN_vs and DN_1s). **B-F)** Representation of Mean ±SEM of background-corrected Per antibody signal for each cell cluster on the left panels (B, s-LN_vs; C, l-LN_vs; D, LN_ds; E, DN_1s and F, DN_2s). Numbers in bars indicate *n*. *p<0.05; **p<0.01 and ***p<0.001 by Mann-Whitney *U* test (α= 0.05).

The less rhythmic clock neurons in both genders were the l-LN_vs (Figure 3.13 C and Figure 3.14 C). These clock neurons have been consistently reported as unable of maintaining molecular rhythms in *free run* (Yang and Sehgal, 2001; Veleri *et al.*, 2003; Grima *et al.*, 2004). Interestingly, comparison of the control clock cells showed a previously uncharacterised gender dimorphism. Female LN_ds and DNs exhibited a smaller difference between time points (Figure 3.13 D, E, F) than male ones and (Figure 3.14 D, E, F). As a consequence, the female dorsal cells with reduced *Rho1* levels showed greater differences among time points than the ones in control brains (Figure 3.13). Male clock cells displayed strong rhythms regardless of the presence of the RNAi, with the aforementioned exception of the l-LN_vs (Figure 3.14). The low *n* could be accounted for the gender differences for the DN_2s, but this is not the case for the LN_ds and DN_1s. The strong molecular cycle of the male clock could be related to the phenotypic gender differences found in locomotor behaviour, as more rhythmic individuals are expected to contribute to the population group than in females. It is not known how a pre-selection of arrhythmic-only males could have affected these results. Further categorical analysis based on Per protein cellular subcellular localisation showed the same results than signal analysis, including weakened rhythms in the l-LN_vs and female control dorsal clusters overall (Supplementary Table 5). The similarities between both analyses evidence that regardless of the genotype, clock cells tended to exhibit either strong nuclear accumulation or very low Per levels, as expected from a cycling clock in the selected time points.

These results constitute another difference with the previously mentioned work characterising the effects of Rho1 upregulation in the PDF-expressing neurons. Justin Blau group reported a phase shift of approximately 6 hours for the males DN_1s (females were not assayed) (Petsakou, Sapsis and Blau, 2015). The phase delay was detected with both Vri and PDP1 and was not observed in the PDF/Rho1-overexpressing s-LN_vs (Petsakou, Sapsis and Blau, 2015). This phenotypic discrepancy is difficult to explain, although *Rho1* overexpression is of course expected not to cause the same effects than the genetic knockdown.

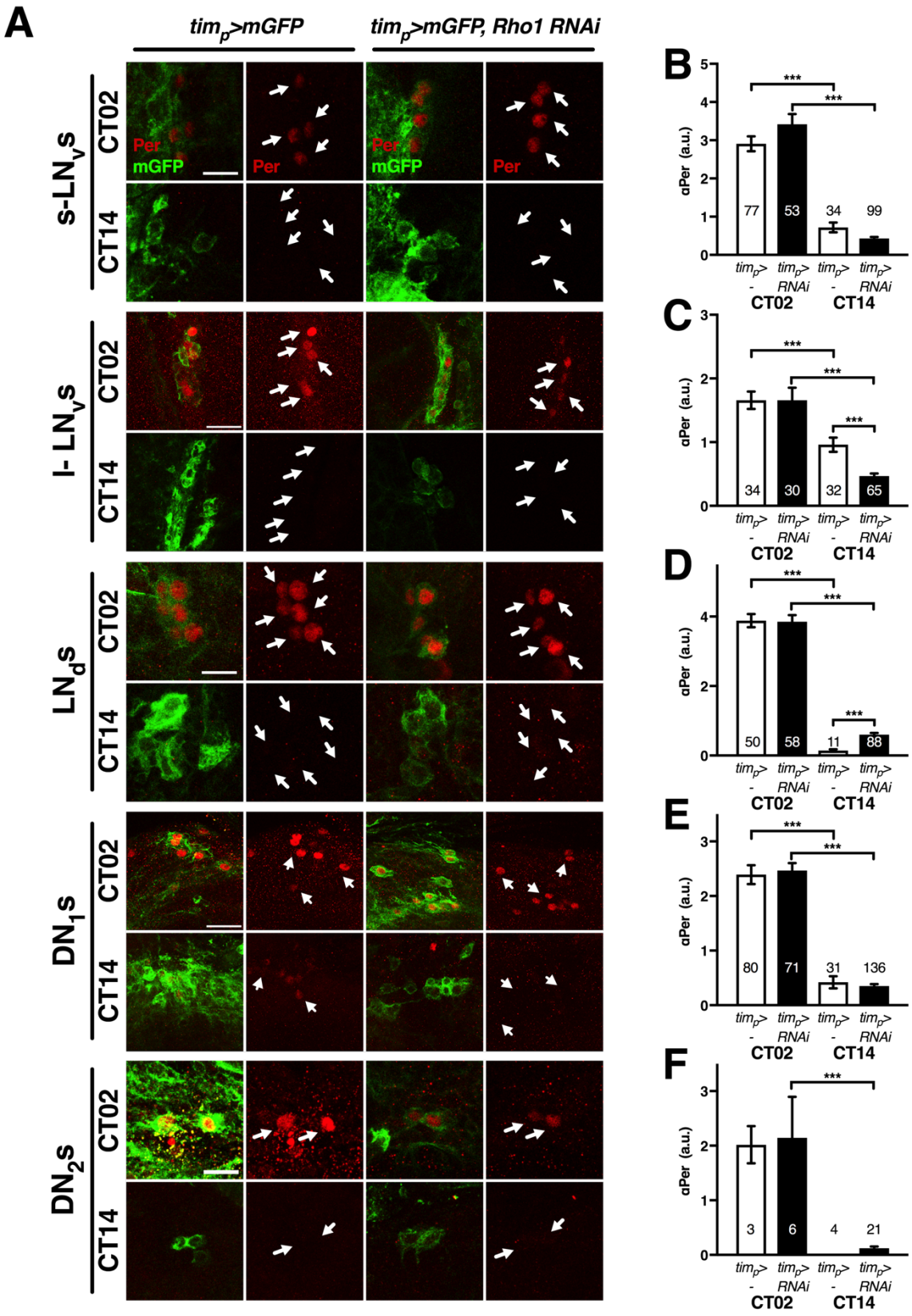

Figure 3.14. Persistence of Per molecular rhythms upon *Rho1* RNAi (*JF02809*) knockdown in the male clock cells. **A)** Representative pictures of the analysed clock cell clusters at CT02 (top

rows) and CT14 (bottom rows) on the second day of exposure to DD (26 and 38 hours after last lights-off, respectively). Per each given genotype (columns), left panels display mGFP and Per channel, with Per channel alone in right panels. White arrows indicate nuclei or nuclei cluster for DN_1s. Scale bar represents 10 µm (s-LN_vs, LN_ds and DN_2s) or 20 µm (l-LN_vs and DN_1s). **B-F)** Representation of Mean ±SEM of background-corrected Per antibody signal for each cell cluster on the left panels (B, s-LN_vs; C, l-LN_vs; D, LN_ds; E, DN_1s and F, DN_2s). Numbers in bars indicate *n*. **p<0.01 and ***p<0.001 by Mann-Whitney *U* test (α= 0.05).

The clock cells are expected to maintain the normal rhythms during the LD days (ZT times) where normal activity rhythms are evoked by the flies (Chapter 3.2 and 3.3). If the molecular oscillators are unaffected by *Rho1* knockdown at least during the first hours of *free run*, it is possible that the GTPase somehow intervenes in the communication across the circuit. A communication defect among the clock clusters could compromise the resulting behavioural output without affecting the molecular oscillators first. Therefore, study of the *Drosophila* main clock inside the brains revealed that *Rho1* knockdown inside the clock cells leads to the uncoupling of a working and functional clock from its locomotor output in the animal.

3.4.3 *Rho1* knockdown disrupts the clock output at the s-LN_v dorsal projections

The hypothesis of the defect in cellular communication, as well as the spatial mapping of the locomotor defects point to Rho1 having a role inside the PDF-expressing neurons. As previously explained, rhythms related to PDF-signalling correspond to one of the earliest known outputs of the molecular clock. Although the neuropeptide expression is not directly clock-controlled, its mobilization to the s-LN_v axonal termini follow daily rhythms, with more elevated levels after the dawn and reduced after dusk, in phase with Per protein rhythms (Helfrich-Forster, 2000; Park *et al.*, 2000; Shafer, Rosbash and Truman, 2002; Hermann-Luibl *et al.*, 2014). Additionally, the axonal termini undergo a process of daily remodelling which increases the number of synaptic areas with the dorsal receptor cells in the same way (Fernandez, Berni and Ceriani, 2008; Gorostiza *et al.*, 2014). These mechanisms altogether constitute a gating system, that in theory increases PDF-signalling during the first hours of the (real or subjective) day, and decreases it during early night.

This time, brains were interrogated with the employment of a PDF antibody, which fairly represent the morphology of the s-LN_vs (Fernandez, Berni and Ceriani, 2008). mGFP was not used as it would be impossible to distinguish the s-LN_v projections from the dorsal cells with the

employment of the *tim(UAS)-Gal4* driver. Unlike when interrogating the molecular oscillators (Chapter 3.4.2), isogenic undriven controls were used for these assays. Brains were again dissected on the second day in DD conditions as in the previous experiment (see Chapter 3.4.2).

Sholl score, as previously employed (Fernandez, Berni and Ceriani, 2008) and analysed with Mann-Whitney *U* test confirmed that in normal brains dorsal termini of the s-LN_vs exhibited a daily remodelling, with an open state (higher Sholl score) in the early times of the surrogate day (CT02) compared to the early hours of the subjective night (CT14) (Figure 3.15). Females and males showed similar rhythms when *Rho1* levels were not altered inside the clock circuitry (Figure 3.15 A, B). However, the axonal complexity remained unchanged across the two time points with *Rho1* knockdown inside the clock cells. Under these conditions, neither female or male dorsal termini displayed any rhythm at al (Figure 3.15 A, B). Inspection of the data suggested that depleted Rho1 levels compromises the arborisation of these axonal termini and thus they fail to display a complexity equivalent to the one found in control counterparts. This led to the greatest differences being found two hours after the subjective dawn: the dorsal termini of *Rho1* deficit s-LN_vs remained "collapsed", compared to the "extended" state of the control axons. Strikingly, the same effect was found by Justin Blau group when overexpressing Rho1 and characterising the dorsal termini in LD, while the flies overexpressing the $Rho1^{DN}$ isoform showed an open state (Petsakou, Sapsis and Blau, 2015). While in all the cases the consequences are effective lack of daily remodelling of these axons, the nature of it seems different. The results of this experiment are therefore not totally consistent with published literature, and both phenotypes could be integrated if *Rho1* knockdown, as presented in this thesis, could indeed be causing developmental defects. They do, interestingly, support the previously described difference with the $Rho1^{DN}$ isoform, which failed to reduce rhythmicity as RNAi expression did (See Chapter 3.3.2).

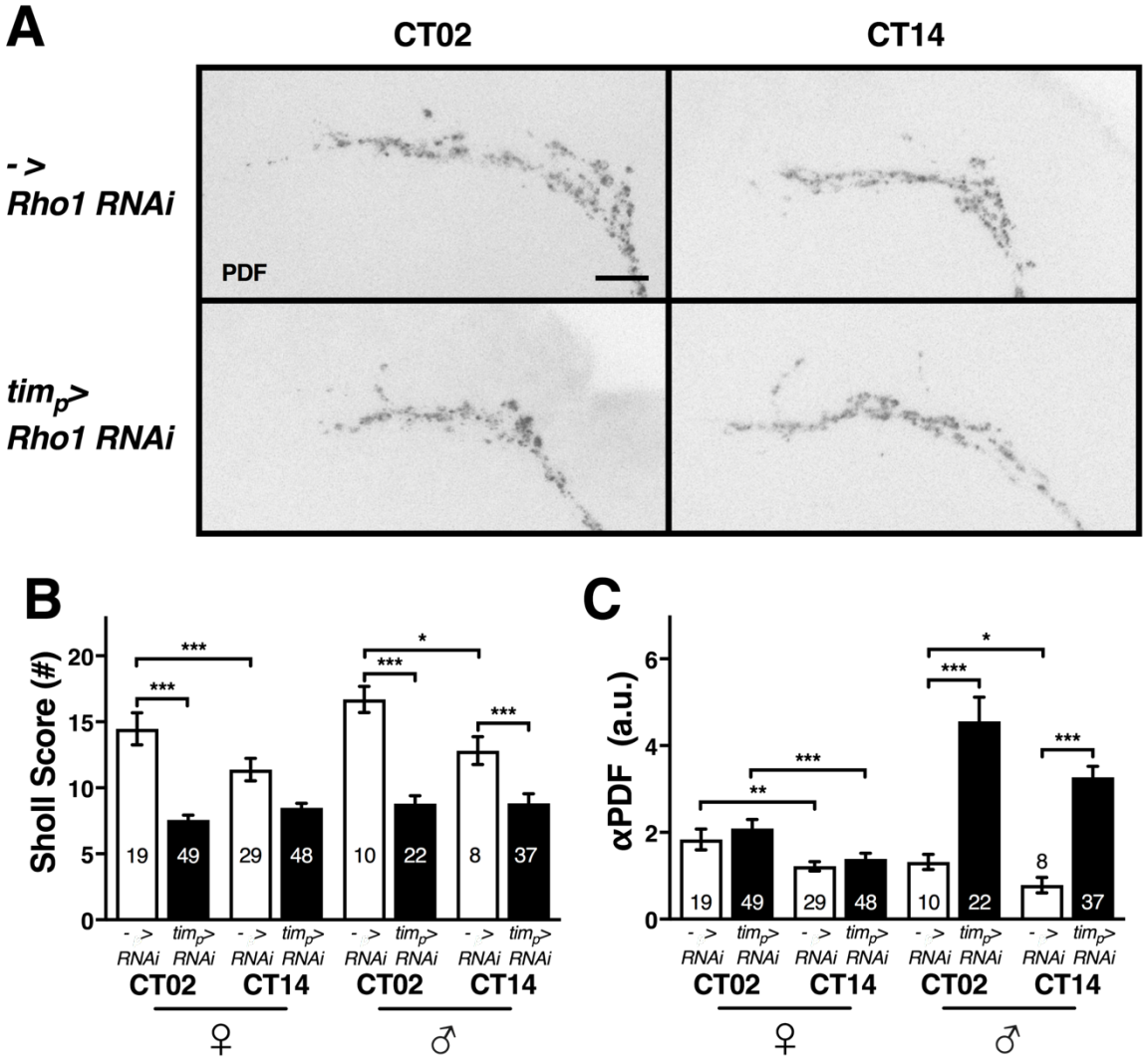

Figure 3.15. Effects of *Rho1* RNAi (*JF02809*) knockdown inside the clock cells upon the daily rhythms associated to PDF at the s-LN$_v$ dorsal termini in *free run*. A) Grayscale-inverted representative pictures of s-LN$_v$ axonal termini (antiPDF antibody) corresponding to the given genotypes (rows) and time points (columns) at the second day in DD. Scale bar represents 10 µm. **B)** Representation of Mean ±SEM of the axonal complexity with Sholl Analysis of populations corresponding to panel A. Numbers in bars indicate **C)** Representation of Mean ±SEM of the anti-PDF signal intensity (background-corrected) in the dorsal horn region of the s-LN$_v$ dorsal termini for the same brains. Numbers in bars indicate *n*. *p<0.05; **p<0.01 and ***p<0.001 by Mann-Whitney *U* test (α= 0.05) for both Sholl Score and antiPDF signal.

The same experimental setup with the PDF antibody allowed to measure the daily rhythms of the neuropeptide itself, in order to address the question whether *Rho1* knockdown would imbalance this process (Helfrich-Forster *et al.*, 2000; Park *et al.*, 2000). PDF levels reached the maximum levels at CT02, with a correspondent low at CT14, in both genotypes and genders (Figure 3.15 C). Noteworthy, the male s-LN_vs exhibited higher levels of PDF at the dorsal termini with *Rho1* knockdown (Figure 3.15 C), albeit still displaying a strong difference between time points. As the different genotypes were tested at the same time, we believe this may indeed be a consequence of targeting *Rho1* levels.

The same genotypes were subjected to a similar experiment, but under LD cycles (dissections at ZT02 and ZT14) (Figure 3.16 A). Under these conditions, the s-LN_vs failed again to remodel their axonal termini in the same way isogenic controls did (Figure 3.16 B). The dorsal termini with reduced Rho1 levels were not, interestingly, as "collapsed" as those in DD (Figure 3.15 B). Interestingly, the phenotype in LD indeed reconciled with the effects caused by adult-only $Rho1^{DN}$ expression as shown in the literature (Petsakou, Sapsis and Blau, 2015). PDF levels maintained the expected cycling (weaker in the case of control females) with a possible increase in the *in situ* accumulation for the male brains expressing the RNAi at ZT02 (Figure 3.16 C). The striking elevated signal in the male experimental axons in DD was not found again in LD, though (Figure 3.15 C).

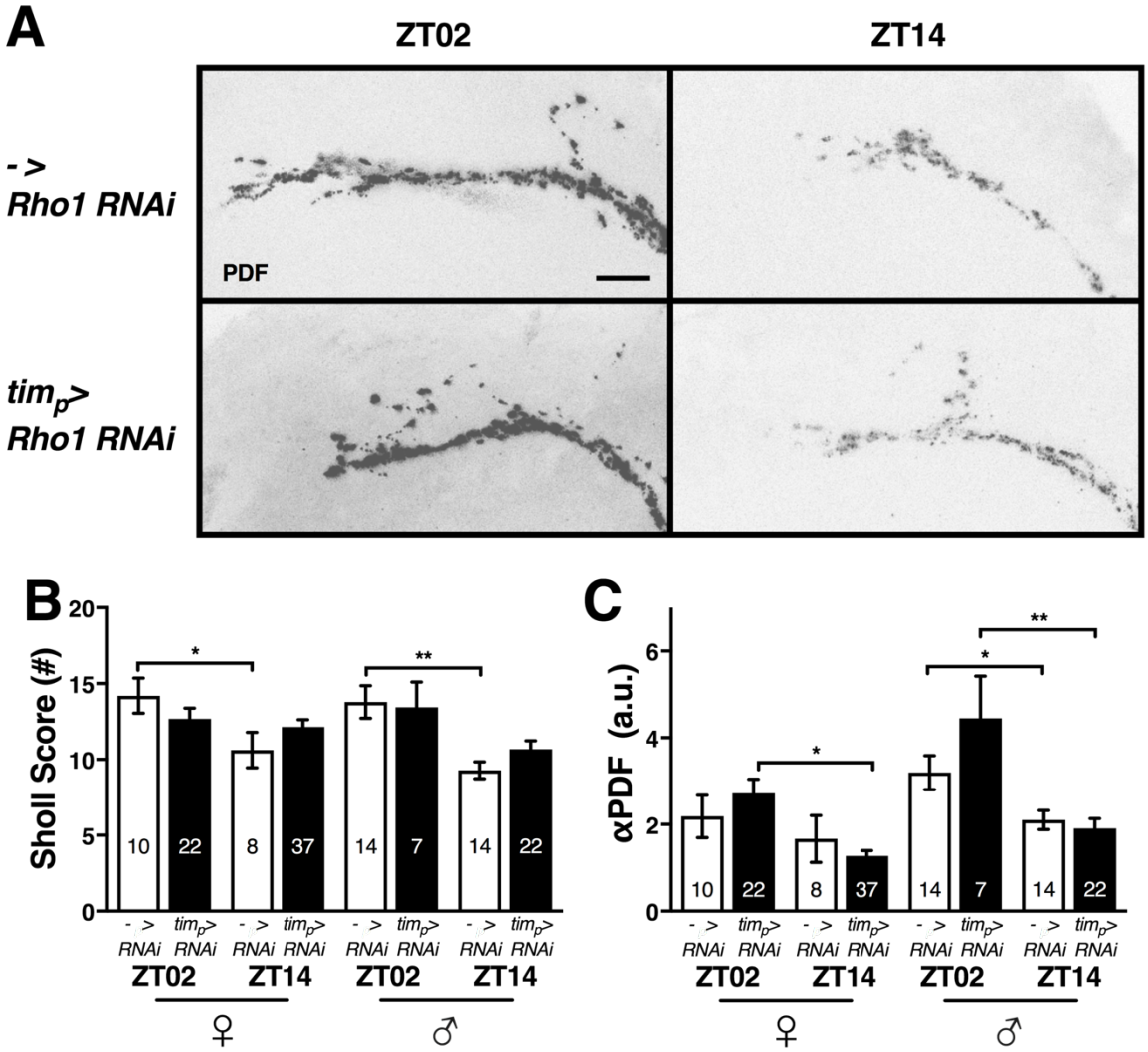

Figure 3.16. Effects of *Rho1* RNAi (*JF02809*) knockdown inside the clock cells upon the daily rhythms associated to PDF at the s-LN$_v$ dorsal termini under LD cycles. A) Grayscale-inverted representative pictures of s-LN$_v$ axonal termini (antiPDF antibody) corresponding to the given genotypes (rows) and time points (columns) during LD cycles. Scale bar represents 10 µm. **B)** Representation of Mean ±SEM of the axonal complexity with Sholl Analysis of populations corresponding to panel A. Numbers in bars indicate **C)** Representation of Mean ±SEM of the anti-PDF signal intensity (background-corrected) in the dorsal horn region of the s-LN$_v$ dorsal termini for the same brains. Numbers in bars indicate *n*. *p<0.05 and **p<0.01 by Mann-Whitney *U* test (α= 0.05) for both Sholl Score and antiPDF signal.

Therefore, the most important conclusion based on the results upon interrogation of the clock cells, is that the reduction in *Rho1* levels uncouples the molecular oscillator from the adult behavioural rhythms. During the second day in *free run*, Per protein maintains the expected rhythms inside affected neurons, contrasting with the concurrent arrhythmic response of the animals. The unaltered expression rhythms of the Per protein correlate with a defect in the rhythms of arborisation of the s-LN_v axonal termini. This defect is already present when flies are under LD cycles, and thus precede to the behavioural arrhythmia. These data reinforce the special requirement of Rho1 inside the PDF-expressing neurons, and points specifically to the s-LN_vs as causative agents of the *Rho1*-deficit genotypes. As the brains were studied with *Rho1* knockdown inside the whole clock circuitry, and no further studies have been done for the l-LN_vs, the cell-autonomous nature of this phenotype cannot be confirmed.

3.5 Interactions between Rho1 and PDF-signalling

3.5.1 Uncovering the role of Rho1 inside the clock circuitry

By this point, the research project has found a role of the small GTPase Rho1 in the adult circadian locomotor behaviour of the fruit flies. This role is carried in fully developed clock cells, with a specific function of Rho1 inside the PDF-expressing neurons. The behavioural arrhythmia of the affected flies contrasts with the normal working of their main clock neurons inside the circuit. A possible connection between these two opposing conditions was also found, after determining that *Rho1* depletion prevents the normal daily axonal remodelling of the PDF-expressing s-LN_vs. These results suggest communication defects related to the s-LN_vs, but do not indicate what kind of role into circadian behaviour Rho1 may have inside these specific neurons.

As already stated, interrogation of the clock neurons suggested that instead of affecting the molecular oscillators themselves, Rho1 is involved in their ways of communication. These constitute a complex and not fully characterised network (See Chapter 1.3.5). The specific spatial restriction of some components (e.g., neuropeptides expressed only at some clock neurons) along the inherent dynamism of the circuit when facing different conditions (See Chapter 1.3.4-7) allows the employment of both genetics and behavioural assays for studying the clock circuit. Although the possible intervening elements extend beyond the scope of this project, the specific requirement of Rho1 inside the PDF-expressing clock neurons immediately pointed out to a possible interaction between the small GTPase and this critical neuropeptide for clock synchrony and output.

3.5.2 Red Light rescues rhythmicity of *Rho1* deficit flies

As presented in Chapter 1.3.4.3, red wavelengths can act as a Cry-independent light cue and entrain the clock neurons throughout the compound eyes (Hanai, Hamasaka and Ishida, 2008). There exist a series of still unidentified clock neurons that take the role of pacemakers during RR conditions and whose cycling oscillator allows the persistence of rhythms, in contrast to the Cry-induced arrhythmia in LL (Emery *et al.*, 2000a; Emery *et al.*, 2000b). These neurons receive red light input from the l-LN_vs, that respectively have previously acquired the information from the compound eyes (Helfrich-Forster *et al.*, 2007a). As this information pathway includes some of the

targeted cells with Rho1 knockdown in previous experiments, the depletion of the small GTPase could disrupt the process.

Diverse previously characterised genotypes in DD were studied in RR conditions, where diverse genotypes can maintain their rhythms opposite to traditional *free run* (Cusumano *et al.*, 2009). The transition from the LD phase was done after the lights-on event instead of before it like in DD, but the same procedure was applied otherwise, and this allowed to analyse the same genotype between different conditions. Figure 3.17 shows the actograms or diverse genotypes (previously studied in LD to DD) in LD to RR, with the genotypes being analysed in Figure 3.18 and Supplementary Figure 1.

Figure 3.18 shows results for the $Rho1^{1B}$ mutant allele and the selective expression of the *JF02809* (*Rho1* RNAi 1) construct inside the clock cells [*tim(UAS)-Gal4 driver*]. Remarkably, flies with reduced *Rho1* levels in both backgrounds retained a remarkable rhythmicity in RR, greatly contrasting with their arrhythmic outcome in DD (Figure 3.17, comparison with actograms in Figure 3.1 and Figure 3.3). All the involved genotypes displayed the characteristic phase shift found in RR conditions, with activity ramping up towards the then extinct *lights-off* event (compared to the disappearance of the *siesta* period without further shifts in DD, like shown in Figure 3.1 and Figure 3.3). Statistical analysis of the female flies carrying a copy of the $Rho1^{1B}$ allele revealed that the rhythmicity of the flies was totally restored in RR, being indistinguishable from control counterparts regarding population frequencies (Figure 3.18 A) or RRP (Figure 3.18 B) of rhythmic individuals. For expression of the *Rho1* RNAi 1, the recovery was not total as the RNAi expression still managed to reduce rhythmicity in RR, yet with a remarkable improvement over DD (Figure 3.18 D, E). In the case of $Rho1^{1B}/+$ males, these individuals barely displayed a compromised rhythmicity in DD, while Rho1 RNAi males exhibited a total recovery (Figure 3.18 A, B, D, E). The flies corresponding to the $Rho1^{1B}$ assay did not experience a period lengthening in RR compared to DD as the ones from the RNAi 1 ones did (Figure 3.18 C, F). As RR conditions tend to increase the endogenous period length, this could be an issue related to the w^{1118} background of the $Rho1^{1B}$ assays. For the RNAi 1 flies, RR conditions masked the increased period length found in DD conditions (See Chapter 3.3) and suspected to be caused by the presence of the *tim(UAS)-Gal4* driver rather than by the RNAi expression (Figure 3.18 G).

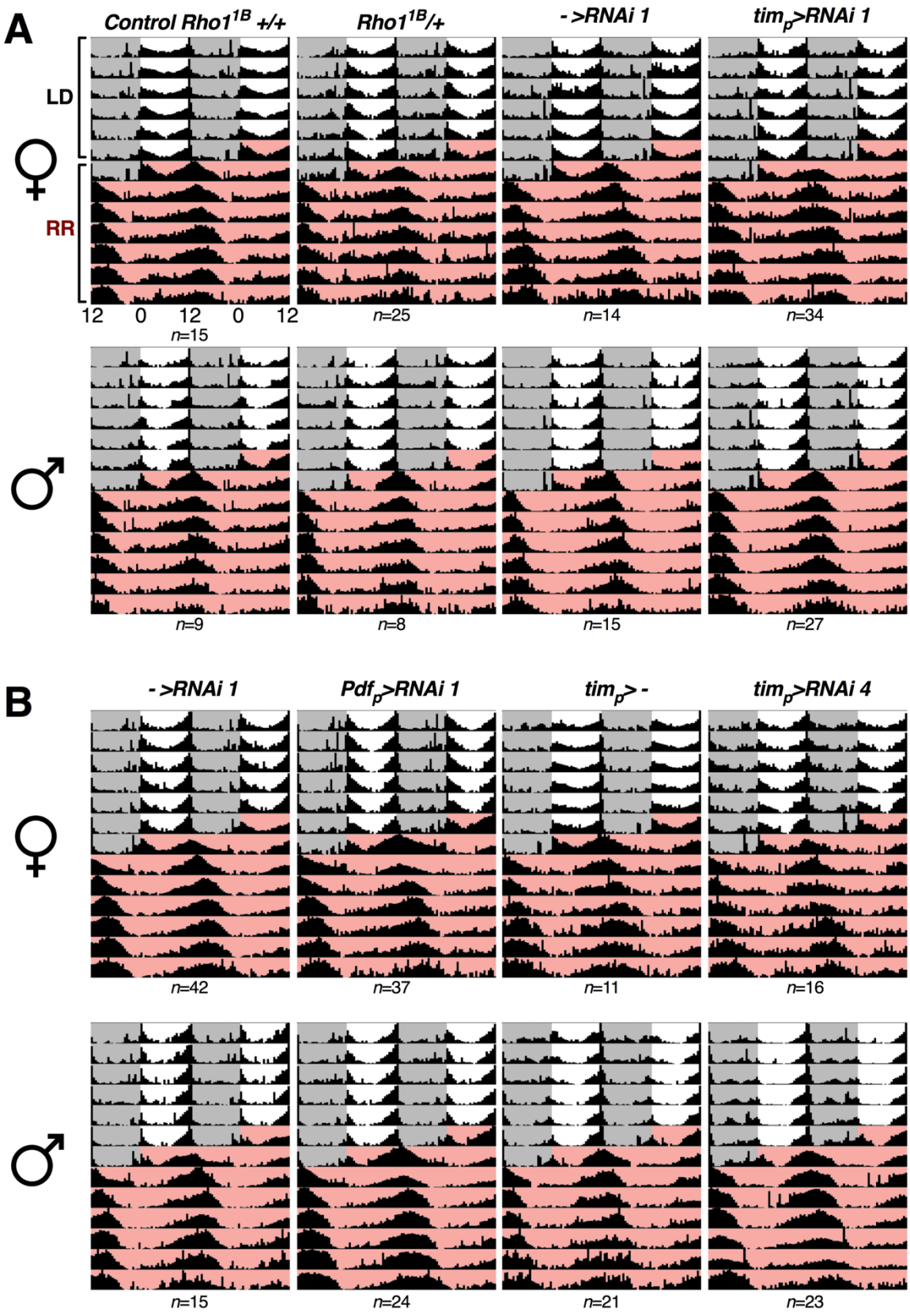

Figure 3.17. Circadian locomotor activity of *Rho1*-deficit flies in RR conditions. Adults of both genders are entrained for 6 days in LD and transferred to RR conditions on day 7 (during the light period), at a constant temperature of 23 °C. The quantified data from the next 7 days

in RR are found in Figure 3.18 and Supplementary Figure 1. Column titles indicate given genotype (with RNAi 1 representing data for the *JF02809* construct and RNAi 4 representing the *Rho1.770-1310* construct), and rows represent females (top) and males (bottom). White background, light period; grey background, dark period; red background, constant red light. *n* numbers are indicated below the actograms. Actograms represent the normalised population average. The actograms of the genotypes in DD are found in Figure 3.1, Figure 3.3 and Figure 3.12.

The surprising behaviour of Rho1 deficit flies in RR prompted to subject other genotypes to the same conditions and test the effectivity of the phenotypic rescue (Figure 3.17 and Supplementary Figure 1. Flies with the RNAi 1 expressed only in the PDF neurons exhibit the same type of rescue, partial for females and total for males (Supplementary Figure 1 A, B). The rescue was better for the females expressing the dubious RNA1 4 (*Rho1.770-1310*) (Figure 3.17 and Supplementary Figure 1 D, E). In both genders, experimental flies for the Pdf_p*>RNAi 1* assay displayed longer rhythms in RR than in DD, while this extension was masked in the tim_p*>RNAi 4* in a similar way than tim_p*>RNAi 1* (Supplementary Figure 1 C, F). These data would suggest that if the found period extension with Rho1 RNAis is just a consequence of the presence of the Gal4 drivers, the *Pdf-Gal4* construct exerts a stronger effect on it, and thus is still observable while comparing DD versus RR (Supplementary Figure 1 C). The increased variance of the experimental females (caused by the not fully rescued rhythmicity) in RR would be the cause of the lack of detectable period extension compared to their control counterparts in the same conditions, opposite to the results in males (Supplementary Figure 1 C).

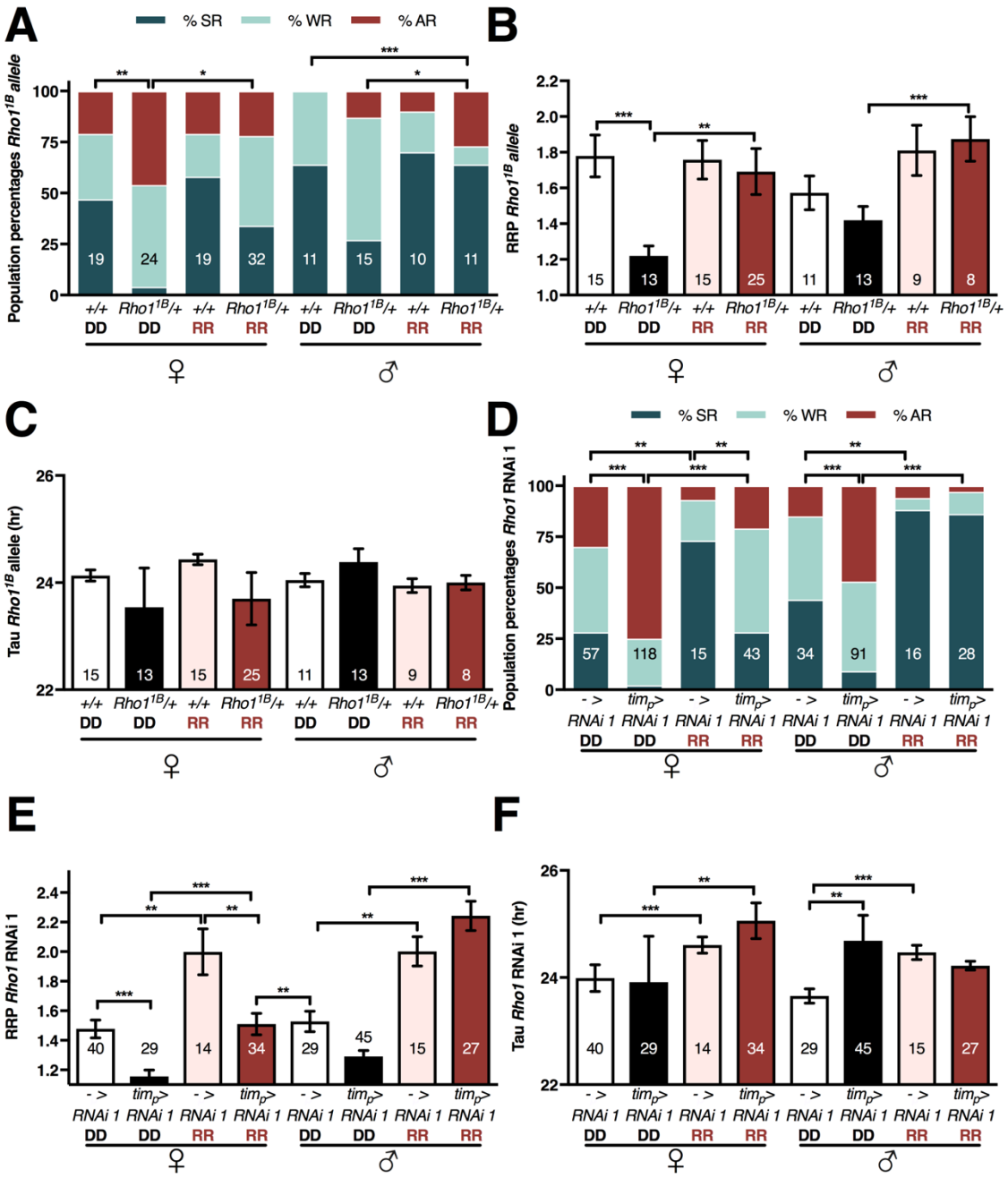

Figure 3.18. Effects of red light on circadian locomotor activity of *Rho1*-deficit flies. **A** and **D)** Distribution of frequencies (Strongly Rhythmic, SR; Weakly Rhythmic, WR or Arrhythmic, AR) for flies carrying the *Rho1*^{1B} mutant allele (A) or expressing the *Rho1* RNAi *JF02809* inside the clock cells (D), as well as isogenic controls. **B** and **E)** Relative Rhythmic Power (RRP) of SR and WR flies for flies carrying the *Rho1*^{1B} mutant allele (B) or expressing the *Rho1* RNAi inside the clock cells (E), as well as isogenic controls. **C** and **F)** Period Length (Tau) of SR and WR flies for flies carrying the *Rho1*^{1B} mutant allele (C) or expressing the *Rho1* RNAi inside the clock cells (F), as well as isogenic controls. Data from genotypes in DD was previously presented in Figure 3.2 and Figure 3.4 and repeated here for better comparison. Bars represent Mean ±SEM and numbers in bars indicate *n*,

with the total number of flies originated from 6 (*Rho1*^{1B} allele in DD), 5 (*Rho1*^{1B} allele in RR), 10 (*JF02809* in DD) and 3 (*JF02809* in RR) crosses. For population percentages panels (A, D), *p<0.05; **p<0.01 and **p<0.001 by Fisher's Exact test. For RRP (B, E) and Tau (F) panels, *p<0.05; **P<0.01 and ***p<0.001 by Mann-Whitney *U* test (α= 0.05). No differences were found for Tau with the *Rho1*^{1B} mutant.

A question to be asked after these surprising results in RR conditions was whether flies with *Rho1* deficit could have their clock indirectly entrained by RD cycles, similar to organisms with undisrupted visual pathways (see Chapter 1.3.4.3) (Hanai, Hamasaka and Ishida, 2008). While this constituted a fair assumption given the recovered rhythmicity under constant red light, RD conditions may provide additional information about the working of the clock circuit, evidenced by the abnormal behaviour of flies lacking PDF-signalling (Cusumano *et al.*, 2009). Consequently, RD activity of flies expressing the Rho1 RNAi inside the clock cells was studied, and compared to both controls and *Pdf* and *Pdfr* mutants (data kindly provided by the laboratory members Ines Lin and Charles Hurdle). As previously reported (Cusumano *et al.*, 2009), flies without the neuropeptide signalling lost their evening anticipatory peaks in RD conditions, compared to the stereotyped profile in LD or the presence of the peak in flies with wild-type *Pdf* gene (Figure 3.19). *Rho1* knockdown flies on the other hand displayed no apparent changes in their activity pattern between both conditions. Their activity pattern was also identical to undriven isogenic controls in both genders (Figure 3.19). These observations proved again that the red light-dependent pathways are not affected by reduced *Rho1* levels inside the clock cells, and that this time cue can reach the clock cells and entrain them in conditions of extinction of light just like in RR. But more importantly, as was evidenced in previous assays and displayed here back to back, RD constituted another condition with phenotypic differences between *Rho1* knockdown and PDF-signalling deficit.

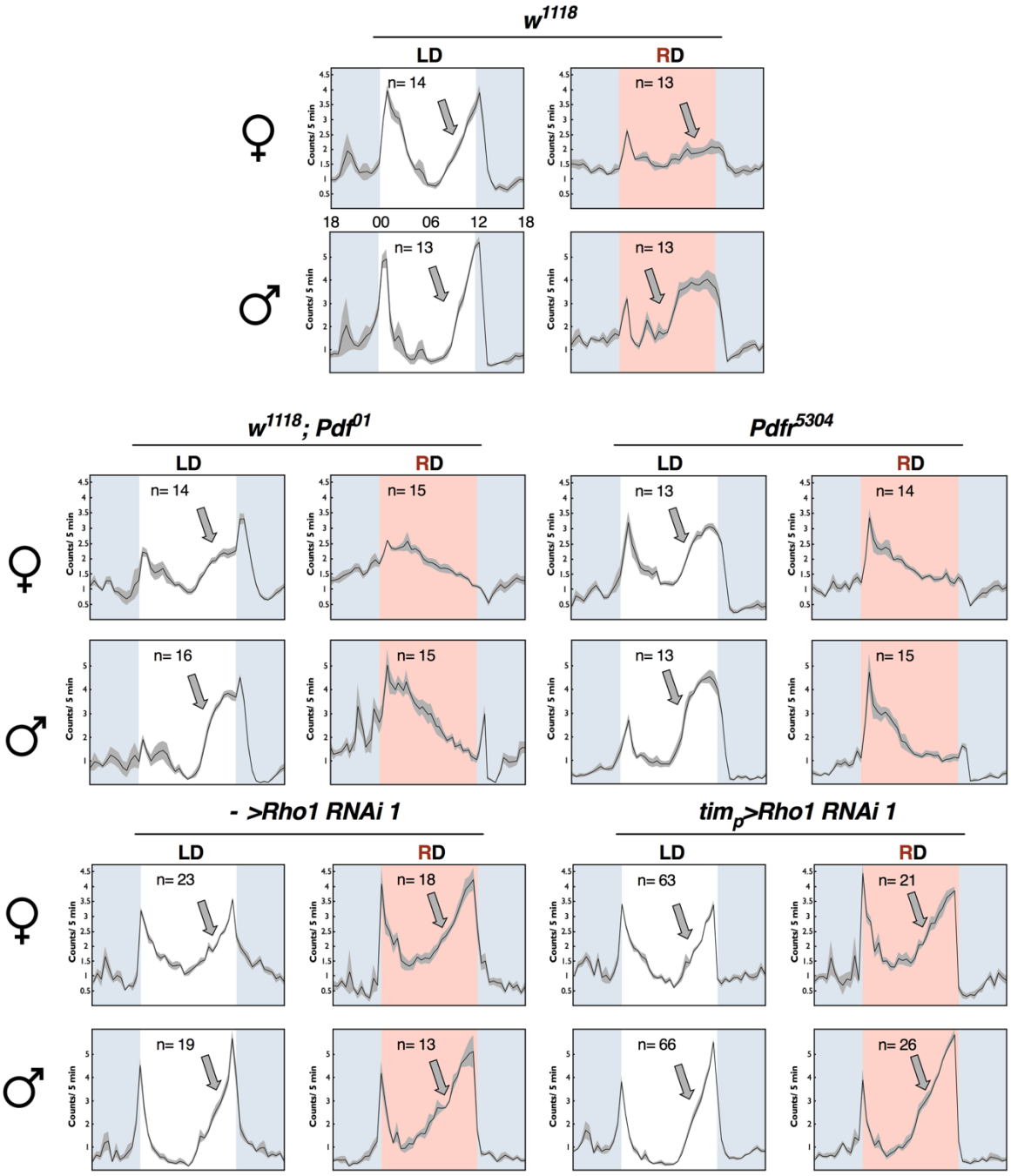

Figure 3.19. Behavioural differences during entrainment phase between *Pdf* mutants and *Rho1* RNAi (*JF02809*) knockdown. Activity profiles display a population average at the given conditions (12:12 LD or RD) at a constant temperature of 23 °C. Column titles indicate genotypes (top row) and conditions (bottom row). Rows indicate gender of the populations. Activities profiles display counts per each 30-min bin (Mean ±SEM) with *lights-on* event occurring at ZT00 and *lights-off* event at ZT12. White background, light phase; grey blue background, dark phase; red background, red light phase. Arrows indicate the presence of evening anticipatory activity. Experimental data from w^{1118} controls, Pdf^{01} and $Pdfr^{5304}$ were collected by Ines Lin and Charles Hurdle.

The wild-type behaviour displayed by *Rho1* deficient flies subjected to the influx of red light provided the project with information about the state of the communications inside the clock circuit when this gene is being targeted. Importantly, they showed that the not yet fully characterised red light circuit is relatively intact and unaffected by reduced *Rho1* levels. Flies lacking PDF-signalling also exhibit recovery. The presence of the evening anticipatory peak in RD cycles is dependent of functional activation of PDFR inside the non-morning cells (Cusumano *et al.*, 2009). As this peak is present in *Rho1* knockdown flies, this constitutes an evidence that PDF-signalling is not interrupted by the depletion of the small GTPase.

3.5.3 *Rho1* knockdown fails to reduce rhythmicity in the $Pdfr^{5304}$ mutant background

As previously detailed in the Introduction chapter, Pdf^{01} mutants already manifest an altered behaviour during the phase of entrainment (Renn *et al.*, 1999). This phenotype is perfectly reproduced by assaying flies expressing a *Pdf* RNAi construct within the *tim* cells, as well as $Pdfr^{5304}$ mutants (Figure 3.19). Firstly, behaviour of the flies under LD cycles of both genotypes is different. The morning anticipatory activity of flies with deficiencies in PDF-signalling is absent, while in different genetic backgrounds this was not the case for *Rho1* deficit (See more in Chapter 3.6). Moreover, in *Pdf* mutants flies the evening anticipatory activity is advanced and reaches a plateau (and hence a change in its shape) before dusk. This effect is not present in flies with *Rho1* knockdown (Figure 3.19). The presence of normal evening anticipatory activity in LD, and the persistence of it in RD (Figure 3.19) clearly indicated that the depletion of the small GTPase is indeed not downregulating PDF-signalling across the clock circuitry.

Although the precise levels of *Rho1* inside the clock cells are difficult to quantify and comparing different genetic backgrounds is not totally informative, reduced *Rho1* levels seem to be more detrimental to rhythmicity than loss of PDF-signalling at least in females. Research articles usually describe the phenotype of the latter as a progressive loss of rhythmicity in *free run* (Renn *et al.*, 1999; Hyun *et al.*, 2005; Lear *et al.*, 2005). *Rho1* knockdown flies, on the other hand, manifest an almost immediate arrhythmia when external light cycles are gone (see Chapter 3.2 and 3.3). Comparison of the rhythmicity among early and late days in *free run* for either *Rho1* or *Pdf* knockdown flies was not successful because Clocklab failed in finding any rhythm at all with the reduced number of input days (data not shown).

Finally, flies without PDF-signalling that achieve to display some rhythmicity have a shorter period length (Renn *et al.*, 1999). Period shortening was not found in any of the *Rho1* deficit flies on the other hand (See Chapter 3.2 and 3.3). Because the *tim(UAS)-Gal4* and *Pdf-Gal4* constructs stochastically lengthen the period, the difference may not be observable when the driver is present. However, period shortening was not found in flies with chromosome deficiencies affecting *Rho1* gene (See Chapter 3.2). More importantly, the shorter Period length of Pdf^{01} flies manifest more strongly under RR conditions, unlike many other genotypes that normally display and increased period length in these conditions compared to DD (Cusumano *et al.*, 2009). This effect was again not observed in *Rho1*-deficit flies, which besides an increased rhythmicity extended their endogenous rhythms in the same way than their control counterparts (Figure 3.17 and Figure 3.18). Interestingly, the insertion site effect of the *tim(UAS)-Gal4* driver on the period length is still present when Pdf is targeted with an RNAi (Supplementary Table 1), but absent in the Pdf^{01} mutant background (Appendix B Table 1).

All these data support the conclusion that the *Rho1* knockdown phenotype was not downregulating PDF-signalling. This would mean the small GTPase is not required for the successful delivery of the neuropeptide to the PDFR-expressing clock neurons, and that therefore PDF-signalling is still happening in the *Rho1* knockdown clock circuitry.

Regulation of PDF-signalling is complex and not fully understood, and includes among others many control mechanisms that make the neuropeptide to timely accumulate at the s-LN_v dorsal projections. This rhythm is not affected by neuropeptide overexpression, suggesting the existence of a post-translational brake that restricts the pool of neuropeptide that can be mobilized (Helfrich-Forster *et al.*, 2000). Interestingly expression of PDF inside neurons whose terminals reach the periphery of the s-LN_v dorsal termini resulted in arrhythmia in DD, contrasting with a normal LD behaviour. This phenotype is remarkably similar to *Rho1* knockdown, and correlates with the neuropeptide being present, with no rhythm at all, at the dorsal protocerebrum (Helfrich-Forster *et al.*, 2000). Therefore, it was postulated then that Rho1 may still have a function in the regulation of PDF-signalling, leading to aberrant cell communication when depleted.

Firstly, a technical issue to solve was that both the employed *Rho1* RNAi (*JF02809*) construct and the *Pdf* gene are located at the third chromosome. A recombination to generate a chromosome carrying both the Pdf^{01} allele and the *Rho1* RNAi 1 was ruled out because of the lack of visual markers for both elements (like a w^+ rescue of the eye colour, very common in transgenic constructs). Instead, a *Pdfr* mutant background was introduced as this gene is located on the X

chromosome and the phenotype is identical to *Pdf*^{01} (Figure 3.19)(Hyun *et al.*, 2005; Lear, Zhang and Allada, 2009). The loss-of-function *Pdf*^{5304} was introduced in both parental stocks in a homozygous way at both paternal lines. Previously, the *UASDcr2w* element was substituted by a third chromosome carrying the same construct (Dietzl *et al.*, 2007).

Figure 3.20 shows the experimental results of the interaction between *Rho1* knockdown and the *Pdfr*^{5304} mutant allele. Firstly, analysis confirmed that in a *Pdfr*$^{+}$ background (*w*^{1118} X chromosome), the phenotype caused by *JF02809* Rho1 RNAi was reproduced with the exchange of UASdcr2 elements (Figure 3.20). During LD days, experimental females displayed a more evident altered with an increased activity during the night phase (Figure 3.20), which could be due to the background, as pointed out by the weak rhythmicity of the control individuals (Figure 3.20 B, C). As previously presented in Figure 3.19, the presence of the *Pdfr*^{5304} mutant allele altered the stereotypical LD pattern of the flies (Figure 3.20) and also increased the basal level of arrhythmic flies regardless of further modifications (Figure 3.20 B). However, inspection of the weakly and strongly rhythmic flies revealed several interesting observations when comparing control and experimental genotypes. Firstly, these crosses showed that *Rho1* knockdown with the construct is more detrimental to the circadian behaviour than the *Pdfr*^{5304} homozygous mutant. While this had been previously observed as a trend, this is the first assay that can compare both deficits in a very similar background (excluding the mentioned X Chromosomes). This difference allowed for uncovering the second and most crucial observation. It was determined that flies with both *Rho1* knockdown and compromised PDF-signalling resembled the *Pdfr*^{5304} mutants alone more than *Rho1* knockdown alone ones. This was found in the distribution of frequencies (Figure 3.20 B), RRP analysis (Figure 3.20 C) but even with visual comparison of the actograms. The weak and shorter than 24 hour DD rhythms associated to the lack of PDF-signalling were noticeable when compared to the overall arrhythmia caused by *Rho1* knockdown in the *Pdfr*$^{+}$ background, especially in females (Figure 3.20 A). These behavioural data indicated that *Rho1* interact with PDF-signalling, and that the removal of it makes *Rho1* knockdown superfluous and unable of further reducing the rhythmicity. In other words, the *Pdfr*^{5304} phenotype was epistatic to *Rho1* knockdown and "rescued" the small GTPase deficient phenotype. No changes were detected in the endogenous period length, again probably due to the data dispersion associated to poorly rhythmic flies (Figure 3.20 D). Observation of the activity right after the transition to DD (Supplementary Figure 2) revealed that the experimental flies (especially females) display an immediate dampening of their rhythms compared to the controls shortly after transition. Flies with depletion of *Rho1* inside their clock cells in the *Pdfr*^{5304} mutant background exhibited the same behaviour as their control counterparts (Supplementary Figure 2).

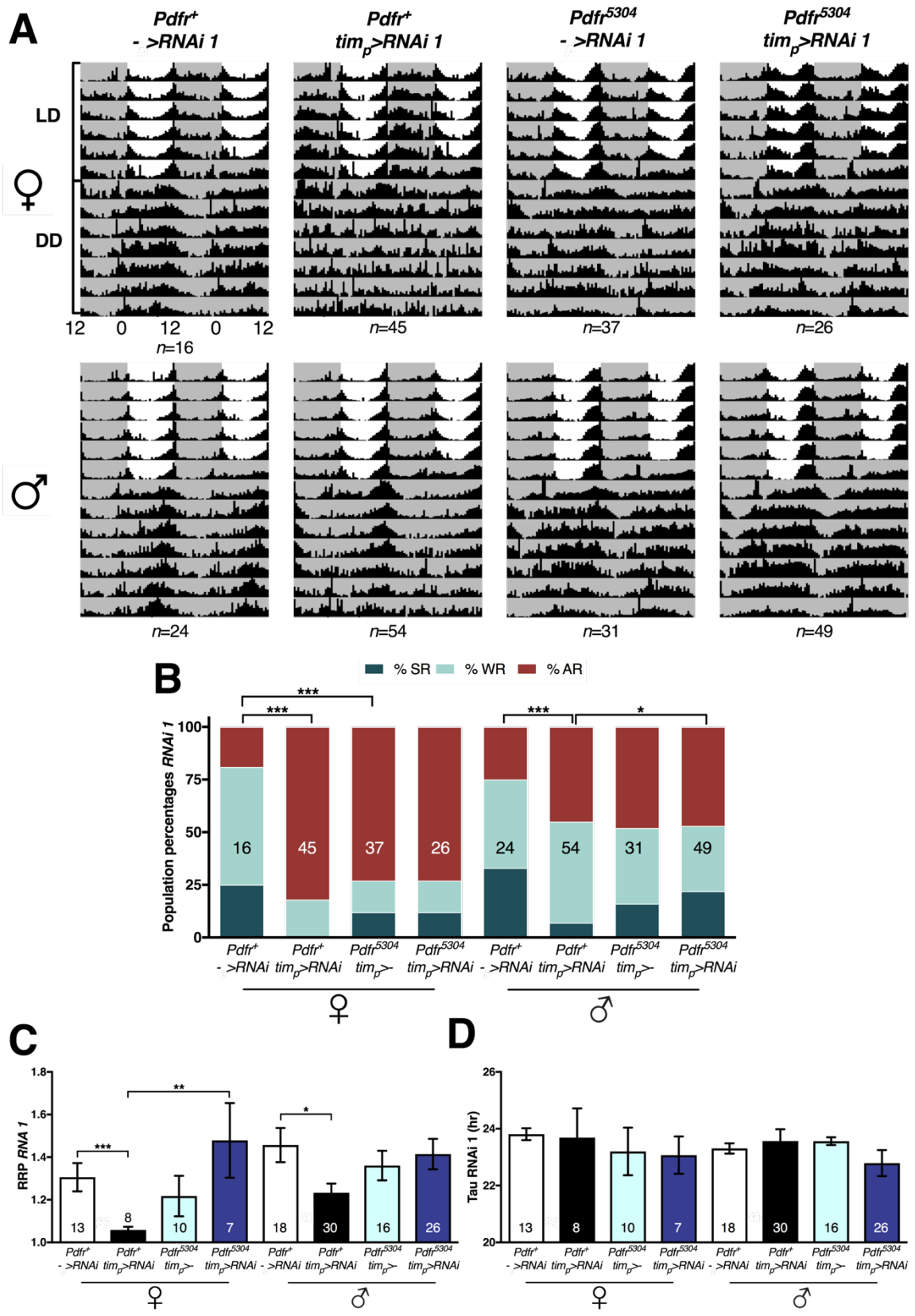

Figure 3.20. Interactions between *Rho1* RNAi (*JF02809*) knockdown inside the clock cells and the *Pdfr*^{5304} mutant. A) Adults of both genders are entrained for 6 days in LD and transferred to

DD conditions on day 7 (during the light period), at a constant temperature of 23 °C. The quantified data from the next 7 days in DD and *n* numbers are found in the next panels. Column titles indicate given genotype (with RNAi 1 representing data for the *JF02809* construct), and rows represent females (top) and males (bottom). White background, light period; grey background, dark period. Actograms represent the normalised population average. **B** Distribution of frequencies (Strongly Rhythmic, SR; Weakly Rhythmic, WR or Arrhythmic, AR) for flies expressing the *Rho1* RNAi inside the clock cells as well as isogenic controls. **C)** Relative Rhythmic Power (RRP) of SR and WR flies for flies expressing the *Rho1* RNAi inside the clock cells, as well as isogenic controls. **D)** Period Length (Tau) of SR and WR flies for flies expressing the *Rho1* RNAi inside the clock cells, as well as isogenic controls. Bars represent Mean ±SEM and numbers in bars indicate *n*, with the total number of flies originated from 2 ($Pdfr^{+}$ background) and 3 ($Pdfr^{5304}$ background) crosses. For population percentages column (B), *p<0.05 and ***p<0.001 by Fisher's Exact test. For RRP panel(C), *p<0.05; **P<0.01 and ***p<0.001 by Mann-Whitney *U* test (α= 0.05). No differences were found for Tau (D).

Taken together, the data from this chapter indicate that the small GTPase Rho1 is involved in the normal working of PDF-signalling. While Rho1 does not seem to be required for the release of the neuropeptide, its depletion deregulates the pathway and leads to intrinsic arrhythmia in absence of external cues. This interaction can be tied to the found effects caused by *Rho1* knockdown in behaviour, where the knockdown inside the PDF-expressing neurons is sufficient to reproduce the phenotype (See Chapter 3.3.3). They can also be related to the morphological defects found inside these neurons, with a compromised axonal remodelling at the s-LN_vs (See Chapter 3.4.3). This would represent a previously unknown mechanism part of the complex gating system that guarantees the correct signalling by this neuropeptide, key element of the *Drosophila melanogaster* clock circuitry.

3.6 Impact of Rho1 upon environmental effects on circadian behaviour

3.6.1 Introduction

The previous subchapters have successfully characterised the circadian phenotype caused by depletion of Rho1 levels inside a specific subpopulation of the *Drosophila* clock cells. The current model is established around the small GTPase having a role in PDF-signalling, deregulating it when removed from the PDF-expressing neurons. This disruption of PDF-signalling is stochastic to the clock circuitry once Rho1 levels have been reduced, but the animals manage to overcome it when facing the 12:12 LD cycle employed as entrainment cue. Yet, the abnormal neuropeptide signalling could be causing an effect even with the presence of environmental cycles.

One of the earliest and most striking results of the first experiments targeting to *Rho1* (See Chapter 3.2 and 3.3) was the apparent phenotypic normality of the involved genotypes during the entraining phase in LD. This represented a significant dissimilarity with the immediate arrhythmia appearing after the extinction of the light cues. While many clock-related mutants are able to respond to (but not to be entrained by) external zeitgebers, they usually display changed LD activity profiles. These can show either mere acute response to the emergence of external cues (per^{01} mutant) or changes in their anticipatory activity (Pdf^{01} mutant)(Renn *et al.*, 1999; Grima *et al.*, 2004). Apparently, this was not true for *Rho1* targeting or its mutants, as shown in previous experiments. Still, it was hypothesised that the arrhythmic behaviour in DD could be anticipated by a detectable effect on the response to LD cycles. The reasoning also implied that while 12:12 cycles lead to a stereotypical activity response (See Chapter 1.3.7), different environmental cues that change the profile could reveal effects caused by Rho1 depletion via a differential response (Currie, Goda and Wijnen, 2009). Corroborating this possibility required, first of all, a comparative way of analysing the LD behaviour.

3.6.2 Development of a quantifiable measure of environmental effect

Raw data from the DAM system only provides the number of activity bouts (number of times the IR sensor is crossed in a given bin size) which need to be further analysed in order to draw conclusions about the activity rhythms. Similar to other more widely studied characteristics like the strength of the rhythm (RRP in this thesis) or the period length, there is no standardized method of quantifying and analysing the fly activity. As the activity of a fly changes when facing different environmental cycles or when the working of the clock is altered, there are measurable differences in the amount of activity within specific time ranges (See Chapter 1.3.7).

The development of a variable that could measure the activity profile of a fly was performed following two main requirements. Firstly, it should be consistent enough to be resilient to individual variability. Secondly, it should be tested by studying the changes of control populations when facing different environments. Observations of data in 12:12 LD cycles showed that the total activity (number of bouts) is highly variable among individuals, and influenced by factors ranging from the genetic background to uncontrolled variables like the actual length of the tube per a given fly, the available food, etc. The keeping of flies during previous assays for six days at entrainment conditions provided a way of averaging the data, although the dispersion was still significant. Following many published works that rely on ratios or indexes (always relating the time range of interest to the total of the same fly)(Sheeba, Fogle and Holmes, 2010; Zhang *et al.*, 2010a), percentages of the total activity were used instead.

As detailed in the Introduction, *Lights-on* and *Lights-off* are considered standing features of the stereotypical behaviour under luminal cycles (see Chapter 1.3.7). Consequently, the anticipatory activity preceding both events are widely studied, as they allow to easily identify circadian mutants by mere observation of the data (Wheeler *et al.*, 1993; Renn *et al.*, 1999). Clocklab was employed to quantify activity within the time ranges of interest, both as actual bouts and percentage of the total daily activity (See Chapter 2.3.3). The morning anticipatory activity was recorded in the four hours preceding *lights-on* (ZT20-ZT24) and the evening anticipatory activity in the four hours preceding *lights-off* (ZT08-ZT12). Although it was recorded, data corresponding to the four hours after both events were not firstly taken into consideration because of the masking effect evoked by the light responses (Se Chapter 1.3.7)(Lu *et al.*, 2008). As explained in Chapter 2.3.3, the time ranges were displaced a bin before the emergence of the light because the slight and inconstant discoordination between incubator and computer clocks.

After several tests, a new variable was designed and named “Evening-Morning Index” (E-M Index), by subtracting the morning anticipatory activity from the evening anticipatory one, and normalizing the result with the original evening anticipatory activity (see Chapter 1.3.7). An index closer to 1 denotes a weak component of the morning anticipatory activity with respect to the evening anticipatory one, while an index closer to 0 denotes the opposite situation. Activity preceding the dusk is usually on average higher than the one preceding the dawn, but for some individuals this was not the case and as explained in Chapter 3.3.3 their indexes were automatically converted to 0 in order to avoid affecting other data. This design detects differences between genotypes (Mann-Whitney *U* test), but also changes in the behavioural response of a given genotype when facing different environmental cycles (Kruskal-Wallis test).

The reduction of the morning anticipatory activity caused by an *in-phase* temperature cycle leads to a more elevated Index compared to constant temperature LD cycles. Conversely, an *anti-phase* temperature cycle causes a reduction of the index for the opposite reason, resulting in an opposed response to *in-phase* temperature cycles, bearing more similarities with the 12:12 LD cycle with constant temperature (Currie, Goda and Wijnen, 2009). The conservation of this response throughout all the control analysed genotypes (see next Chapter) supports the usage of the E-M Index as an indicator of the environmental response of the adult locomotor behaviour.

3.6.3 Deficiencies in *Rho1* increase the locomotor behaviour sensitivity to environmental signals.

Flies carrying a copy of the loss-of-function $Rho1^{1B}$ allele were previously shown to display a reduced rhythmicity in free run after entraining under LD cycles (See Chapter 3.2). Like with many other further experiments, these flies were firstly considered to display a normal LD behaviour, opposing to their inability to sustain rhythms in DD (Actograms in Figure 3.1 A, Figure 3.3 and others). However, quantitative analysis of the activity revealed that $Rho1^{1B}/+$ females already started exhibiting an abnormal behaviour under LD cycles, something not entirely apparent via visual observation (Figure 3.21 A, grey profiles). The activity preceding the *lights-on* event was increased in $Rho1^{1B}$/+ individuals compared to isogenic controls (Figure 3.21 A, grey arrow) and this caused a reduction in the calculated E-M index (Figure 3.21 B, grey/black bars). The same genotypes were subjected to two additional LD cycles with *in-phase* (18-25 °C) and *anti-phase* (25-18 °C) temperature cycles as described in Chapter 2.3.3. The increased anticipatory activity and the subsequent reduction of the E-M index were absent when an *in-phase* temperature cycle was added to the LD cycle (Figure 3.21 A, B, purple profiles and bars), indicating that *Rho1* deficit failed to cause a behavioural change under these conditions. The differential response was evoked again however when the LD phase was complemented with an *anti-phase* temperature cycle (Figure 3.21 A, B, orange profiles and bars). Opposite to female individuals, the $Rho1^{1B}$ allele failed to cause detectable changes in the male behaviour (Figure 3.21 A, C). One of the possible reasons was that the response of the controls facing an *anti-phase* temperature cycle seemed to elicit a response similar to the expected in experimental counterparts (Figure 3.21 A, bottom left orange profile compared to bottom right). However, this lack of effect was not entirely surprising as the *free run* activity of these males was not compromised with the same intensity than female individuals (See Chapter 3.2). This could be, therefore, another example of the gender variation found across this project. Kruskal-Wallis test showed that all the studied genotypes varied their responses across the different environmental cycles, supporting the strength of the E-M index as

an indicator of the behavioural response of the flies (Figure 3.21 B, C, gray boxes). This difference was caused by the increase of the E-M Index during the *in-phase* cycles opposite to the reduced value under *anti-phase* cycles. This effect is consistent with published results about how these conditions modify the fly behaviour (Currie, Goda and Wijnen, 2009).

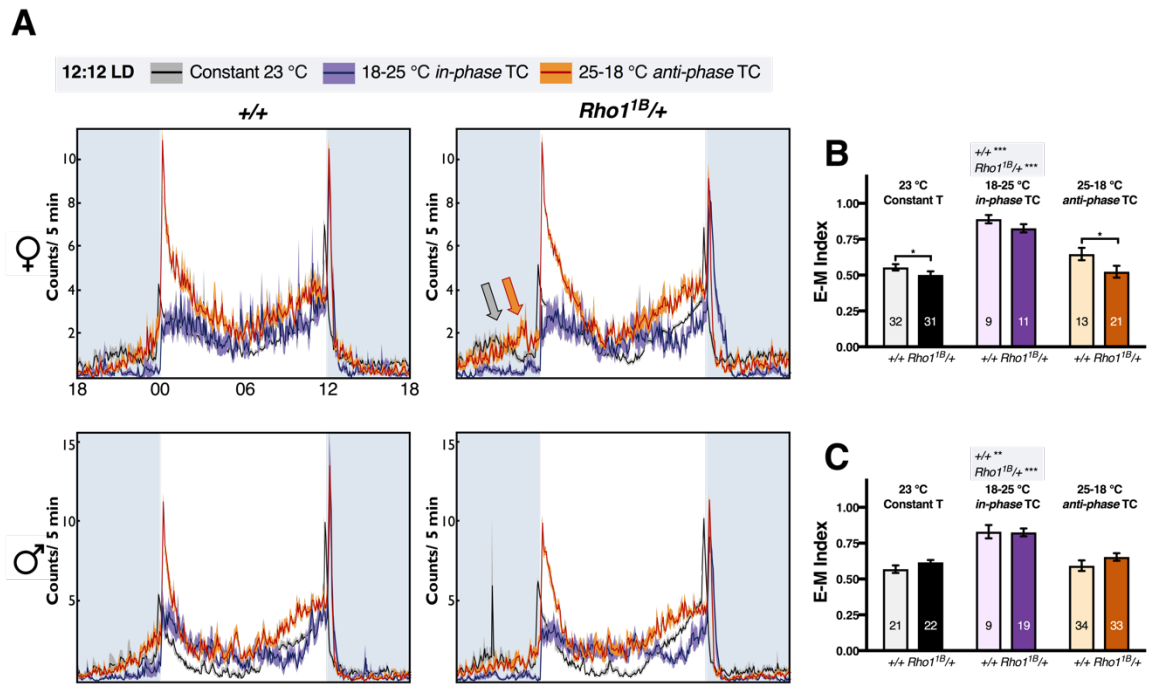

Figure 3.21. Behavioural impact of heterozygous loss of *Rho1* function under different light and temperature interactions. A) Female (top row) and male (bottom row) population average activity profiles over the course of 6 days facing the given environmental conditions (grey, 12:12 LD at constant 23 °C; purple, 12:12 LD with *in-phase* 18-25 °C temperature cycle; and orange, 12:12 LD with *anti-phase* 25-18 °C temperature cycle). Activities profiles display counts per each 5-min bin (Mean ±SEM) with *lights-on* event occurring at ZT00 and *lights-off* event at ZT12. White background, light phase; grey blue background, dark phase. Arrows indicate increased morning anticipatory activity in the given genotypes and environments. **B** and **C**). Quantification (Mean ±SEM) of Evening-Morning Index (E-M Index) as explained in Material and Methods for females (B) and males (C) at the different environments. Bars represent Mean ±SEM and numbers in bars indicate *n*, with the total number of flies originated from 6 ($Rho1^{1B}$ in 12:12 LD at 23 °C), 1 ($Rho1^{1B}$ in 12:12 LD with *in-phase* 18-25 °C temperature cycle) and 3 ($Rho1^{1B}$ in 12:12 LD with *anti-phase* 25-18 °C temperature cycle) crosses. Asterisks in boxes indicate the results of the Kruskal-Wallis test for the same genotype and different environments. *p<0.05; **p<0.01 and ***p<0.001 by Mann-Whitney *U* test (α= 0.05, comparisons among genotypes) or Kruskal-Wallis test (α=

0.05, comparisons for a given genotypes across the three different environments, shown in the legend).

As RNAi interference was proved to be a more useful tool for analysing the role of Rho1 in the circadian behaviour once it was spatially restricted, these flies were also subjected to the same multi-environmental analysis. Consistent with the effect found for both genders in DD, both females and males expressing the Rho1 RNAi 1 (*JF02809*) construct inside the clock cells reproduced the phenotype of the $Rho1^{1B}/+$ females when facing the three environmental cycles (Figure 3.22). Indeed, the response of both genders was almost identical, correlating with the arrhythmia found in *free run* in both cases (Figure 3.4). Plain observation of the activity profiles (Figure 3.22 A) detected an increased morning anticipatory activity under constant temperature LD cycles (grey profiles) and with and *anti-phase* temperature cycle (orange profiles).

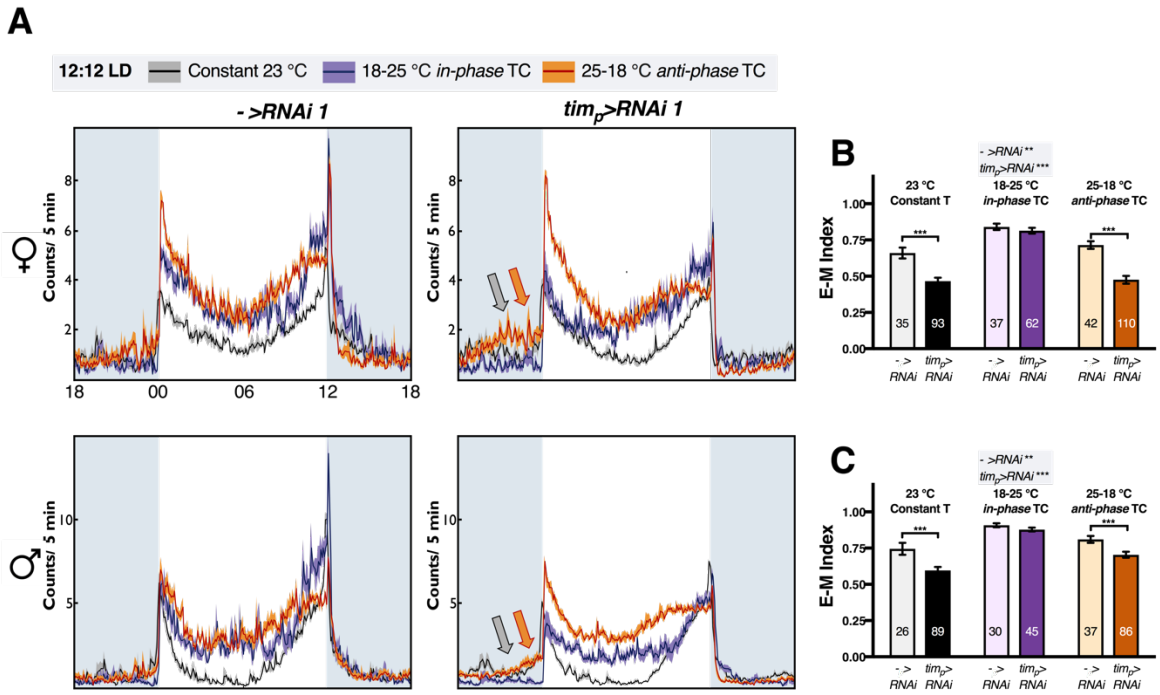

Figure 3.22. Behavioural impact of reduced *Rho1* levels inside the clock cells (*JF02809* construct) under different light and temperature interactions. A) Female (top row) and male (bottom row) population average activity profiles over the course of 6 days facing the given environmental conditions (grey, 12:12 LD at constant 23 °C; purple, 12:12 LD with *in-phase* 18-25 °C temperature cycle; and orange, 12:12 LD with *anti-phase* 25-18 °C temperature cycle). Activities profiles display counts per each 5-min bin (Mean ±SEM) with *lights-on*

event occurring at ZT00 and *lights-off* event at ZT12. White background, light phase; grey blue background, dark phase. Arrows indicate increased morning anticipatory activity in the given genotypes and environments. **B** and **C**). Quantification (Mean ±SEM) of Evening-Morning Index (E-M Index) as explained in Material and Methods for females (B) and males (C) at the different environments. Bars represent Mean ±SEM and numbers in bars indicate *n*, with the total number of flies originated from 10 (*JF02809* in 12:12 LD at 23 °C), 3 (*JF02809* in 12:12 LD with *in-phase* 18-25 °C temperature cycle) and 4 (*JF02809* in 12:12 LD with *anti-phase* 25-18 °C temperature cycle) crosses. ***p<0.001 by Mann-Whitney *U* test (α= 0.05, comparisons among genotypes) or Kruskal-Wallis test (α= 0.05, comparisons for a given genotypes across the three different environments, shown in the legend).

Similar results were found also for the Rho1 RNAi 4 inside the clock cells, and for the expression of the *JF02809* construct inside the PDF-expressing neurons (Supplementary Figure 3 and Supplementary Figure 4). The gender component was frequently present, with the most striking results found in females. Consistently in all these assays, in-phase light and temperature cycles failed to evoke any differential response by experimental flies. An early interpretation of the data suggested that the main effect caused by Rho1 depletion was an overall weakening of the clock which would compromise the maintenance of the rhythms during the dark phase of the LD cycle. As a consequence, the "increase" in the morning anticipatory activity is probably not a real anticipation but the onset of the arrhythmic behaviour, which is inhibited by the *lights-on* event. This effect would be annulated by the presence of an *in-phase* temperature cycle, as the decreasing temperature would force the flies to reduce the activity. This would occur by the animals either trying to follow the temperature cycle or suffering a clock-independent activity decrease that the weakened clock cannot compensate. When the opposite circumstance happened, and the flies faced an *anti-phase* temperature cycle, it prompted the animals into increasing their activity, again as a consequence of the weakened clock. This hypothesis would explain the immediate arrhythmic behaviour of the individuals once devoid of external cues, and in constant requirement of temporal reinforcement by the light phase (See Chapter 4).

The study of the E-M Index was applied to further variations of the LD cycles in order to extract more information of the nature of the *Rho1* deficit phenotype. The behavioural recovery of *Rho1* knockdown flies under RR conditions (See Chapter 3.5.2) prompted to study the response of the mentioned flies when using red light as an entrainment cue. This revealed that, opposite to the behaviour of flies lacking PDF-signalling (Cusumano *et al.*, 2009), *Rho1* deficit organisms maintain

"wild-type"-like activity patterns in RD (Figure 3.19). E-M Index analysis showed that the manifested phenotype in white light cycles was still present, with experimental flies of both genders showing an increased activity in the hours preceding the lights-on event and thus reducing their index (Figure 3.23). Opposite to the situation in RR, RD cycles cannot therefore rescue the experimental phenotype. Both outcomes lead to the same possibility of Rho1 not having an effect in the red light informational pathways. Specifically, they diminish the contribution of the PDF-expressing neurons to the rhythms in red light, as suggested by previous works, unpublished or not (see Appendix B)(Cusumano *et al.*, 2009).

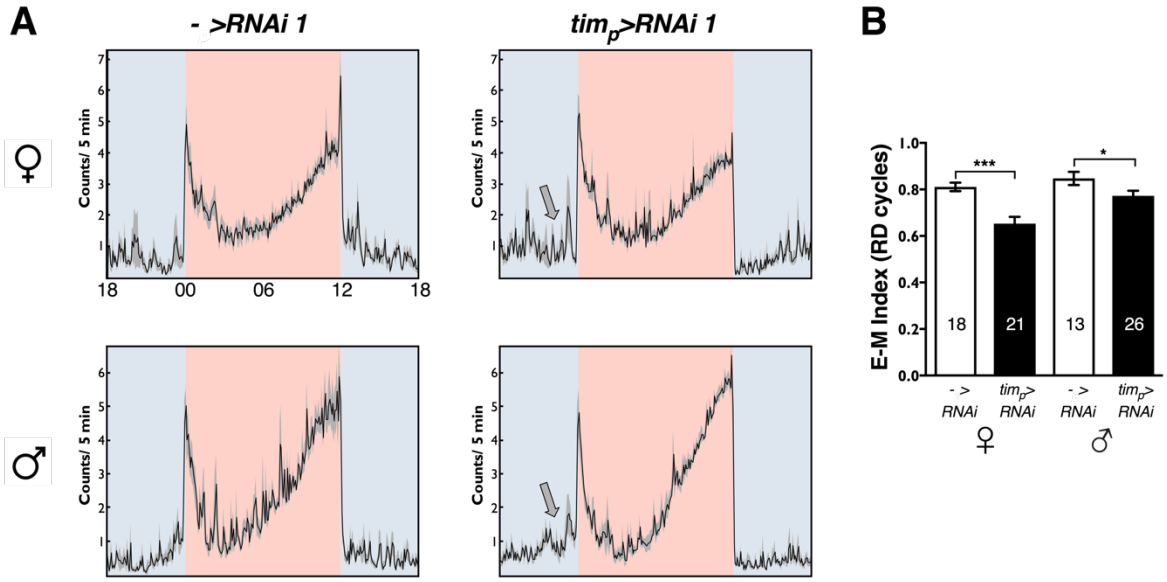

Figure 3.23. Behavioural impact of reduced *Rho1* levels inside the clock cells under RD cycles. A) Female (top row) and male (bottom row) population average activity profiles over the course of 6 days facing 12:12 Red Light-Dark (RD) cycles at constant 23 °C. Activities profiles display counts per each 5-min bin (Mean ±SEM) with *lights-on* event occurring at ZT00 and *lights-off* event at ZT12. Arrows indicate increased morning anticipatory activity in the given genotypes and environments. **B**). Quantification (Mean ±SEM) of Evening-Morning Index (E-M Index) as explained in Material and Methods for females and males. Numbers in bars indicate *n* and flies are originated from one single cross. *p<0.05 and ***p<0.001 by Mann-Whitney *U* test (α= 0.05).

The high reproducibility of the environmental phenotype was challenged by analysing the LD activity of flies where depletion of the PDF receptor overcame the effects caused by *Rho1*

knockdown (See Chapter 3.5.3). Comparison of genotypes arisen from a common background excluding the *Pdfr*-carrying X chromosome drew some interesting conclusions (Figure 3.24). Opposite to the effects of the first assay (See Chapter 3.2 and Figure 3.22), expression of the *JF02809* construct did not affect the male E-M index in the w^{1118} background (Figure 3.24 A, B). This shares resemblance to the unreduced E-M index in males carrying the $Rho1^{1B}$ mutant allele, in the same X chromosome background (Figure 3.21). As the same RNAi can reduce male E-M Index in another background (Figure 3.22) this could be a consequence of the X chromosome, or just the same gender dimorphic effect found elsewhere in this project. Secondly, the $Pdfr^{5304}$ background tended to increase the E-M Index (Figure 3.24 B). This was hypothesised as a consequence of the lack of morning anticipatory activity of these mutants, although it does not entirely take into account the change in the evening anticipatory activity pattern (as the index is sensitive to the actual amount of activity and not the shape of it). Finally, consistent with behaviour in DD (Figure 3.20), downregulation of Rho1 failed to reduce the index in the $Pdfr^{5304}$ background (Figure 3.24 B). While this may not be entirely surprising for males because of the lack of effect in a $Pdfr^{+}$ background, the trend was actually inverted in females, the only single occurrence found in these experiments (Figure 3.24 B). This therefore constitutes another phenotype where the phenotype of the $Pdfr^{5304}$ mutation was dominant to the *Rho1* deficient one.

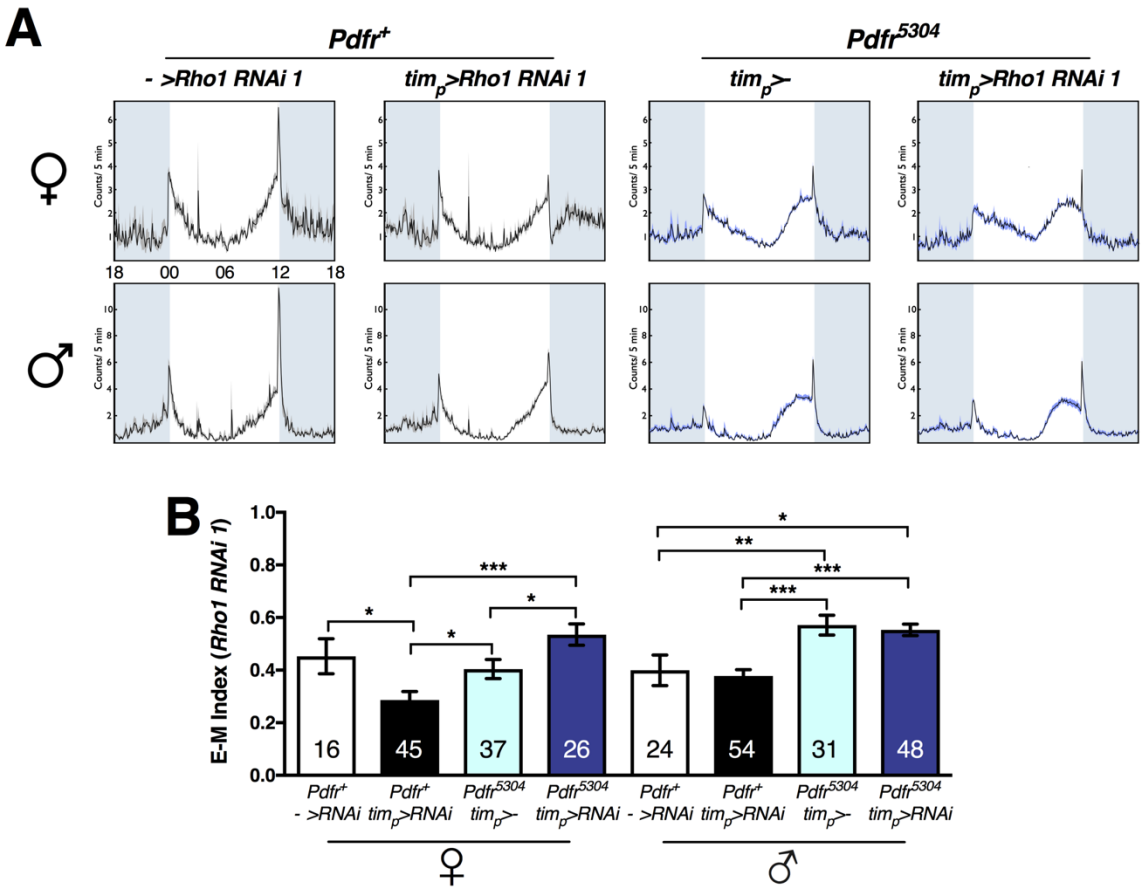

Figure 3.24. Behavioural impact of reduced *Rho1* levels (*JF02809* RNAi expression) inside the clock cells lacking PDF-signalling. Female (top row) and male (bottom row) population average activity profiles over the course of 6 days facing 12:12 LD cycles at constant 23 °C. Columns separate the given genotypes. Activity profiles display counts per each 5-min bin (Mean ±SEM) with *lights-on* event occurring at ZT00 and *lights-off* event at ZT12. **B)** Quantification (Mean ±SEM) of Evening-Morning Index (E-M Index) as explained in Material and Methods for both genders. *Free run* behaviour of these genotypes is analysed in Figure 3.21. Bars represent Mean ±SEM and numbers in bars indicate *n*, with the total number of flies originated from 2 ($Pdfr^{+}$ background) and 3 ($Pdfr^{5304}$ background) crosses. *p<0.05; **p<0.01 and ***p<0.001 by Mann-Whitney *U* test (α= 0.05).

The versatility of the characterisation of the fly activity with the E-M Index prompted it usage under different photoperiod lengths. Along temperature differences, longer or shorter day lengths are a characteristic of seasons, and thus how the clock adapts to them as been linked to seasonality (Stoleru *et al.*, 2007; Pegoraro *et al.*, 2014). Flies expressing the Rho1 RNAi 1 inside the clock cells and subjected to a short photoperiod (10:14 LD) did not exhibited a reduction in their

E-M Index for both genders, but actually a trend towards an increase (Figure 3.25 B, C). The trend was reversed, similar to 12:12 LD cycles, when flies faced a long photoperiod (14:10 LD) (Figure 3.25 B, C). Considering the working hypothesis of the weakened clock, how the photoperiod length affects the response, and specifically how a shorter light phase could reverse the response, requires further interpretation (See Chapter 4).

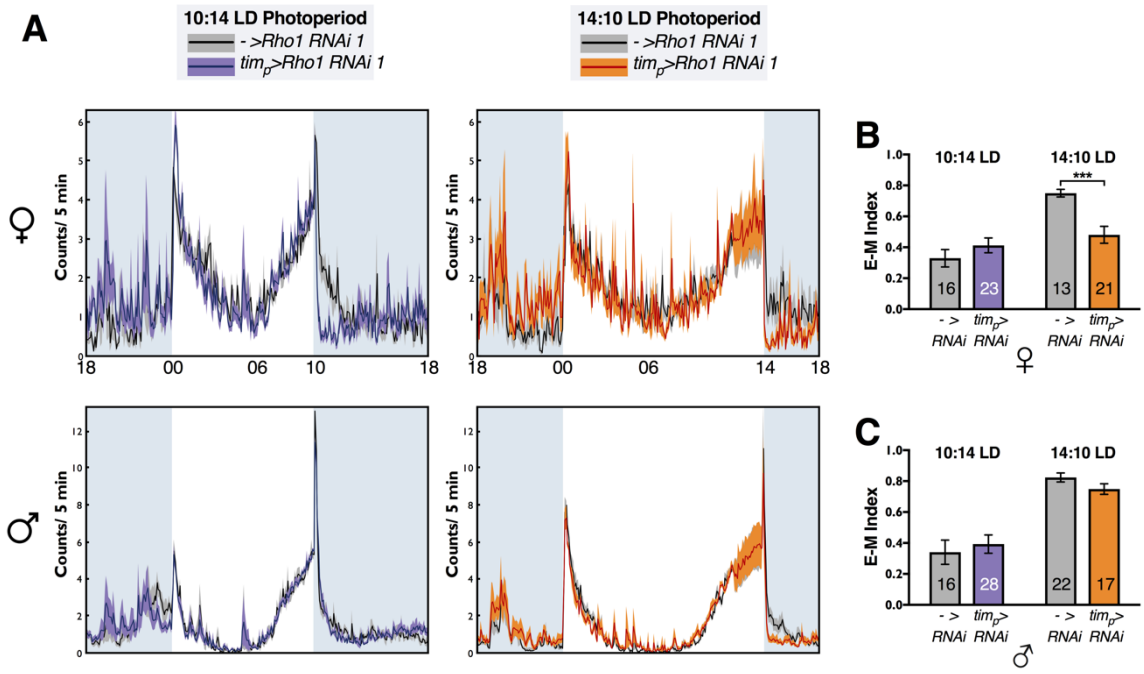

Figure 3.25. Behavioural impact of reduced *Rho1* levels (*JF02809* RNAi expression) inside the clock cells under different photoperiod lengths. A) Female (top row) and male (bottom row) population average activity profiles over the course of 6 days facing short days (10:14 LD, left column) or long days (14:10 LD, right column) at constant 23 °C. Activities profiles display counts per each 5-min bin (Mean ±SEM) with *lights-on* event occurring at ZT00 at both cycles, and *lights-off* event at ZT10 (10:14 LD) or ZT14 (14:10 LD). **B** and **C**) Quantification (Mean ±SEM) of Evening-Morning Index (E-M Index) as explained in Material and Methods for females (B) and males (C) under both cycles. Numbers in bars indicate *n* and flies are originated from a single cross per each condition. ***p<0.001 by Mann-Whitney *U* test (α= 0.05).

The consistent effect upon female E-M Index compared to the more resilient male index drew similarities with the gender dimorphic effect found in the DD behaviour. When comparing the E-M Index (12:12 LD cycle) of diverse *Rho1*-deficient genotypes against their corresponding *free run* RRP (SR and WR flies only) it was found that it was the case in females (Figure 3.26, left graph).

Males on the other hand showed no correlation (Figure 3.26, right graph). Nevertheless, all the compared genotypes showed the same trend when comparing control (Figure 3.26, blank circles) versus experimental genotypes (filled circles), regarding changes in RRP and E-M Index. It is important to take into account this is a correlation comparing two slightly different populations per variable, by excluding flies corresponding to faulty assays, and mainly arrhythmic individuals from the RRP analysis. This comparison clearly shows, regardless, the profound gender dimorphic effect of the reduction in *Rho1* levels.

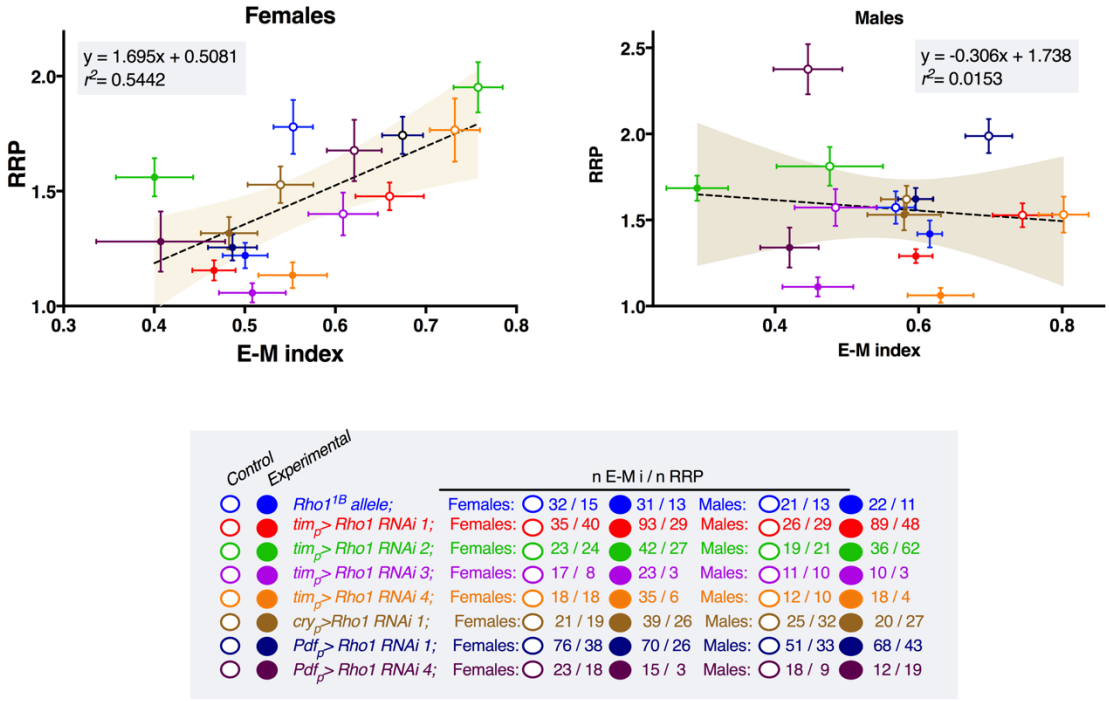

Figure 3.26. Study of the correlation between altered response to LD cycles and *free run* rhythmicity with reduced levels of Rho1. Graphs display Evening-Morning index (also E-M I, x-axis) against the correspondent Relative Rhythmic Power (RRP, Y-axis) for female (left) and male (right) populations. Within each graph, control (white-filled circles) and experimental (colour-filled circles) of each given genotype pair (colours) are represented, as well as the calculated equation and r^2 with lineal regression. The equation is shown as the dotted line, with the coloured background representing the 95% confidence interval. Legend box below the graphic panels displays the colour code for the genotypes and indicate the *n* number for the two different assays. Many of these genotypes were previously presented in this Chapter or in Chapters 3.2 and 3.3 (RRP in *free run*). Data for E-M index only includes flies with six complete days in LD, and data for RRP only includes weakly and strongly rhythmic flies, discarding arrhythmic individuals.

In conclusion, consistent with the *free run* phenotype characterised in previous chapter, selective targeting of *Rho1* inside the clock cells leads to a disturbance of the normal activity pattern when facing environmental cues. Flies with reduced levels of the small GTPase would change their response when facing different environmental cycles, which according to the developed hypothesis are due to a weakened clock. The reason of this compromised oscillator, as presented in previous chapter, would be a deregulation of the normal PDF-signalling across the clock circuitry. As a consequence, the study of the role of the small GTPase revealed that defects in the neuropeptide signalling pathway can impact in the environmental response of the fly. While some information about loss of PDF and its effect on temperature cycles (Busza, Murad and Emery, 2007) or the daily temperature rhythm are known (Goda *et al.*, 2016), the phenotypic differences between this condition and the *Rho1* deficit determine new possibilities for studying the environmental responses related to the neuropeptide.

Chapter 4: Discussion of results

4.1 Main findings of this research

This project started with the goal of understanding the relationship between local deficiencies of the *Rho1* gene products and the emergence of circadian phenotypes. A prior PhD thesis reported that the small GTPase Rho1 had a role in temperature re-entrainment and that it contributed to *Drosophila melanogaster* circadian rhythms (N Rao, unpublished). The research presented here employed diverse techniques and tools to characterise the role of Rho1 in linking the molecular clock to the resulting rhythmic locomotor behaviour.

Numerous experiments confirmed that precise control of *Rho1* expression levels inside the clock cells is necessary for the correct establishment of adult locomotor activity rhythms (Chapter 3.2 and 3.3). Acute knockdown inside adult clock neurons was sufficient to negatively affect the rhythmicity of the flies (Chapter 3.3.2), suggesting but not confirming a post-developmental contribution of the small GTPase to the circadian behaviour. Selective gene targeting inside different clock cell clusters pointed to a specific requirement of the small GTPase inside the PDF-expressing neurons (Chapter 3.3.3). This brought up the hypothesis of a possible effect of Rho1 on signal communication pathways across the clock circuitry, as these neurons act as the core pacemaker cells in DD conditions. The near complete rescue of these arrhythmic phenotypes under constant red light (RR) conditions (Chapter 3.5.2), demonstrated that any developmental or adult impact of *Rho1* knockdown on the cells and signals of the clock circuit was still permissive of clock-controlled behaviour. Consistently, a gender dimorphic effect was found, as males tended to exhibit a milder phenotype

The effective lack of circadian behaviour contrasted with the relatively normal behavioural response of the flies to LD cycles (Chapter 3.2 and 3.3). The stereotyped anticipatory activity before *lights-on* and *lights-off* events was still present, with the former even manifesting a detectable increase (Chapter 3.6.3). The development of a measure to assess the evening versus morning anticipation of flies revealed that, when presented with different light/dark and temperature profiles, reduced *Rho1* levels were associated with an increased environmental sensitivity (Chapter 3.6.3). This is consistent with the notion that flies with depleted *Rho1* levels exhibit a weakened brain clock.

Examination of the molecular and cellular clock circuits of the *Drosophila* brain clarified the origin of the behavioural abnormalities (Chapter 3.4). Reduced *Rho1* levels did not cause distinguishable effects on the molecular clock across the different clock-bearing neurons, including the PDF-

expressing neurons. These neurons displayed persistent clock gene expression rhythms after the transition to DD conditions, revealing uncoupling between molecular oscillations and locomotor behaviour (Chapter 3.4.2). Instead, a defect was found at the level of the PDF^{+} s-LN_v dorsal termini. *Rho1* knockdown blunted the stereotypical rhythm of daily axonal remodelling exhibited by these projections (Chapter 3.4.3). The rhythm of expansion and contraction of the dorsal s-LN_v termini is thought to control the timing of release of PDF and other signals towards the dorsal region of the brain.

Finally, experiments studying the interaction between *Rho1* knockdown and PDF-signalling demonstrated that targeting *Rho1* in a mutant background for the latter failed to cause further behavioural effects (Chapter 3.5.3). The phenotype associated with the PDFR mutant ($Pdfr^{5304}$) overcame the *Rho1* knockdown one not only in *free run* but also during LD cycles (Chapter 3.6.3). Furthermore, the arrhythmia of the combined mutant genotype, although highly significant, was improved compared to *Rho1* knockdown alone. This suggests that the effects caused by Rho1 depletion have an effect via PDF-signalling, and are effectively negated by the removal of the pathway.

The assembled data, therefore, reveal a previously unknown partnership between a critical regulator of the actin cytoskeleton (and thus cellular life) and one of the key time-of-day signals across the *Drosophila* clock circuits. Specific targeting of an actin-modulated cellular component disrupts the signals connecting molecular oscillator function to output pathways. As a result, the circadian behaviour of the animal is disrupted, and more easily modulated by temperature-driven responses. This chapter presents a detailed discussion of the characterization of the Rho1 genotype in a circadian rhythms context.

4.2 General discussion

4.2.1 General considerations about the role of Rho1 and the adult *Drosophila* circadian behaviour.

This project has uncovered a complex requirement of the small GTPase Rho1 in the establishment of the proper circadian behaviour of the fruit fly. Although *Rho1* is an essential gene for eukaryotic cells, the heterozygous presence of a chromosome deficiency including the gene (*Df(2R)ED2457*) or a null allele ($Rho1^{1B}$) is enough for disrupting the normal locomotor behaviour

of adult flies in DD conditions (Chapter 3.2). Yet, a single wild-type copy of *Rho1* is sufficient for apparently normal development (Magie *et al.*, 1999; Magie and Parkhurst, 2005). The lack of a circadian phenotype in $Rho1^{E3.10}$ heterozygotes is consistent with the notion that this is not a null allele in spite of its recessive lethal developmental phenotype, but rather a mislocalization mutant (Halsell, Chu and Kiehart, 2000; Magie and Parkhurst, 2005). The behavioural arrhythmia caused by reduced *Rho1* levels was successfully phenocopied by selective knockdown of the gene inside the clock neurons (Chapter 3.3.1).

The behavioural *Rho1* knockdown phenotype is highly specific and not explained by cell mortalityl. Consistent with the survival of functional PDF neurons, LD activity profiles did not resemble those of flies with targeted ablation of these cells (Renn *et al.*, 1999; Grima *et al.*, 2004; Stoleru *et al.*, 2004). Furthermore, the PDF neurons exhibited normal gross morphology and daily accumulation of Per protein (Chapter 3.4.2). It is possible that developmental expression of the RNAi constructs caused subtler lasting defects in the targeted neurons that contributed to part of the observed phenotype and accounted for the weaker phenotype associated with adult-only RNAi (Chapter 3.3.2). However, it is also possible that the more extensive behavioural arrhythmia for constitutive rather than adult-only *Rho1* knockdown can be explained simply by the fact that the transgenic *dsRho1* accumulated for a longer period and to possibly higher levels in the s-LN_vs in the former setting. In fact, due to poor survival at 29 °C, the DD behavioural analyses for the adult-only knockdown flies were started without prior 29 °C LD exposure limiting the time for RNAi accumulation. The aforementioned work detailing effects of Rho1 overexpression inside the PDF-expressing neurons confirmed this effect to be exclusively post-developmental (Petsakou, Sapsis and Blau, 2015).

The presence of working molecular oscillators throughout the clock circuits (Chapter 3.4.2), indeed, supports the idea that overall cellular fitness of the clock neurons was relatively unaffected by the applied level of *Rho1* knockdown. A more complete loss of *Rho1* using *tim(UAS)-gal4*-driven knockdown might have interfered with highly dynamic actin networks in the cell and triggered loss of basic cell functions in all clock-bearing cells and associated lethality (Celeste Morley, Sun and Bierer, 2003; Pawlowski *et al.*, 2010; Falahzadeh, Banaei-Esfahani and Shahhoseini, 2015). Even with only two assayed time points (Chapter 3.4.2), differences between CT02 and CT14 were striking enough to assume the normal working of the molecular oscillator. The rapid loss of circadian locomotor behaviour of these flies in DD contrasts with the persistence of widespread molecular oscillator function for at least a number of days under these conditions. A very similar result was recently published, showing normal cycling of all the main clock clusters

despite absence of the s-LN_v dorsal termini (Agrawal and Hardin, 2016). Based on these results one of the original hypotheses could be rejected right away; namely, that Rho1 acted on circadian behaviour by intervening in the complex cycle of phosphorylation events taking place in the molecular clock (See Chapter 1.3.2). Some of these events could, still, have been disrupted for Per and other clock components not immunoassayed for this project, and Western blotting experiment could confirm the state of the phosphorylation cycles under depletion of Rho1. As longer term experiments were not carried out in DD, it is not known for how long these clocks would continue to display rhythms. Nevertheless, the *Rho1* knockdown phenotype is distinct from that of the Pdf^{01} and $Pdfr^{5304}$ mutants, which exhibit gradual loss of both molecular and behavioural rhythms in DD, as opposed to the mismatched molecular rhythmicity and behavioural arrhythmicity found in the former (Lin, Stormo and Taghert, 2004; Lear, Zhang and Allada, 2009).

Last but not least, functionality of the clock circuit apart from the s-LN_vs was confirmed as the flies were able to overcome the effects caused by Rho1 depletion under constant red light (Chapter 3.5.2). A functional clock inside a specific subset of non-PDF clock cells is necessary for this to happen (See Appendix B). The RR rescue of the *Rho1* phenotype means that the circuitry required under this condition remains functional, despite the loss of pacemaker function in DD, a role carried by the PDF-expressing s-LN_vs (Renn *et al.*, 1999; Wu, Cao and Nitabach, 2008; Shafer and Taghert, 2009).

The great versatility of the Gal4/UAS system and availability of drivers allowed spatiotemporal mapping of the *Rho1* knockdown phenotype (Chapter 3.3.3). Considering the gender component and the phenotypic rescue with *Pdf-Gal80*, we favour the hypothesis that *Rho1* levels in the adult PDF-expressing clock cells are rate limiting for circadian behaviour. This is further supported by recent observations that have shown that the activity of Rho1 is subjected to circadian control inside these cells (Petsakou, Sapsis and Blau, 2015). Again, genetically targeted *Rho1* knockdown inside the PDF^+ clock cells did not reproduce the behavioural phenotype associated with their ablation or peptidergic silencing of these neurons (Renn *et al.*, 1999).

While molecular clock oscillations remained unaffected by *Rho1* knockdown (Chapter 3.4.2), the daily rhythms of expansion and collapse of the s-LN_v dorsal termini were dampened (Chapter 3.4.3). Interestingly, behavioural rhythms in RR exhibit a decreased dependence on PDF (See Appendix B) (Cusumano *et al.*, 2009). Moreover, while a functional clock inside the PDF neurons is sufficient for driving rhythms in DD, it cannot act as the pacemaker in RR (See Appendix B). Therefore, the conditional DD-specific behavioural phenotype of reduced *Rho1* levels is consistent with disrupted signalling from the s-LN_vs. Specific developmental loss of the s-LN_v dorsal

projections has been shown to phenocopy the DD behavioural arrhythmia and a relatively normal LD profile observed for *Rho1* knockdown (Agrawal and Hardin, 2016). The specific requirement of Rho1 inside the PDF-expressing neurons, and the phenotypic dominance of the *Pdfr*^{5304} mutant, suggest a change in PDF-signalling as the mechanistic cause of the *Rho1* phenotype. This raises a number of questions about how Rho1 could interact with the neuropeptide and other related communication signals, and what the resulting effect in downstream components of the clock circuit might be.

As previously presented in Chapter 3 and in this subchapter, recent published results (Petsakou, Sapsis and Blau, 2015), showed that adult overexpression of *Rho1*, similar to some of the studied phenotypes in this project, led to behavioural arrhythmia in association with blunting of the s-LN$_v$ axonal remodelling. This article also identified rhythms in Rho1 activity in the s-LN$_v$ axons, further supporting the link between Rho1 dosage, s-LN$_v$ axonal remodelling and circadian behaviour (see next subchapter). The localized need for cycling Rho1 activity rhythms in the s-LN$_v$s might also explain the haploinsufficient behavioural phenotype observed for heterozygous deficiency or deletion mutants impacting *Rho1* (Chapter 3.2 and 3.3.2). In contrast to our observations for *Rho1* knockdown, however, this study did find a local molecular oscillator defect in the DN$_1$s (See Chapter 3.4.2). This difference might be attributable to the use of over-expression rather than knockdown or to the fact that the experimental temperature was 30 °C instead of the ambient 23 °C employed in our analyses. Nevertheless, the lack of a molecular oscillator defect in the *Rho1* knockdown phenotype is consistent with similar observations in association with the specific loss of dorsal s-LN$_v$ projections upon knockdown or loss-of-function of *Lar* (see Chapter 4.2.4)(Agrawal and Hardin, 2016). Furthermore, neural activity phases have recently been shown to be controlled via peptidergic signalling independently from molecular oscillator phase, and it is likely that inhibition of PDF-signalling would not immediately impact upon the downstream clocks (see Chapter 4.2.3 and 4.2.4)(Liang, Holy and Taghert, 2016;2017).

4.2.2 Rho1 and the regulation of the axonal remodelling of the s-LN$_v$s

The normal oscillations inside the clock cells (Chapter 3.4.2) and the arrhythmic behaviour of the adult individuals (Chapter 3.2 and 3.3) can be reconciled with the mechanical defect at the s-LN$_v$ dorsal termini (Chapter 3.4.3). In normal conditions, the rhythmic remodelling of these axons (as well as PDF accumulation) is clock-controlled (Park *et al.*, 2000; Fernandez, Berni and Ceriani, 2008). Therefore, the *Rho1* phenotype not only uncouples the molecular oscillators from the

behavioural output, but also disconnects the axonal remodelling of the s-LN_vs from their molecular oscillators. A similar and reversible phenomenon, although affecting PDF accumulation mostly, is caused by acute electrical silencing of the PDF neurons (Depetris-Chauvin *et al.*, 2011). Although many of the experiments regarding the *Rho1* phenotype have been performed *in free run*, the presence of the defect during LD (Figure 3.16) suggests that the some of its consequences might arise under entrained conditions. Despite the presence of light cues, the activity of the flies during the entrainment phase already showed signs of a defective clock (Chapter 3.6.3). Accordingly, the blunting of the arborisation rhythms at the s-LN_v dorsal termini could, in principle, account for all the features of the *Rho1* phenotype.

The observation that *Rho1* product dosage is critical to the daily remodelling of the s-LN_v axonal projections is consistent with both the recognised role of Rho1 in neuronal actin dynamics (Prokop *et al.*, 2013; Antoine-Bertrand, Fu and Lamarche-Vane, 2016), and more specific studies centred on the remodelling of these axons, even with other genetic manipulations of Rho1 function in the PDF neurons (Fernandez, Berni and Ceriani, 2008; Pirooznia *et al.*, 2012; Depetris-Chauvin *et al.*, 2014; Gorostiza *et al.*, 2014; Petsakou, Sapsis and Blau, 2015). The Sholl analysis protocol was implemented (Chapter 3.4.3) as originally published (Fernandez, Berni and Ceriani, 2008) and successfully reproduced (Depetris-Chauvin *et al.*, 2014; Gorostiza *et al.*, 2014). The protocol has some limits that need to be considered though. One of them is its restriction to the bi-dimensional structure, because it is limited to maximum Z-projections. Despite published results showing that either 3D or 2D approaches bring up similar results (Petsakou, Sapsis and Blau, 2015), the axons are three-dimensional structures and therefore study of Z-projections is prone to underestimate differences. Manual counting of the number of crosses was chosen as method because of false positives resulting from unspecific staining or aberrant puncta when employing available plugins. Other alternative methods were assessed, such as manual drawing 2D neuronal skeletons (which is also subjected to human bias in order to avoid the automatized process to be interfered by staining). The use of a set of overlaid concentric circles, however, proved to be the most efficient method with the most reproducible results.

Experimental differences between LD and DD, with a more collapsed state of the s-LN_v axons in the latter, can be tied to the published rhythmic dampening caused by overexpression of the dominant negative *Rho1* isoform (Petsakou, Sapsis and Blau, 2015). The results were comparable when the axons were studied in LD cycles, but not when RNAi axons in DD were compared with mutant axons in LD (there is no available information about the effects of $Rho1^{DN}$ in the s-LN_v axons in DD) (Petsakou, Sapsis and Blau, 2015). It is important to consider that the greatest

discrepancy between this project and the previous research is the lack of phenotype when overexpressing $Rho1^{DN}$ (Chapter 3.3.2), which was expected to reproduce the RNAi effects. This makes difficult to compared the results from this project with the use of RNAi and the reported effects of the mutant isoform (indeed this could explain differences on environmental responses between both, as seen in Chapter 3.6.3 and discussed in Chapter 4.2.5) The difference in axonal complexity found in this project between both environments suggest that while uncontrolled RNAi expression blunt the arborisation rhythms, it does not *per se* collapse the structures. This phenotypic difference on the cellular level contrasts with other more abrupt developmental effects that cause more detrimental effects over these axons, including their disappearance (Agrawal and Hardin, 2016; Gunawardhana and Hardin, 2017).

Structural plasticity in the brain, although not fully understood in post-developmental stages, enables adaptations in neuronal wiring in response to environmental stimuli or internal changes in the context of memory establishment or behavioural responses (Sweatt, 2016). It constitutes an umbrella term, ranging from *de novo* neurogenesis to the structural modification of already existent neurons, for example in flies after eclosion (Gogolla, Galimberti and Caroni, 2007; Rekart, Holahan and Routtenberg, 2007; Yasunaga *et al.*, 2010; Gu, Janoschka and Ge, 2013). The daily remodelling of the s-LN_v axonal projections constitutes an example of the latter, with presumed complex regulatory mechanisms that establish the daily rhythms. Experimental data have shown that the arborisations renew the close contacts and synaptic sites as well, acting as a switch system for intercellular communication (Fernandez, Berni and Ceriani, 2008; Gorostiza *et al.*, 2014; Tang *et al.*, 2017). Matrix metalloproteinases (Mmp), especially Mmp1, intervene in the process of remodelling (Depetris-Chauvin *et al.*, 2014). This is unsurprising because of the known role of these proteins in (at least in peripheral nervous system) neuronal plasticity (Yasunaga *et al.*, 2010; Fujioka *et al.*, 2012). Notably, Mmp1 specifically interacts with PDF at the s-LN_v dorsal termini (Yasunaga *et al.*, 2010; Depetris-Chauvin *et al.*, 2014). There are no direct known interactions between Rho1 and Mmp1, albeit metalloproteinases are involved in interaction with actin cytoskeleton during cell migration and wound healing (Glasheen *et al.*, 2010; Stevens and Page-McCaw, 2012; Raza, Vanderploeg and Jacobs, 2017).

4.2.3 Effects upon PDF-signalling by depletion of Rho1

PDF-signalling constitutes one of several communication pathways from the s-LN_v dorsal termini. While these structures do not require PDF for their formation, the daily remodelling rhythms were reportedly dampened upon downregulation of *Pdf* (Renn *et al.*, 1999; Depetris-Chauvin *et al.*,

2014). The ectopic overexpression of *Pdf* inside the s-LN_vs, which normally does not affect the rhythmic accumulation of the neuropeptide, can slightly rescue the dampening of arborisation rhythms found upon *vri* depletion (Helfrich-Forster *et al.*, 2000; Gunawardhana and Hardin, 2017). In contrast, the *Rho1* knockdown phenotype maintains rhythms in neuropeptide accumulation at the dorsal s-LN_v termini (Chapter 3.4.3). This persistence of PDF rhythms indicates they have not been uncoupled from the s-LN_v molecular clock, as found for example if these neurons are acutely silenced (Park *et al.*, 2000; Depetris-Chauvin *et al.*, 2011). In that instance, PDF levels are lowered at CT02, opposite to the data from *Rho1* knockdown. Indeed, our experimental set up may have uncovered an increase in the amount of neuropeptide at the male dorsal termini in DD, which is not found in LD. Although there is a published case of daily rhythms in PDF accumulation with the loss of the s-LN_v clocks (and with uncertain effect over the axonal remodelling)(Prakash, Nambiar and Sheeba, 2017), we consider that the defect in the dorsal termini correspond to a mechanistic process independent from the neuropeptide (as explained in Chapter 4.2.2). Still, the experimental data suggest an interaction between the small GTPase and PDF-signalling, which is rendered ineffective with the removal of the latter (Chapter 3.5.3).

As stated in Chapter 3.5.1, there exist many differences between the *Rho1* knockdown phenotype and those of mutants blocking all PDF-signalling. The latter are characterized by a progressive loss of rhythmicity when flies are moved to DD conditions (Renn *et al.*, 1999; Hyun *et al.*, 2005; Liang, Holy and Taghert, 2016). The epistatic effect of the $Pdfr^{5304}$ mutant allele (Chapter 3.5.3) (Hyun *et al.*, 2005; Im and Taghert, 2010), relative to clock-targeted *Rho1* knockdown suggests that the behavioural phenotype of *Rho1* knockdown is mediated via disruption of PDF-signalling. Several studies have found an association between defective PDF-signalling in the dorsal protocerebrum and behavioural phenotypes combining DD arrhythmia with apparently normal LD activity profiles (See Chapter 4.2.3 and 4.2.4) (Helfrich-Forster *et al.*, 2000; Agrawal and Hardin, 2016). The traditional dual oscillator model presented the PDF-expressing neurons as a functional unit (M-cells), whose removal causes major changes in the LD activity (Renn *et al.*, 1999; Stoleru *et al.*, 2004). Later studies found specific differences between the contribution of small and large LN_vs to the activity profile (Sheeba *et al.*, 2008a; Wulbeck, Grieshaber and Helfrich-Forster, 2008; Shafer and Taghert, 2009; Schlichting *et al.*, 2016). More recently, it has been shown that the removal of the s-LN_v dorsal axons has no consequences for daily LD behaviour, despite constitutive arrhythmicity in in DD (Agrawal and Hardin, 2016). These observations are, therefore, consistent with a specific defect in the dorsal s-LN_vs termini as the cause for the *Rho1* knockdown behavioural phenotype.

Although the defect at the s-LN_v dorsal termini suggests this cell population is responsible of the effects caused by Rho1 depletion, they are not the only PDF-expressing neurons. However, the developmental lethality with the *R6* (s-LN_vs) and *c929* (l-LN_vs) Gal4 driver lines prevented direct genetic mapping of the s-LN_vs as the site of action of Rho1 in the establishment of circadian behaviour. This lethality is consistent with detrimental effects caused by the off-clock targets of these drivers (Taghert *et al.*, 2001; Head *et al.*, 2015). Interpretation of the results of this thesis in a broader context, however, suggests that the l-LN_vs do not contribute to the behavioural phenotype. While scientists consider the s-LN_v dorsal termini as important output centres for this cell type, no equivalent is currently known for the l-LN_vs besides the accessory medulla or aMe, which is also expected to receive signals from the s-LN_vs. Despite the importance of the aMe for overall rhythmicity in many invertebrates (Helfrich-Forster, Stengl and Homberg, 1998; Loesel and Homberg, 2001; Reischig and Stengl, 2003), its functional description in *Drosophila melanogaster* has been rather limited. The aMe receives contacts from the LN_vs, some LN_ds (including the single ITP and Cry^+), DN_1s and DN_3s (Shafer *et al.*, 2006; Helfrich-Forster *et al.*, 2007a; Johard *et al.*, 2009). This probably means that all anatomically clustered sets of clock neurons except the LPNs and DN_2s make one or more direct contacts with the aMe. Therefore, all cell clusters known to express PDFR have projections there (Howe, 2004; Helfrich-Forster, 2005b; Im and Taghert, 2010; Im, Li and Taghert, 2011). Experiments with mutants have indicated that the PDF neuropeptide in the aMe lengthens the period length, while the one reaching the dorsal part of the brain enhances the short period component (Wulbeck, Grieshaber and Helfrich-Forster, 2008; Lear, Zhang and Allada, 2009). Although this information is not useful for interpreting the *Rho1* phenotype (as no long or short rhythmic components have been found in the experimental flies), it shows that PDF-signalling from the dorsal s-LN_v projections versus that in the aMe may have different effects on the resulting locomotor behaviour.

Functional l-LN_vs could account for the rescued rhythmicity in RR (Chapter 3.5.2), as these neurons have been implicated in connecting the compound eyes to the clock circuitry, hence being critical for non-blue light input (Helfrich-Forster *et al.*, 2007a; Muraro and Ceriani, 2015). While the H-B eyelets signal to the s-LN_vs, they are apparently not sufficient for driving entrainment to by red light/dark rhythms for example (Helfrich-Forster *et al.*, 2002; Hanai, Hamasaka and Ishida, 2008). The $PDFR^-$ l-LN_vs contact the aMe and are thought to release PDF there that induces cAMP signalling in the s-LN_vs and perhaps other PDFR-expressing neurons) (Schlichting *et al.*, 2016). In the presence of red light cues which cannot directly entrain the molecular clock (See Chapter 1.3.4.1), this circuit would relay red light information from the visual systems to this area. This integration of red light input into the network would also be

instrumental in mediating the rescue of the circadian behaviour in RR for both Rho1 deficient (Chapter 3.5.2) and other PDF-signalling deficient mutant genotypes (Cusumano *et al.*, 2009). The contribution of Cry^+ LN_ds and DNs to the phenotypic rescue in RR is not known, partially due to the little knowledge of the clock circuit hierarchy under these environmental conditions as previously described (See Appendix B).

Activity profiles during LD cycles provide further insight in possible contributions of the l-LN_vs and s-LN_vs to the *Rho1* knockdown phenotype, and the dual role of PDF-signalling as well. The phase of the evening anticipatory activity, which is advanced in the Pdf^{01} mutant, relies mostly on PDF from the l-LN_vs (Shafer and Taghert, 2009; Zhang *et al.*, 2010a; Schlichting *et al.*, 2016). On the other hand, signalling from the s-LN_vs to the DN_1s is the most important determinant of the morning anticipatory activity directly preceding *lights-on* (Chapter 3.6.3) (Shafer and Taghert, 2009; Zhang *et al.*, 2010a). Some studies have reported the contribution of the l-LN_vs to the activity before *lights-on* either in the context of their hyperexcitation or huntingtin-induced degradation of their s-LN_vs counterparts leaving them as the sole PDF neurons (Sheeba *et al.*, 2008a; Sheeba, Fogle and Holmes, 2010); in both cases dark-associated activity was increased throughout the night rather than specifically in association with direct anticipation of *lights-on*, not unlike the change observed for *Rho1* knockdown. Thus, clock-targeted *Rho1* knockdown results in a similar LD behaviour profile as was observed with Huntingtin-Q128-mediated s-LN_v ablation (Chapter 3.6.3) (Sheeba, Fogle and Holmes, 2010), suggesting that *Rho1* deficit in the s-LN_vs might also be responsible for the increased late night activity observed under LD conditions.

As introduced in Chapter 1, PDF-signalling can be studied in the peptidergic cell, the receptive cell and the extracellular signalling space between them as well as downstream outputs (Chapter 1.3.5). Disruption of PDF-signalling by PDF-neuron-targeted *Rho1* knockdown likely occurs at the level of actin-mediated remodelling of the dorsal s-LN_v termini. However, as the s-LN_vs also express PDFR it is, in principle, possible that *Rho1* knockdown interferes with PDF receptivity in the s-LN_vs.

Analysis of the s-LN_v dorsal termini (Chapter 3.4.3) suggest that PDF expression and distribution remain relatively normal. While the remodelling defect in the s-LN_v termini suggests that secreted PDF would not efficiently reach its intended targets it remains unclear to what extent PDF release occurs in the first place. It is possible that Rho1 activity is required for the last steps involved in vesicle release into the extracellular space. Although Rho1 and related pathways do not have characterised roles in vesicle trafficking in neurons, in diverse cell types they act upon cell polarity, and subsequent control of endocytic/exocytic pathways (Symons and Rusk, 2003). The

circadian control of PDF processing and secretion is not entirely understood. While *Pdf* mRNA does not show conclusive daily rhythms, the accumulation of PDF at the dorsal termini does (Renn *et al.*, 1999; Helfrich-Forster *et al.*, 2000; Park *et al.*, 2000). The observation that PDF overexpression in the PDF cells does not cause defects in behavioural rhythmicity is probably explained by the moderating influence of posttranscriptional control mechanisms regulating neuropeptide synthesis, processing, transport and release (Helfrich-Forster *et al.*, 2000). The coincidence of increased axonal arborisation and PDF accumulation in the dorsal protocerebrum suggests that spreading of the axonal termini enhances PDF-signalling during the early hours of the (subjective) day. Such a peak in release of PDF during the early hours of the day would match with the reported maximum of s-LN_v electrical activity (Cao *et al.*, 2013). As previously mentioned, the uncoupling between neuropeptide rhythms and the axonal remodelling could lead to a deregulation in the pathway, suggesting that Rho1 indeed acts upstream of PDFR activation.

The scientific consensus states that the s-LN_vs are subjected to autocrine signalling by their own neuropeptide molecules, and probably paracrine (short range) from the l-LN_vs at the accessory medulla, place of action for PDF in many invertebrates (Shafer *et al.*, 2008; Wulbeck, Grieshaber and Helfrich-Forster, 2008; Wei *et al.*, 2014; Schlichting *et al.*, 2016; Liang, Holy and Taghert, 2017). It is not known if PDFR exhibits specific subcellular locations within the s-LN_vs as detailed expression analysis are lacking. Nevertheless, it is worth considering whether *Rho1* knockdown might affect PDF-induced responses in the s-LN_vs at the level of PDFR or further downstream. If Rho1 acted downstream of PDFR this would restrict its activity in PDF cells to s-LN_vs, as l-LN_vs lack PDFR expression (Helfrich-Forster, 2005b; Hyun *et al.*, 2005; Lear *et al.*, 2005; Mertens *et al.*, 2005; Shafer *et al.*, 2008). The increase in cAMP levels upon PDFR activation (Shafer *et al.*, 2008) acts via two downstream pathways. The molecular clock is synchronized by effects on Per and Tim via PKA (Li *et al.*, 2014b; Seluzicki *et al.*, 2014), while cAMP also promotes depolarization of the neurons and therefore their firing rate. As explained in Chapter 1.3.5, this constitutes another temporal cue across the clock circuit (Kunst *et al.*, 2014; Cavey *et al.*, 2016). PKA and cAMP-signalling can communicate with the actin dynamics regulators and produce changes in the cytoskeleton, in some cellular types (Scott and Leopardi, 2003; Howe, 2004). If the increase of the electrical activity of the s-LN_vs in the morning is causally related to the maximum release of PDF, autocrine signalling from the neuropeptide could, in principle, be responsible for the former (Cao *et al.*, 2013). There exists a negative feedback response, however, as the s-LN_v Ca^{2+} currents, exponents of electrical activity (Simons, 1988; Yao *et al.*, 2012; Bushey, Tononi and Cirelli, 2015), are reduced upon PDFR activation (Liang, Holy and Taghert, 2017). Instead, neuronal activation

likely triggers the release of PDF, in analogy to the regulation of other neuropeptides (Ludwig *et al.*, 2002), and analysis of the Ca^{2+} currents of the s-LN_vs also suggests this (Liang, Holy and Taghert, 2017). In summary, there are currently no results that support the hypothesis that Rho1 functions downstream of PDFR. In fact, mutations interfering with PDF responsiveness in the s-LN_vs exhibit phenotypes that contrast with those observed for Rho1 knockdown, as the former exhibit strong rhythms with lengthened period rather than the weakened rhythms of normal periodicity observed for *Rho1* knockdown (Klose *et al.*, 2016).

4.2.4 Consequences of aberrant signalling from the s-LN_vs

Detailed inspection of the data and interpretation in the previous subchapters allow us to focus on the signalling defect arising in the dorsal protocerebrum as a consequence of the loss of rhythmic remodelling in the s-LN_v dorsal termini. A recent study reported that selective knockdown of the Leukocyte antigen-related (Lar) transmembrane phosphatase inside the PDF-expressing clock neurons leads to the specific developmental loss of the dorsal s-LN_v axons (Agrawal and Hardin, 2016). Although the cellular phenotype for clock-targeted *Rho1* knockdown (Chapter 3.4.2) as well as *Rho1* overexpression (Petsakou, Sapsis and Blau, 2015) is subtler, the resulting behavioural phenotypes are remarkably similar. Both *Rho1* and *Lar* knockdown result in constitutively arrhythmic behaviour in DD conditions, with flies exhibiting a rather normal behaviour during LD entrainment (Agrawal and Hardin, 2016). Moreover, targeting either *Lar* or *Rho1* did not disrupt molecular clock oscillations in spite of the observed behavioural arrhythmia. A search in the online database STRING (Szklarczyk *et al.*, 2017) showed that the RhoGEF Trio forms a complex with Lar, probably for coordinating purposes rather than an actual role of Lar on Rho1-signalling (Debant *et al.*, 1996). As presented in Chapter 1, Trio has been mostly characterised in the developing nervous system, something consistent with the developmental *Lar* knockdown (Bateman, Shu and Van Vactor, 2000; Shivalkar and Giniger, 2012; Agrawal and Hardin, 2016).

As explained in the previous subchapter, *Rho1* knockdown is thought to impact behaviour via its impact on PDF-signalling (Chapter 3.5.3). However, complete disruption of PDF-signalling would cause changes in the molecular clocks, as PDFR-mediated activation of PKA is known to act on clock components (Lin, Stormo and Taghert, 2004; Li *et al.*, 2014b; Seluzicki *et al.*, 2014).

PDF-signalling acts to desynchronise calcium currents among different clusters, in part via negative feedback effect on the s-LN_v neurons (Liang, Holy and Taghert, 2016;2017). The phases of these Ca^{2+} rhythms match the maximum electrical activity of the different cell clusters, where it

has been described. Moreover, peak Ca^{2+} in M- and E- cells occurs ~5h before their respective associated behavioural activity peaks (Liang, Holy and Taghert, 2016;2017). If PDFR is not functional, the phases of the Ca^{2+} currents of different clock cell clusters largely collapse to the same phase (Liang, Holy and Taghert, 2016). Importantly, this means that PDF-signalling is responsible for maintaining cell-type specific phase relationships between Ca^{2+} rhythms and molecular oscillators. For example, the s-LN_vs and the LN_ds have very similar Per cycling, but almost *anti-phase* Ca^{2+} rhythms caused by PDF-signalling (Lin, Stormo and Taghert, 2004; Liang, Holy and Taghert, 2016;2017). In contrast, disruption of PDF-signalling does not initially prevent the clock cells from synchrony in their molecular oscillators either (Lear, Zhang and Allada, 2009) although this can emerge after prolonged time in DD.

Due to their proximity to the s-LN_v dorsal termini, the DN_1s are clock cells of special interest in order to explain the *Rho1* phenotype. Seven of these neurons normally express PDFR (Im, Li and Taghert, 2011), but they are often analysed altogether. Many studies investigate the DN_{1p}s because of the available Gal4 drivers, but projections from the DN_{1a}s are found close to the s-LN_v dorsal termini, and hence could interact in the same way (Shafer *et al.*, 2006). Activation of PDF-signalling pathways in the DN_{1p}s is necessary for the appearance of the morning anticipatory behaviour (Zhang *et al.*, 2010a), and this is considered to be caused by their discreet contacts with the s-LN_v dorsal termini (Seluzicki *et al.*, 2014). Focal application of ectopic neuropeptide depolarizes the DN_{1p}s and increases both the firing rate and the intracellular Ca^{2+} levels (Seluzicki *et al.*, 2014; Flourakis *et al.*, 2015). In normal conditions, the peak phases in Ca^{2+} for s-LN_vs and DN_1s are relatively close in the late night (Liang, Holy and Taghert, 2017), and, therefore, the signalling towards the DN_1s is thought to reach its peak in late night/early morning. Well-timed activation of the s-LN_v-to-DN_1 route is critical for some of the known connections between the circadian clock and locomotor behaviour, and a disruption caused by depletion of Rho1 could contribute to behavioural arrhythmia (Cavanaugh *et al.*, 2014; Cavey *et al.*, 2016). The requirement of a precise temporal activation of the DH44-expressing neurons of the Pars Intercerebralis (See Chapter 1.3.7) for the correct establishment of a circadian behaviour is demonstrated by the arrhythmia induced by both ablation or ectopic activation of them (Cavanaugh *et al.*, 2014). The peak levels of Ca^{2+} inside these neurons at subjective dusk (Cavey *et al.*, 2016) imply increased spontaneous activity during those times (Simons, 1988; Bushey, Tononi and Cirelli, 2015), and the changes throughout the day are clock-controlled (Cavey *et al.*, 2016). Additionally, PDF-signalling towards the DN_1s cause them to release the sleep-inhibiting DH31. This normally contributes to the awake state in the morning, but ectopic DH31 expression in night causes the same effect (See Chapter 1.3.6) (Kunst *et al.*, 2014). While sleep has not been studied

in this project, this phenomenon could still contribute to the behavioural phenotype. Modulation of the midday siesta, which is a feature of DH31-related phenotypes, is, however, not observed for *Rho1* knockdown (Kunst *et al.*, 2014; Guo *et al.*, 2016). Closing the clock circuit, the DN_1s exert some inhibitory effects on s-LN_v and LN_d neuronal activity (Guo *et al.*, 2016).

Although, recent studies have highlighted output circuits involving the DN_1s, several other E-cells are contacted by the s-LN_v axonal termini. In particular, new synapses are established in the late hours of the day with some of the LN_ds and the fifth s-LN_v (Gorostiza *et al.*, 2014). They are all part of the same network that spreads at the dorsal region of the brain, where the identity of the different contributing neurons has traditionally been obscured by the technical limitations (Kaneko and Hall, 2000; Schubert, Helfrich-Forster and Rieger, 2016). The dorsal region of the brain is also subjected to effects from neuropeptides other than PDF, and the intersection of multiple signals in this region raises the question whether the *Rho1* knockdown phenotype may have disturbed neuropeptidergic pathways other than PDF. One of the most interesting candidates, in this regard, is sNPF, expressed by the four PDF^+ s-LN_vs and two of the Cry^+ LN_ds (Johard *et al.*, 2009). The 3 Cry^+ LN_ds express PDFR, influence the neuronal state of the DN_1s via sNPF, but this effect is inhibited by PDF (Johard *et al.*, 2009; Beckwith and Ceriani, 2015; Liang, Holy and Taghert, 2017). The Ca^{2+} currents of the DN_1s are the most sensitive to the removal of sNPF from the s-LN_vs and, interestingly, do not affect the molecular clock under these conditions (Liang, Holy and Taghert, 2017). While ITP could have been affected by *Rho1* knockdown, it is expressed in the 5^{th} s-LN_v and one of the LN_ds, but not in the PDF neurons, casting doubts about it involvement (Hermann-Luibl *et al.*, 2014; Yoshii *et al.*, 2015; Schlichting *et al.*, 2016). Moreover, a driver found to be expressed in the ITP-expressing clock neurons (R*54D11*, see Supplementary Table 3 and Appendix B.3.2)(Johard *et al.*, 2009; Yoshii *et al.*, 2015) did not affect the rhythmicity of the flies. Another characterised driver targeting (among many others) the E-Cells (*R78G02*)(Schlichting *et al.*, 2016) was used to drive *Rho1* RNAi expression, with the goal of confirming the s-LN_vs as the place of action of Rho1. This experiment resulted in poor female rhythmicity, but also in developmental death of all the males but one (Supplementary Table 3). This was probably caused by off targets of the driver (at least 15 non-clock neurons in the adult brain) (Schlichting *et al.*, 2016) and supports the interpretation that these females exhibited arrhythmia because of developmental defects. Apart from all the previously discussed possibilities, the s-LN_v dorsal termini also contact neurons outside the circadian network that are of interest for possible involvement in mediating output(Gorostiza *et al.*, 2014).

4.2.5 Environmental sensitivity of a weakened clock by Rho1 depletion

Besides the inability of flies with reduced levels of *Rho1* to sustain behavioural rhythms in DD, results in Chapter 3.6 also revealed behavioural abnormalities when flies were subjected to environmental cues. The Evening-Morning Index proved to be a robust tool to quantify the activity of the animals under different conditions and compare them. The data (Chapter 3.6 and Appendix A.4) showed that the E-M Index for experimental genotypes (at both constant temperature and *anti-phase* temperature cycles) was decreased due to an increase in the activity during the hours preceding the *lights-on* event. Interpretation of this result may be easier in the constant temperature LD setting. However, with the growing realisation that a simple dual oscillator model does not describe the Drosophila neural clock circuit well (Pittendrigh and Daan, 1976; Helfrich-Forster, 2009), even in this context, the precise causative mechanism is not entirely clear.

The effect of PDF-signalling from the s-LN_vs on functional E-cells constitutes the first stage of the circuit that causes morning anticipatory activity (Lear, Zhang and Allada, 2009; Zhang *et al.*, 2010a; Yoshii, Rieger and Helfrich-Forster, 2012). A reduced input of this pathway does not account for the increased anticipatory activity found in the *Rho1* genotype, as deficiencies of PDF usually lead to its disappearance (Lear, Zhang and Allada, 2009; Shafer and Taghert, 2009). Equally, the collapsed s-LN_v dorsal termini are expected to display reduced synaptic contacts with the $DN1_p$s, cells considered to be specifically critical for the morning peak (Zhang *et al.*, 2010a; Gorostiza *et al.*, 2014). The explanation to the *Rho1* phenotype in LD could be found in the myriad of connections between clock cells, immediate output centres and activity/sleep hubs in the dorsal region (Crocker *et al.*, 2010; Cavanaugh *et al.*, 2014; Park *et al.*, 2014; Cavey *et al.*, 2016). If the s-LN_v dorsal termini were unable of sending signals at all, they would be functionally equivalent to the loss axons with *Lar* knockdown (Agrawal and Hardin, 2016). As l-LN_vs remain apparently unnafected in both genotypes, they would still employ PDF-signalling in order to establish the normal the evening anticipatory peak by action of the E-cells (Grima *et al.*, 2004; Schlichting *et al.*, 2016). This would imply two characteristics: 1) that light would exert an inhibitory effect on the *Rho1* knockdown-mediated behavioural phenotype, which is consistent with the behaviour of the flies and the emergence of arrhythmia in the dark; and 2) that the "morning anticipatory activity" would not be anticipatory at all, but the actual emergence of the arrhythmic behaviour, which would be suppressed by light.

The modification of the stereotyped LD behaviour when temperature cycles are present puts into context the notion of the blue light as the most intense of the zeitgebers, pointing out that its

effect can still be modulated by others (Busza, Murad and Emery, 2007; Currie, Goda and Wijnen, 2009). Naturally aligned light and temperature cycles tend to reinforce effective coupling of fly activity with the external environment, whereas misaligned light and temperature cues can help reveal their separate impact (Currie, Goda and Wijnen, 2009). It is important to state that temperature cycles can drive activity rhythms independently from the clock with colder temperatures tending to suppress activity, and that a functional oscillator normally counteracts out-of-phase temperature-driven responses (Currie, Goda and Wijnen, 2009; Menegazzi, Yoshii and Helfrich-Forster, 2012). The interaction between temperature-driven and clock-mediated control of behaviour may, therefore, explain why the increase in the morning anticipatory activity of *Rho1*-deficit flies in 12:12 LD cycles at constant temperature disappears upon superposition of an *in-phase*, but not an *anti-phase* temperature cycle. If locomotor activity just reacted in a clock-independent manner, it would ramp up with increasing temperatures and trough at the decreasing phase. This tendency is most evident in clock mutant flies, indicating the role of a functional clock in restraining this behavioural output (Currie, Goda and Wijnen, 2009). E-cells are more prone to follow temperature cycles if M-cells are compromised, something that could fit with the *Rho1* knockdown phenotype during the dark phase or DD (Busza, Murad and Emery, 2007). However, the activity of *Rho1*-deficient flies during the light phase is never as affected as per^{01} individuals, whose activity dramatically ramps up with temperature (Menegazzi, Yoshii and Helfrich-Forster, 2012). This lends further suppport to the conclusion that the clock of the *Rho1* phenotype is not as defective as in those mutants, especially when light is present.

Interestingly, a shorter photoperiod (10:14 LD, Figure 3.25) rescued the E-M index with experimental flies actually possibly displaying reduced activity in the hours preceeding *lights-on* (Supplementary Table 8). The behaviour of the flies subjected to long photoperiod cycles (14:10 LD, Figure 3.25), underscores the difference between the Rho1 knockdown and Pdf^{01} phenotypes (Chapter 3.5.1). Pdf^{01} mutants cannot delay their evening anticipatory peak as the day extends (Yoshii *et al.*, 2009a; Schlichting *et al.*, 2016). It is worth noting that even wild-type flies will display an apparent activity plateau in the evening preceeding *lights-off* if the photoperiod is long enough (Yoshii *et al.*, 2009b), as happens also with *Rho1* knockdown individuals (Figure 3.25). Different results were reported in comparison to the phenotype of overexpressing $Rho1^{DN}$ to the PDF neurons (Petsakou, Sapsis and Blau, 2015). The latter study reported that excess of Rho1 increased the morning anticipatory activity during short photoperiods, while the expression of $Rho1^{DN}$ reduced it during long photoperiods (Petsakou, Sapsis and Blau, 2015). For the experiments involving *Rho1* knockdown and heterozygosity for the $Rho1^{1B}$ mutant allele, an opposite relationship was described between *Rho1* levels and morning anticipation (Figure 3.25

and Supplementary Table 8). We cannot explain this discrepancy with the current data, besides the difference in temperature used for these experiments (23 °C versus 30 °C in the latter to disable the Gal80^{TS})(Petsakou, Sapsis and Blau, 2015) As previously mentioned, this represent another conflict between this project and the published article, centered around the use of the dominant negative isoform (which, nevertheless, reportedly causes a different effect than the loss-of-function *Rho1^{1B}* allele).

4.2.6 The role of Rho1-signalling in the establishment of the circadian behaviour

As stated in Chapter 1.4, actin dynamics and intervening factors have been traditionally studied in motile cells rather than neurons, although some specific roles are being uncovered for this cell type. Some of these functions are involved in morphological features of dendrites, axons and other types of cell-to-cell contacts, thus offering a possible explanation of the s-LN$_v$ dorsal termini phenotype (Newsome *et al.*, 2000; Tashiro, Minden and Yuste, 2000; Schmidt and Debant, 2014). These interactions underline the delicate requirements for neurons of actin dynamics, whose regulators have clinical significance (Ba *et al.*, 2016; Hu and Selzer, 2017). Recent studies report roles of the Rho1-signalling pathway and related modules in synapsis (Tolias, Duman and Um, 2011; Ba and Nadif Kasri, 2017). Among the most recent results, it has been determined that RhoA is upregulated after spinal cord injury, and its inhibition or knockdown has therapeutic applications for promoting neuron survival and lesion recovery (Conrad *et al.*, 2005; Wu and Xu, 2016; Hu and Selzer, 2017).

The hypothesis that Rho1-signalling control of actin dynamics has a role in the establishment of the circadian behaviour is supported by the actual requirement of the Myosin Light Chain (MLC or Sqh) in the remodelling of the s-LN$_v$ dorsal termini (Edwards and Kiehart, 1996; Petsakou, Sapsis and Blau, 2015). At the start of this project, several other Rho1-signalling components were tested for mutant phenotypes affecting circadian behaviour and some of these results merit mentioning here. As presented in supplementary material (Supplementary Table 1 and Supplementary Table 2), one of the transgenic knockdown constructs (*dsRhoGEF2$^{9635R-3}$*) for the gene encoding the Guanine Nucleotide Exchange factor RhoGEF2 (Barrett, Leptin and Settleman, 1997) showed consistently reduced rhythmicity in DD, albeit with a lengthened period when expressed with the *tim(UAS)-Gal4* driver. A second, independent knockdown allele for the same gene (*dsRhoGEF2^{JF01747}*) resulted in a gender-specific weakening of rhythms (Supplementary Table 1). The overexpression of the *RhoGEF2$^{\Delta PDZ}$* mutant isoform, which is functional, but mis-localised, in clock-bearing cells caused no specific circadian behavioural defect(Jelen *et al.*, 2003; Wenzl *et*

al., 2010). Similar to the negative results for the $Rho1^{E3.10}$ mutant (Chapter 3.2), this might be explained by the differences between epithelium and neurons regarding specific sites of action inside the cells. Additional experiments are needed to resolve whether RhoGEF2 manipulation causes the similar molecular and defects as *Rho1* knockdown. There is precedent, however, for related phenotypes found in association with manipulation of Rho1 GEF activity in the case of Puratrophin-1-like (Pura) inside the PDF neurons (Petsakou, Sapsis and Blau, 2015). The genetic reagents tested did not reveal a consistent behavioural phenotype for Rho kinase (Rok), which acts as an important output actuator of Rho1 (Mizuno *et al.*, 1999; Amano, Nakayama and Kaibuchi, 2010). This was the case for clock-targeting of transgenic knockdown or over-expression of a constitutively active version of Rok. The latter, did, however, practically rescued the circadian phenotype of *Rho1* knockdown in a genetic interaction study (Supplementary Table 1 and Supplementary Table 4).

4.2.7 Sexual dimorphism and the role of Rho1 in the circadian behaviour

As introduced in Chapter 1.3.9, female and male individuals exhibit differences regarding their clock circuitry and output behaviour, determined by developmental but also post-mating factors (Helfrich-Forster, 2000; Lee, Bahn and Park, 2006; Guo *et al.*, 2016; Khericha, Kolenchery and Tauber, 2016). Of special importance, given the hypothetical model of how Rho1 may impact PDF-signalling in the dorsal brain, are the DN_1s, which are more excited in males, but also unlike female counterparts sensitive to sexual cues (Hanafusa *et al.*, 2013; Guo *et al.*, 2016). The most reported dimorphic contribution of these neurons is the daytime sleep, which was not quantified in this study but, based on activity profiles and actograms, appeared unchanged by Rho1 depletion (Chapter 3.6)(Guo *et al.*, 2016).

Throughout the realisation of the project, behaviour appeared consistently less affected for males than females as measured by the locomotor assays (Chapter 3.2, 3.3, 3.5 and 3.6). Most of the experiments include the presence of a *UASDcr2* construct on the X chromosome, which could account for gender effects in the resulting progeny. However, the stronger phenotype for females was still found for genotypes with heterozygosity for either the chromosomal deficiency *(2R)ED2457* or the $Rho1^{1B}$ deletion mutant (Chapter 3.2), and for transgenic genotypes where the expression of the *JF02809* construct was enhanced by an *UASDcr2w* insertion on the third chromosome (Chapter 3.5.3). This reproducibility across different genotypes and backgrounds suggests that females are indeed more sensitive to a reduced *Rho1* dosage in their PDF neurons.

As illustrated in Figure 3.26, for female flies *Rho1* deficit-induced phenotypic changes in the EM index during LD correlate well with the degree of behavioural arrhythmia, as measured by relative rhythmic power, during DD. This is not the case for males, however, as pointed out by the negligible r^2 coefficient. Expression of *Rho1* RNAi 2 (*TRiP.HMS00375*) inside the clock cells did not affect male rhythmicity in DD (Figure 3.3), but dramatically reduced the experimental E-M index. On the other hand, expression of *Rho1* RNAi 3 (*Rho1.325-786*) caused a very strong effect on males (Figure 3.3), but did not change the Index (Figure 3.26).

Immunostaining experiments determined that the PDF neuropeptide maintains cyclic accumulation at the s-LN_v dorsal termini despite depletion of *Rho1* levels (as seen in Chapter 3.4.3 and discussed in Chapter 4.2.2). The same experiments also revealed, however, that the levels of the neuropeptide inside male dorsal termini were considerably higher than in females, at least in DD (Figure 3.15). Perhaps this is a consequence of the increase in *Pdf* mRNA reported for males (Park and Hall, 1998). Most previous studies have not taken into account gender differences and focussed exclusively on males (Park *et al.*, 2000; Depetris-Chauvin *et al.*, 2014). As a consequence, the results presented in Chapter 3.4.3 may represent the first example where both genders were independently examined regarding PDF accumulation at their s-LN_v dorsal termini. The aforementioned phenotype caused by overexpressing mutant huntingtin also resulted in increased but rhythmic PDF levels in males (with females not being assayed) (Prakash, Nambiar and Sheeba, 2017).

The milder male *Rho1* knockdown phenotypes imply either that PDF-signalling is less suppressed in this gender or that male behaviour is less sensitive to PDF-signalling defects. The increased PDF staining in male s-LN_v projections may be relevant to the former possibility. As for the latter explanation, at this point we can only speculate why male circadian behaviour might be less dependent on PDF. Perhaps there is a role for sexually dimorphic expression or function of neuropeptides. In a clock-independent manner, PDF and NPF [with the reported gender dimorphic expression (Lee, Bahn and Park, 2006; Hermann *et al.*, 2012)] from the s-LN_v and LN_ds are required for the males to extend the mating time. This trait increases the reproductive chances within a population and constitute an example of clock components providing males with improved fitness (Kim, Jan and Jan, 2013). As sexual activity may influence the male DN_1s, (Hanafusa *et al.*, 2013) there could also be an underlying feedback mechanism between the male core clock and mating in analogy to the mating-induced locomotor behaviour change observed in females. (Isaac *et al.*, 2010).

4.3 Conclusions

In summary, the results of this research project have led to the following conclusions:

1. A precise control of the available pool of the small GTPase Rho1 is required inside the adult *Drosophila melanogaster* PDF neurons in order to allow the persistence of circadian behaviour in DD.

2. Flies with a *Rho1* deficit in their PDF neurons exhibit locomotor behaviour that has increased environmental sensitivity, consistent with a weakened brain clock.

3. The *Rho1* knockdown phenotype pairs behavioural arrhythmia with unimpaired molecular oscillator function.

4. *Rho1* knockdown abolishes rhythmic remodelling of the s-LN_v dorsal projections, but not rhythms of PDF in the dorsal brain.

5. Red light environmental conditions that shift the pacemaker role to include E neurons rescue the arrhythmic phenotype of Rho1 knockdown without impacting its s-LN_v projections remodelling defect.

6. Loss-of-function mutation of the Pdfr gene is epistatic to clock-targeted *Rho1* knockdown for its behavioural phenotype.

Summing up the discussion of the experimental results, we propose a model for the role of Rho1 in the clock circuit that is depicted in Figure 4.1.

1. Rho1-mediated axonal remodelling of the s-LN_vs intervenes in the gating system that allows rhythmic PDF-signalling from the s-LN_vs to the E-cells and subsequent output centres (Cavanaugh *et al.*, 2014; Gorostiza *et al.*, 2014; Cavey *et al.*, 2016). The activity of the small GTPase itself is regulated by the clock-controlled RhoGEF Pura (Petsakou, Sapsis and Blau, 2015).
2. Depletion of the small GTPase levels dampen the rhythm of s-LN_v projection expansion/contraction, abrogating the precise control of PDF-signalling, and associated patterns of neural activity.

3. During LD cycles, the presence of the zeitgeber is sufficient to overcome disruption of the circuit (Agrawal and Hardin, 2016). The defect at the dorsal protocerebrum is sufficient, however, to increase the activity of the flies in the last hours of the night in a temperature-sensitive manner. Similarly, the compromised clock causes abnormal behavioural responses when external cues are conflicted.
4. The lack of a *lights-on* event with the transition to DD exposes the consequences of the PDF-signalling deficit from the s-LN$_v$ dorsal termini. This causes behavioural arrhythmia and the effective loss of the locomotor circadian behaviour in females, with a milder effect in males.
5. The presence of red light bypasses s-LN$_v$ signalling to the dorsal brain, presumably via the compound eyes, l-LN$_v$s, accessory medulla (Helfrich-Forster *et al.*, 2007a; Hanai, Hamasaka and Ishida, 2008), and the "red light pacemakers" (including E-cells, see Appendix B). This allows the establishment of circadian behaviour despite depletion of *Rho1* inside the s-LN$_v$s.

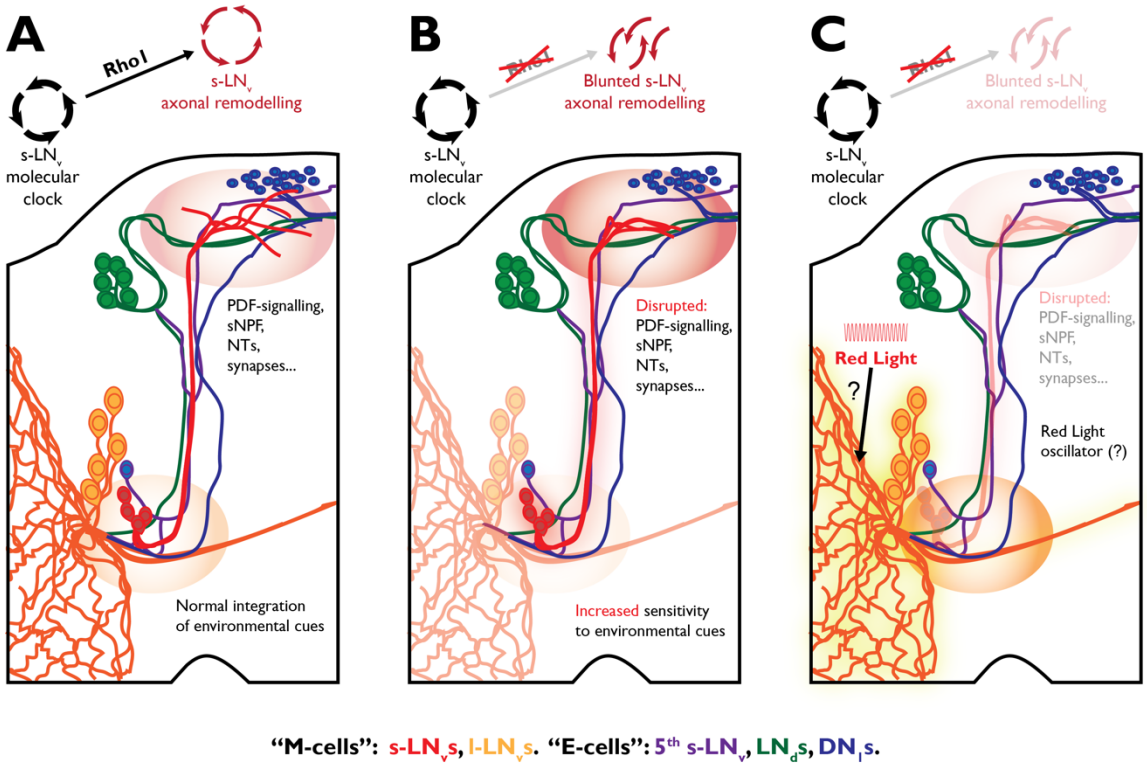

Figure 4.1. Model for the role of Rho1 in the establishment of the *Drosophila melanogaster* circadian behaviour. This graphic model is based on the described and discussed data, discussed data, as well as published observations. The DN$_2$, DN$_3$ and LPN clock clusters are

not included in this model. The inclusion of all the LN_ds and DN_1s as E-cells has a purpose of simplification but only some members of each cluster are actual "E-cells" as explained in Chapter 1.3.7. **A)** The PDF-expressing neurons or M-cells coordinate LD responses with the E-cells at the dorsal region of the brain (red area) and the accessory Medulla (orange area). Rho1 intervenes in the clock-controlled remodelling of the s-LN_v dorsal termini, regulating related pathways including PDF-signalling. The s-LN_vs assume the role of *pacemaker* neurons in DD. **B)** The depletion of *Rho1* blunts the s-LN_v axonal remodelling and uncouples it from the s-LN_v clock. This disturbs the signalling towards the E-cells in the dorsal region of the brain (red area). As a result, the locomotor circadian behaviour is lost in DD, and flies also exhibit anomalous activity during the dark phase in LD and increased sensitivity to environmental cues. **C)** The presence of red light (RR conditions) is sensed by the compound eyes and presumably relayed to the l-LN_vs. These neurons signal via the accessory Medulla (orange area) to the yet uncharacterised red light *pacemaker* neurons (presumably related to the E-cells, see Appendix B), which drive rhythmic behaviour in RR. The defect in the s-LN_v dorsal termini persists as *Rho1* is still depleted, but its effect on the dorsal signalling is marginalised in this environment.

4.4 Future outcomes

New questions have arisen during the course of this project that provide hypotheses for future studies. As a final consideration of this project, the following future experimental objectives are proposed:

1. Characterization of the neuronal activity of the clock neurons in the presence of *Rho1* knockdown. As the state of the molecular clock cannot explain the characteristic arrhythmic behaviour of the *Rho1* phenotype, we hypothesized that this phenotype was attributable to defective intercellular communication and associated mis-regulation of neuronal activity. While electrophysiological studies of clock neurons are challenging and rarely performed outside of the l-LN_vs (Sheeba *et al.*, 2008b), there currently exist several imaging-based analyses of the neuronal state (Yao *et al.*, 2012). The published studies about PDF- and sNPF-signalling and their effect on Ca^{2+} currents across the clock circuit are of special interest for further characterising the Rho1 phenotype originating in the s-LN_vs (Liang, Holy and Taghert, 2016;2017). Voltage-dependent fluorescence is the basis of the ArcLight technique, which allows imaging of neuronal membrane potential in vivo and has been published for the s-LN_vs as proof of concept (Jin *et al.*, 2012; Cao *et al.*, 2013; Guo *et al.*, 2016).

2. Confirmation that *Rho1* knockdown cell-autonomously affects the adult s-LN_vs. The spatial and temporal mapping of the *Rho1* phenotype was challenging because of Rho1's essential function and has not yet included separate knockdown in s-LN_v versus l-LN_v neurons. However, additional expression tools are available that should make this possible. For example, the driver line *R78G01* specifically targets l-LN_vs, but not s-LN_vs (Yoshii *et al.*, 2015).

3. Study of the possible interactions between *Rho1* dosage and further signalling output from the s-LN_vs. Although the $Pdfr^{5304}$ mutant is epistatic to *Rho1* knockdown, it is likely that the blunting of the axonal remodelling rhythm disturbs other signals besides PDF (Gorostiza *et al.*, 2014; Beckwith and Ceriani, 2015). Alteration of the neurotransmitter-based feedback routes between the s-LN_vs and the dorsal clock neurons is expected to be affected in the context of the *Rho1* phenotype (Guo *et al.*, 2016; Frenkel *et al.*, 2017). It would also be possible to study connections between the s-LN_v dorsal termini and

downstream neurons via the GPF Reconstitution Across Synaptic Partners (GRASP) technique (Cavanaugh *et al.*, 2014; Gorostiza *et al.*, 2014). *Rho1* dosage could be manipulated in a spatiotemporally targeted manner (e.g., using GeneSwitch)(Nicholson *et al.*, 2008; Guo *et al.*, 2014) or for more convenient combination of genetic tools by chromosomal mutants (such as heterozygosity for the $Rho1^{1B}$ allele). Moreover, the phenotype could be further studied downstream of the s-LN_vs, by interrogating output routes of the affected clock clusters that correlate with behavioural phenotypes (Cavanaugh *et al.*, 2014; Frenkel *et al.*, 2017). Altogether, this will provide more information about the way that Rho1 deficits impact signalling downstream of the s-LN_vs.

4. In-depth analysis of the female molecular oscillators. As was shown in Chapter 3.4.2, the female control clock cells exhibited local differences in their Per rhythms relative to their male counterparts. We acknowledge that two time points are not enough resolution to characterise the molecular oscillator and that there is a relative lack of female *Drosophila* molecular clock studies in literature. Therefore, this constitutes an important question to address in order to gain better understanding of the gender contributions to circadian behaviour. The experiments suggested in the previous objectives could also find differences in the clock circuit (See Appendix B.3).

Appendix A : Supplementary results and tables for Chapter 3

A.1 Summary of locomotor assay results

Env	Genotype	G	N(c)	%SR•%WR•%AR	Tau ±SEM(hr)	RRP ±SEM
DD	w^{1118}; +/SM6B;	F	29(6)	59 •24 •17	24.25 ±0.07	1.69 ±0.08
	w^{1118}; +/Df(2R)ED2457;	F	26	15 •31•54**	24.00 ±0.39	1.36 ±0.11*
	w^{1118}; +/SM6B;	M	19	11•63•26	24.53 ±0.69	1.33 ±0.09
	w^{1118}; +/Df(2R)ED2457;	M	19	0•37•63*	24.93 ±0.64	1.17 ±0.07
	w^{1118}; +/CyO;	F	19(6)	47•32•21	24.13 ±0.10	1.78 ±0.12
	w^{1118}; +/$Rho1^{1B}$;	F	24	4•50•46**	23.54 ±0.73	1.22 ±0.06***
	w^{1118}; +/CyO;	M	11	64•36•0	24.05 ±0.13	1.57 ±0.09
	w^{1118}; +/$Rho1^{1B}$;	M	15	27•60•13	24.38 ±0.25	1.42 ±0.08
	w^{1118}/w^{1118}N; +/CyO;	F	9(1)	11•56•33	23.50 ±0.84	1.25 ±0.09
	w^{1118}/w^{1118}N; +/$Rho1^{E3.10}$;	F	16	25•25•50	23.94 ±0.11	1.58 ±0.10*
	w^{1118}; +/CyO;	M	9	78•22•0	23.61 ±0.11	1.82 ±0.14
	w^{1118}; +/$Rho1^{E3.10}$;	M	11	73•27•0	24.18 ±0.15**	1.83 ±0.14
RR	w^{1118}; +/CyO;	F	19(5)	58•21•21	24.43 ±0.10	1.76 ±0.11
	w^{1118}; +/$Rho1^{1B}$;	F	32	34•44•22†	23.70 ±0.49	1.69 ±0.13††
	w^{1118}; +/CyO;	M	10	70•20•10	23.94 ±0.13	1.81 ±0.14
	w^{1118}; +/$Rho1^{1B}$;	M	11	64•9•27†	24.00 ±0.13	1.87 ±0.12††

Summary Table 1. *Rho1* levels influence the adult circadian locomotor behaviour of the adult fly. Adult flies were entrained in LD for 6 days and transferred to DD or RR conditions at a constant temperature of 23 °C. *Free run* behaviour was analysed during 7 days, skipping the first day of transition to DD/RR as described in Methodology. **Env,** type of environment, DD or RR. **Genotype,** chromosome dotation of interest for the assay. **Gender**, female (F) or male (M) flies. **N(c)**, total number of involved flies (number of crosses/assays, applied for the four genotypes: experimental and isogenic control for both genders). **%SR•%WR•%AR**, percentage of flies classified as Strongly Rhythmic (SR), Weakly Rhythmic (WR) or Arrhythmic (AR). **Tau ±SEM**, mean Period Length (hours) ±Standard Error of the Mean (SEM). **RRP ±SEM**, mean Relative Rhythmic Power (no units) ±SEM. *p<0.05; **p<0.01 and ***p<0.001 by Fisher's Exact test (%SR•%WR•%AR) or Mann-Whitney *U* test (α= 0.05, Tau and RRP) while comparing the experimental genotype with the isogenic control. †p<0.05 and ††p<0.01 by Fisher's Exact test (%SR•%WR•%AR) or Mann-Whitney *U* test (α= 0.05, Tau and RRP) while comparing the same genotype among different environmental conditions.

Env	Genotype	G	N(c)	%SR•%WR•%AR	Tau ±SEM(hr)	RRP ±SEM
DD	*; CyO/+; UASdsRho1^{JF02809}/+*	F	57 (10)	28 •42•30	23.99 ±0.25‡‡	1.48 ±0.06
	; tim(UAS)-Gal4/+; UASdsRho1^{JF02809}/+	F	118	2•23•75***‡‡‡	23.91 ±0.86	1.15 ±0.04***‡‡‡
	; CyO/+; UASdsRho1^{JF02809}/+	M	34	44•41•15	23.65 ±0.13	1.53 ±0.07
	; tim(UAS)-Gal4/+; UASdsRho1^{JF02809}/+	M	19	0•37•63*	24.93 ±0.64	1.17 ±0.07
	; CyO/+; UASdsRho1^{HMS00375}/+	F	25 (3)	80•16•4	23.96 ±0.11	1.95 ±0.11
	; tim(UAS)-Gal4/+; UASdsRho1^{HMS00375}/+	F	50	26•28•46***	24.20 ±0.16	1.56 ±0.08*
	; CyO/+; UASdsRho1^{HMS00375}/+	M	21	71•29•0	23.52 ±0.09	1.81 ±0.11
	; tim(UAS)-Gal4/+; UASdsRho1^{HMS00375}/+	M	78	40•40•20*	24.81 ±0.20***	1.68 ±0.07
	; CyO/+; UASdsRho1$^{325-786}$/+	F	16 (2)	31•19•50	24.12 ±0.20	1.40 ±0.09
	; tim(UAS)-Gal4/+; UASdsRho1$^{325-786}$/+	F	23	13•0•87*	21± 1*	1.06 ±0.05*
	; CyO/+; UASdsRho1$^{325-786}$/+	M	11	46•45•9	24.8 ±0.81	1.57 ±0.11
	; tim(UAS)-Gal4/+; UASdsRho1$^{325-786}$/+	M	10	30•0•70**	28.5 ±3.12	1.11 ±0.05*
	; tim(UAS)-Gal4/CyO;	F	23 (3)	43•35•22	24.31 ±0.19	1.77 ±0.04
	; tim(UAS)-Gal4/UASdsRho1$^{770-1310}$;	F	40	0•15•85***	25.92 ±2.45	1.13 ±0.06**
	; tim(UAS)-Gal4/CyO;	M	12	33•50•17	24.75 ±0.28	1.53 ±0.10
	; tim(UAS)-Gal4/UASdsRho1$^{770-1310}$;	M	18	0•22•78***	27.37 ±1.28	1.06 ±0.04*
RR	*; CyO/+; UASdsRho1^{JF02809}*	F	15 (3)	73•20•7††	24.61 ±0.15†††	2.00 ±0.15††
	; tim(UAS)-Gal4/+; UASdsRho1^{JF02809}/+	F	43	28•51•21**†††	25.06 ±0.33††	1.51 ±0.07**†††
	; CyO/+; UASdsRho1^{JF02809}	M	16	88•6•6††	24.47 ±0.13††	2.00 ±0.1†††
	; tim(UAS)-Gal4/+; UASdsRho1^{JF02809}/+	M	28	86•11•3†††	24.22 ±0.08	2.24 ±0.1†††
	; tim(UAS)-Gal4/CyO;	F	12 (3)	92•0•8†	24.59 ±0.15	2.48 ±0.14††
	; tim(UAS)-Gal4/UASdsRho1$^{770-1310}$;	F	18	67•22•11†††	25.06 ±0.20	1.80 ±0.11**†††
	; tim(UAS)-Gal4/CyO;	M	25	95•5•0†††	24.5 ±0.21	2.44 ±0.12†††
	; tim(UAS)-Gal4/UASdsRho1$^{770-1310}$;	M	21	95•5•0†††	24.59 ±0.11	2.28 ±0.09†††

Summary Table 2. *Rho1* genetic knockdown inside the clock cells with diverse RNAi constructs.

Adult flies were entrained in LD for 6 days and transferred to DD or RR conditions at a constant temperature of 23 °C. *Free run* behaviour was analysed during 7 days, skipping the first day of transition to DD/RR as described in Methodology. **Env,** type of environment, DD or RR. **Genotype,** chromosome dotation of interest for the assay. All the flies carry a copy of the *UASdcr2w* construct in the X chromosome (homozygous for males). **G,** gender, female (F) or male (M) flies. **N(c)**, total number of involved flies (number of crosses/assays, applied for the four genotypes: experimental and isogenic control for both genders). **%SR•%WR•%AR**, percentage of flies classified as Strongly Rhythmic (SR), Weakly Rhythmic (WR) or Arrhythmic (AR). **Tau ±SEM**, mean Period Length (hours) ±Standard Error of the Mean (SEM). **RRP ±SEM**, mean Relative Rhythmic Power (no units) ±SEM. *p<0.05; **p<0.01 and ***p<0.001 by Fisher's Exact test (%SR•%WR•%AR) or Mann-Whitney *U* test (α= 0.05, Tau and RRP) while comparing the experimental genotype with the isogenic control. †p<0.05 and ††p<0.01 by Fisher's Exact test (%SR•%WR•%AR) or Mann-Whitney *U*

test (α= 0.05, Tau and RRP) while comparing the same genotype among different environmental conditions.

Genotype	G	N(c)	%SR•%WR•%AR	Tau ±SEM(hr)	RRP ±SEM
w^{1118}; CyO/+; UASRho1.Sph/	F	17 (4)	59•29•12	24.45 ±0.17	1.91 ±0.13
w^{1118}; tim(UAS)-Gal4/+; UASRho1.Sph/	F	30	20•43•37*	23.97 ±0.83**	1.40 ±0.09**
w^{1118}; CyO/+; UASRho1.Sph/	M	10	90•10•0	24 ±0.09	1.99 ±0.12
w^{1118}; tim(UAS)-Gal4/+; UASRho1.Sph/	M	19	56•39•5	23.64 ±0.07**	1.97 ±0.11
w^{1118}; CyO/+; UASRho1^{V14}(CAT)/	F	7(1)	100•0•0	23.71 ±0.18	2.26 ±0.17
w^{1118}; tim(UAS)-Gal4/+; UASRho1^{V14}(CAT)/	F	9	0•67•33***	24.08 ±1.41	1.11 ±0.05***
w^{1118}; CyO/+; UASRho1^{V14}(CAT)/	M	9	67•33•0	23.61 ±0.18	1.79 ±0.16
w^{1118}; tim(UAS)-Gal4/+; UASRho1^{V14}(CAT)/	M	12	42•33•25	23 ±0.17	1.67 ±0.18
w^{1118}; CyO/+; UASRho1^{N19}(DN)/	F	7(1)	57•14•29	23.5 ±0.16	1.79 ±0.17
w^{1118}; tim(UAS)-Gal4/+; UASRho1^{N19}(DN)/	F	10	20•60•20	23.69 ±0.21	1.39 ±0.08*
w^{1118}; CyO/+; UASRho1^{N19}(DN)/	M	3	34•66•0	24 ±0.5	1.78 ±0.51
w^{1118}; tim(UAS)-Gal4/+; UASRho1^{N19}(DN)/	M	10	70•30•0	23.4 ±0.39	1.81 ±0.13
w^{1118}; tim(UAS)-Gal4/Rho1^{1B}; UASRho1.Sph/	F	20 (4)	30•55•15*	24.62 ±0.13††	1.47 ±0.10†
w^{1118}; tim(UAS)-Gal4/Rho1^{1B}; UASRho1.Sph/	M	14	7•72•21$^{††‡‡###}$	24.22 ±0.21	1.30 ±0.06$^{†‡‡#}$

Summary Table 3. Expression of Rho1 isoforms inside the clock neurons. Adult flies were entrained in LD for 6 days and transferred to DD at a constant temperature of 23 °C. *Free run* behaviour was analysed during 7 days, skipping the first day of transition to DD as described in Methodology. **Genotype,** chromosome dotation of interest for the assay. All the flies carry the *UASDcr2w* (X) construct. **Gender**, female (F) or male (M) flies. **N**, total number of involved flies. **%SR•%WR•%AR**, percentage of flies classified as Strongly Rhythmic (SR), Weakly Rhythmic (WR) or Arrhythmic (AR). **Tau ±SEM**, mean Period Length (hours) ±Standard Error of the Mean (SEM). **RRP ±SEM**, mean Relative Rhythmic Power (no units) ±SEM. *p<0.05; **p<0.01 and ***p<0.001 by Fisher's Exact test (%SR•%WR•%AR) or Mann-Whitney *U* test (α= 0.05, Tau and RRP) against isogenic controls. For the *w^{1118}; tim(U)Gal4/Rho1^{1B}; UASRho1.Sph/* genotypes, symbols indicate differences against *w^{1118}; +/CyO* (†, found in Summary Table 1); *w^{1118}; Rho1^{1B}/CyO*; flies (*, found in Summary Table 1); *w^{1118}; CyO/+; UASRho1.Sph/* (‡, found in this table) and *w^{1118}; tim(U)Gal4/+; UASRho1.Sph/* (#, found in this table).

Temp	Genotype	G	N (c)	%SR•%WR•%AR	Tau ±SEM(hr)	RRP ±SEM
17 °C	*UASdcr2w; tubGal80^{TS}/CyO; UASdsRho1^{JF02809}/+*	F	26 **(4)**	27•54•19	23.52 ±0.08	1.40 ±0.06
	UASdcr2w; tubGal80^{TS}/tim(UAS)-Gal4; UASdsRho1^{JF02809}/+	F	33	27•61•12	23.51 ±0.30	1.45 ±0.06
	UASdcr2w; tubGal80^{TS}/CyO; UASdsRho1^{JF02809}/+	M	21	7•62•31	23.10 ±0.32	1.24 ±0.03
	UASdcr2w; tubGal80^{TS}/tim(UAS)-Gal4; UASdsRho1^{JF02809}/+	M	29	10•76•14	24.19 ±0.64	1.34 ±0.10
29 °C	*UASdcr2w; tubGal80^{TS}/CyO; UASdsRho1^{JF02809}/+*	F	37 **(7)**	54•24•22	23.78 ±0.07	1.69 ±0.08
	UASdcr2w; tubGal80^{TS}/tim(UAS)-Gal4; UASdsRho1^{JF02809}/+	F	52	21•33•46**	23.86 ±0.18	1.44 ±0.07*
	UASdcr2w; tubGal80^{TS}/CyO; UASdsRho1^{JF02809}/+	M	25	68•16•16	24.05 ±0.13	2.15 ±0.13
	UASdcr2w; tubGal80^{TS}/tim(UAS)-Gal4; UASdsRho1^{JF02809}/+	M	25	76•20•4	23.73 ±0.07	1.80 ±0.08*

Summary Table 4. Post-developmental *Rho1* knockdown inside the clock neurons. Flies were raised at 17 °C (*permissive* conditions with RNAi expression inhibited by *tubGal80^{TS}*) and entrained with 12:12 LD cycles. Adults were then transferred to DD remaining at 17 °C (top rows) or 29 °C (*restrictive* conditions, bottom rows) which allowed the RNAi expression. **Temp,** temperature in DD conditions. **Genotype,** chromosome dotation of interest for the assay. **G,** gender, female (F) or male (M) flies. **N(c)**, total number of involved flies (number of crosses/assays, applied for the four genotypes: experimental and isogenic control for both genders). **%SR•%WR•%AR**, percentage of flies classified as Strongly Rhythmic (SR), Weakly Rhythmic (WR) or Arrhythmic (AR). **Tau ±SEM**, mean Period Length (hours) ±Standard Error of the Mean (SEM). **RRP ±SEM**, mean Relative Rhythmic Power (no units) ±SEM. *p<0.05; **p<0.01 and ***p<0.001 by Fisher's Exact test (%SR•%WR•%AR) or Mann-Whitney *U* test (α= 0.05, Tau and RRP) while comparing the experimental genotype with the isogenic control.

Genotype	G	N(c)	%SR•%WR•%AR	Tau ±SEM(hr)	RRP ±SEM
; tim(UAS)-Gal4/CyO;	F	31 **(5)**	36 •35•29	24.20 ±0.45	1.50 ±0.08
; tim(UAS)-Gal4/CyO;	M	34	53•32•15	24.60 ±0.09	1.70 ±0.07
; RepoGal80/CyO; UASdsRho1^{JF02809}	F	16 **(1)**	44•19•37	23.65 ±0.11‡‡	1.73 ±0.12
; tim(UAS)-Gal4/RepoGal80; UASdsRho1^{JF02809}/+	F	15	0•7•93$^{‡‡‡###}$	34.5	1.01
; tim(UAS)-Gal4/CyO; UASdsRho1^{JF02809}/+	F	8	0•0•100$^{‡‡‡#}$	-	-
; RepoGal80/CyO; UASdsRho1^{JF02809}	M	13	46•39•15	23.50 ±0.58	1.58 ±0.14
; tim(UAS)-Gal4/RepoGal80; UASdsRho1^{JF02809}/+	M	6	0•67•33‡	25.25 ±0.92	1.13 ±0.03$^{‡‡‡#}$
; tim(UAS)-Gal4/CyO; UASdsRho1^{JF02809}/+	M	9	0•44•56$^{‡‡#}$	24.62 ±1.20	1.08 ±0.02$^{‡‡‡##}$
; PdfGal80/CyO; UASdsRho1^{JF02809}	F	12 **(3)**	50•42•8	23.77 ±0.18‡	1.61 ±0.12
; tim(UAS)-Gal4/ PdfGal80; UASdsRho1^{JF02809}/+	F	32	9 •44•47$^{‡##}$	24.41 ±0.55	1.37 ±0.09
; tim(UAS)-Gal4/CyO; UASdsRho1^{JF02809}/+	F	9	0•67•33$^{#}$	27.33 ±0.2.15	1.08 ±0.03$^{‡‡###*}$
; PdfGal80/CyO; UASdsRho1^{JF02809}	M	13	62•38•0	23.61 ±0.20‡‡‡	1.61 ±0.12
; tim(UAS)-Gal4/ PdfGal80; UASdsRho1^{JF02809}/+	M	37	32•46•16	23.76 ±0.09‡‡‡	1.65 ±0.09
; tim(UAS)-Gal4/CyO; UASdsRho1^{JF02809}/+	M	23	4•48•48$^{‡‡‡###***}$	24.67 ±0.64	1.22 ±0.05$^{‡‡‡###**}$
;; TM6B/UASdsRho1^{JF02809}	F	24 **(6)**	37•42•21	23.37 ±0.07	1.53 ±0.08
;; cry-Gal4-13/UASdsRho1^{JF02809}	F	46	13•43•44**	24.31 ±0.54	1.32 ±0.07*
;; TM6B/UASdsRho1^{JF02809}	M	40	38•42•20	24.06 ±0.42	1.62 ±0.08
;; cry-Gal4-13/UASdsRho1^{JF02809}	M	31	42•45•13	23.41 ±0.35	1.53 ±0.09

Summary Table 5. Spatial mapping of the *Rho1* knockdown (*JF02909*) phenotype. Adult flies were entrained in LD for 6 days and transferred to DD conditions at a constant temperature of 23 °C. *Free run* behaviour was analysed during 7 days, skipping the first day of transition to DD as described in Methodology. **Genotype,** chromosome dotation of interest for the assay. All the flies carry a copy of the *UASdcr2w* construct in the X chromosome (homozygous for males). **G,** gender, female (F) or male (M) flies. **N(c)**, total number of involved flies (number of crosses/assays, applied for the four genotypes: experimental and isogenic control for both genders). **%SR•%WR•%AR**, percentage of flies classified as Strongly Rhythmic (SR), Weakly Rhythmic (WR) or Arrhythmic (AR). **Tau ±SEM**, mean Period Length (hours) ±Standard Error of the Mean (SEM). **RRP ±SEM**, mean Relative Rhythmic Power (no units) ±SEM. *p<0.05; **p<0.01 and ***p<0.001 by Fisher's Exact test (%SR•%WR•%AR) or Mann-Whitney *U* test (α= 0.05, Tau and RRP) while comparing the experimental genotype against *tim(UAS)-Gal4* driver line (‡); Gal80 and RNAI construct line (#), and isogenic (controls or driver+Gal80 flies) genotypes (*)

Env	Genotype	G	N(c)	%SR•%WR•%AR	Tau ±SEM(hr)	RRP ±SEM
DD	*; CyO/+; UASdsRho1^{JF02809}/+*	F	43 (3)	56•32•12	23.68 ±0.10	1.74 ±0.08
	; Pdf-Gal4/CyO;	F	18	62•24•14	24.83 ±0.07**	1.79 ±0.12
	; Pdf-Gal4/+; UASdsRho1^{JF02809}/+	F	62	6•44•50***‡‡‡	24.61 ±0.27***‡‡‡	1.25 ±0.06***‡‡‡
	; CyO/+; UASdsRho1^{JF02809}/+	M	34	73•21•6	23.56 ±0.06	1.99 ±0.10
	; Pdf-Gal4/CyO;	M	16	75•25•0	24.59 ±0.12***	1.82 ±0.09
	; Pdf-Gal4/+; UASdsRho1^{JF02809}/+	M	47	49•43•9	23.94 ±0.21*‡‡‡	1.62 ±0.06*‡
	; Pdf-Gal4/CyO;	F	25 (2)	80•16•4	23.96 ±0.11	1.95 ±0.11
	; Pdf-Gal4/UASdsRho1$^{770-1310}$;	F	50	26•28•46***	24.20 ±0.16	1.56 ±0.08*
	; Pdf-Gal4/CyO;	M	21	71•29•0	23.52 ±0.09	1.81 ±0.11
	; Pdf-Gal4/UASdsRho1$^{770-1310}$;	M	78	40•40•20*	24.81 ±0.20***	1.68 ±0.07
RR	*; CyO; UASdsRho1^{JF02809}/+*	F	15 (3)	73•20•7††	24.61 ±0.15†††	2.00 ±0.15††
	; Pdf-Gal4/+; UASdsRho1^{JF02809}/+	F	43	28•51•21**†††	25.06 ±0.33††	1.51 ±0.07**†††
	; CyO; UASdsRho1^{JF02809}/+	M	16	88•6•6††	24.47 ±0.13††	2.00 ±0.1†††
	; Pdf-Gal4/+; UASdsRho1^{JF02809}/+	M	28	86•11•3†††	24.22 ±0.08	2.24 ±0.1†††

Summary Table 6. *Rho1* knockdown inside the PDF-expressing neurons. Adult flies were entrained in LD for 6 days and transferred to DD/ RR conditions at a constant temperature of 23 °C. *Free run* behaviour was analysed during 7 days, skipping the first day of transition to DD/RR as described in Methodology. **Env,** type of environment, DD or RR. **Genotype,** chromosome dotation of interest for the assay. All the flies carry the *UASDcr2w* (X) construct. **G,** gender, female (F) or male (M) flies. **N(c)**, total number of involved flies (number of crosses/assays, applied for the four genotypes: experimental and isogenic control for both genders). **%SR•%WR•%AR**, percentage of flies classified as Strongly Rhythmic (SR), Weakly Rhythmic (WR) or Arrhythmic (AR). **Tau ±SEM**, mean Period Length (hours) ±Standard Error of the Mean (SEM). **RRP ±SEM**, mean Relative Rhythmic Power (no units) ±SEM. *p<0.05; **p<0.01 and ***p<0.001 by Fisher's Exact test (%SR•%WR•%AR) or Mann-Whitney *U* test (α= 0.05, Tau and RRP) against isogenic controls (*), *Gal4* driver parental line (‡), or the given genotype in DD conditions (†).

Genotype	G	N(c)	%SR•%WR•%AR	Tau ±SEM(hr)	RRP ±SEM
w^{1118}; CyO/; UASdsRho1^{JF02809}/UASDcr2w	F	16**(2)**	25•56•19	23.81 ±0.32	1.31 ±0.06
w^{1118}; tim(UAS)-Gal4/; UASdsRho1^{JF02809}/UASDcr2w	F	45	0•18•82***	23.69 ±1.03	1.06 ±0.01***
Pdfr^{4304}; tim(UAS)-Gal4/CyO; UASDcr2w	F	37**(4)**	22•5•73†††	23.20 ±0.83	1.22 ±0.09
Pdfr^{4304}; tim(UAS)-Gal4/CyO; UASdsRho1^{JF02809}/UASDcr2w	F	26	15•12•73	23.07 ±0.66	1.48 ±0.17††
w^{1118}; CyO/; UASdsRho1^{JF02809}/UASDcr2w	M	24**(2)**	42•33•25	23.30 ±0.18	1.46 ±0.08
w^{1118}; tim(UAS)-Gal4/; UASdsRho1^{JF02809}/UASDcr2w	M	54	48•7•45***	23.57 ±0.42	1.23 ±0.04*
Pdfr^{4304}; tim(UAS)-Gal4/CyO; UASDcr2w	M	31**(4)**	36•16•48	23.56 ±0.14	1.36 ±0.07
Pdfr^{4304}; tim(UAS)-Gal4/CyO; UASdsRho1^{JF02809}/UASDcr2w	M	49	31•22•47†	22.79 ±0.46	1.41 ±0.07

Summary Table 7. Interaction between *Rho1* knockdown and the removal of PDF-signalling with the *Pdfr^{5304}* mutant. Adult flies were entrained in LD for 6 days and transferred to DD at a constant temperature of 23 °C. *Free run* behaviour was analysed during 7 days, skipping the first day of transition to DD as described in Methodology. **Genotype,** chromosome dotation of interest for the assay. **G**, gender, female (F) or male (M) flies. **N(c)**, total number of involved flies (number of crosses/assays, applied for the control and following experimental genotype). **%SR•%WR•%AR**, percentage of flies classified as Strongly Rhythmic (SR), Weakly Rhythmic (WR) or Arrhythmic (AR). **Tau ±SEM**, mean Period Length (hours) ±Standard Error of the Mean (SEM). **RRP ±SEM**, mean Relative Rhythmic Power (no units) ±SEM. *p<0.05; **p<0.01 and ***p<0.001 by Fisher's Exact Test (%SR•%WR•%AR) or Mann-Whitney *U* test (α= 0.05, Tau and RRP) against controls (*) or the genotypes in *Pdfr^{+}* background (†).

A.2 Supplementary data of locomotor assays

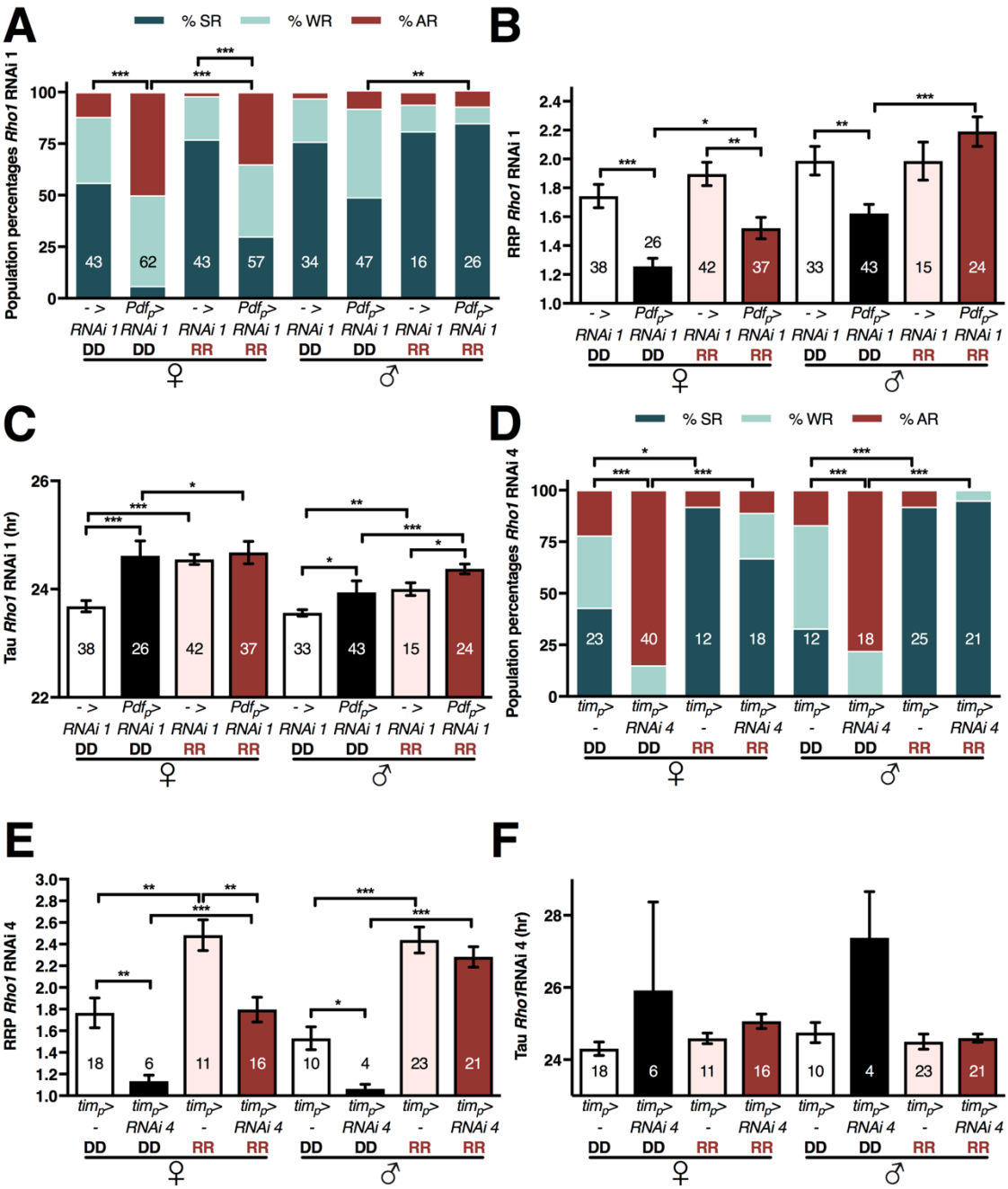

Supplementary Figure 1. Effects of red light on circadian locomotor activity of *Rho1*-deficit flies (additional genotypes). **A** and **D**) Distribution of frequencies (Strongly Rhythmic, SR; Weakly Rhythmic, WR or Arrhythmic, AR) for flies expressing the *Rho1* RNAi 1 inside the PDF$^+$ cells (A) or expressing the *Rho1* RNAi 4 inside the clock cells (D), as well as isogenic controls. **B** and **E)** Relative Rhythmic Power (RRP) of SR and WR flies for flies expressing the *Rho1* RNAi 1 inside the PDF$^+$ cells (B) or expressing the *Rho1* RNAi 4 inside the clock cells (E), as well as isogenic controls. **C** and **F)** Period Length (Tau) of SR and WR flies for flies expressing the *Rho1* RNAi 1 inside the PDF$^+$ cells (C) or expressing the *Rho1* RNAi 4 inside

the clock cells (F), as well as isogenic controls. Data from genotypes in DD was previously presented in Chapter 3.3.1 and 3.3.4 and repeated here for better comparison. Bars represent Mean ±SEM and numbers in bars indicate *n*, with the total number of flies originated from 3 (*JF02809* in DD), 3 (*JF02809* in RR), 3 (*Rho1.770-1310* in DD) and 3 (*Rho1.770-1310* in RR) crosses. For population percentages panels (A, D), *p<0.05; **p<0.01 and **p<0.001 by Fisher's Exact test. For RRP (B, E) and Tau (C) panels, *p<0.05; **P<0.01 and ***p<0.001 by Mann-Whitney *U* test (α= 0.05). No differences were found for Tau with expression of the RNAi 4.

Genotype	G	N(c)	%SR•%WR•%AR	Tau ±SEM(hr)	RRP ±SEM
; CyO/UASdsRok$^{9774R-3}$;	F	11(1)	18 •27 •55	24.60 ±0.29	1.81 ±0.10
; tim(UAS)-Gal4/UASdsRok$^{9774R-3}$;	F	48	48•40•12**	24.36 ±0.11	1.51 ±0.15
; CyO/UASdsRok$^{9774R-3}$;	M	7	43•29•28	24.6 ± 0.29	1.65 ±0.23
; tim(UAS)-Gal4/UASdsRok$^{9774R-3}$;	M	24	59•33•8	24.73 ±0.11	1.73 ±0.10
; CyO/; UASdsRok$^{9774R-2}$/	F	6(1)	17•50•33	24.37 ±0.12	1.41 ±0.09
; tim(UAS)-Gal4/; UASdsRok$^{9774R-2}$/	F	43	46•49•5	23.95 ±0.23	1.51 ±0.06
; CyO/; UASdsRok$^{9774R-2}$/	M	8	63•37•0	23.56 ±0.81	1.69 ±0.19
; tim(UAS)-Gal4/; UASdsRok$^{9774R-2}$/	M	23	78•22•0	24.59 ±0.11	1.93 ±0.09
; CyO/; UASdsWasp^{JF01975}/	F	14(1)	78•22•0	23.38 ±0.08	1.90 ±0.09
; tim(UAS)-Gal4/; UASdsWasp^{JF01975}/	F	18	0•43•57***	25.08 ±1.47	1.13 ±0.05***
; CyO/; UASdsWasp^{JF01975}/	M	12	66•33•0	23.12 ±0.14	1.72 ±0.14
; tim(UAS)-Gal4/; UASdsWasp^{JF01975}/	M	5	0•40•60**	20.50 ±3	1.13 ±0.01
; CyO/UASdsWasp^{HMS01534};	F	14(1)	14•36•50	23.43 ±0.38	1.44 ±0.16
; tim(UAS)-Gal4/UASdsWasp^{HMS01534};	F	25	12•48•40	23.57±0.30	1.33 ±0.10
; CyO/UASdsWasp^{HMS01534};	M	12	50•50•0	23.42 ±0.15	1.70 ±0.16
; tim(UAS)-Gal4/UASdsWasp^{HMS01534};	M	18	50•44•6	23.68 ±0.21	1.52 ±0.11
; CyO/; UASdsPbl^{GL01092}/	F	16(2)	44•50•6	24.93 ±1.51	1.70 ±0.13
; tim(UAS)-Gal4/; UASdsPbl^{GL01092}/	F	24	63•33•4	24.15 ±0.13**	1.71 ±0.13
; CyO/; UASdsPbl^{GL01092}/	M	10	90•10•0	23.65 ±0.11	2.32 ±0.20
; tim(UAS)-Gal4/; UASdsPbl^{GL01092}/	M	32	81•19•0	24.46 ±0.07***	2.02 ±0.08
; CyO/; UASdschic^{HMS00550}/	F	5(1)	80•20•0	24.20 ±0.37	1.97 ±0.24
; tim(UAS)-Gal4/; UASdschic^{HMS00550}/	F	22	37•36•27	23.65 ±0.11	1.60 ±0.11
; CyO/; UASdschic^{HMS00550}/	M	7	43•57•0	23.71 ±0.15	1.73 ±0.17
; tim(UAS)-Gal4/; UASdschic^{HMS00550}/	M	23	83•17•0	24.35 ±0.09**	1.93 ±0.08
; CyO/; UASdsRhoGEF2^{JF01747}/	F	15(1)	93•7•0	23.63 ±0.06	2.40 ±0.16
; tim(UAS)-Gal4/; UASdsRhoGEF2^{JF01747}/	F	29	55•35•10*	23.02 ±0.10***	1.72 ±0.09***
; CyO/; UASdsRhoGEF2^{JF01747}/	M	9	56•33•11	23.50 ±0.16	1.70 ±0.21
; tim(UAS)-Gal4/; UASdsRhoGEF2^{JF01747}/	M	30	74•23•3	23.38 ±0.08	1.86 ±0.09
; CyO/UASdsRhoGEF2$^{9635R-3}$;	F	14(1)	36•36•28	23.90 ±0.12	1.66 ±0.12
; tim(UAS)-Gal4/UASdsRhoGEF2$^{9635R-3}$;	F	42	0•48•52***	27.27 ±0.85***	1.17 ±0.03***
; CyO/UASdsRhoGEF2$^{9635R-3}$;	M	10	90•0•10	24.28 ±0.14	1.92 ±0.10
; tim(UAS)-Gal4/UASdsRhoGEF2$^{9635R-3}$;	M	45	18•62•20***	28.15 ±0.45***	1.32 ±0.04***
; tim(UAS)-Gal4/; TM6B/	F	3(1)	66•33•0	24.67 ±0.33	1.71 ±0.26
; tim(UAS)-Gal4/; UASdsPdf^{JF01820}/	F	11	9•27•64*	24.75 ±1.27	1.33 ±0.21
; tim(UAS)-Gal4/; TM6B/	M	3	34•33•33	23 ±1	1.35 ±0.27
; tim(UAS)-Gal4/; UASdsPdf^{JF01820}/	M	12	17•50•33	24.25 ±0.19	1.34 ±0.14
; tim(UAS)-Gal4/; UASdsRho1^{JF02809}/cryGal80	F	50(5)	14•38•48	23.92 ±0.53	1.37 ±0.07
; tim(UAS)-Gal4/; UASdsRho1^{JF02809}/TM6B	F	15	0•27•73	22.12 ±1.21	1.27 ±0.09
; tim(UAS)-Gal4/; UASdsRho1^{JF02809}/cryGal80	M	42	28•48•24	23.53 ±0.39	1.46 ±0.07
; tim(UAS)-Gal4/; UASdsRho1^{JF02809}/TM6B	M	9	0•67•33	25.17 ±1.70	1.17 ±0.04*
; tim(UAS)-Gal4/; TM6B/Pdf^{01}	F	34(3)	76•15•9	24.90 ±0.11	2.01 ±0.09
; tim(UAS)-Gal4/; UASdsRho1^{JF02809}/ Pdf^{01}	F	14	7•29•64***	23.3 ±0.46***	1.25 ±0.12***
; tim(UAS)-Gal4/; TM6B/Pdf^{01}	M	20	80•20•0	24.2 ±0.99	2.01 ±0.12
; tim(UAS)-Gal4/; UASdsRho1^{JF02809}/ Pdf^{01}	M	20	15•40•45***	24.59 ±0.77***	1.34 ±0.12**

Supplementary Table 1. Supplementary data for RNAi knockdowns inside the clock cells. Adult flies were entrained in LD for 6 days and transferred to DD at a constant temperature of 23 ˚C. *Free run* behaviour was analysed during 7 days, skipping the first day of transition to DD as described in Methodology. **Genotype,** chromosome dotation of interest for the assay. All the flies carry the *UASdcr2w* (X) construct, heterozygous for females. **G**, gender, female (F) or male (M) flies. **N(c)**, total number of involved flies (number of crosses/assays, applied for the four genotypes: experimental and isogenic control for both genders). **%SR•%WR•%AR**, percentage of flies classified as Strongly Rhythmic (SR), Weakly Rhythmic (WR) or Arrhythmic (AR). **Tau ±SEM**, mean Period Length (hours) ±Standard Error of the Mean (SEM). **RRP ±SEM**, mean Relative Rhythmic Power (no units) ±SEM. *p<0.05; **p<0.01 and ***p<0.001 by Fisher's Exact Test (%SR•%WR•%AR) or Mann-Whitney *U* test (α= 0.05, Tau and RRP) against isogenic controls.

Genotype	G	N(c)	%SR•%WR•%AR	Tau ±SEM(hr)	RRP ±SEM
; CyO/; UASdsRho1^{JF02809}/ UAStub::GFP	F	23(3)	61•26•13	24.45 ±0.17	1.91 ±0.13
UASdcr2w; Pdf-Gal4/CyO; UAStub::GFP/	F	26	23•39•38*	23.97 ±0.83**	1.40 ±0.09**
; CyO/; UASdsRho1^{JF02809}/ UAStub::GFP	M	21	70•23•7	24.00 ±0.09	1.99 ±0.12
UASdcr2w; Pdf-Gal4/CyO; UAStub::GFP/	M	30	67•24•9	23.64 ±0.07**	1.97 ±0.11
; CyO/UASdsRok$^{9774R-3}$; UAStub::GFP/	F	4(2)	100•0•0	24.25 ±0.43	1.89 ±0.13
; Pdf-Gal4/UASdsRok$^{9774R-3}$; UAStub::GFP/	F	20	15•50•35**	25.04 ±0.68	1.33 ±0.08**
; Cy0/UASdsRok$^{9774R-3}$; UAStub::GFP/	M	2	100•0•0	24 ±0.00	1.76 ±0.28
; Pdf-Gal4/UASdsRok$^{9774R-3}$; UAStub::GFP/	M	8	56•44•0	24.42 ±0.15	1.55 ±0.10
; CyO/; UASdsRok$^{9774R-2}$/ UAStub::GFP	F	4(3)	100•0•0	23.62 ±0.37	1.80 ±0.13
; Pdf-Gal4/; UASdsRok$^{9774R-2}$/ UAStub::GFP	F	16	38•37•25	25.16 ±0.59*	1.56 ±0.08
; CyO/; UASdsRok$^{9774R-2}$/ UAStub::GFP	M	3	100•0•0	23.83 ±0.17	1.88 ±0.11
; Pdf-Gal4/; UASdsRok$^{9774R-2}$/ UAStub::GFP	M	9	56•44•0	24.22 ±0.12	1.76 ±0.15
; CyO/UASdsRhoGEF2$^{9635R-3}$; UAStub::GFP/	F	14(2)	29•57•14	24.29 ±0.14	1.44 ±0.11
; Pdf-Gal4/UASdsRhoGEF2$^{9635R-3}$; UAStub::GFP/	F	19	0•21•79***	23.87 ±2.70	1.04 ±0.01*
; CyO/UASdsRhoGEF2$^{9635R-3}$; UAStub::GFP/	M	9	56•33•11	23.94 ±0.17	1.74 ±0.14
; Pdf-Gal4/UASdsRhoGEF2$^{9635R-3}$; UAStub::GFP/	M	19	5•53•42**	25.32 ±0.91	1.09 ±0.04***

Supplementary Table 2. Supplementary data for RNAi knockdowns inside the PDF-expressing cells. Adult flies were entrained in LD for 6 days and transferred to DD at a constant temperature of 23 °C. *Free run* behaviour was analysed during 7 days, skipping the first day of transition to DD as described in Methodology. **Genotype,** chromosome dotation of interest for the assay. All the flies carry the *UASdcr2w* (X) construct, heterozygous for females. **G**, gender, female (F) or male (M) flies. **N(c)**, total number of involved flies (number of crosses/assays, applied for the four genotypes: experimental and isogenic control for both genders). **%SR•%WR•%AR**, percentage of flies classified as Strongly Rhythmic (SR), Weakly Rhythmic (WR) or Arrhythmic (AR). **Tau ±SEM**, mean Period Length (hours) ±Standard Error of the Mean (SEM). **RRP ±SEM**, mean Relative Rhythmic Power (no units) ±SEM. *p<0.05; **p<0.01 and ***p<0.001 by Fisher's Exact Test (%SR•%WR•%AR) or Mann-Whitney *U* test (α= 0.05, Tau and RRP) against isogenic controls.

Genotype	G	N(c)	%SR•%WR•%AR	Tau ±SEM(hr)	RRP ±SEM
; CyO/; UASdsRho1^{JF02809}/;	F	16(1)	69•25•6	24.17 ±0.06	1.88 ±0.15
; Pdf-Gal4/CyO; UASdsRho1^{JF02809}/;	F	17	20•53•27*	24.5 ±0.33	1.39 ±0.08*
; CyO/; R54D11-Gal4/UASdsRho1^{JF02809};	F	17	35•35•30	23.54 ± 0.13***	1.70 ±0.19
; CyO/; R78G02-Gal4/UASdsRho1^{JF02809};	F	11	9•55•36**	24.07 ±0.25	1.32 ±0.16*
; CyO/; UASdsRho1^{JF02809}/;	M	13	69•31•0	24.19 ±0.09	1.57 ±0.07
; Pdf-Gal4/CyO; UASdsRho1^{JF02809}/;	M	11	27•46•27*	23.56 ±0.22	1.51 ±0.13
; CyO/; R54D11-Gal4/UASdsRho1^{JF02809};	M	16	69•18•12	23.61 ±0.12	1.92 ±0.13*
; CyO/; R78G02-Gal4/UASdsRho1^{JF02809};	M	1	0•100•0	25.5 ±0	1.00 ±0

Supplementary Table 3. Supplementary data for expression of the *JF02809* construct in additional drivers. Adult flies were entrained in LD for 6 days and transferred to DD at a constant temperature of 23 °C. *Free run* behaviour was analysed during 7 days, skipping the first day of transition to DD as described in Methodology. **Genotype,** chromosome dotation of interest for the assay. All the flies carry the *UASdcr2w* (X) construct, heterozygous for females. **G**, gender, female (F) or male (M) flies. **N(c)**, total number of involved flies (number of crosses/assays, applied for the four genotypes: experimental and isogenic control for both genders). **%SR•%WR•%AR**, percentage of flies classified as Strongly Rhythmic (SR), Weakly Rhythmic (WR) or Arrhythmic (AR). **Tau ±SEM**, mean Period Length (hours) ±Standard Error of the Mean (SEM). **RRP ±SEM**, mean Relative Rhythmic Power (no units) ±SEM. *p<0.05; **p<0.01 and ***p<0.001 by Fisher's Exact Test (%SR•%WR•%AR) or Mann-Whitney *U* test (α= 0.05, Tau and RRP) against progeny from the control cross (*Berlin K* flies).

Genotype	G	N(c)	%SR•%WR•%AR	Tau ±SEM(hr)	RRP ±SEM
UASdcr2w/; CyO/; UASLuc/	F	24 (1)	67•25•8	23.59 ±0.29	2.21 ±0.15
UASdcr2w/; tim(UAS)-Gal4/; UASLuc/	F	23	57•35•8	23.19 ±0.06	1.76 ±0.11*
UASdcr2w; CyO/; UASLuc/	M	11	64•27•9	23.35 ±0.18	2.16 ±0.11
UASdcr2w; tim(UAS)-Gal4/; UASLuc/	M	28	86•11•3	23.56 ±0.07	1.72 ±0.13*
UASdcr2w/; CyO/; UASRhoGEF2$^{\Delta PDZ}$/	F	18 (3)	94•6•0	24.11 ±0.12	1.94 ±0.09
UASdcr2w/; tim(UAS)-Gal4/; UASRhoGEF2$^{\Delta PDZ}$/	F	29	83•17•0	23.60 ±0.11**	1.95 ±0.08
UASdcr2w; CyO/; UASRhoGEF2$^{\Delta PDZ}$/	M	31	68•32•0	24.04 ±0.31	2.16 ±0.11
UASdcr2w; tim(UAS)-Gal4/; UASRhoGEF2$^{\Delta PDZ}$/	M	14	86•14•0	24.16 ±0.06**	1.91 ±0.11
UASdcr2w/; CyO/; UASWasp/	F	15 (1)	93•7•0	23.4 ±0.05	2.36 ±0.14
UASdcr2w/; tim(UAS)-Gal4/; UASWasp/	F	29	41•28•31	24.05 ±0.17*	1.74 ±0.12**
UASdcr2w; CyO/; UASWasp/	M	14	93•7•0	23.64 ±0.06	2.41 ±0.12
UASdcr2w; tim(UAS)-Gal4/; UASWasp/	M	21	90•10•0	24.17 ±0.14**	2.31 ±0.11
UASdcr2w; tim(UAS)-Gal4; UASmCD8::GFP	F	45 (6)	7•47•46	24.40 ±0.81	1.18 ±0.04
UASdcr2w/; CyO/; UASdsRho1^{JF02809}/UASmCD8::GFP	F	16	0•50•50	24.06 ±0.48	1.18 ±0.05
UASdcr2w/; tim(UAS)-Gal4/; UASdsRho1^{JF02809}/UASmCD8::GFP	F	63	0•41•59	23.86 ±1.03	1.10 ±0.02
UASdcr2w; tim(UAS)-Gal4; UASmCD8::GFP	M	32	38•56•6	23.92 ±0.33	1.58 ±0.09
UASdcr2w; CyO/; UASdsRho1^{JF02809}/UASmCD8::GFP	M	7	29•57•14	23.67 ±0.17	1.49 ±0.11
UASdcr2w; tim(UAS)-Gal4/; UASdsRho1^{JF02809}/UASmCD8::GFP	M	61	00•44•56‡‡‡**	25.07 ±0.98	1.10 ±0.01 ‡‡‡***
UASdcr2w; tim(U)Gal4/UASRok.CAT;	F	17 (1)	88•6•6	24.69± 0.10	2.13 ±0.08
UASdcr2w/; CyO/UASRok.CAT; UASdsRho1^{JF02809}/	F	9	67•22•11	23.94 ±0.37‡	2.18 ±0.23
UASdcr2w/; tim(UAS)-Gal4/UASRok.CAT; UASdsRho1^{JF02809}/	F	29	7•31•62 ‡‡‡***	25.04 ±1.16	1.28 ±0.10 ‡‡‡**
UASdcr2w; tim(UAS)-Gal4/UASRok.CAT;	M	8	88•12•0	24.25 ±0.09	2.19 ±0.19
UASdcr2w/; CyO/UASRok.CAT; UASdsRho1^{JF02809}/	M	11	73•27•0	23.41 ±0.13‡‡	2.20 ±0.25
UASdcr2w/; tim(UAS)-Gal4/UASRok.CAT; UASdsRho1^{JF02809}/	M	30	40•37•23	24.41 ±0.44**	1.63 ±0.11‡

Supplementary Table 4. Additional locomotor assays involving ectopic expression inside the clock cells. Adult flies were entrained in LD for 6 days and transferred to DD conditions at a constant temperature of 23 °C. *Free run* behaviour was analysed during 7 days, skipping the first day of transition to DD as described in Methodology. **Genotype,** chromosome dotation of interest for the assay. **G (gender)**, female (F) or male (M) flies. **N(c)**, total number of involved flies (number of crosses/assays, applied for the four genotypes: experimental and isogenic control for both genders). **%SR•%WR•%AR**, percentage of flies classified as

Strongly Rhythmic (SR), Weakly Rhythmic (WR) or Arrhythmic (AR). **Tau ±SEM**, mean Period Length (hours) ±Standard Error of the Mean (SEM). **RRP ±SEM**, mean Relative Rhythmic Power (no units) ±SEM. *p<0.05; **p<0.01 and ***p<0.001 by Fisher's Exact test (%SR•%WR•%AR) or Mann-Whitney *U* test (α= 0.05, Tau and RRP) while comparing the experimental genotype against isogenic controls (*) and driver parental line *(JF02809+mCD8::GFP* and *Rok^{CAT}+JF02809* assays) (‡).

A.3 Supplementary data for molecular clock analysis in the *Rho1* knockdown

Cluster	G	Time	Genotype	N	αPer ±SEM	%N•%CN•%A
s-LN$_v$s	F	CT02	*tim(UAS)-Gal4;*	29	2.08 ±0.20	86•0•14
			tim(UAS)-Gal4; UASdsRho1^{JF02809}	66	2.65 ±0.28	94•0•6
		CT14	*tim(UAS)-Gal4;*	48	0.60 ±0.07$^{\#\#\#}$	17•8•75$^{\#\#\#}$
			tim(UAS)-Gal4; UASdsRho1^{JF02809}	90	0.39 ±0.04$^{*\#\#\#}$	14•0•86$^{*\#\#\#}$
	M	CT02	*tim(UAS)-Gal4;*	77	2.91 ±0.19	96•1•3
			tim(UAS)-Gal4; UASdsRho1^{JF02809}	53	3.42 ±0.27	87•0•13*
		CT14	*tim(UAS)-Gal4;*	34	0.72 ±0.13$^{\#\#\#}$	12•3•85$^{\#\#\#}$
			tim(UAS)-Gal4; UASdsRho1^{JF02809}	99	0.43 ±0.04$^{\#\#\#}$	30•3•67$^{\#\#\#}$
l-LN$_v$s	F	CT02	*tim(UAS)-Gal4;*	19	1.45 ±0.14	89•11•0
			tim(UAS)-Gal4; UASdsRho1^{JF02809}	66	1.91 ±0.22	92•0•8*
		CT14	*tim(UAS)-Gal4;*	32	1.25 ±0.15	62•0•38$^{\#\#\#}$
			tim(UAS)-Gal4; UASdsRho1^{JF02809}	69	0.51 ±0.05$^{***\#\#\#}$	33•2•65$^{*\#\#\#}$
	M	CT02	*tim(UAS)-Gal4;*	34	1.66 ±0.14	100•0•0
			tim(UAS)-Gal4; UASdsRho1^{JF02809}	30	1.66 ±0.20	80•0•20**
		CT14	*tim(UAS)-Gal4;*	32	0.96 ±0.11$^{\#\#\#}$	47•0•53$^{\#\#\#}$
			tim(UAS)-Gal4; UASdsRho1^{JF02809}	65	0.47 ±0.04$^{***\#\#\#}$	46•0•54$^{\#\#}$
LN$_d$s	F	CT02	*tim(UAS)-Gal4;*	26	2.37 ±0.33	100•0•0
			tim(UAS)-Gal4; UASdsRho1^{JF02809}	77	2.49 ±0.18	94•1•5
		CT14	*tim(UAS)-Gal4;*	25	1.42 ±0.15$^{\#}$	64•16•20$^{\#\#\#}$
			tim(UAS)-Gal4; UASdsRho1^{JF02809}	84	0.38 ±0.04$^{***\#\#\#}$	23•0•77$^{***\#\#\#}$
	M	CT02	*tim(UAS)-Gal4;*	50	3.88 ±0.19	100•0•0
			tim(UAS)-Gal4; UASdsRho1^{JF02809}	58	3.85 ±0.19	95•3•2
		CT14	*tim(UAS)-Gal4;*	11	0.14 ±0.03$^{\#\#\#}$	0•0•100$^{\#\#\#}$
			tim(UAS)-Gal4; UASdsRho1^{JF02809}	84	0.60 ±0.05$^{***\#\#\#}$	32•7•61$^{*\#\#\#}$
DN$_1$s	F	CT02	*tim(UAS)-Gal4;*	80	2.28 ±0.17	94•5•1
			tim(UAS)-Gal4; UASdsRho1^{JF02809}	140	1.47 ±0.10***	93•0•7**
		CT14	*tim(UAS)-Gal4;*	57	1.74 ±0.14	47•30•23$^{\#\#\#}$
			tim(UAS)-Gal4; UASdsRho1^{JF02809}	153	1.28 ±0.12$^{***\#\#\#}$	47•3•50$^{***\#\#\#}$
	M	CT02	*tim(UAS)-Gal4;*	81	2.39 ±0.17	91•0•9
			tim(UAS)-Gal4; UASdsRho1^{JF02809}	70	2.47 ±0.14	91•0•9

		CT14	*tim(UAS)-Gal4;*	31	0.42 ±0.11$^{\#\#\#}$	3•0•97$^{\#\#\#}$
			tim(UAS)-Gal4; UASdsRho1^{JF02809}	136	0.35 ±0.03$^{\#\#\#}$	21•1•78$^{\#\#\#}$
DN_2s	F	CT02	*tim(UAS)-Gal4;*	8	1.29 ±0.14	100•0•0
			tim(UAS)-Gal4; UASdsRho1^{JF02809}	19	1.23 ±0.19	89•0•11
		CT14	*tim(UAS)-Gal4;*	8	1.04 ±0.07	75•0•25
			tim(UAS)-Gal4; UASdsRho1^{JF02809}	23	0.48 ±0.11$^{*\#\#}$	48•0•52$^{\#\#}$
	M	CT02	*tim(UAS)-Gal4;*	3	2.02 ±0.34	100•0•0
			tim(UAS)-Gal4; UASdsRho1^{JF02809}	6	2.14 ±0.76	67•0•33
		CT14	*tim(UAS)-Gal4;*	4	0 ±0	0•0•100$^{\#}$
			tim(UAS)-Gal4; UASdsRho1^{JF02809}	21	0.12 ±0.03$^{\#\#}$	10•0•90$^{\#}$

Supplementary Table 5. Quantification of Per antibody signal inside the clock cells. Adult flies were entrained in 12:12 LD cycles and transferred to DD at a constant temperature of 23 °C. Brain dissections were performed on the second day under these conditions. **G,** Gender, female (F) or male (M) flies. **Time,** CT02 (26 hours after transition to DD) OR CT14 (38 hours after transition to DD). **Genotype,** chromosome dotation of interest for the assay. All the assayed genotypes carry *UASDcr2w* (X) and *UASCD8::mGFP* (III) constructs. **N**, total number of involved brains per gender/time point/genotype. **αPer ±SEM,** mean background-corrected quantified signal for Per antibody ±Standard Error of the Mean (SEM). **%N•%CN•%A,** percentage of clock cells classified based on Per localization as Nuclear (N), Cytoplasmic or nuclear-cytoplasmic (CN) or Absent (A). *p<0.05 and ***p<0.001 by Mann-Whitney *U* test (α= 0.05) or Fisher's Exact test (%N•%CN•%A) against driver-only controls (*) or complementary time point for the same genotype (#).

A.4 Supplementary and summary data for experiments on LD cycles

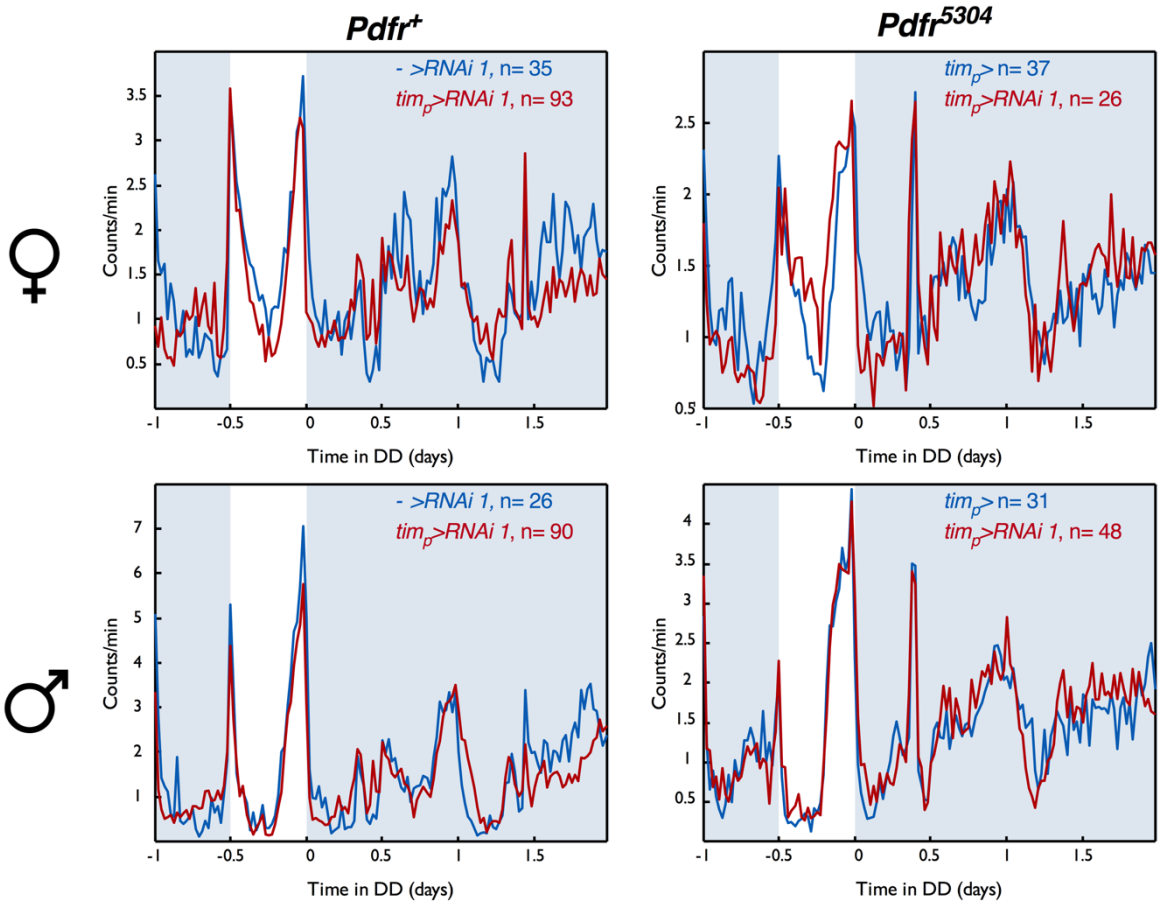

Supplementary Figure 2. Activity of flies expressing the *Rho1* RNAi (*JF02809*) in the *Pdfr*$^{+}$ and the *Pdfr*^{5304} backgrounds. The time series depict the average activity in the last day in LD conditions (constant temperature of 23 °C and the first two days in DD, with a bin size of 30 minutes. Columns indicate the genetic background of the *Pdfr* gene, and rows female (top) and male (bottom) populations. White background, light phase; grey blue background, dark phase. The subjective *lights-on* correspond to the time 0.5 in the graphs. The *Pdfr*$^{+}$ populations correspond to the flies firstly assayed in DD in Chapter 3.2.

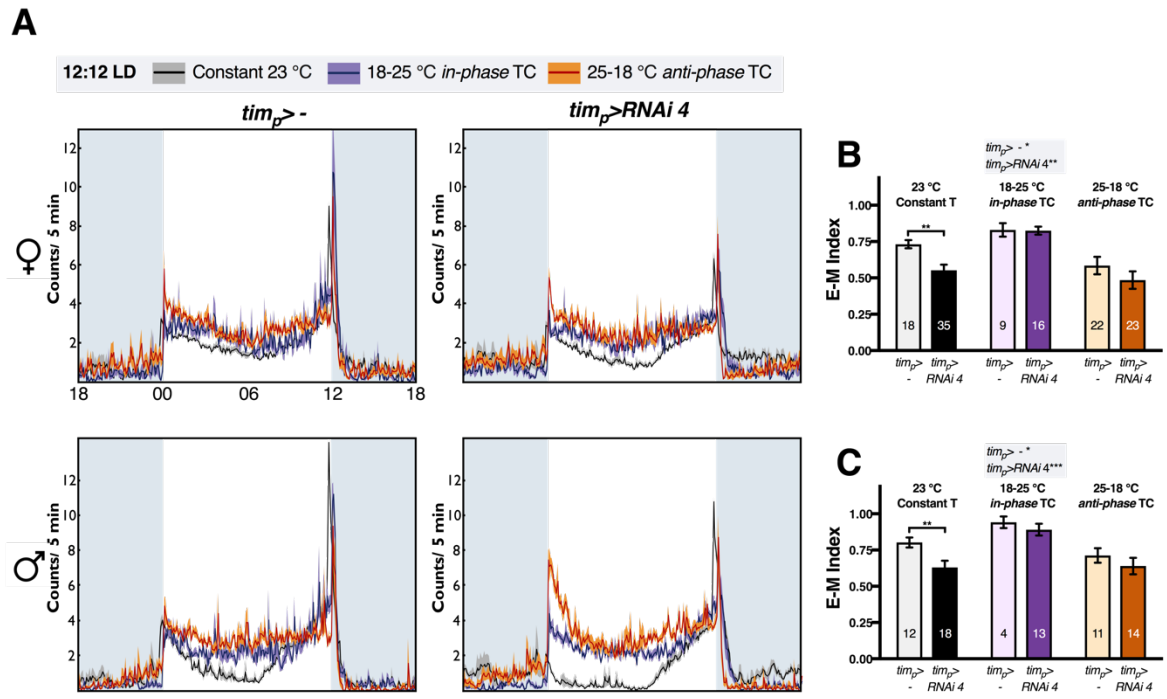

Supplementary Figure 3. Behavioural impact of reduced *Rho1* levels inside the clock cells (*Rho1.770-1310* construct) under different light and temperature interactions. A) Female (top row) and male (bottom row) population average activity profiles over the course of 6 days facing the given environmental conditions (grey, 12:12 LD at constant 23 °C; purple, 12:12 LD with *in-phase* 18-25 °C temperature cycle; and orange, 12:12 LD with *anti-phase* 25-18 °C temperature cycle). Activities profiles display counts per each 5-min bin (Mean ±SEM) with *lights-on* event occurring at ZT00 and *lights-off* event at ZT12. White background, light phase; grey blue background, dark phase. Arrows indicate increased morning anticipatory activity in the given genotypes and environments. **B** and **C**). Quantification (Mean ±SEM) of Evening-Morning Index (E-M Index) as explained in Material and Methods for females (B) and males (C) at the different environments. Bars represent Mean ±SEM and numbers in bars indicate *n*, with the total number of flies originated from 3 (*770-1310* in 12:12 LD at 23 °C), 2 (*770-1310* in 12:12 LD with *in-phase* 18-25 °C temperature cycle) and 2 (*770-1310* in 12:12 LD with *anti-phase* 25-18 °C temperature cycle) crosses. *p<0.05; **p<0.01 and ***p<0.001 by Mann-Whitney *U* test (α= 0.05, comparisons among genotypes) or Kruskal-Wallis test (α= 0.05, comparisons for a given genotypes across the three different environments, shown in the legend).

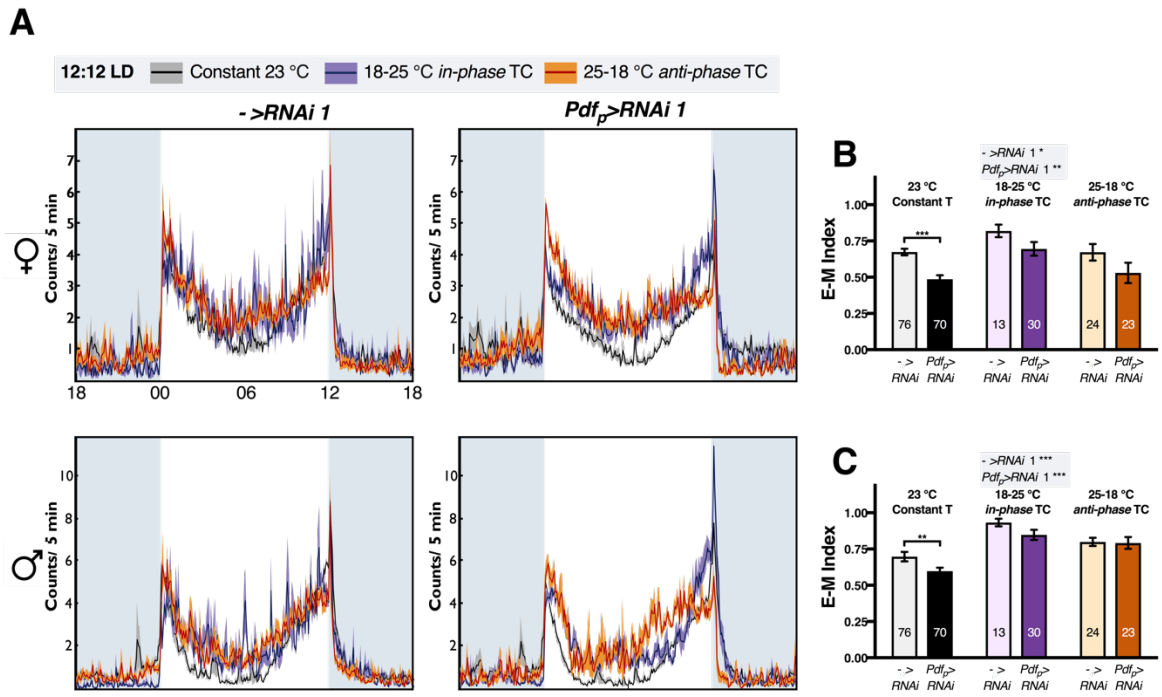

Supplementary Figure 4. Behavioural impact of reduced *Rho1* levels inside the PDF neurons (*JF02809* construct) under different light and temperature interactions. A) Female (top row) and male (bottom row) population average activity profiles over the course of 6 days facing the given environmental conditions (grey, 12:12 LD at constant 23 °C; purple, 12:12 LD with *in-phase* 18-25 °C temperature cycle; and orange, 12:12 LD with *anti-phase* 25-18 °C temperature cycle). Activities profiles display counts per each 5-min bin (Mean ±SEM) with *lights-on* event occurring at ZT00 and *lights-off* event at ZT12. White background, light phase; grey blue background, dark phase. Arrows indicate increased morning anticipatory activity in the given genotypes and environments. **B** and **C**). Quantification (Mean ±SEM) of Evening-Morning Index (E-M Index) as explained in Material and Methods for females (B) and males (C) at the different environments. Bars represent Mean ±SEM and numbers in bars indicate *n*, with the total number of flies originated from 3 (*JF02809* in 12:12 LD at 23 °C), 2 (*JF02809* in 12:12 LD with *in-phase* 18-25 °C temperature cycle) and 3 (*JF02809* in 12:12 LD with *anti-phase* 25-18 °C temperature cycle) crosses. *p<0.05; **p<0.01 and ***p<0.001 by Mann-Whitney *U* test (α= 0.05, comparisons among genotypes) or Kruskal-Wallis test (α= 0.05, comparisons for a given genotypes across the three different environments, shown in the legend).

G	Genotype (K-W test)	Environment (N, c)	% M-act ±SEM	% E-act ±SEM	E-M I ±SEM
F	*w^{1118}; +/CyO;* (***)	CT (32, 6)	12.69 ±0.56	29.22 ±0.85	0.55 ±0.02
		IP (9, 1)	3.28 ±0.0.75	32.04 ±1.63	0.89 ±0.03
		AP (29, 3)	8.72 ±1.01	25.80 ± 0.66	0.65 ±0.04
	w^{1118}; +/$Rho1^{1B}$; (***)	CT (31, 6)	14.27 ±0.63	29.62 ±1.03	0.50 ±0.02*
		IP (11, 1)	4.33 ±0.63	25.38 ±0.95	0.83 ±0.03
		AP (34, 3)	11.25 ±0.80	25.30 ± 0.89	0.52 ±0.04*
M	*w^{1118}; +/CyO;* (***)	CT (21, 6)	17.31 ±0.76	41.14 ±1.37	0.57 ±0.02
		IP (9, 1)	4.57 ±1.31	27.01 ±1.15	0.83 ±0.05
		AP (34, 3)	12.55 ±0.99	32.04 ± 0.71	0.59 ±0.04
	w^{1118}; +/$Rho1^{1B}$; (***)	CT (22, 6)	14.89 ±0.47	39.53 ±1.20	0.62 ±0.02
		IP (19, 1)	3.95 ±0.58	25.33 ±1.37	0.82 ±0.03
		AP (33, 3)	10.24 ±0.56	30.57 ± 0.68	0.65 ±0.03
F	*UASDcr2w/; CyO/;*	CT (35, 10)	8.30 ±0.63	27.40 ±1.10	0.66 ±0.03
	$UASdsRho1^{JF02809}$/ (***)	IP (37, 3)	4.09 ±0.47	29.54 ±1.04	0.84 ±0.02
		AP (42, 4)	7.39 ±0.50	28.47 ± 0.89	0.71 ±0.02
	UASDcr2w/; tim(UAS)-Gal4/;	CT (93, 10)	13.71 ±0.52	27.43 ±0.73	0.47 ±0.02***
	$UASdsRho1^{JF02809}$/ (***)	IP (62, 3)	5.81 ±0.49	34.40 ±0.89	0.81 ±0.02
		AP (110, 4)	12.79 ±0.60	25.22 ± 0.63	0.48 ±0.03***
M	*UASDcr2w; CyO/;*	CT (26, 10)	8.54 ±1.01	40.55 ±2.37	0.74 ±0.04
	$UASdsRho1^{JF02809}$/ (***)	IP (30, 3)	3.17 ±0.46	36.88 ±1.17	0.91 ±0.01
		AP (37, 4)	5.49 ±0.59	31.97 ± 1.28	0.81 ±0.02
	UASDcr2w; tim(UAS)-Gal4/;	CT (89, 10)	14.37 ±0.57	40.02 ±1.18	0.60 ±0.02***
	$UASdsRho1^{JF02809}$/ (***)	IP (45, 3)	4.00 ±0.39	35.94 ±1.04	0.88 ±0.01
		AP (86, 4)	8.54 ±0.49	31.70 ± 0.77	0.70 ±0.02***
F	*UASDcr2w/; tim(UAS)-*	CT (18, 3)	7.71 ±0.62	30.13 ±1.06	0.73 ±0.03
	Gal4/CyO; (*)	IP (9, 2)	4.55 ±1.15	27.30 ±1.69	0.82 ±0.05
		AP (22, 2)	9.47 ±1.13	25.36 ± 0.97	0.58 ±0.06
	UASDcr2w/; tim(UAS)-Gal4/	CT (35, 3)	11.34 ±0.60	28.17 ±1.16	0.55 ±0.04**
	$UASdsRho1^{770-1310}$; (**)	IP (16, 2)	6.62 ±0.82	28.55 ±2.03	0.73 ±0.04
		AP (23, 2)	11.62 ±1.23	23.35 ± 1.26	0.48 ±0.06
M	*UASDcr2w; tim(UAS)-*	CT (12, 3)	8.12 ±1.27	43.03 ±2.03	0.80 ±0.03
	Gal4/CyO; (*)	IP (4, 2)	1.68 ±1.07	32.98 ±2.40	0.94 ±0.04
		AP (11, 2)	8.32 ±1.34	29.43 ± 1.31	0.71 ±0.05
	UASDcr2w; tim(UAS)-Gal4/	CT (18, 3)	13.08 ±0.99	39.05 ±2.31	0.63 ±0.05**
	$UASdsRho1^{770-1310}$; (***)	IP (13, 2)	2.78 ±0.76	32.23 ±2.55	0.89 ±0.04
		AP (14, 2)	9.48 ±1.11	28.19 ± 1.51	0.64 ±0.06
F	*UASDcr2w/; CyO/;*	CT (76, 3)	9.33 ±0.49	30.99 ±0.74	0.67 ±0.02
	$UASdsRho1^{JF02809}$/ (*)	IP (13, 2)	4.55 ±0.94	29.27 ±2.28	0.81±0.04
		AP (24, 3)	7.77±1.14	26.64 ± 1.58	0.67 ±0.06
	UASDcr2w/; Pdf-Gal4/;	CT (70, 3)	13.64 ±0.50	28.82 ±0.96	0.49 ±0.03***
	$UASdsRho1^{JF02809}$/ (***)	IP (30, 2)	7.44 ±1.05	29.21 ±1.61	0.70 ±0.05
		AP (23, 3)	11.28 ±1.61	25.15 ± 1.33	0.53 ±0.07
M	*UASDcr2w; CyO/;*	CT (51, 3)	9.88 ±0.76	38.40 ±1.40	0.70 ±0.03
	$UASdsRho1^{JF02809}$/ (***)	IP (10, 2)	2.31 ±0.92	35.22 ±2.07	0.93 ±0.03
		AP (19, 3)	6.42 ±0.94	34.10 ±1.81	0.80 ±0.033
	UASDcr2w; Pdf-Gal4/;	CT (68, 3)	13.16 ±0.62	35.55 ±0.94	0.60 ±0.02**
	$UASdsRho1^{JF02809}$/ (***)	IP (23, 2)	4.56 ±0.90	34.39 ±1.53	0.85 ±0.03
		AP (10, 3)	6.85 ±1.17	35.24 ± 1.92	0.79 ±0.04

Supplementary Table 6. Quantification of LD activity for *Rho1*-deficit genotypes. Adult flies remained for six days in the given environmental conditions. **G,** Gender, female (F) or male (M) flies. **Genotype (K-W test),** chromosome dotation of interest for the assay, with the

result of the Kruskal-Wallis test (α= 0.05) for the three environments**. Environment (N, c),** type of environment complementary to the LD cycle: constant temperature of 23 °C (CT), *in-phase* 18-25 °C temperature cycle (IP) or *anti-phase* 25-18 °C temperature cycle (AP), along number of involved individuals (N) and number of crosses/assays (c). **% M-act ±SEM,** mean of the percentage of the total activity in the four hours preceding *lights-on* ±Standard Error of the Mean (SEM). **% E-act ±SEM,** mean of the percentage of the total activity in the four hours preceding *lights-off* ±SEM. **E-M I ±SEM,** mean of Evening-Morning Index [(E-act - M-act)/(E-act)] ±SEM. *p<0.05; **p<0.01 and ***p<0.001 by Mann-Whitney *U* test (α= 0.05) compared to isogenic controls or by Kruskal-Wallis test (α= 0.05) when comparing a genotype in different environments.

G	Genotype	N(c)	% M-act ±SEM	% E-act ±SEM	E-M I ±SEM
F	*UASDcr2w/; CyO/+; UASdsRho1^{HMS00375}/+*	23(3)	6.74 ±0.71	29.27 ±1.25	0.76 ±0.03
	UASDcr2w/; tim(UAS)-Gal4/+; UASdsRho1^{HMS00375}/+	42	14.46 ±0.93	24.02 ±1.03	0.40 ±0.04***
M	*UASDcr2w; CyO/+; UASdsRho1^{HMS00375}/+*	19	14.80 ±1.45	33.63 ±2.79	0.48 ±0.07
	UASDcr2w; tim(UAS)-Gal4/+; UASdsRho1^{HMS00375}/+	36	18.75 ±0.97	26.01 ±1.27	0.29 ±0.04*
F	*UASDcr2w/; CyO/+; UASdsRho1$^{325-786}$/+*	17(2)	10.67 ±0.91	27.77 ±0.82	0.61 ±0.04
	UASDcr2w/; tim(UAS)-Gal4/+; UASdsRho1$^{325-786}$/+	23	12.90 ±0.73	27.15 ±0.94	0.51 ±0.04
M	*UASDcr2w; CyO/+; UASdsRho1$^{325-786}$/+*	11	17.56 ±1.59	35.29 ±1.68	0.48 ±0.06
	UASDcr2w; tim(UAS)-Gal4/+; UASdsRho1$^{325-786}$/+	10	16.72 ±1.04	32.62 ±2.45	0.46 ±0.04
F	*UASDcr2w/;; TM6B/UASdsRho1^{JF02809}*	21(3)	13.75 ±0.60	32.44 ±2.03	0.54 ±0.04
	UASDcr2w/;; cry-Gal413/ UASdsRho1^{JF02809}	39	14.44 ±0.60	29.65 ±0.93	0.48 ±0.03
M	*UASDcr2w;; TM6B/UASdsRho1^{JF02809}*	25	13.68 ±0.85	35.30 ±1.56	0.58 ±0.04
	UASDcr2w;; cry-Gal4-13/ UASdsRho1^{JF02809}	20	15.08 ±1.16	39.65 ±2.07	0.58 ±0.05
F	*w^{1118}; CyO/; UASdsRho1^{JF02809}/UASDcr2w*	16(2)	12.69 ±1.20	25.99 ±1.99	0.45 ±0.07
	w^{1118}; tim(UAS)-Gal4/; UASdsRho1^{JF02809}/UASDcr2w	45	15.71 ±0.67	21.95 ±0.80	0.29 ±0.03*
	Pdfr^{4304}; tim(UAS)-Gal4/CyO; UASDcr2w	37(4)	14.66 ±0.58	26.34 ±1.67	0.40 ±0.04
	Pdfr^{4304}; tim(UAS)-Gal4/CyO; UASdsRho1^{JF02809}/UASDcr2w	26	12.38 ±0.57	29.55 ±1.55	0.53 ±0.04 *†††
M	*w^{1118}; CyO/; UASdsRho1^{JF02809}/UASDcr2w*	24(2)	19.02 ±1.48	35.37 ±2.76	0.40 ±0.06
	w^{1118}; tim(UAS)-Gal4/; UASdsRho1^{JF02809}/UASDcr2w	54	20.29 ±0.56	34.00 ±0.96	0.38 ±0.02
	Pdfr^{4304}; tim(UAS)-Gal4/CyO; UASDcr2w	31(4)	17.05 ±1.17	42.12 ±1.66	0.57 ±0.04††
	Pdfr^{4304}; tim(UAS)-Gal4/CyO; UASdsRho1^{JF02809}/UASDcr2w	48	17.20 ±0.68	39.91 ±0.97	0.55 ±0.03†††

Supplementary Table 7. Quantification of LD activity for supplementary genotypes. Adult flies remained for six days under 12:12 LD cycles, at a constant temperature of 23 °C. **Env,** environmental conditions. **G,** gender, female (F) or male (M) flies. **Genotype,** chromosome dotation of interest for the assay**. N(c)**, total number of involved flies and number of crosses/assays (c). **% M-act ±SEM,** mean of the percentage of the total activity in the four hours preceding *lights-on* ±Standard Error of the Mean (SEM). **% E-act ±SEM,** mean of the percentage of the total activity in the four hours preceding *lights-off* ±SEM. **E-M I ±SEM,** mean of Evening-Morning Index [(E-act - M-act)/(E-act)] ±SEM. *p<0.05; **p<0.01 and ***p<0.001 by Mann-Whitney *U* test (α= 0.05) against controls (*) or the genotypes in $Pdfr^{+}$ background (†).

Env	G	Genotype	N	% M-act ±SEM	% E-act ±SEM	E-M I ±SEM
12:12 RD	**F**	*UASDcr2w/; CyO/; $UASdsRho1^{JF02809}$/*	18	6.40 ±0.59	34.70 ±1.28	0.81 ±0.02
		UASDcr2w/; tim(UAS)-Gal4/; $UASdsRho1^{JF02809}$/	21	11.06 ±0.73	33.36 ±1.34	0.65 ±0.03 ***
	M	*UASDcr2w; CyO/; $UASdsRho1^{JF02809}$/*	13	5.92 ±1.07	43.41 ±3.69	0.85 ±0.03
		UASDcr2w; tim(UAS)-Gal4/; $UASdsRho1^{JF02809}$/	26	9.95 ±0.80	46.79 ±1.96	0.77 ±0.02 *
10:14 LD	**F**	*UASDcr2w/; CyO/; $UASdsRho1^{JF02809}$/*	16	17.36 ±1.42	25.49 ±1.91	0.33 ±0.06
		UASDcr2w/; tim(UAS)-Gal4/; $UASdsRho1^{JF02809}$/	23	14.03 ±0.77	25.48 ±1.29	0.41 ±0.05
	M	*UASDcr2w; CyO/; $UASdsRho1^{JF02809}$/*	16	19.02 ±1.77	30.69 ±2.12	0.34 ±0.08
		UASDcr2w; tim(UAS)-Gal4/; $UASdsRho1^{JF02809}$/	28	15.53 ±1.41	26.04 ±1.00	0.39 ±0.06
14:10 LD	**F**	*UASDcr2w/; CyO/; $UASdsRho1^{JF02809}$/*	13	6.41 ±0.54	26.35 ±1.22	0.75 ±0.02
		UASDcr2w/; tim(UAS)-Gal4/; $UASdsRho1^{JF02809}$/	21	13.34 ±1.12	27.49 ±1.27	0.48 ±0.05 ***
	M	*UASDcr2w; CyO/; $UASdsRho1^{JF02809}$/*	22	6.62 ±0.93	40.75 ±1.61	0.82 ±0.03
		UASDcr2w; tim(UAS)-Gal4/; $UASdsRho1^{JF02809}$/	27	9.21 ±0.99	41.08 ±1.77	0.75 ±0.03

Supplementary Table 8. Quantification of LD activity for flies expressing the *JF02809* RNAi under different environmental conditions. Adult flies remained for six days in the given environmental conditions, at a constant temperature of 23 °C. **Env,** environmental conditions. **G,** gender, female (F) or male (M) flies. **Genotype,** chromosome dotation of interest for the assay**. N**, total number of involved flies (1 assay/cross for all the genotypes). **% M-act ±SEM,** mean of the percentage of the total activity in the four hours preceding

lights-on ±Standard Error of the Mean (SEM). **% E-act ±SEM,** mean of the percentage of the total activity in the four hours preceding *lights-off* ±SEM. **E-M I ±SEM,** mean of Evening-Morning Index [(E-act - M-act)/(E-act)] ±SEM. *p<0.05; **p<0.01 and ***p<0.001 by Mann-Whitney *U* test (α= 0.05) compared to isogenic controls.

Appendix B : Characterization of the *red light oscillator* inside the *Drosophila melanogaster* clock circuitry

B.1 Introduction

The results presented in this Appendix are part of a joint project by several members from our laboratory to address the origin of the behavioural rhythms in RR conditions. The project is still ongoing, but the current data provide with additional information to help interpreting the main results of the Rho1 project.

As presented in Chapter 1.3.4.1, red light is a zeitgeber that can be indirectly received by the clock cells. While many neurons in the clock circuit respond to blue light stimulation with Cry (Berndt *et al.*, 2007; VanVickle-Chavez and Van Gelder, 2007), the visual systems are required for the sensing of red light. Red light seems to be perceived specifically by both Rhodopsin 1 and 6 (Rh1, Rh6) inside the compound eyes (Hanai, Hamasaka and Ishida, 2008). Their role in red light sensing is redundant as long as one of the two is found in this photoreceptor structure. The $Rh6^{+}$ H-B eyelets (see Chapter 1.3.4.1) do not contribute to this at least under determined light conditions (Yasuyama and Meinertzhagen, 1999; Hanai, Hamasaka and Ishida, 2008). The weaker and indirect transmission of light cues to the clock cells is the probable reason red light entrainment takes approximately twice as long as direct blue light stimulation of the Cry expressing neurons (Hanai and Ishida, 2009). This also permits circadian researchers to give brief exposures of red light to the experimental subjects without evoking the *lights-on* response. The lack of one of the two involved Rhodopsins could, indeed, increase the entrainment time (Hanai and Ishida, 2009).

Flies can be entrained by red light [as well as additional wavelengths other than blue (Hanai and Ishida, 2009)]. Constant red light conditions (RR) allowed flies to maintain self-sustained rhythms (Cusumano *et al.*, 2009) in contrast to the arrhythmia induced by constantwhite light exposure. This *free run* behaviour in RR conditions is often characterised by a phase delay that centres the active phase of locomotor behaviour around subjective evening (compared to the midday in DD)(Cusumano *et al.*, 2009). The behaviour of wild-type flies in RR resembles that of *cry* mutants in LL (Emery *et al.*, 2000a; Dolezelova, Dolezel and Hall, 2007). More intriguingly, it was shown that the Pdf^{01} mutant, arrhythmic in DD, exhibited improved rhythms under constant red light (Renn *et al.*, 1999; Cusumano *et al.*, 2009). And finally, as presented in this thesis, RR conditions can overcome the arrhythmia caused by *Rho1* deficit inside the clock circuit (See Chapter 3.5.2).

Therefore, the behavioural arrhythmia of both *Pdf*^{01} mutants (Renn *et al.*, 1999; Cusumano *et al.*, 2009) and *Rho1* knockdown (Chapters 3.4.3 and 3.5.2) is in RR. This raises the question, which cells (and related signal(s)) take the role of pacemaker cells in RR?

B.2 Methodology

The experimental protocols followed for the locomotor assays are fully described in Chapter 2.3, including maintenance of the flies, data gathering and methods of analysis.

The nature of this genetic screen required the specific rescue of *per* gene inside clock cells of interest. With *per* located in the X chromosome (DrosDel Project, 2007), it would require to introduce the *per*^{01} background in all the involved stocks in order to study both genders. Therefore

All the Gal4 drivers and construct are listed and described in Chapter 2.1.2. The parental line employed as maternal stock was *ywper*^{01}*;; UASper16* (F Rouyer). The *per*^{01} mutant was isolated and firstly characterized by Konopka and Benzer (Konopka and Benzer, 1971). The *per16* construct has been successfully employed by circadian researchers to selectively rescue *per* gene in the mutant background (Blanchardon *et al.*, 2001; Grima *et al.*, 2004). Only male offspring were analysed.

B.3 Results

B.3.1 Red light reduces the impact of the *Pdf*^{01} mutant in a gender-dependent manner

Flies of both genders with or without expression of PDF were tested in DD and RR conditions (Appendix B Figure 1, Appendix B Table 1). The goal was to reproduce the reported behavioural rescue of *Pdf*^{01} individuals under these environmental conditions (Cusumano *et al.*, 2009). The *tim(U)Gal4* driver was part of the background genotype for this analysis, and accounts for the >24-hour endogenous rhythm of the animals (Appendix B Table 1). Analysis of the data showed that the *Pdf*^{01} mutant individuals lost their rhythms in DD compared to the wild-type individuals, as expected (Appendix B Table 1)(Renn *et al.*, 1999). In RR, strikingly, only *Pdf*^{01} males showed a clear improvement in rhythmicity compared to the population in DD (Appendix B Table 1). For both genders, the loss of PDF still caused detrimental effects when compared to wild-type individuals, which exhibited an improvement in RR compared to DD (Appendix B Table 1). The data suggest, therefore, that PDF-signalling is not as critical for behavioural rhythmicity in RR as in DD conditions, but that still has an impact, especially in females.

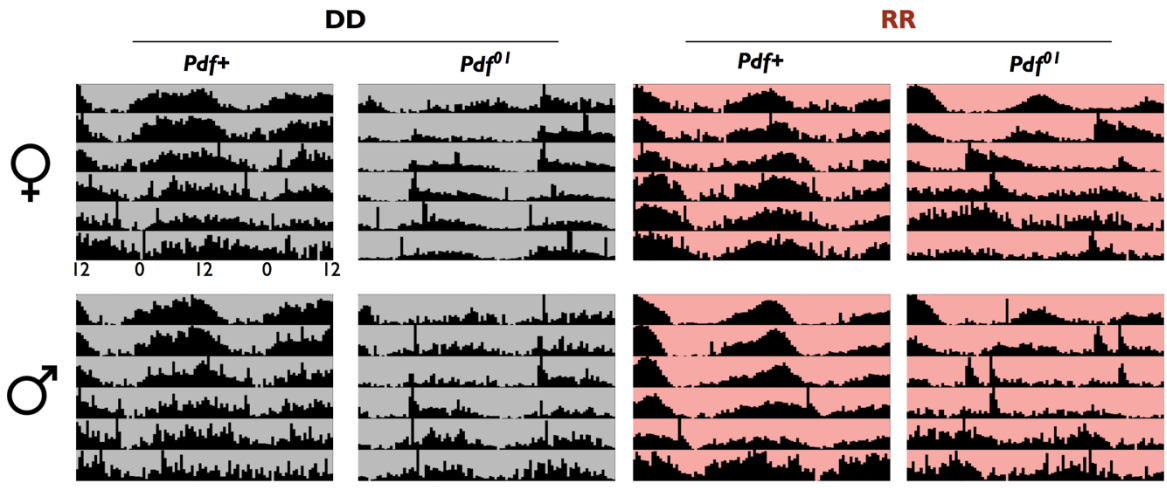

Appendix B Figure 1. Locomotor activity of the *Pdf*^{01} mutant in DD and RR conditions. Adult flies are entrained for 6 days in LD (not shown in this figure) and transferred to DD or RR conditions on day 7, at a constant temperature of 23 °C. Data from the next 7 days in DD or RR is found in Appendix B Table 1. Column titles indicate conditions (first row) and genotypes (Second row), with actogram rows displaying females (top) and males (bottom). Grey background, dark phase; red background, red light phase. Actograms represent the population average and are normalised within each population.

Env	Genotype	G	N(c)	%SR•%WR•%AR	Tau ±SEM(hr)	RRP ±SEM
DD	*UASDcr2w; tim(U)/CyO; +*	F	23 (5)	43•35•22	24.31 ±0.18	1.77 ±0.14
	UASDcr2w; tim(U)/CyO; Pdf^{01}	F	55	7•31•62***	23.43 ±0.35***	1.32 ±0.07**
	UASDcr2w; tim(U)/CyO; +	M	12	33•50•17	24.75 ±0.28	1.53 ±0.10
	UASDcr2w; tim(U)/CyO; Pdf^{01}	M	40	3•35•62**	23.23 ±0.24**	1.17 ±0.05**
RR	*UASDcr2w; tim(U)/CyO; +*	F	12 (5)	92•0•8†	24.59 ±0.15	2.48 ±0.14††
	UASDcr2w; tim(U)/CyO; Pdf^{01}	F	14	21•36•43***	22.25 ±0.96***††	1.56 ±0.17**
	UASDcr2w; tim(U)/CyO; +	M	25	92•0•8†††	24.5 ±0.21	2.44 ±0.12†††
	UASDcr2w; tim(U)/CyO; Pdf^{01}	M	13	39•23•38***††	21.56 ±0.15***††	1.56 ±0.50***†

Appendix B Table 1. Loss of *Pdf* in DD and RR conditions. Adult flies were entrained in LD for 6 days and transferred to DD and RR conditions at a constant temperature of 23 °C. *Free run* behaviour was analysed during 7 days, skipping the first day of transition to DD or RR as described in Material and Methods. **Env,** environment DD or RR conditions. **Genotype:** chromosome dotation of interest for the assay. **G**, gender, female (F) or male (M) flies. **N(c)**, total number of involved flies (number of crosses/assays, applied for the four genotypes: experimental and isogenic control for both genders). **%SR•%WR•%AR**, percentage of flies classified as Strongly Rhythmic (SR), Weakly Rhythmic (WR) or Arrhythmic (AR); **Tau ±SEM**, mean Period Length (hours) ±Standard Error of the Mean (SEM). **RRP ±SEM**, mean Relative Rhythmic Power (no units) ±SEM. *p<0.05; **p<0.01 and ***p<0.001 by Fisher's Exact Test (%SR•%WR•%AR) or Mann-Whitney *U* test (α= 0.05, Tau and RRP) against wild-type controls (*) or the given genotypes in DD conditions (†).

B.3.2 Red light shifts the free run pacemaker function from the PDF-expressing neurons

The results of the genetic screen have provided some cues about the identity of the red light oscillator. It is important to take into consideration, given the gender dimorphism described in the previous chapter, that these results exclusively refer to male individuals.

per^{01} flies failed to display rhythms in both DD and RR (Appendix B Figure 2, Appendix B Table 2). The behaviour of the *per^{01}* mutant further supports the hypothesis that the rescue of the *Rho1* phenotype in RR requires molecular oscillator function (Chapter 3.5.2).

Males with *per* rescue inside the PDF-expressing neurons exhibited recovery of morning anticipatory activity but absence of evening anticipation in LD (Appendix B Figure 2)(Grima *et al.*, 2004). In DD, they showed strong rhythms, as a consequence of rescue of functional molecular clock inside these pacemaker neurons (Appendix B Figure 2, Appendix B Table 2). However, these flies did not maintain locomotor rhythms in RR (Appendix B Figure 2, Appendix B Table 2). This

result implies that, unlike in DD, the PDF-expressing neurons are not the *pacemaker* cells in RR. This conclusion is consistent with the phenotypic improvements of the Pdf^{01} mutant in RR (Appendix B Table 1)(Cusumano *et al.*, 2009) and the rescue of the *Rho1* knockdown phenotype, now known to linked to the s-LN_v function. per rescue in only s-LN_v s (*R6*) or l-LN_vs (*c929*) resulted in poor rhythmicity in DD and RR equally (Helfrich-Forster *et al.*, 2007a; Park *et al.*, 2008). While the *R6* Gal4 driver rescued the morning anticipatory activity as described in literature (Appendix B Figure 2)(Cusumano *et al.*, 2009), there was no published information regarding behavioural rescue in DD. Experiments with *Pdf* and *c929* drivers confirmed that the l-LN_vs, despite their possible role in linking the clock circuit with the visual systems in RR, cannot drive rhythms in this condition (Helfrich-Forster *et al.*, 2007a; Hanai, Hamasaka and Ishida, 2008).

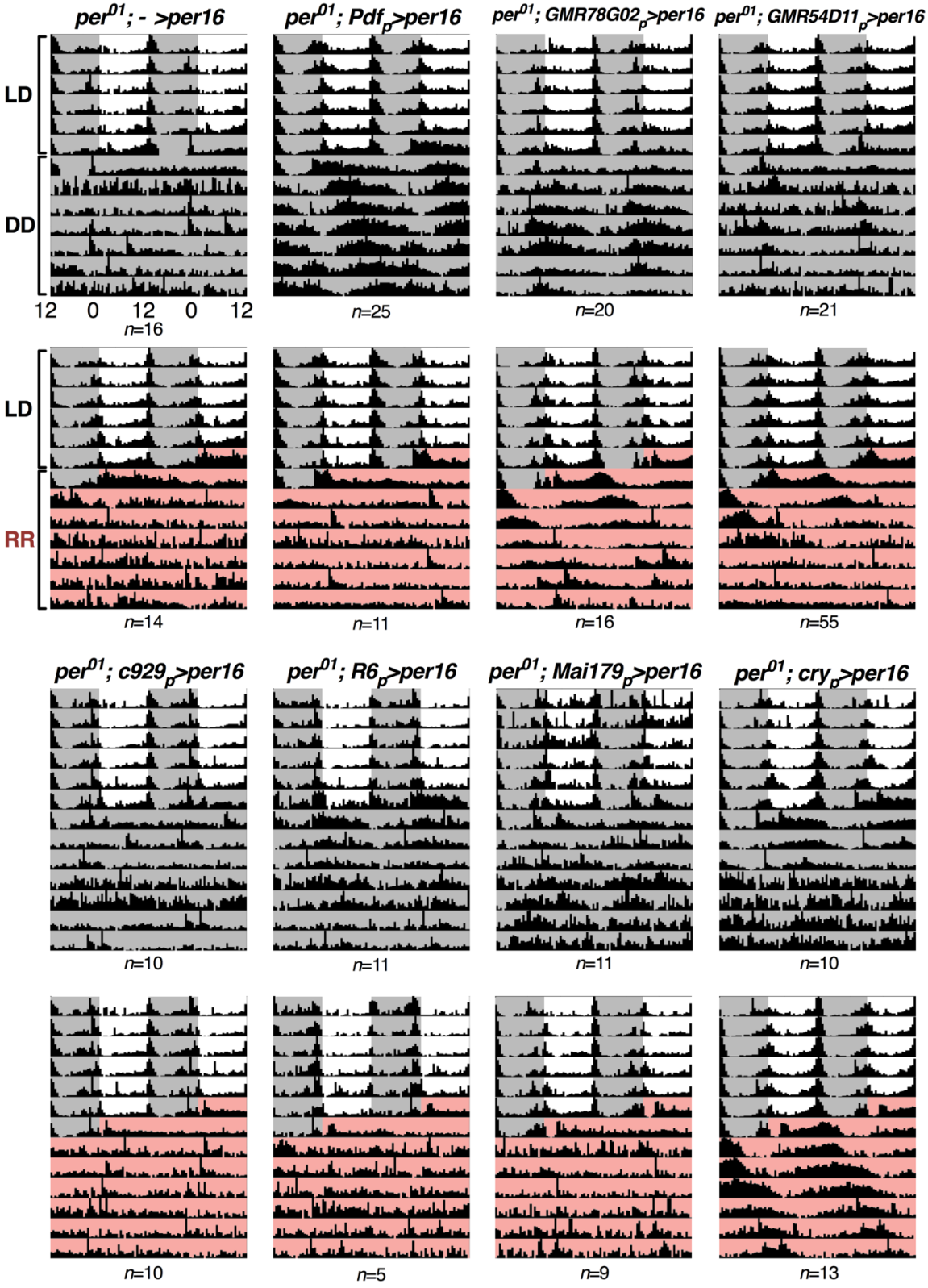

Appendix B Figure 2. Locomotor activity on DD and RR conditions with selective *per* rescues.

Male flies are entrained for 6 days in LD and transferred to DD or RR conditions on day 7, at a constant temperature of 23 °C. Data from the next 7 days in DD or RR is found in Appendix B Table 2. Column titles indicate given genotype, and rows represent DD (top) and RR (bottom). White background, light phase; grey background, dark phase; red

background, red light phase. Actograms represent the population average and are normalised within each population.

The hypothesis of the E-cells acting as the red light pacemaker was tested with lines from the Janelia Farm project (Pfeiffer *et al.*, 2011). The *R78G02* driver (related to the *Spr* gene) is expressed in the 5th s-LN$_v$ and three cry$^+$ LN$_d$s. This was functionally confirmed because specific rescue of *Pdfr* with this driver was sufficient for rescue of evening anticipatory activity in the *Pdfr^{5304}* mutant background (Schlichting *et al.*, 2016). The *R54D11* driver has been published as a method of targeting the ITP-expressing cells (the 5th s-LN$_v$ and one LN$_d$, plus very weak expression in a couple of PDF-expressing neurons)(Johard *et al.*, 2009; Yoshii *et al.*, 2015). These drivers showed weak (*R78G02*) or non-significant (*R54D11*) rescue of rhythmicity for the *per^{01}* mutant in DD (Appendix B Figure 2, Appendix B Table 2), whereas rescue of rhythmicity for both of these drivers in RR was incomplete but significantly better than that for negative control (Appendix B Figure 2, Appendix B Table 2). Moreover, both genotypes exhibited a clear period lengthening in clock neurons, albeit not for a rescue (Guo *et al.*, 2016).

Additionally, E-cells (and M cells) were targeted with *Mai179* (Grima *et al.*, 2004). The rhythmicity was very poor in DD and marginally different from negative control in RR (Appendix B Figure 2, Appendix B Table 2). While this driver has been repeatedly shown to rescue per expression inside both E and M clock cells, its strength is attenuated in DD at least inside the s-LN$_v$s (Grima *et al.*, 2004; Picot *et al.*, 2007). Indeed, the transgenic rescue of *per^{01}* arrhythmia with this driver can be improved by co-introduction of *Pdf-Gal4* (Grima *et al.*, 2004). Expression of *per* in a very similar group of clock cells with *DvPdf* (the domain of expression for *Pdf* in the *Drosophila virilis* species, which includes the 5th s-LN$_v$ and some LN$_d$s in *melanogaster*)(Bahn, Lee and Park, 2009), failed to rescue any behaviour in LD, DD or RR. Importantly, this driver has been used for successfully targeting clock neurons, albeit not for a rescue (Guo *et al.*, 2016).

Finally, the rescue of per inside all the *cry*-expressing neurons evoked a wild-type response in LD and DD (Appendix B Figure 2, Appendix B Table 2), again as expected by published data with the driver (Zhao *et al.*, 2003; Grima *et al.*, 2004; Klarsfeld *et al.*, 2004). When these flies were transferred to RR, they exhibited strong rhythms, even improving the rhythmicity compared to the group in DD (Appendix B Figure 2, Appendix B Table 2).

Env	Genotype	N(c)	%SR•%WR•%AR	Tau ±SEM(hr)	RRP ±SEM
DD	***ywper^{01}; ; UASper16***	16(1)	0•13•87	21.50 ±6	1.13 ±0.04
	ywper^{01}; CyO/; UASper16/	19(3)	5•21•74	24.83 ±4.78	1.10 ±0.02
	ywper^{01}; Pdf-Gal4/; UASper16/	25(3)	56•24•20‡‡‡	25.85 ±0.20	1.82 ±0.11**
	ywper^{01}; ; GMR78G02-Gal4/ UASper16	20(3)	15•60•25‡‡‡	24.57 ±0.55	1.29 ±0.09

	ywper^{01}; ; GMR54D11-Gal4/ UASper16	21(2)	0•38•62	22.94 ±1.47	1.15 ±0.03
	ywper^{01}; c929-Gal4/; UASper16	10(1)	0•20•80	24.5 ±9	1.14 ±0.04
	ywper^{01}; CyO/; UASper16/	2(1)	0•50•50	33.5 ±0	1.13 ±0
	ywper^{01}; R6-Gal4/; UASper16/	11(1)	9•9•82	23.75 ±0.75	1.62 ±0.32
	ywper^{01}; Mai179-Gal4/; UASper16	11(2)	0•0•100	-	-
	ywper^{01}; ; cry-Gal4-13/UASper16	10(1)	10•60•30‡‡	26.64 ±1.29	1.29 ±0.07
	ywper^{01}; dvPdf-Gal4/; Uasper16	14(1)	0•36•64	24.9 ±3.19	1.02 ±0.01
RR	***ywper^{01}; ; UASper16***	14(2)	0•0•100	-	-
	ywper^{01}; CyO/; UASper16/	6(1)	0•17•83	24 ±0	1.10 ±0
	ywper^{01}; Pdf-Gal4/; UASper16/	11(1)	0•9•91†††	31.5 ±0	1.02 ±0
	ywper^{01}; ; GMR78G02-Gal4/ UASper16	16(1)	13•75•12‡‡‡	28.71 ±0.32†††	1.31 ±0.06
	ywper^{01}; ; GMR54D11-Gal4/ UASper16	55(2)	4•38•58‡‡	28.52 ±0.44†††	1.16 ±0.04
	ywper^{01}; c929-Gal4/; UASper16	10(1)	0•10•90	31.5 ±0	1.06 ±0
	ywper^{01}; CyO/; UASper16/	6(1)	0•0•100	-	-
	ywper^{01}; R6-Gal4/; UASper16/	5(1)	0•20•80	24 ±0	1.04±0
	ywper^{01}; Mai179-Gal4/; UASper16	9(3)	0•44•56†‡	18.125 ±2.39	1.24 ±0.10
	ywper^{01}; ; cry-Gal4-13/UASper16	13(2)	69•16•15‡‡‡	26.68 ± 0.33	1.70 ±0.09††
	ywper^{01}; dvPdf-Gal4/; Uasper16	17(1)	0•24•76	27.5 ±1.77	1.07 ±0.05

Appendix B Table 2. Male locomotor activity on DD and RR conditions with selective *per* rescues. Adult flies were entrained in LD for 6 days and transferred to DD and RR conditions at a constant temperature of 23 °C. *Free run* behaviour was analysed during 7 days, skipping the first day of transition to DD or RR as described in Material and Methods. **Env**, environment, DD or RR conditions. **Genotype,** chromosome dotation of interest for the assay. **N(c)**, total number of involved flies (number of crosses/assays). **%SR•%WR•%AR**, percentage of flies classified as Strongly Rhythmic (SR), Weakly Rhythmic (WR) or Arrhythmic (AR). **Tau ±SEM**, mean Period Length (hours) ±Standard Error of the Mean (SEM). **RRP ±SEM**, mean Relative Rhythmic Power (no units) ±SEM. *p<0.05; **p<0.01 and ***p<0.001 by Fisher's Exact Test (%SR•%WR•%AR) or Mann-Whitney *U* test (α= 0.05, Tau and RRP) against isogenic controls (*Pdf* and *R6* assays) (*); the *per^{01}* parental line at the given environmental conditions (‡) or the given genotypes in RR conditions (†).

B.4 Conclusions of the preliminary results

The results presented in this Appendix have drawn the following conclusions regarding the effect of red light on the *Drosophila melanogaster* circadian clock:

1) RR diminishes the importance of PDF-signalling in its *free run* state. Flies lacking PDF-signalling altogether exhibit a partial rescue of circadian behaviour in RR and this is further diminished for females. Therefore, PDF-signalling, while less important in RR, still contributes to circadian locomotor rhythms in this condition in a sexually dimorphic manner.

2) The s-LN_vs lose their status as pacemaker neurons when flies are exposed to RR. This result reveals a reorganisation of the clock hierarchy.

3) A working clock inside both M- and E- cells is sufficient for full rescue of behavioural rhythms in RR. Considering that rescue of *per* expression in the M-cells alone cannot reverse the arrhythmic phenotype of per^{01} flies, and that E-cell-only drivers produce partial rescue of this phenotype, it appears likely that oscillator function in both sets of cells contributes the circadian behaviour in RR.

Together with the main results from this thesis, it could be argued that both selective rescues and the *Rho1* phenotype suggest that signalling from the s-LN_v dorsal termini is not as important for rhythmicity in RR than in DD, at least in males. Unfortunately, the experimental design of the *per* rescue screen has not allowed the assessment of female individuals. The conditional behavioural differences for the Pdf^{01} mutant, however, indicates that exposure to RR uncovers a circuit-level difference between both genders.

The search of the red light oscillator will continue in our laboratory, and complementary approaches (i.e., selective disruption of the clock instead of selective rescue) will be used for mapping out the cells responsible for driving the behavioural rhythms under these environmental conditions.

Bibliography

Agrawal, P. and Hardin, P.E. (2016) 'The Drosophila Receptor Protein Tyrosine Phosphatase LAR Is Required for Development of Circadian Pacemaker Neuron Processes That Support Rhythmic Activity in Constant Darkness But Not during Light/Dark Cycles', *J Neurosci*, 36(13), pp. 3860-70.

Akten, B. *et al.* (2009) 'Ribosomal s6 kinase cooperates with casein kinase 2 to modulate the Drosophila circadian molecular oscillator', *J Neurosci*, 29(2), pp. 466-75.

Alberts, B. *et al.* (2002) 'General Principles of Cell Communication', in *Molecular Biology of the Cell*. 4th edn. New York: Garland Science.

Aldaz, S., Escudero, L.M. and Freeman, M. (2013) 'Dual role of myosin II during Drosophila imaginal disc metamorphosis', *Nat Commun*, 4, p. 1761.

Allada, R. and Chung, B.Y. (2010) 'Circadian organization of behavior and physiology in Drosophila', *Annu Rev Physiol*, 72, pp. 605-24.

Allada, R. *et al.* (1998) 'A mutant Drosophila homolog of mammalian Clock disrupts circadian rhythms and transcription of period and timeless', *Cell*, 93(5), pp. 791-804.

Allende, J.E. and Allende, C.C. (1995) 'Protein kinases. 4. Protein kinase CK2: an enzyme with multiple substrates and a puzzling regulation', *Faseb j*, 9(5), pp. 313-23.

Alward, R.R. (1988) 'Are you a lark or an owl on the night shift?', *Am J Nurs*, 88(10), pp. 1337-9.

Amano, M., Nakayama, M. and Kaibuchi, K. (2010) 'Rho-kinase/ROCK: A key regulator of the cytoskeleton and cell polarity', *Cytoskeleton (Hoboken)*, 67(9), pp. 545-54.

An, S. *et al.* (2013) 'A neuropeptide speeds circadian entrainment by reducing intercellular synchrony', *Proc Natl Acad Sci U S A*, 110(46), pp. E4355-61.

Antoine-Bertrand, J., Fu, M. and Lamarche-Vane, N. (2016) 'Direct measurement of oscillatory RhoA activity in embryonic cortical neurons stimulated with the axon guidance cue netrin-1 using FRET', *Biol Cell*.

Archer, S.N. *et al.* (2003) 'A length polymorphism in the circadian clock gene Per3 is linked to delayed sleep phase syndrome and extreme diurnal preference', *Sleep*, 26(4), pp. 413-5.

Aschoff, J. (1960) 'Exogenous and endogenous components in circadian rhythms', *Cold Spring Harb Symp Quant Biol*, 25, pp. 11-28.

Ashburner, M., Golic, K.G. and Hawley, R.S. (2005) *Drosophila: a laboratory handbook*. 2nd edn.

Aton, S.J. *et al.* (2005) 'Vasoactive intestinal polypeptide mediates circadian rhythmicity and synchrony in mammalian clock neurons', *Nat Neurosci*, 8(4), pp. 476-83.

Aton, S.J. and Herzog, E.D. (2005) 'Come together, right...now: synchronization of rhythms in a mammalian circadian clock', *Neuron*, 48(4), pp. 531-4.

Attrill, H. *et al.* (2016) 'FlyBase: establishing a Gene Group resource for Drosophila melanogaster', *Nucleic Acids Res*, 44(D1), pp. D786-92.

Awasaki, T. *et al.* (2008) 'Organization and postembryonic development of glial cells in the adult central brain of Drosophila', *J Neurosci*, 28(51), pp. 13742-53.

Ba, W. and Nadif Kasri, N. (2017) 'RhoGTPases at the synapse: An embarrassment of choice', *Small GTPases*, 8(2), pp. 106-113.

Ba, W. *et al.* (2016) 'TRIO loss of function is associated with mild intellectual disability and affects dendritic branching and synapse function', *Hum Mol Genet*, 25(5), pp. 892-902.

Bae, K. *et al.* (2001) 'Differential functions of mPer1, mPer2, and mPer3 in the SCN circadian clock', *Neuron*, 30(2), pp. 525-36.

Bae, K. *et al.* (1998) 'Circadian regulation of a Drosophila homolog of the mammalian Clock gene: PER and TIM function as positive regulators', *Mol Cell Biol*, 18(10), pp. 6142-51.

Bahn, J.H., Lee, G. and Park, J.H. (2009) 'Comparative analysis of Pdf-mediated circadian behaviors between Drosophila melanogaster and D. virilis', *Genetics*, 181(3), pp. 965-75.

Bainbridge, S.P. and Bownes, M. (1981) 'Staging the metamorphosis of Drosophila melanogaster', *J Embryol Exp Morphol*, 66, pp. 57-80.

Baker, C.L., Loros, J.J. and Dunlap, J.C. (2012) 'The circadian clock of Neurospora crassa', *FEMS Microbiol Rev*, 36(1), pp. 95-110.

Barrett, K. (2005) Barrett constructs and insertions.

Barrett, K., Leptin, M. and Settleman, J. (1997) 'The Rho GTPase and a putative RhoGEF mediate a signaling pathway for the cell shape changes in Drosophila gastrulation', *Cell*, 91(7), pp. 905-15.

Barrett, R.K. and Takahashi, J.S. (1995) 'Temperature compensation and temperature entrainment of the chick pineal cell circadian clock', *J Neurosci*, 15(8), pp. 5681-92.

Bateman, J., Shu, H. and Van Vactor, D. (2000) 'The guanine nucleotide exchange factor trio mediates axonal development in the Drosophila embryo', *Neuron*, 26(1), pp. 93-106.

Beaver, L.M. *et al.* (2002) 'Loss of circadian clock function decreases reproductive fitness in males of Drosophila melanogaster', *Proc Natl Acad Sci U S A*, 99(4), pp. 2134-9.

Beaver, L.M. *et al.* (2010) 'Circadian clock regulates response to pesticides in Drosophila via conserved Pdp1 pathway', *Toxicol Sci*, 115(2), pp. 513-20.

Bechtel, W. (2015) 'Circadian Rhythms and Mood Disorders: Are the Phenomena and Mechanisms Causally Related?', *Front Psychiatry*, 6, p. 118.

Beckwith, E.J. and Ceriani, M.F. (2015) 'Communication between circadian clusters: The key to a plastic network', *FEBS Lett*, 589(22), pp. 3336-42.

Bedrosian, T.A. and Nelson, R.J. (2013) 'Sundowning syndrome in aging and dementia: research in mouse models', *Exp Neurol*, 243, pp. 67-73.

Belle, M.D. *et al.* (2014) 'Acute suppressive and long-term phase modulation actions of orexin on the Mammalian circadian clock', *J Neurosci*, 34(10), pp. 3607-21.

Bellen, H. (2012) Bellen insertions.

Benito, J., Zheng, H. and Hardin, P.E. (2007) 'PDP1epsilon functions downstream of the circadian oscillator to mediate behavioral rhythms', *J Neurosci*, 27(10), pp. 2539-47.

Benna, C. *et al.* (2010) 'Drosophila timeless2 is required for chromosome stability and circadian photoreception', *Curr Biol*, 20(4), pp. 346-52.

Bernards, A. (2003) 'GAPs galore! A survey of putative Ras superfamily GTPase activating proteins in man and Drosophila', *Biochim Biophys Acta*, 1603(2), pp. 47-82.

Berndt, A. *et al.* (2007) 'A novel photoreaction mechanism for the circadian blue light photoreceptor Drosophila cryptochrome', *J Biol Chem*, 282(17), pp. 13011-21.

Billuart, P. *et al.* (2001) 'Regulating axon branch stability: the role of p190 RhoGAP in repressing a retraction signaling pathway', *Cell*, 107(2), pp. 195-207.

Bishop, A.L. and Hall, A. (2000) 'Rho GTPases and their effector proteins', *Biochem J*, 348 Pt 2, pp. 241-55.

Blanchardon, E. *et al.* (2001) 'Defining the role of Drosophila lateral neurons in the control of circadian rhythms in motor activity and eclosion by targeted genetic ablation and PERIOD protein overexpression', *Eur J Neurosci*, 13(5), pp. 871-88.

Blau, J. and Young, M.W. (1999) 'Cycling vrille expression is required for a functional Drosophila clock', *Cell*, 99(6), pp. 661-71.

Boureux, A. *et al.* (2007) 'Evolution of the Rho family of ras-like GTPases in eukaryotes', *Mol Biol Evol*, 24(1), pp. 203-16.

Bradshaw, W.E. and Holzapfel, C.M. (2010) 'What season is it anyway? Circadian tracking vs. photoperiodic anticipation in insects', *J Biol Rhythms*, 25(3), pp. 155-65.

Brainard, G.C. *et al.* (2001) 'Action spectrum for melatonin regulation in humans: evidence for a novel circadian photoreceptor', *J Neurosci*, 21(16), pp. 6405-12.

Brand, A.H. and Perrimon, N. (1993) 'Targeted gene expression as a means of altering cell fates and generating dominant phenotypes', *Development*, 118(2), pp. 401-15.

Brugnera, E. *et al.* (2002) 'Unconventional Rac-GEF activity is mediated through the Dock180-ELMO complex', *Nat Cell Biol*, 4(8), pp. 574-82.

Bushey, D., Tononi, G. and Cirelli, C. (2015) 'Sleep- and wake-dependent changes in neuronal activity and reactivity demonstrated in fly neurons using in vivo calcium imaging', *Proc Natl Acad Sci U S A*, 112(15), pp. 4785-90.

Busza, A. *et al.* (2004) 'Roles of the two Drosophila CRYPTOCHROME structural domains in circadian photoreception', *Science*, 304(5676), pp. 1503-6.

Busza, A., Murad, A. and Emery, P. (2007) 'Interactions between circadian neurons control temperature synchronization of Drosophila behavior', *J Neurosci*, 27(40), pp. 10722-33.

Campbell, S.S. and Tobler, I. (1984) 'Animal sleep: a review of sleep duration across phylogeny', *Neurosci Biobehav Rev*, 8(3), pp. 269-300.

Cao, G. and Nitabach, M.N. (2008) 'Circadian control of membrane excitability in Drosophila melanogaster lateral ventral clock neurons', *J Neurosci*, 28(25), pp. 6493-501.

Cao, G. *et al.* (2013) 'Genetically targeted optical electrophysiology in intact neural circuits', *Cell*, 154(4), pp. 904-13.

Carlier, M.F. *et al.* (1997) 'Actin depolymerizing factor (ADF/cofilin) enhances the rate of filament turnover: implication in actin-based motility', *J Cell Biol*, 136(6), pp. 1307-22.

Carrera, P. *et al.* (1998) 'A modifier screen in the eye reveals control genes for Kruppel activity in the Drosophila embryo', *Proc Natl Acad Sci U S A*, 95(18), pp. 10779-84.

Castrillon, D.H. and Wasserman, S.A. (1994) 'Diaphanous is required for cytokinesis in Drosophila and shares domains of similarity with the products of the limb deformity gene', *Development*, 120(12), pp. 3367-77.

Catterson, J.H. *et al.* (2010) 'Dietary modulation of Drosophila sleep-wake behaviour', *PLoS One*, 5(8), p. e12062.

Cavanaugh, D.J. *et al.* (2014) 'Identification of a circadian output circuit for rest:activity rhythms in Drosophila', *Cell*, 157(3), pp. 689-701.

Cavey, M. *et al.* (2016) 'Circadian rhythms in neuronal activity propagate through output circuits', *Nat Neurosci*.

Celeste Morley, S., Sun, G.P. and Bierer, B.E. (2003) 'Inhibition of actin polymerization enhances commitment to and execution of apoptosis induced by withdrawal of trophic support', *J Cell Biochem*, 88(5), pp. 1066-76.

Ceriani, M.F. *et al.* (1999) 'Light-dependent sequestration of TIMELESS by CRYPTOCHROME', *Science*, 285(5427), pp. 553-6.

Chang, A.M. *et al.* (2015) 'Evening use of light-emitting eReaders negatively affects sleep, circadian timing, and next-morning alertness', *Proc Natl Acad Sci U S A*, 112(4), pp. 1232-7.

Chen, C. *et al.* (2015) 'Drosophila Ionotropic Receptor 25a mediates circadian clock resetting by temperature', *Nature*.

Chen, J. and Condron, B.G. (2008) 'Branch architecture of the fly larval abdominal serotonergic neurons', *Dev Biol*, 320(1), pp. 30-8.

Chen, J. *et al.* (2001) 'Cofilin/ADF is required for cell motility during Drosophila ovary development and oogenesis', *Nat Cell Biol*, 3(2), pp. 204-9.

Chen, K.F. *et al.* (2014) 'The central molecular clock is robust in the face of behavioural arrhythmia in a Drosophila model of Alzheimer's disease', *Dis Model Mech*, 7(4), pp. 445-58.

Chen, X. and Rosbash, M. (2016) 'mir-276a strengthens Drosophila circadian rhythms by regulating timeless expression', *Proc Natl Acad Sci U S A*, 113(21), pp. E2965-72.

Cherfils, J. and Zeghouf, M. (2013) 'Regulation of small GTPases by GEFs, GAPs, and GDIs', *Physiol Rev*, 93(1), pp. 269-309.

Chiou, Y.Y. *et al.* (2016) 'Mammalian Period represses and de-represses transcription by displacing CLOCK-BMAL1 from promoters in a Cryptochrome-dependent manner', *Proc Natl Acad Sci U S A*, 113(41), pp. E6072-e6079.

Chiu, J.C., Ko, H.W. and Edery, I. (2011) 'NEMO/NLK phosphorylates PERIOD to initiate a time-delay phosphorylation circuit that sets circadian clock speed', *Cell*, 145(3), pp. 357-70.

Chiu, J.C. *et al.* (2008) 'The phospho-occupancy of an atypical SLIMB-binding site on PERIOD that is phosphorylated by DOUBLETIME controls the pace of the clock', *Genes Dev*, 22(13), pp. 1758-72.

Chung, B.Y. *et al.* (2009) 'The GABA(A) receptor RDL acts in peptidergic PDF neurons to promote sleep in Drosophila', *Curr Biol*, 19(5), pp. 386-90.

Cingolani, L.A. and Goda, Y. (2008) 'Actin in action: the interplay between the actin cytoskeleton and synaptic efficacy', *Nat Rev Neurosci*, 9(5), pp. 344-56.

Collins, B. *et al.* (2014) 'Differentially timed extracellular signals synchronize pacemaker neuron clocks', *PLoS Biol*, 12(9), p. e1001959.

Collins, B.H., Rosato, E. and Kyriacou, C.P. (2004) 'Seasonal behavior in Drosophila melanogaster requires the photoreceptors, the circadian clock, and phospholipase C', *Proc Natl Acad Sci U S A*, 101(7), pp. 1945-50.

Conrad, S. *et al.* (2005) 'Prolonged lesional expression of RhoA and RhoB following spinal cord injury', *J Comp Neurol*, 487(2), pp. 166-75.

Costa, G. (2003) 'Shift work and occupational medicine: an overview', *Occup Med (Lond)*, 53(2), pp. 83-8.

Costa, R. *et al.* (1992) 'A latitudinal cline in a Drosophila clock gene', *Proc Biol Sci*, 250(1327), pp. 43-9.

Crocker, A. *et al.* (2010) 'Identification of a neural circuit that underlies the effects of octopamine on sleep:wake behavior', *Neuron*, 65(5), pp. 670-81.

CSHP (2006) 'Paraformaldehyde in PBS', *Cold Spring Harbor Protocols*, 2006(1), p. pdb.rec9959.

CSHP (2010) 'PB (0.1 M phosphate buffer pH 7.2)', *Cold Spring Harbor Protocols*.

Currie, J., Goda, T. and Wijnen, H. (2009) 'Selective entrainment of the Drosophila circadian clock to daily gradients in environmental temperature', *BMC Biol*, 7, p. 49.

Curtin, K.D., Huang, Z.J. and Rosbash, M. (1995) 'Temporally regulated nuclear entry of the Drosophila period protein contributes to the circadian clock', *Neuron*, 14(2), pp. 365-72.

Cusumano, P. *et al.* (2009) 'PDF-modulated visual inputs and cryptochrome define diurnal behavior in Drosophila', *Nat Neurosci*, 12(11), pp. 1431-7.

Cyran, S.A. *et al.* (2003) 'vrille, Pdp1, and dClock form a second feedback loop in the Drosophila circadian clock', *Cell*, 112(3), pp. 329-41.

Cyran, S.A. *et al.* (2005) 'The double-time protein kinase regulates the subcellular localization of the Drosophila clock protein period', *J Neurosci*, 25(22), pp. 5430-7.

Czarna, A. *et al.* (2013) 'Structures of Drosophila cryptochrome and mouse cryptochrome1 provide insight into circadian function', *Cell*, 153(6), pp. 1394-405.

Dahdal, D. *et al.* (2010) 'Drosophila pacemaker neurons require g protein signaling and GABAergic inputs to generate twenty-four hour behavioral rhythms', *Neuron*, 68(5), pp. 964-77.

Dahmus, G.K. *et al.* (1984) 'Similarities in structure and function of calf thymus and Drosophila casein kinase II', *J Biol Chem*, 259(14), pp. 9001-6.

Darlington, T.K. *et al.* (1998) 'Closing the circadian loop: CLOCK-induced transcription of its own inhibitors per and tim', *Science*, 280(5369), pp. 1599-603.

Das, A., Holmes, T.C. and Sheeba, V. (2015) 'dTRPA1 Modulates Afternoon Peak of Activity of Fruit Flies Drosophila melanogaster', *PLoS One*, 10(7), p. e0134213.

Das, A., Holmes, T.C. and Sheeba, V. (2016) 'dTRPA1 in Non-circadian Neurons Modulates Temperature-Dependent Rhythmic Activity in Drosophila melanogaster', *J Biol Rhythms*.

Davis, R.L. and Turner, D.L. (2001) 'Vertebrate hairy and Enhancer of split related proteins: transcriptional repressors regulating cellular differentiation and embryonic patterning', *Oncogene*, 20(58), pp. 8342-57.

de Mairan, J. (1729) 'Observation botanique', *Hist. Acad. Roy. Sci*, pp. 35-36.

de Velasco, B. *et al.* (2007) 'Specification and development of the pars intercerebralis and pars lateralis, neuroendocrine command centers in the Drosophila brain', *Dev Biol*, 302(1), pp. 309-23.

Debant, A. *et al.* (1996) 'The multidomain protein Trio binds the LAR transmembrane tyrosine phosphatase, contains a protein kinase domain, and has separate rac-specific and rho-specific guanine nucleotide exchange factor domains', *Proc Natl Acad Sci U S A*, 93(11), pp. 5466-71.

DeCoursey, P.J. and Krulas, J.R. (1998) 'Behavior of SCN-lesioned chipmunks in natural habitat: a pilot study', *J Biol Rhythms*, 13(3), pp. 229-44.

DeCoursey, P.J., Walker, J.K. and Smith, S.A. (2000) 'A circadian pacemaker in free-living chipmunks: essential for survival?', *J Comp Physiol A*, 186(2), pp. 169-80.

Denhardt, D.T. (1996) 'Signal-transducing protein phosphorylation cascades mediated by Ras/Rho proteins in the mammalian cell: the potential for multiplex signalling', *Biochem J*, 318 (Pt 3), pp. 729-47.

Depetris-Chauvin, A. *et al.* (2011) 'Adult-specific electrical silencing of pacemaker neurons uncouples molecular clock from circadian outputs', *Curr Biol*, 21(21), pp. 1783-93.

Depetris-Chauvin, A. *et al.* (2014) 'Mmp1 processing of the PDF neuropeptide regulates circadian structural plasticity of pacemaker neurons', *PLoS Genet*, 10(10), p. e1004700.

Devlin, P.F. (2002) 'Signs of the time: environmental input to the circadian clock', *J Exp Bot*, 53(374), pp. 1535-50.

Di Cara, F. and King-Jones, K. (2016) 'The Circadian Clock Is a Key Driver of Steroid Hormone Production in Drosophila', *Curr Biol*.

Dietzl, G. *et al.* (2007) 'A genome-wide transgenic RNAi library for conditional gene inactivation in Drosophila', *Nature*, 448(7150), pp. 151-6.

Dillon, C. and Goda, Y. (2005) 'The actin cytoskeleton: integrating form and function at the synapse', *Annu Rev Neurosci*, 28, pp. 25-55.

Dircksen, H. *et al.* (2008) 'Ion transport peptide splice forms in central and peripheral neurons throughout postembryogenesis of Drosophila melanogaster', *J Comp Neurol*, 509(1), pp. 23-41.

Dodd, A.N. *et al.* (2005) 'Plant circadian clocks increase photosynthesis, growth, survival, and competitive advantage', *Science*, 309(5734), pp. 630-3.

Dodson, C.A., Hore, P.J. and Wallace, M.I. (2013) 'A radical sense of direction: signalling and mechanism in cryptochrome magnetoreception', *Trends Biochem Sci*, 38(9), pp. 435-46.

Dolezelova, E., Dolezel, D. and Hall, J.C. (2007) 'Rhythm defects caused by newly engineered null mutations in Drosophila's cryptochrome gene', *Genetics*, 177(1), pp. 329-45.

Dominoni, D.M. *et al.* (2013) 'Clocks for the city: circadian differences between forest and city songbirds', *Proc Biol Sci*, 280(1763), p. 20130593.

DrosDel Project (2007) DrosDel deletion data mapped to Release 5.1 (updated 2007-06-25).

Dubruille, R. *et al.* (2009) 'A constant light-genetic screen identifies KISMET as a regulator of circadian photoresponses', *PLoS Genet*, 5(12), p. e1000787.

Dunlap, J.C. (1999) 'Molecular bases for circadian clocks', *Cell*, 96(2), pp. 271-90.

Dunlap, J.C.L.J.J.D.P.J. (2004) *Chronobiology: Biological Timekeeping*. Sinauer Associates, Sunderland MA.

Dvornyk, V., Vinogradova, O. and Nevo, E. (2003) 'Origin and evolution of circadian clock genes in prokaryotes', *Proc Natl Acad Sci U S A*, 100(5), pp. 2495-500.

Dvorsky, R. and Ahmadian, M.R. (2004) 'Always look on the bright site of Rho: structural implications for a conserved intermolecular interface', *EMBO Rep*, 5(12), pp. 1130-6.

Edwards, K.A. and Kiehart, D.P. (1996) 'Drosophila nonmuscle myosin II has multiple essential roles in imaginal disc and egg chamber morphogenesis', *Development*, 122(5), pp. 1499-511.

Emery, P. *et al.* (1998) 'CRY, a Drosophila clock and light-regulated cryptochrome, is a major contributor to circadian rhythm resetting and photosensitivity', *Cell*, 95(5), pp. 669-79.

Emery, P. *et al.* (2000a) 'A unique circadian-rhythm photoreceptor', *Nature*, 404(6777), pp. 456-7.

Emery, P. *et al.* (2000b) 'Drosophila CRY is a deep brain circadian photoreceptor', *Neuron*, 26(2), pp. 493-504.

Engelen, E. *et al.* (2013) 'Mammalian TIMELESS is involved in period determination and DNA damage-dependent phase advancing of the circadian clock', *PLoS One*, 8(2), p. e56623.

Etienne-Manneville, S. and Hall, A. (2002) 'Rho GTPases in cell biology', *Nature*, 420(6916), pp. 629-35.

Evans, J.A. (2016) 'Collective timekeeping among cells of the master circadian clock', *J Endocrinol*, 230(1), pp. R27-49.

Ewer, J. *et al.* (1992) 'Expression of the period clock gene within different cell types in the brain of Drosophila adults and mosaic analysis of these cells' influence on circadian behavioral rhythms', *J Neurosci*, 12(9), pp. 3321-49.

Falahzadeh, K., Banaei-Esfahani, A. and Shahhoseini, M. (2015) 'The potential roles of actin in the nucleus', *Cell J*, 17(1), pp. 7-14.

Fang, Y., Sathyanarayanan, S. and Sehgal, A. (2007) 'Post-translational regulation of the Drosophila circadian clock requires protein phosphatase 1 (PP1)', *Genes Dev*, 21(12), pp. 1506-18.

Fanto, M. *et al.* (2000) 'Nuclear signaling by Rac and Rho GTPases is required in the establishment of epithelial planar polarity in the Drosophila eye', *Curr Biol*, 10(16), pp. 979-88.

Fedele, G. *et al.* (2014) 'An electromagnetic field disrupts negative geotaxis in Drosophila via a CRY-dependent pathway', *Nat Commun*, 5, p. 4391.

Fernandez, M.P., Berni, J. and Ceriani, M.F. (2008) 'Circadian remodeling of neuronal circuits involved in rhythmic behavior', *PLoS Biol*, 6(3), p. e69.

Fire, A. *et al.* (1998) 'Potent and specific genetic interference by double-stranded RNA in Caenorhabditis elegans', *Nature*, 391(6669), pp. 806-11.

Fischer, J.A. *et al.* (1988) 'GAL4 activates transcription in Drosophila', *Nature*, 332(6167), pp. 853-6.

Flourakis, M. *et al.* (2015) 'A Conserved Bicycle Model for Circadian Clock Control of Membrane Excitability', *Cell*, 162(4), pp. 836-48.

Förster, C. (2010) 'The neuronal network of the endogenous clock', *e-Neuroforum*, 1(1), pp. 17-22.

Frenkel, L. *et al.* (2017) 'Organization of Circadian Behavior Relies on Glycinergic Transmission', *Cell Rep*, 19(1), pp. 72-85.

Frisch, B. *et al.* (1994) 'A promoterless period gene mediates behavioral rhythmicity and cyclical per expression in a restricted subset of the Drosophila nervous system', *Neuron*, 12(3), pp. 555-70.

Fujii, S. and Amrein, H. (2010) 'Ventral lateral and DN1 clock neurons mediate distinct properties of male sex drive rhythm in Drosophila', *Proc Natl Acad Sci U S A*, 107(23), pp. 10590-5.

Fujioka, H. *et al.* (2012) 'Neural functions of matrix metalloproteinases: plasticity, neurogenesis, and disease', *Biochem Res Int*, 2012, p. 789083.

Fuller, P.M., Gooley, J.J. and Saper, C.B. (2006) 'Neurobiology of the sleep-wake cycle: sleep architecture, circadian regulation, and regulatory feedback', *J Biol Rhythms*, 21(6), pp. 482-93.

Gabler, M. *et al.* (2005) 'Trans-splicing of the mod(mdg4) complex locus is conserved between the distantly related species Drosophila melanogaster and D. virilis', *Genetics*, 169(2), pp. 723-36.

Gao, J., Liao, J. and Yang, G.Y. (2009) 'CAAX-box protein, prenylation process and carcinogenesis', *Am J Transl Res*, 1(3), pp. 312-25.

Garbe, D.S. *et al.* (2013) 'Cooperative interaction between phosphorylation sites on PERIOD maintains circadian period in Drosophila', *PLoS Genet*, 9(9), p. e1003749.

Gatto, C.L. and Broadie, K. (2009) 'Temporal requirements of the fragile x mental retardation protein in modulating circadian clock circuit synaptic architecture', *Front Neural Circuits*, 3, p. 8.

Gekakis, N. *et al.* (1998) 'Role of the CLOCK protein in the mammalian circadian mechanism', *Science*, 280(5369), pp. 1564-9.

Gentile, C. *et al.* (2013) 'Cryptochrome antagonizes synchronization of Drosophila's circadian clock to temperature cycles', *Curr Biol*, 23(3), pp. 185-95.

Gibbs, F.P. (1981) 'Temperature dependence of rat circadian pacemaker', *Am J Physiol*, 241(1), pp. R17-20.

Glaser, F.T. and Stanewsky, R. (2005) 'Temperature synchronization of the Drosophila circadian clock', *Curr Biol*, 15(15), pp. 1352-63.

Glaser, F.T. and Stanewsky, R. (2007) 'Synchronization of the Drosophila circadian clock by temperature cycles', *Cold Spring Harb Symp Quant Biol*, 72, pp. 233-42.

Glasheen, B.M. *et al.* (2010) 'A matrix metalloproteinase mediates airway remodeling in Drosophila', *Dev Biol*, 344(2), pp. 772-83.

Glossop, N.R. *et al.* (2003) 'VRILLE feeds back to control circadian transcription of Clock in the Drosophila circadian oscillator', *Neuron*, 37(2), pp. 249-61.

Glossop, N.R., Lyons, L.C. and Hardin, P.E. (1999) 'Interlocked feedback loops within the Drosophila circadian oscillator', *Science*, 286(5440), pp. 766-8.

Goda, T. *et al.* (2011) 'Adult circadian behavior in Drosophila requires developmental expression of cycle, but not period', *PLoS Genet*, 7(7), p. e1002167.

Goda, T., Sharp, B. and Wijnen, H. (2014) 'Temperature-dependent resetting of the molecular circadian oscillator in Drosophila', *Proc Biol Sci*, 281(1793).

Goda, T. *et al.* (2016) 'Drosophila DH31 Neuropeptide and PDF Receptor Regulate Night-Onset Temperature Preference', *J Neurosci*, 36(46), pp. 11739-11754.

Gogolla, N., Galimberti, I. and Caroni, P. (2007) 'Structural plasticity of axon terminals in the adult', *Curr Opin Neurobiol*, 17(5), pp. 516-24.

Golden, S.S. *et al.* (1997) 'CYANOBACTERIAL CIRCADIAN RHYTHMS', *Annu Rev Plant Physiol Plant Mol Biol*, 48, pp. 327-354.

Gorostiza, E.A. *et al.* (2014) 'Circadian Pacemaker Neurons Change Synaptic Contacts across the Day', *Curr Biol*.

Gould, P.D. *et al.* (2006) 'The molecular basis of temperature compensation in the Arabidopsis circadian clock', *Plant Cell*, 18(5), pp. 1177-87.

Goyal, L. *et al.* (2000) 'Induction of apoptosis by Drosophila reaper, hid and grim through inhibition of IAP function', *Embo j*, 19(4), pp. 589-97.

Gray, H.L., Warren; (1918) *Anatomy of the human body*. 20th edn.: Philadelphia, Lea & Febiger.

Green, E.W. *et al.* (2015a) 'Drosophila circadian rhythms in seminatural environments: Summer afternoon component is not an artifact and requires TrpA1 channels', *Proc Natl Acad Sci U S A*.

Green, E.W. *et al.* (2015b) 'Drosophila circadian rhythms in seminatural environments: Summer afternoon component is not an artifact and requires TrpA1 channels', *Proc Natl Acad Sci U S A*, 112(28), pp. 8702-7.

Green, R.M. *et al.* (2002) 'Circadian Rhythms Confer a Higher Level of Fitness to Arabidopsis Plants', *Plant Physiol*, 129(2), pp. 576-84.

Greenberg, L. and Hatini, V. (2011) 'Systematic expression and loss-of-function analysis defines spatially restricted requirements for Drosophila RhoGEFs and RhoGAPs in leg morphogenesis', *Mech Dev*, 128(1-2), pp. 5-17.

Gregory, S.L., Lorensuhewa, N. and Saint, R. (2010) 'Signalling through the RhoGEF Pebble in Drosophila', *IUBMB Life*, 62(4), pp. 290-5.

Grima, B. *et al.* (2004) 'Morning and evening peaks of activity rely on different clock neurons of the Drosophila brain', *Nature*, 431(7010), pp. 869-73.

Grima, B. *et al.* (2012) 'CULLIN-3 controls TIMELESS oscillations in the Drosophila circadian clock', *PLoS Biol*, 10(8), p. e1001367.

Grima, B. *et al.* (2002) 'The F-box protein slimb controls the levels of clock proteins period and timeless', *Nature*, 420(6912), pp. 178-82.

Gu, Y., Janoschka, S. and Ge, S. (2013) 'Neurogenesis and hippocampal plasticity in adult brain', *Curr Top Behav Neurosci*, 15, pp. 31-48.

Guan, R. *et al.* (2013) 'Advances in the studies of roles of Rho/Rho-kinase in diseases and the development of its inhibitors', *Eur J Med Chem*, 70, pp. 613-22.

Guerra, P.A., Gegear, R.J. and Reppert, S.M. (2014) 'A magnetic compass aids monarch butterfly migration', *Nat Commun*, 5, p. 4164.

Gunawardhana, K.L. and Hardin, P.E. (2017) 'VRILLE Controls PDF Neuropeptide Accumulation and Arborization Rhythms in Small Ventrolateral Neurons to Drive Rhythmic Behavior in Drosophila', *Curr Biol*.

Gunsalus, K.C. *et al.* (1995) 'Mutations in twinstar, a Drosophila gene encoding a cofilin/ADF homologue, result in defects in centrosome migration and cytokinesis', *J Cell Biol*, 131(5), pp. 1243-59.

Guo, F. *et al.* (2014) 'PDF neuron firing phase-shifts key circadian activity neurons in Drosophila', *Elife*, 3.

Guo, F. *et al.* (2016) 'Circadian neuron feedback controls the Drosophila sleep-activity profile', *Nature*.

Habas, R., Dawid, I.B. and He, X. (2003) 'Coactivation of Rac and Rho by Wnt/Frizzled signaling is required for vertebrate gastrulation', *Genes Dev*, 17(2), pp. 295-309.

Halberg, F. *et al.* (2003) 'Transdisciplinary unifying implications of circadian findings in the 1950s', *J Circadian Rhythms*, 1(1), p. 2.

Hall, A. and Lalli, G. (2010) 'Rho and Ras GTPases in axon growth, guidance, and branching', *Cold Spring Harb Perspect Biol*, 2(2), p. a001818.

Halsell, S.R., Chu, B.I. and Kiehart, D.P. (2000) 'Genetic analysis demonstrates a direct link between rho signaling and nonmuscle myosin function during Drosophila morphogenesis', *Genetics*, 155(3), pp. 1253-65.

Halsell, S.R. and Kiehart, D.P. (1998) 'Second-site noncomplementation identifies genomic regions required for Drosophila nonmuscle myosin function during morphogenesis', *Genetics*, 148(4), pp. 1845-63.

Hamasaka, Y. and Nassel, D.R. (2006) 'Mapping of serotonin, dopamine, and histamine in relation to different clock neurons in the brain of Drosophila', *J Comp Neurol*, 494(2), pp. 314-30.

Hamasaka, Y. *et al.* (2007) 'Glutamate and its metabotropic receptor in Drosophila clock neuron circuits', *J Comp Neurol*, 505(1), pp. 32-45.

Hamblen, M. *et al.* (1986) 'Germ-line transformation involving DNA from the period locus in Drosophila melanogaster: overlapping genomic fragments that restore circadian and ultradian rhythmicity to per0 and per- mutants', *J Neurogenet*, 3(5), pp. 249-91.

Hanafusa, S. *et al.* (2013) 'Sexual Interactions Influence the Molecular Oscillations in DN1 Pacemaker Neurons in Drosophila melanogaster', *PLoS One*, 8(12), p. e84495.

Hanai, S., Hamasaka, Y. and Ishida, N. (2008) 'Circadian entrainment to red light in Drosophila: requirement of Rhodopsin 1 and Rhodopsin 6', *Neuroreport*, 19(14), pp. 1441-4.

Hanai, S. and Ishida, N. (2009) 'Entrainment of Drosophila circadian clock to green and yellow light by Rh1, Rh5, Rh6 and CRY', *Neuroreport*, 20(8), pp. 755-8.

Hang, C.Y., Kitahashi, T. and Parhar, I.S. (2016) 'Neuronal Organization of Deep Brain Opsin Photoreceptors in Adult Teleosts', *Front Neuroanat*, 10, p. 48.

Hao, H., Allen, D.L. and Hardin, P.E. (1997) 'A circadian enhancer mediates PER-dependent mRNA cycling in Drosophila melanogaster', *Mol Cell Biol*, 17(7), pp. 3687-93.

Hao, H. *et al.* (1999) 'The 69 bp circadian regulatory sequence (CRS) mediates per-like developmental, spatial, and circadian expression and behavioral rescue in Drosophila', *J Neurosci*, 19(3), pp. 987-94.

Harden, N. *et al.* (1996) 'A Drosophila homolog of the Rac- and Cdc42-activated serine/threonine kinase PAK is a potential focal adhesion and focal complex protein that colocalizes with dynamic actin structures', *Mol Cell Biol*, 16(5), pp. 1896-908.

Hardin, P.E., Hall, J.C. and Rosbash, M. (1990) 'Feedback of the Drosophila period gene product on circadian cycling of its messenger RNA levels', *Nature*, 343(6258), pp. 536-40.

Harper, R.E. *et al.* (2016) 'Sensory Conflict Disrupts Activity of the Drosophila Circadian Network', *Cell Rep*, 17(7), pp. 1711-1718.

Hartenstein, V. (2006) 'The neuroendocrine system of invertebrates: a developmental and evolutionary perspective', *J Endocrinol*, 190(3), pp. 555-70.

Hazelrigg, T., Levis, R. and Rubin, G.M. (1984) 'Transformation of white locus DNA in drosophila: dosage compensation, zeste interaction, and position effects', *Cell*, 36(2), pp. 469-81.

He, C. *et al.* (2013) 'Regulation of circadian locomotor rhythm by neuropeptide Y-like system in Drosophila melanogaster', *Insect Mol Biol*, 22(4), pp. 376-88.

Head, L.M. *et al.* (2015) 'The influence of light on temperature preference in Drosophila', *Curr Biol*, 25(8), pp. 1063-8.

Helfrich, C. and Engelmann, W. (1983) 'Circadian rhythm of the locomotor activity in Drosophila melanogaster and its mutants ‘sine oculis’ and ‘small optic lobes’', *Physiological Entomology*, 8(3), pp. 257-272.

Helfrich-Forster, C. (1995) 'The period clock gene is expressed in central nervous system neurons which also produce a neuropeptide that reveals the projections of circadian pacemaker cells within the brain of Drosophila melanogaster', *Proc Natl Acad Sci U S A*, 92(2), pp. 612-6.

Helfrich-Forster, C. (1997) 'Development of pigment-dispersing hormone-immunoreactive neurons in the nervous system of Drosophila melanogaster', *J Comp Neurol*, 380(3), pp. 335-54.

Helfrich-Forster, C. (2000) 'Differential control of morning and evening components in the activity rhythm of Drosophila melanogaster--sex-specific differences suggest a different quality of activity', *J Biol Rhythms*, 15(2), pp. 135-54.

Helfrich-Forster, C. (2004) 'The circadian clock in the brain: a structural and functional comparison between mammals and insects', *J Comp Physiol A Neuroethol Sens Neural Behav Physiol*, 190(8), pp. 601-13.

Helfrich-Forster, C. (2005a) 'Neurobiology of the fruit fly's circadian clock', *Genes Brain Behav*, 4(2), pp. 65-76.

Helfrich-Forster, C. (2005b) 'PDF has found its receptor', *Neuron*, 48(2), pp. 161-3.

Helfrich-Forster, C. (2009) 'Does the morning and evening oscillator model fit better for flies or mice?', *J Biol Rhythms*, 24(4), pp. 259-70.

Helfrich-Förster, C. (1996) 'Drosophila rhythms: from brain to behavior', *Seminars in Cell & Developmental Biology*, 7(6), pp. 791-802.

Helfrich-Forster, C. *et al.* (2002) 'The extraretinal eyelet of Drosophila: development, ultrastructure, and putative circadian function', *J Neurosci*, 22(21), pp. 9255-66.

Helfrich-Forster, C. and Homberg, U. (1993) 'Pigment-dispersing hormone-immunoreactive neurons in the nervous system of wild-type Drosophila melanogaster and of several mutants with altered circadian rhythmicity', *J Comp Neurol*, 337(2), pp. 177-90.

Helfrich-Forster, C. *et al.* (2007a) 'Development and morphology of the clock-gene-expressing lateral neurons of Drosophila melanogaster', *J Comp Neurol*, 500(1), pp. 47-70.

Helfrich-Forster, C., Stengl, M. and Homberg, U. (1998) 'Organization of the circadian system in insects', *Chronobiol Int*, 15(6), pp. 567-94.

Helfrich-Forster, C. *et al.* (2000) 'Ectopic expression of the neuropeptide pigment-dispersing factor alters behavioral rhythms in Drosophila melanogaster', *J Neurosci*, 20(9), pp. 3339-53.

Helfrich-Forster, C. *et al.* (2001) 'The circadian clock of fruit flies is blind after elimination of all known photoreceptors', *Neuron*, 30(1), pp. 249-61.

Helfrich-Forster, C., Wulf, J. and de Belle, J.S. (2002) 'Mushroom body influence on locomotor activity and circadian rhythms in Drosophila melanogaster', *J Neurogenet*, 16(2), pp. 73-109.

Helfrich-Forster, C. *et al.* (2007b) 'The lateral and dorsal neurons of Drosophila melanogaster: new insights about their morphology and function', *Cold Spring Harb Symp Quant Biol*, 72, pp. 517-25.

Hendricks, J.C. *et al.* (2003) 'Gender dimorphism in the role of cycle (BMAL1) in rest, rest regulation, and longevity in Drosophila melanogaster', *J Biol Rhythms*, 18(1), pp. 12-25.

Hermann, C. *et al.* (2012) 'Neuropeptide F immunoreactive clock neurons modify evening locomotor activity and free-running period in Drosophila melanogaster', *J Comp Neurol*, 520(5), pp. 970-87.

Hermann-Luibl, C. *et al.* (2014) 'The ion transport peptide is a new functional clock neuropeptide in the fruit fly Drosophila melanogaster', *J Neurosci*, 34(29), pp. 9522-36.

Highkin, H.R. and Hanson, J.B. (1954) 'Possible Interaction between Light-dark Cycles and Endogenous Daily Rhythms on the Growth of Tomato Plants', *Plant Physiol*, 29(3), pp. 301-2.

Hirsh, J. *et al.* (2010) 'Roles of dopamine in circadian rhythmicity and extreme light sensitivity of circadian entrainment', *Curr Biol*, 20(3), pp. 209-14.

Hlushchenko, I., Koskinen, M. and Hotulainen, P. (2016) 'Dendritic spine actin dynamics in neuronal maturation and synaptic plasticity', *Cytoskeleton (Hoboken)*, 73(9), pp. 435-41.

Ho, K.S. and Sehgal, A. (2005) 'Drosophila melanogaster: an insect model for fundamental studies of sleep', *Methods Enzymol*, 393, pp. 772-93.

Hofmann, W.A. (2009) 'Cell and molecular biology of nuclear actin', *Int Rev Cell Mol Biol*, 273, pp. 219-63.

Honma, S. *et al.* (2012) 'Suprachiasmatic nucleus: cellular clocks and networks', *Prog Brain Res*, 199, pp. 129-41.

Houl, J.H. *et al.* (2008) 'CLOCK expression identifies developing circadian oscillator neurons in the brains of Drosophila embryos', *BMC Neurosci*, 9, p. 119.

Howe, A.K. (2004) 'Regulation of actin-based cell migration by cAMP/PKA', *Biochim Biophys Acta*, 1692(2-3), pp. 159-74.

Hu, J. and Selzer, M.E. (2017) 'RhoA as a target to promote neuronal survival and axon regeneration', *Neural Regen Res*, 12(4), pp. 525-528.

Huang, Z.J., Edery, I. and Rosbash, M. (1993) 'PAS is a dimerization domain common to Drosophila period and several transcription factors', *Nature*, 364(6434), pp. 259-62.

Hung, H.C. *et al.* (2009) 'Sequential and compartment-specific phosphorylation controls the life cycle of the circadian CLOCK protein', *J Biol Chem*, 284(35), pp. 23734-42.

Hunter-Ensor, M., Ousley, A. and Sehgal, A. (1996) 'Regulation of the Drosophila protein timeless suggests a mechanism for resetting the circadian clock by light', *Cell*, 84(5), pp. 677-85.

Hut, R.A. and Beersma, D.G. (2011) 'Evolution of time-keeping mechanisms: early emergence and adaptation to photoperiod', *Philos Trans R Soc Lond B Biol Sci*, 366(1574), pp. 2141-54.

Huveneers, S. and Danen, E.H. (2009) 'Adhesion signaling - crosstalk between integrins, Src and Rho', *J Cell Sci*, 122(Pt 8), pp. 1059-69.

Hyun, S. *et al.* (2005) 'Drosophila GPCR Han is a receptor for the circadian clock neuropeptide PDF', *Neuron*, 48(2), pp. 267-78.

Im, S.H., Li, W. and Taghert, P.H. (2011) 'PDFR and CRY signaling converge in a subset of clock neurons to modulate the amplitude and phase of circadian behavior in Drosophila', *PLoS One*, 6(4), p. e18974.

Im, S.H. and Taghert, P.H. (2010) 'PDF receptor expression reveals direct interactions between circadian oscillators in Drosophila', *J Comp Neurol*, 518(11), pp. 1925-45.

Innocenti, M. *et al.* (2003) 'Phosphoinositide 3-kinase activates Rac by entering in a complex with Eps8, Abi1, and Sos-1', *J Cell Biol*, 160(1), pp. 17-23.

Isaac, R.E. *et al.* (2010) 'Drosophila male sex peptide inhibits siesta sleep and promotes locomotor activity in the post-mated female', *Proc Biol Sci*, 277(1678), pp. 65-70.

ITIS (1996) *Drosophila melanogaster (Meigen, 1830)*. Available at: https://www.itis.gov/ (Accessed: 29th April).

Ito, C. and Tomioka, K. (2016) 'Heterogeneity of the Peripheral Circadian Systems in Drosophila melanogaster: A Review', *Front Physiol*, 7, p. 8.

Ito, M. *et al.* (2004) 'Myosin phosphatase: structure, regulation and function', *Mol Cell Biochem*, 259(1-2), pp. 197-209.

Itoh, T.Q., Matsumoto, A. and Tanimura, T. (2013) 'C-terminal binding protein (CtBP) activates the expression of E-box clock genes with CLOCK/CYCLE in Drosophila', *PLoS One*, 8(4), p. e63113.

Iwase, T. *et al.* (2002) 'Mutation screening of the human Clock gene in circadian rhythm sleep disorders', *Psychiatry Res*, 109(2), pp. 121-8.

Iyer, S.C. *et al.* (2012) 'The RhoGEF trio functions in sculpting class specific dendrite morphogenesis in Drosophila sensory neurons', *PLoS One*, 7(3), p. e33634.

Jackson, F.R. (2011) 'Glial cell modulation of circadian rhythms', *Glia*, 59(9), pp. 1341-50.

Jacobs T. and Hall, C. (2005) 'RHO Family GTPases: RhoGAPs - regulators of the Rho GTPases and more', in Manser, E.J. (ed.) *Proteins and Cell Regulation*. 1st edn. Netherlands: Springer.

Jana, S. *et al.* (2004) 'RNA interference: potential therapeutic targets', *Appl Microbiol Biotechnol*, 65(6), pp. 649-57.

Jaramillo, A.M. *et al.* (2004) 'Pattern of distribution and cycling of SLOB, Slowpoke channel binding protein, in Drosophila', *BMC Neurosci*, 5, p. 3.

Jelen, F. *et al.* (2003) 'PDZ domains - common players in the cell signaling', *Acta Biochim Pol*, 50(4), pp. 985-1017.

Jin, L. *et al.* (2012) 'Single action potentials and subthreshold electrical events imaged in neurons with a fluorescent protein voltage probe', *Neuron*, 75(5), pp. 779-85.

Johard, H.A. *et al.* (2009) 'Peptidergic clock neurons in Drosophila: ion transport peptide and short neuropeptide F in subsets of dorsal and ventral lateral neurons', *J Comp Neurol*, 516(1), pp. 59-73.

Johnson, C.H. (2005) 'Testing the adaptive value of circadian systems', *Methods Enzymol*, 393, pp. 818-37.

Johnson, C.H. (2007) 'Bacterial circadian programs', *Cold Spring Harb Symp Quant Biol*, 72, pp. 395-404.

Johnston, S.A. and Hopper, J.E. (1982) 'Isolation of the yeast regulatory gene GAL4 and analysis of its dosage effects on the galactose/melibiose regulon', *Proc Natl Acad Sci U S A*, 79(22), pp. 6971-5.

Jones, C.R. *et al.* (1999) 'Familial advanced sleep-phase syndrome: A short-period circadian rhythm variant in humans', *Nat Med*, 5(9), pp. 1062-5.

Jones, C.R. *et al.* (2013) 'Genetic basis of human circadian rhythm disorders', *Exp Neurol*, 243, pp. 28-33.

Jursnich, V.A. *et al.* (1990) 'Defective gap-junctional communication associated with imaginal disc overgrowth and degeneration caused by mutations of the dco gene in Drosophila', *Dev Biol*, 140(2), pp. 413-29.

Kadener, S. *et al.* (2009) 'A role for microRNAs in the Drosophila circadian clock', *Genes Dev*, 23(18), pp. 2179-91.

Kadener, S. *et al.* (2007) 'Clockwork Orange is a transcriptional repressor and a new Drosophila circadian pacemaker component', *Genes Dev*, 21(13), pp. 1675-86.

Kalderon, D. (2002) 'Similarities between the Hedgehog and Wnt signaling pathways', *Trends Cell Biol*, 12(11), pp. 523-31.

Kaneko, H. *et al.* (2012) 'Circadian rhythm of temperature preference and its neural control in Drosophila', *Curr Biol*, 22(19), pp. 1851-7.

Kaneko, M. (1998) 'Neural substrates of Drosophila rhythms revealed by mutants and molecular manipulations', *Curr Opin Neurobiol*, 8(5), pp. 652-8.

Kaneko, M. and Hall, J.C. (2000) 'Neuroanatomy of cells expressing clock genes in Drosophila: transgenic manipulation of the period and timeless genes to mark the perikarya of circadian pacemaker neurons and their projections', *J Comp Neurol*, 422(1), pp. 66-94.

Kaneko, M., Hamblen, M.J. and Hall, J.C. (2000) 'Involvement of the period gene in developmental time-memory: effect of the perShort mutation on phase shifts induced by light pulses delivered to Drosophila larvae', *J Biol Rhythms*, 15(1), pp. 13-30.

Kaneko, M., Helfrich-Forster, C. and Hall, J.C. (1997) 'Spatial and temporal expression of the period and timeless genes in the developing nervous system of Drosophila: newly identified pacemaker candidates and novel features of clock gene product cycling', *J Neurosci*, 17(17), pp. 6745-60.

Kantermann, T. *et al.* (2007) 'The human circadian clock's seasonal adjustment is disrupted by daylight saving time', *Curr Biol*, 17(22), pp. 1996-2000.

Karess, R.E. *et al.* (1991) 'The regulatory light chain of nonmuscle myosin is encoded by spaghetti-squash, a gene required for cytokinesis in Drosophila', *Cell*, 65(7), pp. 1177-89.

Katewa, S.D. *et al.* (2016) 'Peripheral Circadian Clocks Mediate Dietary Restriction-Dependent Changes in Lifespan and Fat Metabolism in Drosophila', *Cell Metab*, 23(1), pp. 143-54.

Keene, A.C. *et al.* (2011) 'Distinct visual pathways mediate Drosophila larval light avoidance and circadian clock entrainment', *J Neurosci*, 31(17), pp. 6527-34.

Kelleher, F.C., Rao, A. and Maguire, A. (2014) 'Circadian molecular clocks and cancer', *Cancer Lett*, 342(1), pp. 9-18.

Kher, S.S. *et al.* (2014) 'A novel role for p115RhoGEF in regulation of epithelial plasticity', *PLoS One*, 9(1), p. e85409.

Khericha, M., Kolenchery, J.B. and Tauber, E. (2016) 'Neural and non-neural contributions to sexual dimorphism of mid-day sleep inDrosophila melanogaster: a pilot study', *Physiological Entomology*, pp. n/a-n/a.

Khoo, P. *et al.* (2013) 'In Drosophila, RhoGEF2 cooperates with activated Ras in tumorigenesis through a pathway involving Rho1-Rok-Myosin-II and JNK signalling', *Dis Model Mech*, 6(3), pp. 661-78.

Kidd, P.B., Young, M.W. and Siggia, E.D. (2015) 'Temperature compensation and temperature sensation in the circadian clock', *Proc Natl Acad Sci U S A*, 112(46), pp. E6284-92.

Kim, E.Y. *et al.* (2002a) 'Drosophila CLOCK protein is under posttranscriptional control and influences light-induced activity', *Neuron*, 34(1), pp. 69-81.

Kim, E.Y. and Edery, I. (2006) 'Balance between DBT/CKIepsilon kinase and protein phosphatase activities regulate phosphorylation and stability of Drosophila CLOCK protein', *Proc Natl Acad Sci U S A*, 103(16), pp. 6178-83.

Kim, E.Y. *et al.* (2007) 'A DOUBLETIME kinase binding domain on the Drosophila PERIOD protein is essential for its hyperphosphorylation, transcriptional repression, and circadian clock function', *Mol Cell Biol*, 27(13), pp. 5014-28.

Kim, W.J., Jan, L.Y. and Jan, Y.N. (2013) 'A PDF/NPF neuropeptide signaling circuitry of male Drosophila melanogaster controls rival-induced prolonged mating', *Neuron*, 80(5), pp. 1190-205.

Kim, Y.S. *et al.* (2002b) 'Constitutively active myosin light chain kinase alters axon guidance decisions in Drosophila embryos', *Dev Biol*, 249(2), pp. 367-81.

King, D.P. *et al.* (1997) 'Positional cloning of the mouse circadian clock gene', *Cell*, 89(4), pp. 641-53.

King, H.A. *et al.* (2011) 'Structure of an enclosed dimer formed by the Drosophila period protein', *J Mol Biol*, 413(3), pp. 561-72.

Kivimae, S., Saez, L. and Young, M.W. (2008) 'Activating PER repressor through a DBT-directed phosphorylation switch', *PLoS Biol*, 6(7), p. e183.

Kivimäe, S., Saez, L. and Young, M.W. (2008) 'Activating PER Repressor through a DBT-Directed Phosphorylation Switch', *PLoS Biol*, 6(7).

Klarsfeld, A., Leloup, J.C. and Rouyer, F. (2003) 'Circadian rhythms of locomotor activity in Drosophila', *Behav Processes*, 64(2), pp. 161-175.

Klarsfeld, A. *et al.* (2004) 'Novel features of cryptochrome-mediated photoreception in the brain circadian clock of Drosophila', *J Neurosci*, 24(6), pp. 1468-77.

Klose, M. *et al.* (2016) 'Functional PDF Signaling in the Drosophila Circadian Neural Circuit Is Gated by Ral A-Dependent Modulation', *Neuron*, 90(4), pp. 781-794.

Kloss, B. *et al.* (1998) 'The Drosophila clock gene double-time encodes a protein closely related to human casein kinase Iepsilon', *Cell*, 94(1), pp. 97-107.

Kloss, B. *et al.* (2001) 'Phosphorylation of period is influenced by cycling physical associations of double-time, period, and timeless in the Drosophila clock', *Neuron*, 30(3), pp. 699-706.

Knowles, A. *et al.* (2009) 'The COP9 signalosome is required for light-dependent timeless degradation and Drosophila clock resetting', *J Neurosci*, 29(4), pp. 1152-62.

Ko, H.W., Jiang, J. and Edery, I. (2002) 'Role for Slimb in the degradation of Drosophila Period protein phosphorylated by Doubletime', *Nature*, 420(6916), pp. 673-8.

Ko, H.W. *et al.* (2010) 'A hierarchical phosphorylation cascade that regulates the timing of PERIOD nuclear entry reveals novel roles for proline-directed kinases and GSK-3beta/SGG in circadian clocks', *J Neurosci*, 30(38), pp. 12664-75.

Koh, K., Zheng, X. and Sehgal, A. (2006) 'JETLAG resets the Drosophila circadian clock by promoting light-induced degradation of TIMELESS', *Science*, 312(5781), pp. 1809-12.

Kojima, S. *et al.* (1996) 'A single Drosophila melanogaster myosin light chain kinase gene produces multiple isoforms whose activities are differently regulated', *Genes Cells*, 1(9), pp. 855-71.

Konopka, R.J. and Benzer, S. (1971) 'Clock mutants of Drosophila melanogaster', *Proc Natl Acad Sci U S A*, 68(9), pp. 2112-6.

Koshland, D.E., Jr. (2002) 'Special essay. The seven pillars of life', *Science*, 295(5563), pp. 2215-6.

Krizo, J.A. and Mintz, E.M. (2014) 'Sex differences in behavioral circadian rhythms in laboratory rodents', *Front Endocrinol (Lausanne)*, 5, p. 234.

Krupp, J.J. *et al.* (2013) 'Pigment-dispersing factor modulates pheromone production in clock cells that influence mating in drosophila', *Neuron*, 79(1), pp. 54-68.

Kubli, E. (1992) 'The sex-peptide', *Bioessays*, 14(11), pp. 779-84.

Kumar, S., Chen, D. and Sehgal, A. (2012) 'Dopamine acts through Cryptochrome to promote acute arousal in Drosophila', *Genes Dev*, 26(11), pp. 1224-34.

Kunst, M. *et al.* (2014) 'Calcitonin gene-related peptide neurons mediate sleep-specific circadian output in Drosophila', *Curr Biol*, 24(22), pp. 2652-64.

Lamarche, N. and Hall, A. (1994) 'GAPs for rho-related GTPases', *Trends Genet*, 10(12), pp. 436-40.

Lamba, P. *et al.* (2014) 'Morning and evening oscillators cooperate to reset circadian behavior in response to light input', *Cell Rep*, 7(3), pp. 601-8.

Landgraf, M. (2016) 'Neurogenesis reunited', *Elife*, 5, p. e14955.

Landskron, J. *et al.* (2009) 'A role for the PERIOD:PERIOD homodimer in the Drosophila circadian clock', *PLoS Biol*, 7(4), p. e3.

Larson, D.E., Liberman, Z. and Cagan, R.L. (2008) 'Cellular behavior in the developing Drosophila pupal retina', *Mech Dev*, 125(3-4), pp. 223-32.

Lartey, J. and Lopez Bernal, A. (2009) 'RHO protein regulation of contraction in the human uterus', *Reproduction*, 138(3), pp. 407-24.

Lawrence, P. (1992) *The making of a Fly: The Genetics of Animal Design"*. Oxford: Blackwell Scientific Publications.

Lear, B.C. *et al.* (2005) 'A G protein-coupled receptor, groom-of-PDF, is required for PDF neuron action in circadian behavior', *Neuron*, 48(2), pp. 221-7.

Lear, B.C., Zhang, L. and Allada, R. (2009) 'The neuropeptide PDF acts directly on evening pacemaker neurons to regulate multiple features of circadian behavior', *PLoS Biol*, 7(7), p. e1000154.

Lee, C., Bae, K. and Edery, I. (1998) 'The Drosophila CLOCK protein undergoes daily rhythms in abundance, phosphorylation, and interactions with the PER-TIM complex', *Neuron*, 21(4), pp. 857-67.

Lee, C., Bae, K. and Edery, I. (1999) 'PER and TIM inhibit the DNA binding activity of a Drosophila CLOCK-CYC/dBMAL1 heterodimer without disrupting formation of the heterodimer: a basis for circadian transcription', *Mol Cell Biol*, 19(8), pp. 5316-25.

Lee, E. *et al.* (2016) 'Pacemaker-neuron-dependent disturbance of the molecular clockwork by a Drosophila CLOCK mutant homologous to the mouse Clock mutation', *Proc Natl Acad Sci U S A*, 113(33), pp. E4904-13.

Lee, G., Bahn, J.H. and Park, J.H. (2006) 'Sex- and clock-controlled expression of the neuropeptide F gene in Drosophila', *Proc Natl Acad Sci U S A*, 103(33), pp. 12580-5.

Lee, T. and Luo, L. (1999) 'Mosaic analysis with a repressible cell marker for studies of gene function in neuronal morphogenesis', *Neuron*, 22(3), pp. 451-61.

Lee, T. *et al.* (2000) 'Essential roles of Drosophila RhoA in the regulation of neuroblast proliferation and dendritic but not axonal morphogenesis', *Neuron*, 25(2), pp. 307-16.

Lee, Y. and Montell, C. (2013) 'Drosophila TRPA1 functions in temperature control of circadian rhythm in pacemaker neurons', *J Neurosci*, 33(16), pp. 6716-25.

Levi, F. *et al.* (2010) 'Circadian timing in cancer treatments', *Annu Rev Pharmacol Toxicol*, 50, pp. 377-421.

Levi, F. and Schibler, U. (2007) 'Circadian rhythms: mechanisms and therapeutic implications', *Annu Rev Pharmacol Toxicol*, 47, pp. 593-628.

Levine, J.D. *et al.* (2002) 'Resetting the circadian clock by social experience in Drosophila melanogaster', *Science*, 298(5600), pp. 2010-2.

Li, R. and Zheng, Y. (1997) 'Residues of the Rho family GTPases Rho and Cdc42 that specify sensitivity to Dbl-like guanine nucleotide exchange factors', *J Biol Chem*, 272(8), pp. 4671-9.

Li, X. and Lim, B. (2003) 'RhoGTPases and their role in cancer', *Oncol Res*, 13(6-10), pp. 323-31.

Li, X.T. *et al.* (2014a) '[Current progress in functions of axon guidance molecule Robo and underlying molecular mechanism]', *Sheng Li Xue Bao*, 66(3), pp. 373-85.

Li, Y. *et al.* (2014b) 'PDF and cAMP enhance PER stability in Drosophila clock neurons', *Proc Natl Acad Sci U S A*, 111(13), pp. E1284-90.

Liang, X., Holy, T.E. and Taghert, P.H. (2016) 'Synchronous Drosophila circadian pacemakers display nonsynchronous Ca(2)(+) rhythms in vivo', *Science*, 351(6276), pp. 976-81.

Liang, X., Holy, T.E. and Taghert, P.H. (2017) 'A Series of Suppressive Signals within the Drosophila Circadian Neural Circuit Generates Sequential Daily Outputs', *Neuron*, 94(6), pp. 1173-1189.e4.

Lim, C. *et al.* (2007) 'Targeted inhibition of Pdp1epsilon abolishes the circadian behavior of Drosophila melanogaster', *Biochem Biophys Res Commun*, 364(2), pp. 294-300.

Lim, M.M., Gerstner, J.R. and Holtzman, D.M. (2014) 'The sleep-wake cycle and Alzheimer's disease: what do we know?', *Neurodegener Dis Manag*, 4(5), pp. 351-62.

Lin, C. and Todo, T. (2005) 'The cryptochromes', *Genome Biol*, 6(5), p. 220.

Lin, J.M. *et al.* (2002) 'A role for casein kinase 2alpha in the Drosophila circadian clock', *Nature*, 420(6917), pp. 816-20.

Lin, J.M., Schroeder, A. and Allada, R. (2005) 'In vivo circadian function of casein kinase 2 phosphorylation sites in Drosophila PERIOD', *J Neurosci*, 25(48), pp. 11175-83.

Lin, Y., Stormo, G.D. and Taghert, P.H. (2004) 'The neuropeptide pigment-dispersing factor coordinates pacemaker interactions in the Drosophila circadian system', *J Neurosci*, 24(36), pp. 7951-7.

Lindsley, D.L. and Zimm, G.G. (1992) *The Genome of Drosophila melanogaster*.

Ling, J., Dubruille, R. and Emery, P. (2012) 'KAYAK-alpha modulates circadian transcriptional feedback loops in Drosophila pacemaker neurons', *J Neurosci*, 32(47), pp. 16959-70.

Liu, R. *et al.* (2009) 'Wash functions downstream of Rho and links linear and branched actin nucleation factors', *Development*, 136(16), pp. 2849-60.

Liu, X. *et al.* (1992) 'The period gene encodes a predominantly nuclear protein in adult Drosophila', *J Neurosci*, 12(7), pp. 2735-44.

Liu, Y. and Lehmann, M. (2008) 'A genomic response to the yeast transcription factor GAL4 in Drosophila', *Fly (Austin)*, 2(2), pp. 92-8.

Lloyd, D. and Stupfel, M. (1991) 'The occurrence and functions of ultradian rhythms', *Biol Rev Camb Philos Soc*, 66(3), pp. 275-99.

Loesel, R. and Homberg, U. (2001) 'Anatomy and physiology of neurons with processes in the accessory medulla of the cockroach Leucophaea maderae', *J Comp Neurol*, 439(2), pp. 193-207.

Long, M.A. *et al.* (2005) 'Electrical synapses coordinate activity in the suprachiasmatic nucleus', *Nat Neurosci*, 8(1), pp. 61-6.

Lowrey, P.L. *et al.* (2000) 'Positional syntenic cloning and functional characterization of the mammalian circadian mutation tau', *Science*, 288(5465), pp. 483-92.

Lu, B. *et al.* (2008) 'Circadian modulation of light-induced locomotion responses in Drosophila melanogaster', *Genes Brain Behav*, 7(7), pp. 730-9.

Ludwig, M. *et al.* (2002) 'Intracellular calcium stores regulate activity-dependent neuropeptide release from dendrites', *Nature*, 418(6893), pp. 85-9.

Luo, L. (2000) 'Rho GTPases in neuronal morphogenesis', *Nat Rev Neurosci*, 1(3), pp. 173-80.

Luo, L. (2002) Luo insertions.

Mack, N.A. and Georgiou, M. (2014) 'The interdependence of the Rho GTPases and apicobasal cell polarity', *Small GTPases*, 5(2), p. 10.

Mackay, T.F. (2001) 'Quantitative trait loci in Drosophila', *Nat Rev Genet*, 2(1), pp. 11-20.

Madaule, P. and Axel, R. (1985) 'A novel ras-related gene family', *Cell*, 41(1), pp. 31-40.

Magie, C.R. *et al.* (1999) 'Mutations in the Rho1 small GTPase disrupt morphogenesis and segmentation during early Drosophila development', *Development*, 126(23), pp. 5353-64.

Magie, C.R. and Parkhurst, S.M. (2005) 'Rho1 regulates signaling events required for proper Drosophila embryonic development', *Dev Biol*, 278(1), pp. 144-54.

Mahesh, G. *et al.* (2014) 'Phosphorylation of the transcription activator CLOCK regulates progression through a approximately 24-h feedback loop to influence the circadian period in Drosophila', *J Biol Chem*, 289(28), pp. 19681-93.

Majercak, J. *et al.* (1999) 'How a circadian clock adapts to seasonal decreases in temperature and day length', *Neuron*, 24(1), pp. 219-30.

Mantel, N. (1966) 'Evaluation of survival data and two new rank order statistics arising in its consideration', *Cancer Chemother Rep*, 50(3), pp. 163-70.

Markow, T.A. (2015) 'The secret lives of Drosophila flies', *Elife*, 4.

Martinek, S. *et al.* (2001) 'A role for the segment polarity gene shaggy/GSK-3 in the Drosophila circadian clock', *Cell*, 105(6), pp. 769-79.

Matsumoto, A. *et al.* (2007) 'A functional genomics strategy reveals clockwork orange as a transcriptional regulator in the Drosophila circadian clock', *Genes Dev*, 21(13), pp. 1687-700.

Matsuo, T. and Ishiura, M. (2010) 'New insights into the circadian clock in Chlamydomonas', *Int Rev Cell Mol Biol*, 280, pp. 281-314.

Matus, A. (1999) 'Postsynaptic actin and neuronal plasticity', *Curr Opin Neurobiol*, 9(5), pp. 561-5.

Maury, E., Ramsey, K.M. and Bass, J. (2010) 'Circadian rhythms and metabolic syndrome: from experimental genetics to human disease', *Circ Res*, 106(3), pp. 447-62.

Mazzoni, E.O., Desplan, C. and Blau, J. (2005) 'Circadian pacemaker neurons transmit and modulate visual information to control a rapid behavioral response', *Neuron*, 45(2), pp. 293-300.

McCarthy, D.D. and Seidelmann, K.P. (2009) *Time: From Earth Rotation to Atomic Physics*. Wiley.

McDonald, M.J. and Rosbash, M. (2001) 'Microarray analysis and organization of circadian gene expression in Drosophila', *Cell*, 107(5), pp. 567-78.

McGill, S. *et al.* (1988) 'The molecular analyses of an antimorphic mutation of Drosophila melanogaster, Scutoid', *Genetics*, 119(3), pp. 647-61.

McGuire, S.E. *et al.* (2003) 'Spatiotemporal rescue of memory dysfunction in Drosophila', *Science*, 302(5651), pp. 1765-8.

Mehta, N. and Cheng, H.Y. (2013) 'Micro-managing the circadian clock: The role of microRNAs in biological timekeeping', *J Mol Biol*, 425(19), pp. 3609-24.

Meigen, J.W. (1830) *Systematische Beschreibung der Bekannten Europaischen Zweiflugeligen Insekten*. Digital scanning by Smithsonian Libraries edn.

Meissner, R.A. *et al.* (2008) 'TIMELESS is an important mediator of CK2 effects on circadian clock function in vivo', *J Neurosci*, 28(39), pp. 9732-40.

Menegazzi, P., Yoshii, T. and Helfrich-Forster, C. (2012) 'Laboratory versus nature: the two sides of the Drosophila circadian clock', *J Biol Rhythms*, 27(6), pp. 433-42.

Mertens, I. *et al.* (2005) 'PDF receptor signaling in Drosophila contributes to both circadian and geotactic behaviors', *Neuron*, 48(2), pp. 213-9.

Meuti, M.E. and Denlinger, D.L. (2013) 'Evolutionary links between circadian clocks and photoperiodic diapause in insects', *Integr Comp Biol*, 53(1), pp. 131-43.

Mezan, S. *et al.* (2016) 'PDF Signaling Is an Integral Part of the Drosophila Circadian Molecular Oscillator', *Cell Rep*, 17(3), pp. 708-719.

Michel, S. *et al.* (1993) 'Circadian rhythm in membrane conductance expressed in isolated neurons', *Science*, 259(5092), pp. 239-41.

Miyasako, Y., Umezaki, Y. and Tomioka, K. (2007) 'Separate sets of cerebral clock neurons are responsible for light and temperature entrainment of Drosophila circadian locomotor rhythms', *J Biol Rhythms*, 22(2), pp. 115-26.

Mizuno, T. *et al.* (1999) 'Identification and characterization of Drosophila homolog of Rho-kinase', *Gene*, 238(2), pp. 437-44.

Mohawk, J.A., Green, C.B. and Takahashi, J.S. (2012) 'Central and peripheral circadian clocks in mammals', *Annu Rev Neurosci*, 35, pp. 445-62.

Moon, S.Y. and Zheng, Y. (2003) 'Rho GTPase-activating proteins in cell regulation', *Trends Cell Biol*, 13(1), pp. 13-22.

Moran, D., Softley, R. and Warrant, E.J. (2014) 'Eyeless Mexican cavefish save energy by eliminating the circadian rhythm in metabolism', *PLoS One*, 9(9), p. e107877.

Muraro, N.I. and Ceriani, M.F. (2015) 'Acetylcholine from Visual Circuits Modulates the Activity of Arousal Neurons in Drosophila', *J Neurosci*, 35(50), pp. 16315-27.

Murre, C. *et al.* (1989) 'Interactions between heterologous helix-loop-helix proteins generate complexes that bind specifically to a common DNA sequence', *Cell*, 58(3), pp. 537-44.

Musiek, E.S. and Holtzman, D.M. (2016) 'Mechanisms linking circadian clocks, sleep, and neurodegeneration', *Science*, 354(6315), pp. 1004-1008.

Musiek, E.S., Xiong, D.D. and Holtzman, D.M. (2015) 'Sleep, circadian rhythms, and the pathogenesis of Alzheimer disease', *Exp Mol Med*, 47, p. e148.

Mutterer, J. and Zinck, E. (2013) 'Quick-and-clean article figures with FigureJ', *J Microsc*, 252(1), pp. 89-91.

Myers, E.M., Yu, J. and Sehgal, A. (2003) 'Circadian control of eclosion: interaction between a central and peripheral clock in Drosophila melanogaster', *Curr Biol*, 13(6), pp. 526-33.

Myers, M.P. *et al.* (1996) 'Light-induced degradation of TIMELESS and entrainment of the Drosophila circadian clock', *Science*, 271(5256), pp. 1736-40.

Myers, M.P. *et al.* (1995) 'Positional cloning and sequence analysis of the Drosophila clock gene, timeless', *Science*, 270(5237), pp. 805-8.

Nagoshi, E. *et al.* (2004) 'Circadian gene expression in individual fibroblasts: Cell-autonomous and self-sustained oscillators pass time to daughter cells', *Cell*, 119(5), pp. 693-705.

Nagoshi, E. *et al.* (2010) 'Dissecting differential gene expression within the circadian neuronal circuit of Drosophila', *Nat Neurosci*, 13(1), pp. 60-8.

Nahm, M. and Lee, S. (2011) 'Characterization of the Rho GTPase-Activating Protein RhoGAP68F', *Exp Neurobiol*, 20(1), pp. 29-34.

Nakane, Y. *et al.* (2010) 'A mammalian neural tissue opsin (Opsin 5) is a deep brain photoreceptor in birds', *Proc Natl Acad Sci U S A*, 107(34), pp. 15264-8.

Nassel, D.R. *et al.* (1993) 'Pigment-dispersing hormone-like peptide in the nervous system of the flies Phormia and Drosophila: immunocytochemistry and partial characterization', *J Comp Neurol*, 331(2), pp. 183-98.

Nassel, D.R. and Winther, A.M. (2010) 'Drosophila neuropeptides in regulation of physiology and behavior', *Prog Neurobiol*, 92(1), pp. 42-104.

Nawathean, P., Stoleru, D. and Rosbash, M. (2007) 'A small conserved domain of Drosophila PERIOD is important for circadian phosphorylation, nuclear localization, and transcriptional repressor activity', *Mol Cell Biol*, 27(13), pp. 5002-13.

Neisch, A.L. *et al.* (2010) 'Rho1 regulates apoptosis via activation of the JNK signaling pathway at the plasma membrane', *J Cell Biol*, 189(2), pp. 311-23.

Newsome, T.P. *et al.* (2000) 'Trio combines with dock to regulate Pak activity during photoreceptor axon pathfinding in Drosophila', *Cell*, 101(3), pp. 283-94.

Ng, F.S. and Jackson, F.R. (2015) 'The ROP vesicle release factor is required in adult Drosophila glia for normal circadian behavior', *Front Cell Neurosci*, 9, p. 256.

Ng, F.S., Tangredi, M.M. and Jackson, F.R. (2011) 'Glial cells physiologically modulate clock neurons and circadian behavior in a calcium-dependent manner', *Curr Biol*, 21(8), pp. 625-34.

Ni, J.Q. *et al.* (2009) 'A Drosophila resource of transgenic RNAi lines for neurogenetics', *Genetics*, 182(4), pp. 1089-100.

Ni, J.Q. *et al.* (2008) 'Vector and parameters for targeted transgenic RNA interference in Drosophila melanogaster', *Nat Methods*, 5(1), pp. 49-51.

Ni, J.Q. *et al.* (2010) A genome-scale shRNA resource for transgenic RNAi in Drosophila.

Ni, J.Q. *et al.* (2011a) TRiP germline vectors pVALIUM20, pVALIUM21 and pVALIUM22.

Ni, J.Q. *et al.* (2011b) 'A genome-scale shRNA resource for transgenic RNAi in Drosophila', *Nature Methods*, 8(5), pp. 405-407.

Nicholson, L. *et al.* (2008) 'Spatial and Temporal Control of Gene Expression in Drosophila Using the Inducible GeneSwitch GAL4 System. I. Screen for Larval Nervous System Drivers', *Genetics*, 178(1), pp. 215-34.

Nikhil, K.L., Abhilash, L. and Sharma, V.K. (2016) 'Molecular Correlates of Circadian Clocks in Fruit Fly Drosophila melanogaster Populations Exhibiting early and late Emergence Chronotypes', *J Biol Rhythms*, 31(2), pp. 125-41.

Ohashi, K. *et al.* (2000a) 'A Drosophila homolog of LIM-kinase phosphorylates cofilin and induces actin cytoskeletal reorganization', *Biochem Biophys Res Commun*, 276(3), pp. 1178-85.

Ohashi, K. *et al.* (2000b) 'Rho-associated kinase ROCK activates LIM-kinase 1 by phosphorylation at threonine 508 within the activation loop', *J Biol Chem*, 275(5), pp. 3577-82.

Ojelade, S.A., Acevedo, S.F. and Rothenfluh, A. (2013) 'The role of the actin cytoskeleton in regulating Drosophila behavior', *Rev Neurosci*, 24(5), pp. 471-84.

Okamura, K. *et al.* (2008) 'The Drosophila hairpin RNA pathway generates endogenous short interfering RNAs', *Nature*, 453(7196), pp. 803-6.

Ono, D., Honma, S. and Honma, K. (2016) 'Differential roles of AVP and VIP signaling in the postnatal changes of neural networks for coherent circadian rhythms in the SCN', *Sci Adv*, 2(9), p. e1600960.

Ortiz-Tudela, E. *et al.* (2014) 'The circadian rest-activity rhythm, a potential safety pharmacology endpoint of cancer chemotherapy', *Int J Cancer*, 134(11), pp. 2717-25.

Ouyang, Y. *et al.* (1998) 'Resonating circadian clocks enhance fitness in cyanobacteria', *Proc Natl Acad Sci U S A*, 95(15), pp. 8660-4.

Ozturk, N. *et al.* (2011) 'Reaction mechanism of Drosophila cryptochrome', *Proc Natl Acad Sci U S A*, 108(2), pp. 516-21.

Ozturk, N. *et al.* (2014) 'Mechanism of photosignaling by Drosophila cryptochrome: role of the redox status of the flavin chromophore', *J Biol Chem*, 289(8), pp. 4634-42.

Ozturk, N. *et al.* (2007) 'Structure and function of animal cryptochromes', *Cold Spring Harb Symp Quant Biol*, 72, pp. 119-31.

Pan, H. *et al.* (2015) 'Selection of Reference Genes for RT-qPCR Analysis in the Monarch Butterfly, Danaus plexippus (L.), a Migrating Bio-Indicator', *PLoS One*, 10(6), p. e0129482.

Pantaloni, D. and Carlier, M.F. (1993) 'How profilin promotes actin filament assembly in the presence of thymosin beta 4', *Cell*, 75(5), pp. 1007-14.

Parisky, K.M. *et al.* (2008) 'PDF cells are a GABA-responsive wake-promoting component of the Drosophila sleep circuit', *Neuron*, 60(4), pp. 672-82.

Park, D. and Griffith, L.C. (2006) 'Electrophysiological and anatomical characterization of PDF-positive clock neurons in the intact adult Drosophila brain', *J Neurophysiol*, 95(6), pp. 3955-60.

Park, D. *et al.* (2008) 'Mapping peptidergic cells in Drosophila: where DIMM fits in', *PLoS One*, 3(3), p. e1896.

Park, J.H. and Hall, J.C. (1998) 'Isolation and chronobiological analysis of a neuropeptide pigment-dispersing factor gene in Drosophila melanogaster', *J Biol Rhythms*, 13(3), pp. 219-28.

Park, J.H. *et al.* (2000) 'Differential regulation of circadian pacemaker output by separate clock genes in Drosophila', *Proc Natl Acad Sci U S A*, 97(7), pp. 3608-13.

Park, S. *et al.* (2014) 'SIFamide and SIFamide receptor defines a novel neuropeptide signaling to promote sleep in Drosophila', *Mol Cells*, 37(4), pp. 295-301.

Paul, K.N. *et al.* (2006) 'Diurnal sex differences in the sleep-wake cycle of mice are dependent on gonadal function', *Sleep*, 29(9), pp. 1211-23.

Pawlowski, R. *et al.* (2010) 'An actin-regulated importin alpha/beta-dependent extended bipartite NLS directs nuclear import of MRTF-A', *EMBO J*, 29(20), pp. 3448-58.

Pegoraro, M. *et al.* (2014) 'Role for circadian clock genes in seasonal timing: testing the bunning hypothesis', *PLoS Genet*, 10(9), p. e1004603.

Peng, Y. *et al.* (2003) 'Drosophila free-running rhythms require intercellular communication', *PLoS Biol*, 1(1), p. E13.

Perrimon, N. (2003) *DRSC Functional Genomics Resources (DRSC-FGR)* Available at: http://www.flyrnai.org/RNAi_find_frag_free.html.

Peschel, N. *et al.* (2009) 'Light-dependent interactions between the Drosophila circadian clock factors cryptochrome, jetlag, and timeless', *Curr Biol*, 19(3), pp. 241-7.

Peschel, N. and Helfrich-Forster, C. (2011) 'Setting the clock--by nature: circadian rhythm in the fruitfly Drosophila melanogaster', *FEBS Lett*, 585(10), pp. 1435-42.

Petsakou, A., Sapsis, T.P. and Blau, J. (2015) 'Circadian Rhythms in Rho1 Activity Regulate Neuronal Plasticity and Network Hierarchy', *Cell*.

Pfeiffenberger, C. *et al.* (2010) 'Processing circadian data collected from the Drosophila Activity Monitoring (DAM) System', *Cold Spring Harb Protoc*, 2010(11), p. pdb.prot5519.

Pfeiffer, B.D. *et al.* (2011) GAL4 Driver Collection of Rubin Laboratory at Janelia Farm.

Pfeiffer, B.D. *et al.* (2010) 'Refinement of tools for targeted gene expression in Drosophila', *Genetics*, 186(2), pp. 735-55.

Pham, C.D. *et al.* (2009) 'Ustilago maydis Rho1 and 14-3-3 homologues participate in pathways controlling cell separation and cell polarity', *Eukaryot Cell*, 8(7), pp. 977-89.

Picot, M. *et al.* (2007) 'Light activates output from evening neurons and inhibits output from morning neurons in the Drosophila circadian clock', *PLoS Biol*, 5(11), p. e315.

Piggins, H.D. and Cutler, D.J. (2003) 'The roles of vasoactive intestinal polypeptide in the mammalian circadian clock', *J Endocrinol*, 177(1), pp. 7-15.

Pilgram, G.S. *et al.* (2011) 'The RhoGAP crossveinless-c interacts with Dystrophin and is required for synaptic homeostasis at the Drosophila neuromuscular junction', *J Neurosci*, 31(2), pp. 492-500.

Pili-Floury, S. *et al.* (2004) 'In vivo RNA interference analysis reveals an unexpected role for GNBP1 in the defense against Gram-positive bacterial infection in Drosophila adults', *J Biol Chem*, 279(13), pp. 12848-53.

Pinna, L.A. and Meggio, F. (1997) 'Protein kinase CK2 ("casein kinase-2") and its implication in cell division and proliferation', *Prog Cell Cycle Res*, 3, pp. 77-97.

Pirooznia, S.K. *et al.* (2012) 'Epigenetic regulation of axonal growth of Drosophila pacemaker cells by histone acetyltransferase tip60 controls sleep', *Genetics*, 192(4), pp. 1327-45.

Pittendrigh, C.S. (1954) 'On temperature independence in the clock system controlling emergence time in Drosophila', *Proc Natl Acad Sci U S A*, 40(10), pp. 1018-29.

Pittendrigh, C.S. (1958) 'Perspectives in the study of biological clocks', in Buzzari-Traverso, A.A. (ed.) *Perspectives in marine biology*. University of California Press, Berkeley, pp. 239-268.

Pittendrigh, C.S. (1993) 'Temporal organization: reflections of a Darwinian clock-watcher', *Annu Rev Physiol*, 55, pp. 16-54.

Pittendrigh, C.S. and Daan, S. (1976) 'A functional analysis of circadian pacemakers in nocturnal rodents. V. Pacemaker structure: a clock for all seasons', *J Comp Physiol*, (106), pp. 333-355.

Plautz, J.D. *et al.* (1997) 'Independent photoreceptive circadian clocks throughout Drosophila', *Science*, 278(5343), pp. 1632-5.

Portaluppi, F. *et al.* (1994) 'Progressive disruption of the circadian rhythm of melatonin in fatal familial insomnia', *J Clin Endocrinol Metab*, 78(5), pp. 1075-8.

Prakash, P., Nambiar, A. and Sheeba, V. (2017) 'Oscillating PDF in termini of circadian pacemaker neurons and synchronous molecular clocks in downstream neurons are not sufficient for sustenance of activity rhythms in constant darkness', *PLoS One*, 12(5), p. e0175073.

Preckel, F. *et al.* (2013) 'Morningness-eveningness and educational outcomes: the lark has an advantage over the owl at high school', *Br J Educ Psychol*, 83(Pt 1), pp. 114-34.

Prendergast, B.J., Onishi, K.G. and Zucker, I. (2014) 'Female mice liberated for inclusion in neuroscience and biomedical research', *Neurosci Biobehav Rev*, 40, pp. 1-5.

Price, J.L. *et al.* (1998) 'double-time is a novel Drosophila clock gene that regulates PERIOD protein accumulation', *Cell*, 94(1), pp. 83-95.

Prokop, A. *et al.* (2013) 'Using fly genetics to dissect the cytoskeletal machinery of neurons during axonal growth and maintenance', *J Cell Sci*, 126(Pt 11), pp. 2331-41.

Prokopenko, S.N. *et al.* (1999) 'A putative exchange factor for Rho1 GTPase is required for initiation of cytokinesis in Drosophila', *Genes Dev*, 13(17), pp. 2301-14.

Ptashne, M. (1988) 'How eukaryotic transcriptional activators work', *Nature*, 335(6192), pp. 683-9.

Rao, K.R. and Riehm, J.P. (1988) 'Pigment-dispersing hormones: a novel family of neuropeptides from arthropods', *Peptides*, 9 Suppl 1, pp. 153-9.

Rao, K.R. and Riehm, J.P. (1993) 'Pigment-dispersing hormones', *Ann N Y Acad Sci*, 680, pp. 78-88.

Rasband, W. (2007) *Concentric Circles, an ImageJ plugin*.

Raza, Q.S., Vanderploeg, J.L. and Jacobs, J.R. (2017) 'Matrix Metalloproteinases are required for membrane motility and lumenogenesis during Drosophila heart development', *PLoS One*, 12(2), p. e0171905.

Reddy, K.L. *et al.* (2000) 'The Drosophila PAR domain protein 1 (Pdp1) gene encodes multiple differentially expressed mRNAs and proteins through the use of multiple enhancers and promoters', *Dev Biol*, 224(2), pp. 401-14.

Reischig, T. and Stengl, M. (2003) 'Ectopic transplantation of the accessory medulla restores circadian locomotor rhythms in arrhythmic cockroaches (Leucophaea maderae)', *J Exp Biol*, 206(Pt 11), pp. 1877-86.

Rekart, J.L., Holahan, M.R. and Routtenberg, A. (2007) 'Presynaptic Structural Plasticity and Long-Lasting Memory: Focus on Learning-Induced Redistribution of Hippocampal Mossy Fibers', in Bermudez-Rattoni, F. (ed.) *Neural Plasticity and Memory: From Genes to Brain Imaging*. Boca Raton (FL): CRC Press/Taylor & Francis Taylor & Francis Group, LLC.

Renn, S.C. *et al.* (1999) 'A pdf neuropeptide gene mutation and ablation of PDF neurons each cause severe abnormalities of behavioral circadian rhythms in Drosophila', *Cell*, 99(7), pp. 791-802.

Rezaval, C. *et al.* (2016) 'Activation of Latent Courtship Circuitry in the Brain of Drosophila Females Induces Male-like Behaviors', *Curr Biol*, 26(18), pp. 2508-15.

Ridley, A.J. (2001) 'Rho GTPases and cell migration', *J Cell Sci*, 114(Pt 15), pp. 2713-22.

Ridley, A.J. and Hall, A. (1992) 'The small GTP-binding protein rho regulates the assembly of focal adhesions and actin stress fibers in response to growth factors', *Cell*, 70(3), pp. 389-99.

Rieger, D. *et al.* (2007) 'The fruit fly Drosophila melanogaster favors dim light and times its activity peaks to early dawn and late dusk', *J Biol Rhythms*, 22(5), pp. 387-99.

Rieger, D. *et al.* (2006) 'Functional analysis of circadian pacemaker neurons in Drosophila melanogaster', *J Neurosci*, 26(9), pp. 2531-43.

Rieger, D., Stanewsky, R. and Helfrich-Forster, C. (2003) 'Cryptochrome, compound eyes, Hofbauer-Buchner eyelets, and ocelli play different roles in the entrainment and masking pathway of the locomotor activity rhythm in the fruit fly Drosophila melanogaster', *J Biol Rhythms*, 18(5), pp. 377-91.

Rieger, D. *et al.* (2009) 'Period gene expression in four neurons is sufficient for rhythmic activity of Drosophila melanogaster under dim light conditions', *J Biol Rhythms*, 24(4), pp. 271-82.

Riento, K. and Ridley, A.J. (2003) 'Rocks: multifunctional kinases in cell behaviour', *Nat Rev Mol Cell Biol*, 4(6), pp. 446-56.

Roessingh, S., Wolfgang, W. and Stanewsky, R. (2015) 'Loss of Drosophila melanogaster TRPA1 Function Affects "Siesta" Behavior but Not Synchronization to Temperature Cycles', *J Biol Rhythms*.

Rohatgi, R., Ho, H.Y. and Kirschner, M.W. (2000) 'Mechanism of N-WASP activation by CDC42 and phosphatidylinositol 4, 5-bisphosphate', *J Cell Biol*, 150(6), pp. 1299-310.

Rothenfluh, A., Young, M.W. and Saez, L. (2000) 'A TIMELESS-independent function for PERIOD proteins in the Drosophila clock', *Neuron*, 26(2), pp. 505-14.

Rothwell, W.F. and Sullivan, W. (2007) 'Drosophila embryo dechorionation', *CSH Protoc*, 2007, p. pdb.prot4826.

Ruchhoeft, M.L. *et al.* (1999) 'The neuronal architecture of Xenopus retinal ganglion cells is sculpted by rho-family GTPases in vivo', *J Neurosci*, 19(19), pp. 8454-63.

Ruiz, S. *et al.* (2010) 'Spatio-temporal pattern of cells expressing the clock genes period and timeless and the lineages of period expressing neurons in the embryonic CNS of Drosophila melanogaster', *Gene Expr Patterns*, 10(6), pp. 274-82.

Rusconi, J.C., Hays, R. and Cagan, R.L. (2000) 'Programmed cell death and patterning in Drosophila', *Cell Death Differ*, 7(11), pp. 1063-70.

Rutila, J.E. *et al.* (1998) 'CYCLE is a second bHLH-PAS clock protein essential for circadian rhythmicity and transcription of Drosophila period and timeless', *Cell*, 93(5), pp. 805-14.

Ryder, E. *et al.* (2007) 'The DrosDel deletion collection: a Drosophila genomewide chromosomal deficiency resource', *Genetics*, 177(1), pp. 615-29.

Sabado, V. *et al.* (2017) 'Fluorescence circadian imaging reveals a PDF-dependent transcriptional regulation of the Drosophila molecular clock', *Sci Rep*, 7, p. 41560.

Saez, L. *et al.* (2011) 'A key temporal delay in the circadian cycle of Drosophila is mediated by a nuclear localization signal in the timeless protein', *Genetics*, 188(3), pp. 591-600.

Saez, L. and Young, M.W. (1996) 'Regulation of nuclear entry of the Drosophila clock proteins period and timeless', *Neuron*, 17(5), pp. 911-20.

Sathyanarayanan, S. *et al.* (2004) 'Posttranslational regulation of Drosophila PERIOD protein by protein phosphatase 2A', *Cell*, 116(4), pp. 603-15.

Scemes, E., Spray, D.C. and Meda, P. (2009) 'Connexins, pannexins, innexins: novel roles of "hemi-channels"', *Pflugers Arch*, 457(6), pp. 1207-26.

Schlessinger, K., Hall, A. and Tolwinski, N. (2009) 'Wnt signaling pathways meet Rho GTPases', *Genes Dev*, 23(3), pp. 265-77.

Schlichting, M. *et al.* (2016) 'A Neural Network Underlying Circadian Entrainment and Photoperiodic Adjustment of Sleep and Activity in Drosophila', *J Neurosci*, 36(35), pp. 9084-96.

Schmidt, S. and Debant, A. (2014) 'Function and regulation of the Rho guanine nucleotide exchange factor Trio', *Small GTPases*, 5, p. e29769.

Schmittgen, T.D. and Livak, K.J. (2008) 'Analyzing real-time PCR data by the comparative C(T) method', *Nat Protoc*, 3(6), pp. 1101-8.

Schubert, F., Helfrich-Forster, C. and Rieger, D. (2016) *Poster presented at 16th European Neurobiology of Drosophila (Neurofly) Conference*. Platanias, Crete, Greece.

Scott, G. and Leopardi, S. (2003) 'The cAMP signaling pathway has opposing effects on Rac and Rho in B16F10 cells: implications for dendrite formation in melanocytic cells', *Pigment Cell Res*, 16(2), pp. 139-48.

Sehadova, H. *et al.* (2009) 'Temperature entrainment of Drosophila's circadian clock involves the gene nocte and signaling from peripheral sensory tissues to the brain', *Neuron*, 64(2), pp. 251-66.

Sehgal, A., Price, J. and Young, M.W. (1992) 'Ontogeny of a biological clock in Drosophila melanogaster', *Proc Natl Acad Sci U S A*, 89(4), pp. 1423-7.

Sehgal, A. *et al.* (1994) 'Loss of circadian behavioral rhythms and per RNA oscillations in the Drosophila mutant timeless', *Science*, 263(5153), pp. 1603-6.

Seluzicki, A. *et al.* (2014) 'Dual PDF signaling pathways reset clocks via TIMELESS and acutely excite target neurons to control circadian behavior', *PLoS Biol*, 12(3), p. e1001810.

Sensi, S., Pace Palitti, V. and Guagnano, M.T. (1993) 'Chronobiology in endocrinology', *Ann Ist Super Sanita*, 29(4), pp. 613-31.

Shafer, O.T. *et al.* (2006) 'Reevaluation of Drosophila melanogaster's neuronal circadian pacemakers reveals new neuronal classes', *J Comp Neurol*, 498(2), pp. 180-93.

Shafer, O.T. *et al.* (2008) 'Widespread receptivity to neuropeptide PDF throughout the neuronal circadian clock network of Drosophila revealed by real-time cyclic AMP imaging', *Neuron*, 58(2), pp. 223-37.

Shafer, O.T., Rosbash, M. and Truman, J.W. (2002) 'Sequential nuclear accumulation of the clock proteins period and timeless in the pacemaker neurons of Drosophila melanogaster', *J Neurosci*, 22(14), pp. 5946-54.

Shafer, O.T. and Taghert, P.H. (2009) 'RNA-interference knockdown of Drosophila pigment dispersing factor in neuronal subsets: the anatomical basis of a neuropeptide's circadian functions', *PLoS One*, 4(12), p. e8298.

Shang, Y. *et al.* (2013) 'Short neuropeptide F is a sleep-promoting inhibitory modulator', *Neuron*, 80(1), pp. 171-83.

Shao, W. *et al.* (2010) 'A modifier screen for Bazooka/PAR-3 interacting genes in the Drosophila embryo epithelium', *PLoS One*, 5(4), p. e9938.

Shearman, L.P. *et al.* (1997) 'Two period homologs: circadian expression and photic regulation in the suprachiasmatic nuclei', *Neuron*, 19(6), pp. 1261-9.

Sheeba, V. (2008) 'The Drosophila melanogaster circadian pacemaker circuit', *J Genet*, 87(5), pp. 485-93.

Sheeba, V., Fogle, K.J. and Holmes, T.C. (2010) 'Persistence of morning anticipation behavior and high amplitude morning startle response following functional loss of small ventral lateral neurons in Drosophila', *PLoS One*, 5(7), p. e11628.

Sheeba, V. *et al.* (2008a) 'Large ventral lateral neurons modulate arousal and sleep in Drosophila', *Curr Biol*, 18(20), pp. 1537-45.

Sheeba, V. *et al.* (2008b) 'Circadian- and light-dependent regulation of resting membrane potential and spontaneous action potential firing of Drosophila circadian pacemaker neurons', *J Neurophysiol*, 99(2), pp. 976-88.

Sheeba, V. *et al.* (1999) 'Persistence of eclosion rhythm in Drosophila melanogaster after 600 generations in an aperiodic environment', *Naturwissenschaften*, 86(9), pp. 448-9.

Shinohara, Y. *et al.* (2017) 'Temperature-Sensitive Substrate and Product Binding Underlie Temperature-Compensated Phosphorylation in the Clock', *Mol Cell*, 67(5), pp. 783-798.e20.

Shivalkar, M. and Giniger, E. (2012) 'Control of dendritic morphogenesis by Trio in Drosophila melanogaster', *PLoS One*, 7(3), p. e33737.

Sholl, D.A. (1953) 'Dendritic organization in the neurons of the visual and motor cortices of the cat', *J Anat*, 87(4), pp. 387-406.

Sidote, D. *et al.* (1998) 'Differential effects of light and heat on the Drosophila circadian clock proteins PER and TIM', *Mol Cell Biol*, 18(4), pp. 2004-13.

Simoni, A. *et al.* (2014) 'A mechanosensory pathway to the Drosophila circadian clock', *Science*, 343(6170), pp. 525-8.

Simons, T.J. (1988) 'Calcium and neuronal function', *Neurosurg Rev*, 11(2), pp. 119-29.

Singh, R., Sharma, P.K. and Malviya, R. (2012) 'Circadian cycle and chronotherapeutics: recent trend for the treatment of various biological disorders', *Recent Pat Drug Deliv Formul*, 6(1), pp. 80-91.

Soper, D.S. (2014) *Fisher's Exact Test Calculator for a 2x3 Contingency Table*. Available at: http://www.danielsoper.com/statcalc3/calc.aspx?id=58.

Spindler, S.R. and Hartenstein, V. (2010) 'The Drosophila neural lineages: a model system to study brain development and circuitry', *Dev Genes Evol*, 220(1-2), pp. 1-10.

Sridhar, G.R. and Sanjana, N.S. (2016) 'Sleep, circadian dysrhythmia, obesity and diabetes', *World J Diabetes*, 7(19), pp. 515-522.

Staiger, D. and Koster, T. (2011) 'Spotlight on post-transcriptional control in the circadian system', *Cell Mol Life Sci*, 68(1), pp. 71-83.

Stanewsky, R. *et al.* (1997) 'Temporal and spatial expression patterns of transgenes containing increasing amounts of the Drosophila clock gene period and a lacZ reporter: mapping elements of the PER protein involved in circadian cycling', *J Neurosci*, 17(2), pp. 676-96.

Stanewsky, R. *et al.* (1998) 'The cryb mutation identifies cryptochrome as a circadian photoreceptor in Drosophila', *Cell*, 95(5), pp. 681-92.

Stephan, F.K. and Zucker, I. (1972) 'Circadian rhythms in drinking behavior and locomotor activity of rats are eliminated by hypothalamic lesions', *Proc Natl Acad Sci U S A*, 69(6), pp. 1583-6.

Stevens, L.J. and Page-McCaw, A. (2012) 'A secreted MMP is required for reepithelialization during wound healing', *Mol Biol Cell*, 23(6), pp. 1068-79.

Stoleru, D. *et al.* (2007) 'The Drosophila circadian network is a seasonal timer', *Cell*, 129(1), pp. 207-19.

Stoleru, D. *et al.* (2004) 'Coupled oscillators control morning and evening locomotor behaviour of Drosophila', *Nature*, 431(7010), pp. 862-8.

Strutt, D.I., Weber, U. and Mlodzik, M. (1997) 'The role of RhoA in tissue polarity and Frizzled signalling', *Nature*, 387(6630), pp. 292-5.

Suh, J. and Jackson, F.R. (2007) 'Drosophila ebony activity is required in glia for the circadian regulation of locomotor activity', *Neuron*, 55(3), pp. 435-47.

Sun, Z.S. *et al.* (1997) 'RIGUI, a putative mammalian ortholog of the Drosophila period gene', *Cell*, 90(6), pp. 1003-11.

Suster, M.L. *et al.* (2004) 'Refining GAL4-driven transgene expression in Drosophila with a GAL80 enhancer-trap', *Genesis*, 39(4), pp. 240-5.

Sweatt, J.D. (2016) 'Neural plasticity and behavior - sixty years of conceptual advances', *J Neurochem*, 139 Suppl 2, pp. 179-199.

Sweeney, B.M. (1963) 'Resetting the Biological Clock in Gonyaulax with Ultraviolet Light', *Plant Physiol*, 38(6), pp. 704-8.

Sweeney, B.M. and Hastings, J.W. (1960) 'Effects of temperature upon diurnal rhythms', *Cold Spring Harb Symp Quant Biol*, 25, pp. 87-104.

Symons, M. and Rusk, N. (2003) 'Control of vesicular trafficking by Rho GTPases', *Curr Biol*, 13(10), pp. R409-18.

Szklarczyk, D. *et al.* (2017) 'The STRING database in 2017: quality-controlled protein-protein association networks, made broadly accessible', *Nucleic Acids Res*, 45(D1), pp. D362-d368.

Szular, J. *et al.* (2012) 'Rhodopsin 5- and Rhodopsin 6-mediated clock synchronization in Drosophila melanogaster is independent of retinal phospholipase C-beta signaling', *J Biol Rhythms*, 27(1), pp. 25-36.

Taghert, P.H. *et al.* (2001) 'Multiple amidated neuropeptides are required for normal circadian locomotor rhythms in Drosophila', *J Neurosci*, 21(17), pp. 6673-86.

Taghert, P.H. and Shafer, O.T. (2006) 'Mechanisms of clock output in the Drosophila circadian pacemaker system', *J Biol Rhythms*, 21(6), pp. 445-57.

Tang, X. *et al.* (2013) 'Temperature integration at the AC thermosensory neurons in Drosophila', *J Neurosci*, 33(3), pp. 894-901.

Tang, X. *et al.* (2017) 'The role of PDF neurons in setting the preferred temperature before dawn in Drosophila', *Elife*, 6.

Tanoue, S. *et al.* (2004) 'Circadian clocks in antennal neurons are necessary and sufficient for olfaction rhythms in Drosophila', *Curr Biol*, 14(8), pp. 638-49.

Tashiro, A., Minden, A. and Yuste, R. (2000) 'Regulation of dendritic spine morphology by the rho family of small GTPases: antagonistic roles of Rac and Rho', *Cereb Cortex*, 10(10), pp. 927-38.

Tataroglu, O. and Emery, P. (2014) 'Studying circadian rhythms in Drosophila melanogaster', *Methods*, 68(1), pp. 140-50.

Tissot, M. and Stocker, R.F. (2000) 'Metamorphosis in drosophila and other insects: the fate of neurons throughout the stages', *Prog Neurobiol*, 62(1), pp. 89-111.

Toh, K.L. *et al.* (2001) 'An hPer2 phosphorylation site mutation in familial advanced sleep phase syndrome', *Science*, 291(5506), pp. 1040-3.

Tolias, K.F., Duman, J.G. and Um, K. (2011) 'Control of synapse development and plasticity by Rho GTPase regulatory proteins', *Prog Neurobiol*, 94(2), pp. 133-48.

Tosini, G., Ferguson, I. and Tsubota, K. (2016) 'Effects of blue light on the circadian system and eye physiology', *Mol Vis*, 22, pp. 61-72.

Totsukawa, G. *et al.* (2000) 'Distinct roles of ROCK (Rho-kinase) and MLCK in spatial regulation of MLC phosphorylation for assembly of stress fibers and focal adhesions in 3T3 fibroblasts', *J Cell Biol*, 150(4), pp. 797-806.

Truman, J.W. (1990) 'Metamorphosis of the central nervous system of Drosophila', *J Neurobiol*, 21(7), pp. 1072-84.

Truman, J.W. and Bate, M. (1988) 'Spatial and temporal patterns of neurogenesis in the central nervous system of Drosophila melanogaster', *Dev Biol*, 125(1), pp. 145-57.

Umezaki, Y. and Tomioka, K. (2008) 'Behavioral dissection of the Drosophila circadian multioscillator system that regulates locomotor rhythms', *Zoolog Sci*, 25(11), pp. 1146-55.

Vaidya, A.T. *et al.* (2013) 'Flavin reduction activates Drosophila cryptochrome', *Proc Natl Acad Sci U S A*, 110(51), pp. 20455-60.

Van Roessel, P. *et al.* (2002) 'Two-color GFP imaging demonstrates cell-autonomy of GAL4-driven RNA interference in Drosophila', *Genesis*, 34(1-2), pp. 170-3.

Vanin, S. *et al.* (2012) 'Unexpected features of Drosophila circadian behavioural rhythms under natural conditions', *Nature*, 484(7394), pp. 371-5.

VanVickle-Chavez, S.J. and Van Gelder, R.N. (2007) 'Action spectrum of Drosophila cryptochrome', *J Biol Chem*, 282(14), pp. 10561-6.

Vecsey, C.G., Pirez, N. and Griffith, L.C. (2014) 'The Drosophila neuropeptides PDF and sNPF have opposing electrophysiological and molecular effects on central neurons', *J Neurophysiol*, 111(5), pp. 1033-45.

Veleri, S. *et al.* (2003) 'A self-sustaining, light-entrainable circadian oscillator in the Drosophila brain', *Curr Biol*, 13(20), pp. 1758-67.

Veleri, S. *et al.* (2007) 'Hofbauer-Buchner eyelet affects circadian photosensitivity and coordinates TIM and PER expression in Drosophila clock neurons', *J Biol Rhythms*, 22(1), pp. 29-42.

Verdier, V., Guang Chao, C. and Settleman, J. (2006) 'Rho-kinase regulates tissue morphogenesis via non-muscle myosin and LIM-kinase during Drosophila development', *BMC Dev Biol*, 6, p. 38.

Vereshchagina, N. *et al.* (2004) 'The essential role of PP1beta in Drosophila is to regulate nonmuscle myosin', *Mol Biol Cell*, 15(10), pp. 4395-405.

Verleyen, P. *et al.* (2004) 'Expression of a novel neuropeptide, NVGTLARDFQLPIPNamide, in the larval and adult brain of Drosophila melanogaster', *J Neurochem*, 88(2), pp. 311-9.

Vetter, I.R. and Wittinghofer, A. (2001) 'The guanine nucleotide-binding switch in three dimensions', *Science*, 294(5545), pp. 1299-304.

Vicente-Manzanares, M. *et al.* (2009) 'Non-muscle myosin II takes centre stage in cell adhesion and migration', *Nat Rev Mol Cell Biol*, 10(11), pp. 778-90.

Vigh, B. *et al.* (2002) 'Nonvisual photoreceptors of the deep brain, pineal organs and retina', *Histol Histopathol*, 17(2), pp. 555-90.

Vitaterna, M.H. *et al.* (1994) 'Mutagenesis and mapping of a mouse gene, Clock, essential for circadian behavior', *Science*, 264(5159), pp. 719-25.

Vlachos, S. and Harden, N. (2011) 'Genetic evidence for antagonism between Pak protein kinase and Rho1 small GTPase signaling in regulation of the actin cytoskeleton during Drosophila oogenesis', *Genetics*, 187(2), pp. 501-12.

Wang, Y. *et al.* (2009) 'ROCK isoform regulation of myosin phosphatase and contractility in vascular smooth muscle cells', *Circ Res*, 104(4), pp. 531-40.

Warner, S. and Cook, K. (2009) Warner insertions.

Warner, S.J. and Longmore, G.D. (2009) 'Distinct functions for Rho1 in maintaining adherens junctions and apical tension in remodeling epithelia', *Journal of Cell Biology*, 185(6), pp. 1111-1125.

Watanabe, N. *et al.* (1997) 'p140mDia, a mammalian homolog of Drosophila diaphanous, is a target protein for Rho small GTPase and is a ligand for profilin', *EMBO J*, 16(11), pp. 3044-56.

Watanabe, T., Sato, K. and Kaibuchi, K. (2009) 'Cadherin-mediated intercellular adhesion and signaling cascades involving small GTPases', *Cold Spring Harb Perspect Biol*, 1(3), p. a003020.

Watts, R.J., Hoopfer, E.D. and Luo, L. (2003) 'Axon pruning during Drosophila metamorphosis: evidence for local degeneration and requirement of the ubiquitin-proteasome system', *Neuron*, 38(6), pp. 871-85.

Wear, M.A., Schafer, D.A. and Cooper, J.A. (2000) 'Actin dynamics: assembly and disassembly of actin networks', *Curr Biol*, 10(24), pp. R891-5.

Weber, U. and Mlodzik, M. (2003) UAS-Rho1 insertions.

Wei, H. *et al.* (2014) 'Signaling of pigment-dispersing factor (PDF) in the Madeira cockroach Rhyparobia maderae', *PLoS One*, 9(9), p. e108757.

Wei, L. *et al.* (2000) 'beta(1)-integrin and PI 3-kinase regulate RhoA-dependent activation of skeletal alpha-actin promoter in myoblasts', *Am J Physiol Heart Circ Physiol*, 278(6), pp. H1736-43.

Welsh, D.K. *et al.* (1995) 'Individual neurons dissociated from rat suprachiasmatic nucleus express independently phased circadian firing rhythms', *Neuron*, 14(4), pp. 697-706.

Wennerberg, K., Rossman, K.L. and Der, C.J. (2005) 'The Ras superfamily at a glance', *J Cell Sci*, 118(Pt 5), pp. 843-6.

Wenzl, C. *et al.* (2010) 'Localization of RhoGEF2 during Drosophila cellularization is developmentally controlled by Slam', *Mech Dev*, 127(7-8), pp. 371-84.

West, A.C. and Bechtold, D.A. (2015) 'The cost of circadian desynchrony: Evidence, insights and open questions', *Bioessays*, 37(7), pp. 777-88.

Weston, L., Coutts, A.S. and La Thangue, N.B. (2012) 'Actin nucleators in the nucleus: an emerging theme', *J Cell Sci*, 125(Pt 15), pp. 3519-27.

Wever, R.A. (1984) 'Properties of human sleep-wake cycles: parameters of internally synchronized free-running rhythms', *Sleep*, 7(1), pp. 27-51.

Wheeler, D.A. *et al.* (1993) 'Behavior in light-dark cycles of Drosophila mutants that are arrhythmic, blind, or both', *J Biol Rhythms*, 8(1), pp. 67-94.

Whitehead, K. *et al.* (2009) 'Diurnally entrained anticipatory behavior in archaea', *PLoS One*, 4(5), p. e5485.

Wijnen, H. and Young, M.W. (2008) 'The right period for a Siesta', *Neuron*, 60(6), pp. 943-6.

Winter, C.G. *et al.* (2001) 'Drosophila Rho-associated kinase (Drok) links Frizzled-mediated planar cell polarity signaling to the actin cytoskeleton', *Cell*, 105(1), pp. 81-91.

Wittmann, M. *et al.* (2006) 'Social jetlag: misalignment of biological and social time', *Chronobiol Int*, 23(1-2), pp. 497-509.

Wolfgang, W. *et al.* (2013) 'The Pyrexia transient receptor potential channel mediates circadian clock synchronization to low temperature cycles in Drosophila melanogaster', *Proc Biol Sci*, 280(1768), p. 20130959.

Wollnik, F. (1989) 'Physiology and regulation of biological rhythms in laboratory animals: an overview', *Lab Anim*, 23(2), pp. 107-25.

Wu, J.S. and Luo, L. (2006) 'A protocol for dissecting Drosophila melanogaster brains for live imaging or immunostaining', *Nat Protoc*, 1(4), pp. 2110-5.

Wu, X. and Xu, X.M. (2016) 'RhoA/Rho kinase in spinal cord injury', *Neural Regen Res*, 11(1), pp. 23-7.

Wu, Y., Cao, G. and Nitabach, M.N. (2008) 'Electrical silencing of PDF neurons advances the phase of non-PDF clock neurons in Drosophila', *J Biol Rhythms*, 23(2), pp. 117-28.

Wulbeck, C., Grieshaber, E. and Helfrich-Forster, C. (2008) 'Pigment-dispersing factor (PDF) has different effects on Drosophila's circadian clocks in the accessory medulla and in the dorsal brain', *J Biol Rhythms*, 23(5), pp. 409-24.

Xie, L. *et al.* (2013) 'Sleep drives metabolite clearance from the adult brain', *Science*, 342(6156), pp. 373-7.

Xu, N., Keung, B. and Myat, M.M. (2008) 'Rho GTPase controls invagination and cohesive migration of the Drosophila salivary gland through Crumbs and Rho-kinase', *Dev Biol*, 321(1), pp. 88-100.

Xu, Y. *et al.* (2005) 'Functional consequences of a CKIdelta mutation causing familial advanced sleep phase syndrome', *Nature*, 434(7033), pp. 640-4.

Yang, Z. and Sehgal, A. (2001) 'Role of molecular oscillations in generating behavioral rhythms in Drosophila', *Neuron*, 29(2), pp. 453-67.

Yannielli, P.C. and Harrington, M.E. (2001) 'Neuropeptide Y in the mammalian circadian system: effects on light-induced circadian responses', *Peptides*, 22(3), pp. 547-56.

Yao, Z. *et al.* (2012) 'Analysis of functional neuronal connectivity in the Drosophila brain', *J Neurophysiol*, 108(2), pp. 684-96.

Yasunaga, K. *et al.* (2010) 'Dendrite reshaping of adult Drosophila sensory neurons requires matrix metalloproteinase-mediated modification of the basement membranes', *Dev Cell*, 18(4), pp. 621-32.

Yasuyama, K. and Meinertzhagen, I.A. (1999) 'Extraretinal photoreceptors at the compound eye's posterior margin in Drosophila melanogaster', *J Comp Neurol*, 412(2), pp. 193-202.

Ye, J. *et al.* (2012) 'Primer-BLAST: a tool to design target-specific primers for polymerase chain reaction', *BMC Bioinformatics*, 13, p. 134.

Yoshii, T., Hermann, C. and Helfrich-Forster, C. (2010) 'Cryptochrome-positive and -negative clock neurons in Drosophila entrain differentially to light and temperature', *J Biol Rhythms*, 25(6), pp. 387-98.

Yoshii, T. *et al.* (2015) 'Cryptochrome-dependent and -independent circadian entrainment circuits in Drosophila', *J Neurosci*, 35(15), pp. 6131-41.

Yoshii, T. *et al.* (2005) 'Temperature cycles drive Drosophila circadian oscillation in constant light that otherwise induces behavioural arrhythmicity', *Eur J Neurosci*, 22(5), pp. 1176-84.

Yoshii, T., Rieger, D. and Helfrich-Forster, C. (2012) 'Two clocks in the brain: an update of the morning and evening oscillator model in Drosophila', *Prog Brain Res*, 199, pp. 59-82.

Yoshii, T. *et al.* (2009a) 'Synergic entrainment of Drosophila's circadian clock by light and temperature', *J Biol Rhythms*, 24(6), pp. 452-64.

Yoshii, T. *et al.* (2009b) 'The neuropeptide pigment-dispersing factor adjusts period and phase of Drosophila's clock', *J Neurosci*, 29(8), pp. 2597-610.

Yu, Q. *et al.* (1987) 'Molecular mapping of point mutations in the period gene that stop or speed up biological clocks in Drosophila melanogaster', *Proc Natl Acad Sci U S A*, 84(3), pp. 784-8.

Yu, W. *et al.* (2006) 'PER-dependent rhythms in CLK phosphorylation and E-box binding regulate circadian transcription', *Genes Dev*, 20(6), pp. 723-33.

Yu, X. *et al.* (2010) 'The Cryptochrome Blue Light Receptors', *Arabidopsis Book*, 8, p. e0135.

Zaidi, F.H. *et al.* (2007) 'Short-wavelength light sensitivity of circadian, pupillary, and visual awareness in humans lacking an outer retina', *Curr Biol*, 17(24), pp. 2122-8.

Zeng, H. *et al.* (1996) 'A light-entrainment mechanism for the Drosophila circadian clock', *Nature*, 380(6570), pp. 129-35.

Zerr, D.M. *et al.* (1990) 'Circadian fluctuations of period protein immunoreactivity in the CNS and the visual system of Drosophila', *J Neurosci*, 10(8), pp. 2749-62.

Zhang, L. *et al.* (2010a) 'DN1(p) circadian neurons coordinate acute light and PDF inputs to produce robust daily behavior in Drosophila', *Curr Biol*, 20(7), pp. 591-9.

Zhang, Y. and Emery, P. (2013) 'GW182 controls Drosophila circadian behavior and PDF-receptor signaling', *Neuron*, 78(1), pp. 152-65.

Zhang, Y. *et al.* (2010b) 'Light and temperature control the contribution of specific DN1 neurons to Drosophila circadian behavior', *Curr Biol*, 20(7), pp. 600-5.

Zhao, J. *et al.* (2003) 'Drosophila clock can generate ectopic circadian clocks', *Cell*, 113(6), pp. 755-66.

Zheng, B. *et al.* (2009a) 'Nuclear actin and actin-binding proteins in the regulation of transcription and gene expression', *Febs j*, 276(10), pp. 2669-85.

Zheng, X. *et al.* (2009b) 'An isoform-specific mutant reveals a role of PDP1 epsilon in the circadian oscillator', *J Neurosci*, 29(35), pp. 10920-7.

Zimberg, I.Z. *et al.* (2012) 'Metabolic impact of shift work', *Work*, 41 Suppl 1, pp. 4376-83.

Zimmerman, J.E. *et al.* (2012) 'Genetic background has a major impact on differences in sleep resulting from environmental influences in Drosophila', *Sleep*, 35(4), pp. 545-57.